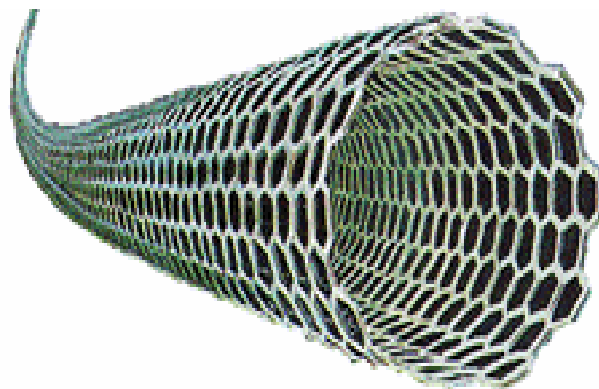


NT05 Tutorial:
Raman Scattering in Carbon Nanotubes

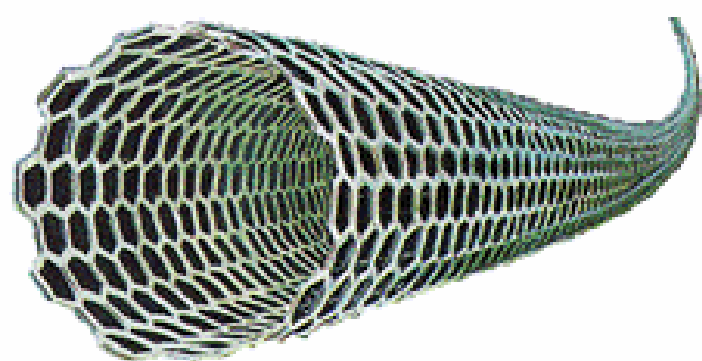
Carbon Nanotubes

Mildred Dresselhaus
MIT
June 26, 2005



Collaborators:

G. Dresselhaus, MIT
G. Samsonidze, MIT
G. Chou, MIT
H. Son, MIT



Collaborators:

A. Jorio, Brazil
M.A. Pimenta, Brazil
A. Souza Filho, Brazil
J. Jiang, Japan
R. Saito, Japan

World Year of Physics 2005

Einstein in the 21st Century

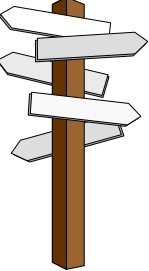


Help make 2005 another *Miraculous Year!*

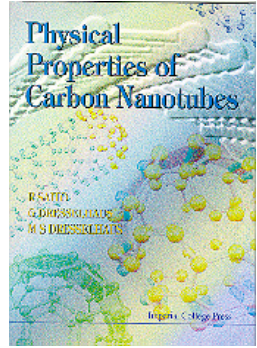
Timed to coincide with the 2005 Centennial Celebration of Albert Einstein's Miraculous Year, the World Year of Physics 2005 will bring the excitement of physics to the public and inspire a new generation of scientists. Visit www.physics2005.org to find out how you can get involved.

www.physics2005.org

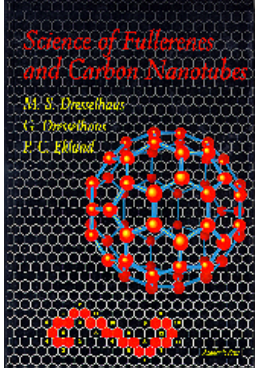




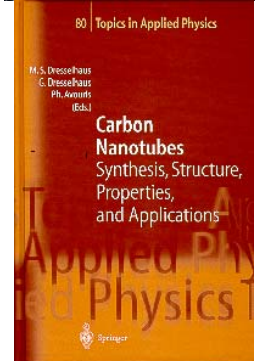
Books on Carbon Nanotubes



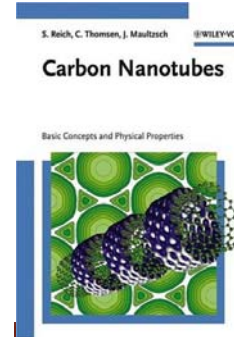
Physical Properties of Carbon Nanotubes (1998), Imperial College Press, UK, R. Saito, M. S. Dresselhaus, G.Dresselhaus



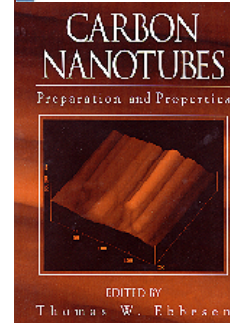
Science of Fullerenes and Carbon Nanotubes, (1996), Academic Press, M. S. Dresselhaus, G. Dresselhaus and P. C. Eklund



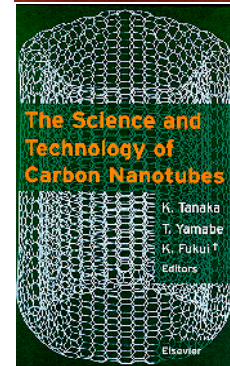
Carbon Nanotubes (2001), Springer, Berlin, Eds. M. S. Dresselhaus, G.Dresselhaus, Ph. Avouris



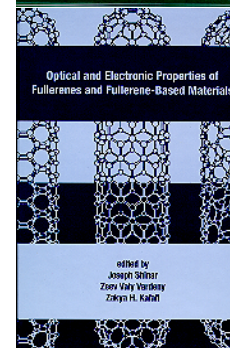
Carbon Nanotubes (2004) Wiley-VCH, S. Reich, C. Thomsen, J. Maultzsch



Carbon Nanotubes, (1997) CRC Press, Ed. T. W. Ebbesen



The Science and Technology of Carbon Nanotubes, (1999) Elsevier, Eds. K. Tanaka, T. Yamabe and K. Yamabe



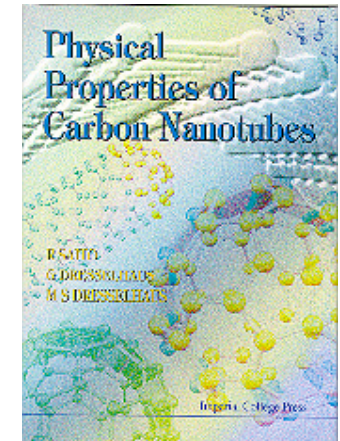
Optical and Electronic Properties of Fullerenes and Fullerene-Based Materials, Marcel Dekker, Inc (1999), Eds. J. Shinar et al.

Review Articles on Raman Scattering in Carbon Nanotubes

- Dresselhaus et al, Physics Reports, “Raman spectroscopy of Carbon Nanotubes”, 47-99 (2005)
- Dresselhaus et al, Carbon **40**, 2043-2061 (2002)
- Dresselhaus et al, Phys. “Raman spectroscopy of Carbon Nanotubes”, book chapter (in press)

Outline

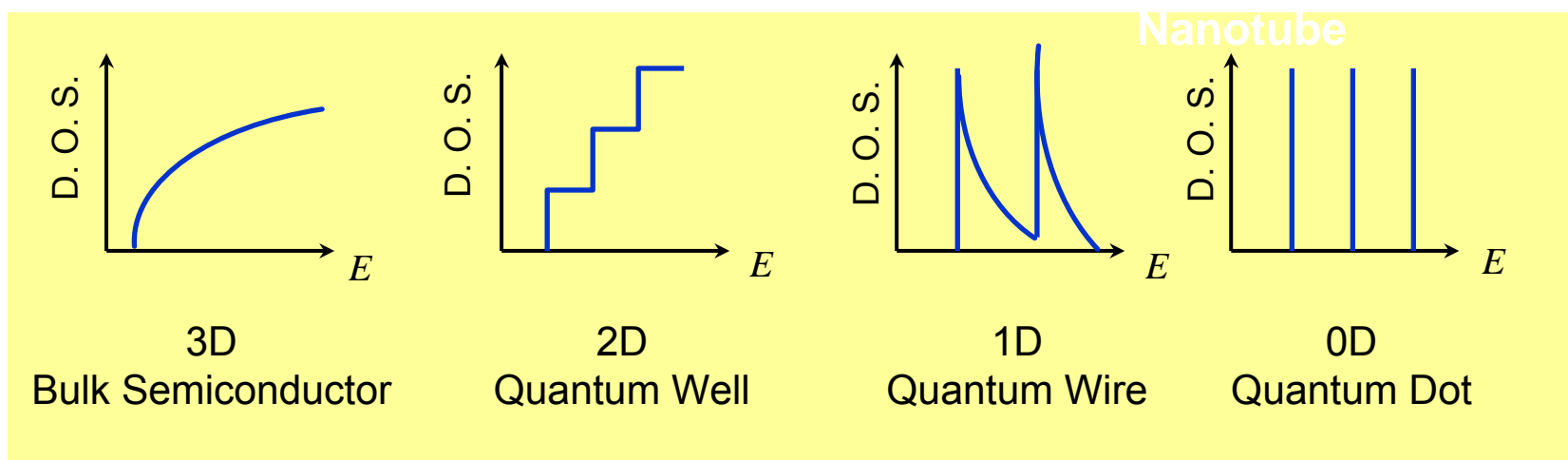
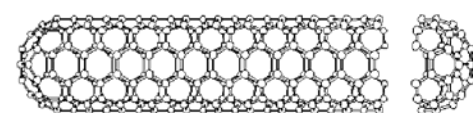
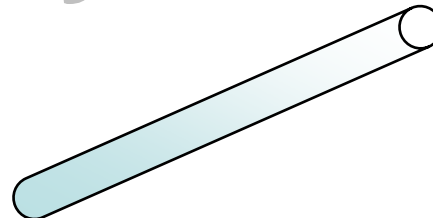
- **Background**
- Phonon Properties
- Overview of Raman Effect
- First-order Raman Processes
 - (the RBM and G-Band)
- Double Resonance Processes
- Photoluminescence
- Excitons



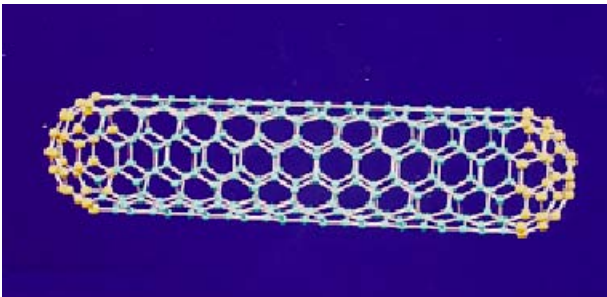
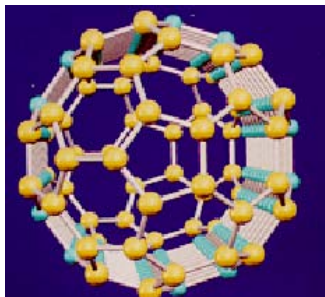
"Physical Properties of Carbon Nanotubes",
by R. Saito, G. Dresselhaus and M.S. Dresselhaus,
Imperial College Press (1998) ISBN 1-86094-093-5

One Dimensional Systems:

- High aspect ratio
- Enhanced density of states
- Single wall carbon nanotubes SWNT: Chirality and diameter-dependent properties

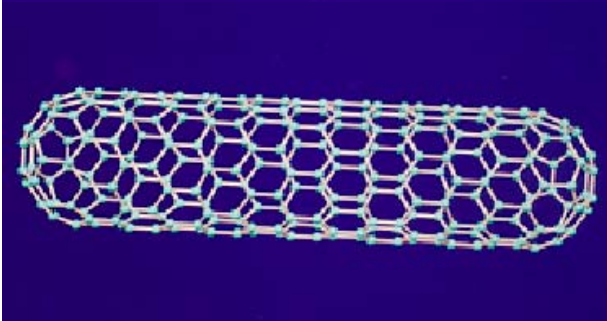
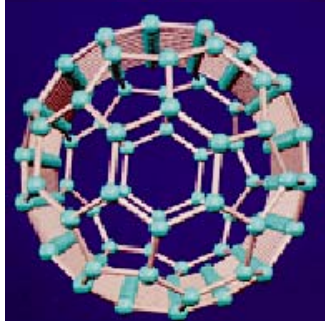


Carbon Nanotubes



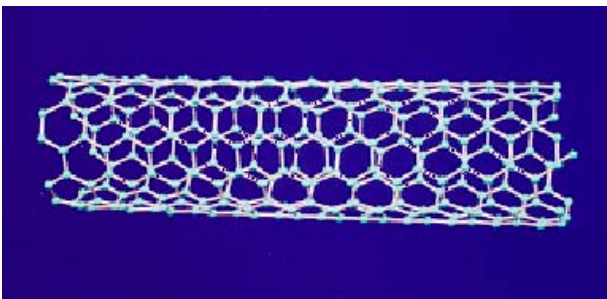
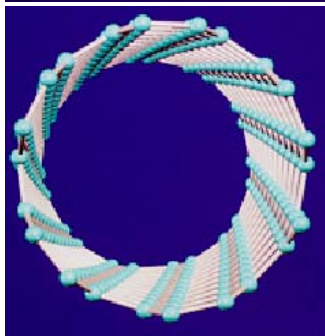
(5,5)

Armchair, symmorphic



(9,0)

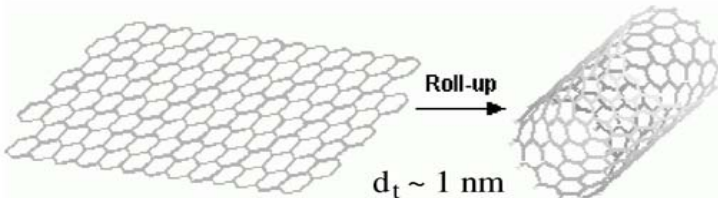
Zigzag, symmorphic



(6,5)

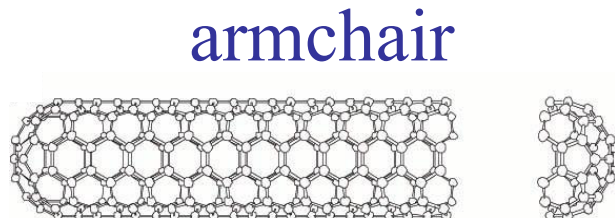
Chiral, non-symmorphic

Unique Properties of Carbon Nanotubes



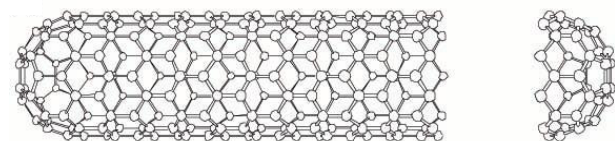
graphene sheet

SWNT

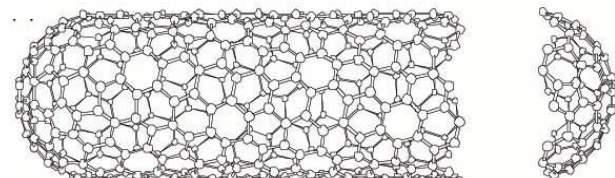


armchair

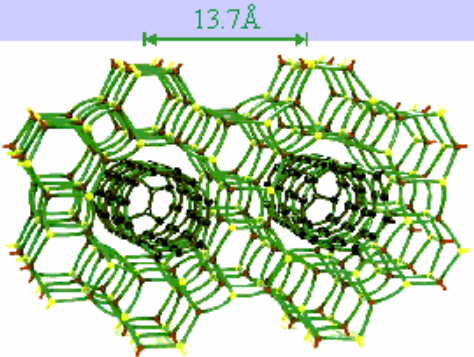
zigzag



chiral



- **Size:** Nanostructures with dimensions of $\sim 1 \text{ nm}$ diameter (~ 10 atoms around the cylinder)
- **Electronic Properties:** Can be either metallic or semiconducting depending on diameter and orientation of the hexagons
- **Mechanical Properties:** Very high strength, modulus, and resiliency. Good properties on both compression and extension.
- **Physics:** 1D density of electronic states
- Single molecule Raman spectroscopy, luminescence, and transport properties.
- Heat pipe, electromagnetic waveguide.

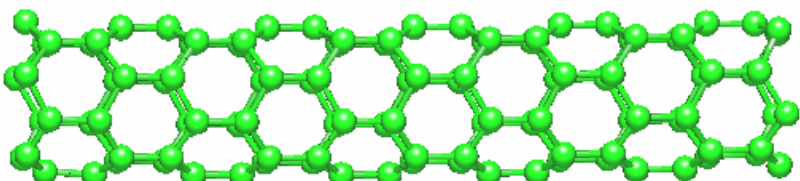


Smallest Nanotubes

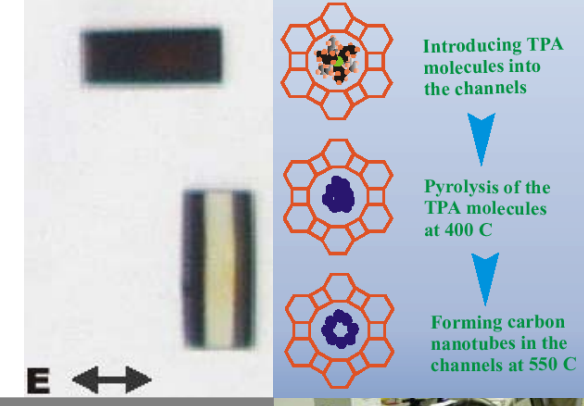
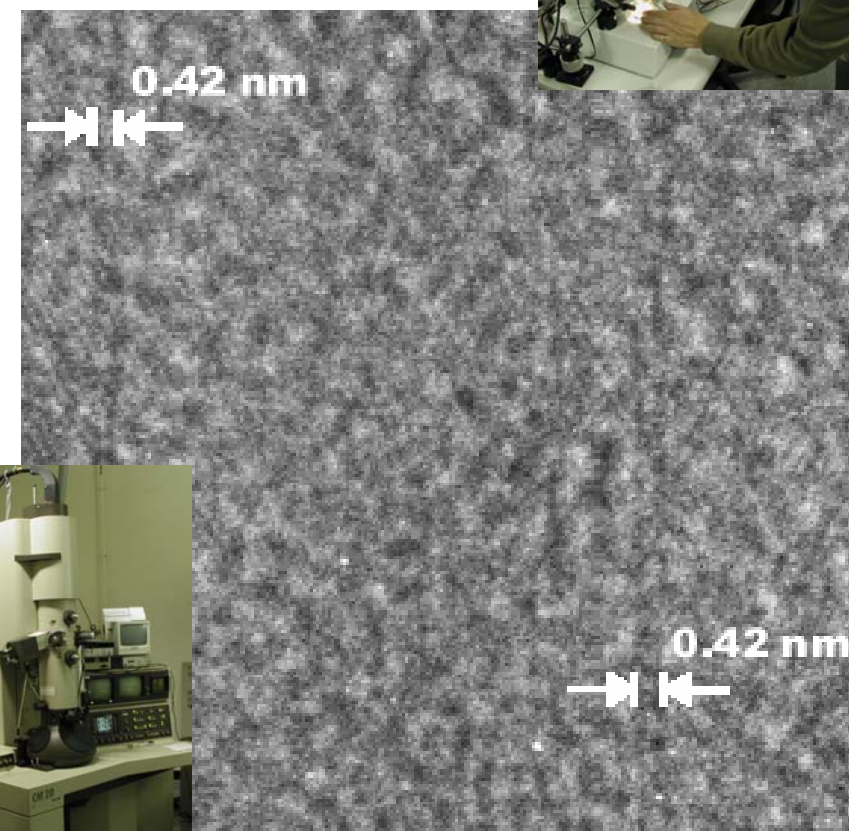
N. Wang *et al.*

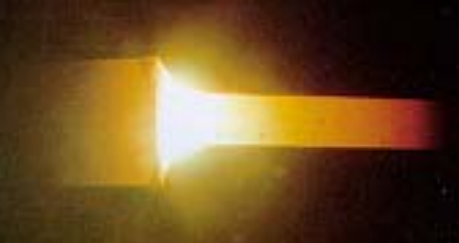
Nature 408, 50 (2000)

- Chiralities (5,0), (3,3), (4,2)
- Diameter 0.42 nm
- 10 Carbon atoms along circumference in (5,0)
- Isolated & Aligned tubes
- Metallic electronic structure
- TEM, Electron diffraction
- Photo Luminescence
- Raman Spectra
- Superconductivity (15 K)



(5,0) zigzag nanotube
same diameter as C_{20} fullerene

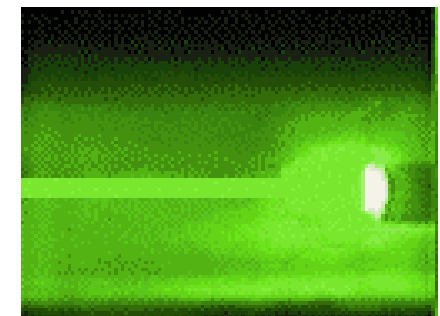




Arc Method: Y. Saito

Synthesis

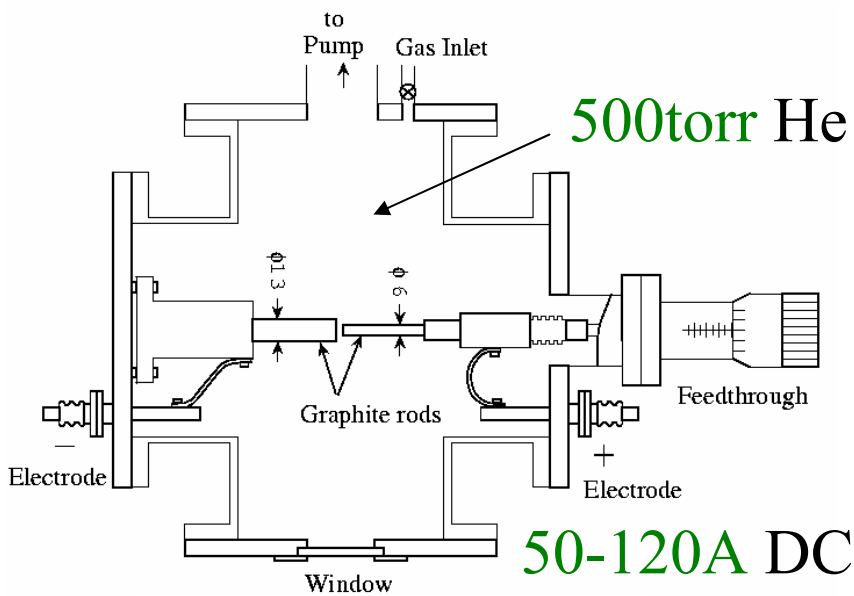
S. Iijima, *Nature* 354 56 (1991)



Laser Ablation:
H. Kataura

- Arc Discharge

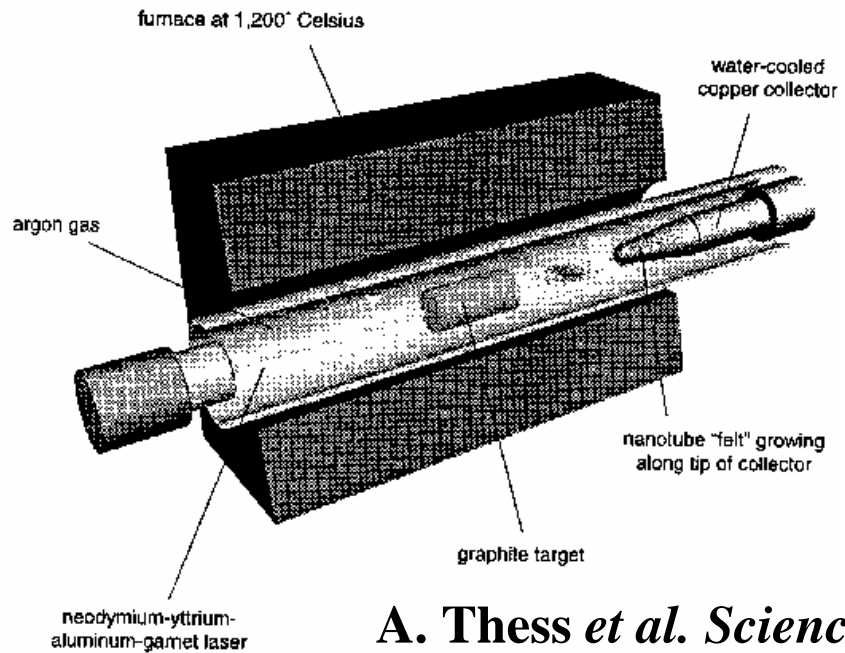
5-20mm diameter carbon rod



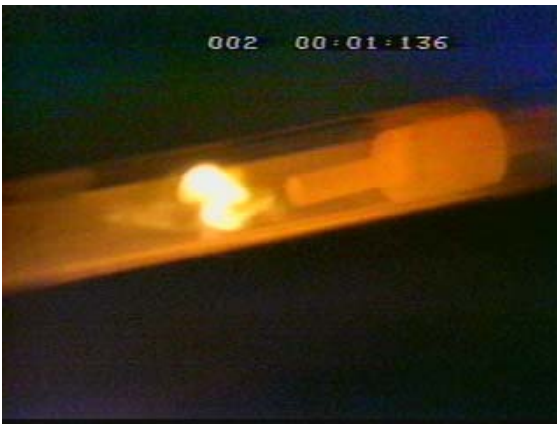
Y. Saito *et al*, *Phys. Rev.* 48 1907 (1993)

- Laser Ablation

Nd-Yb-Al-garnet Laser, 1200°C

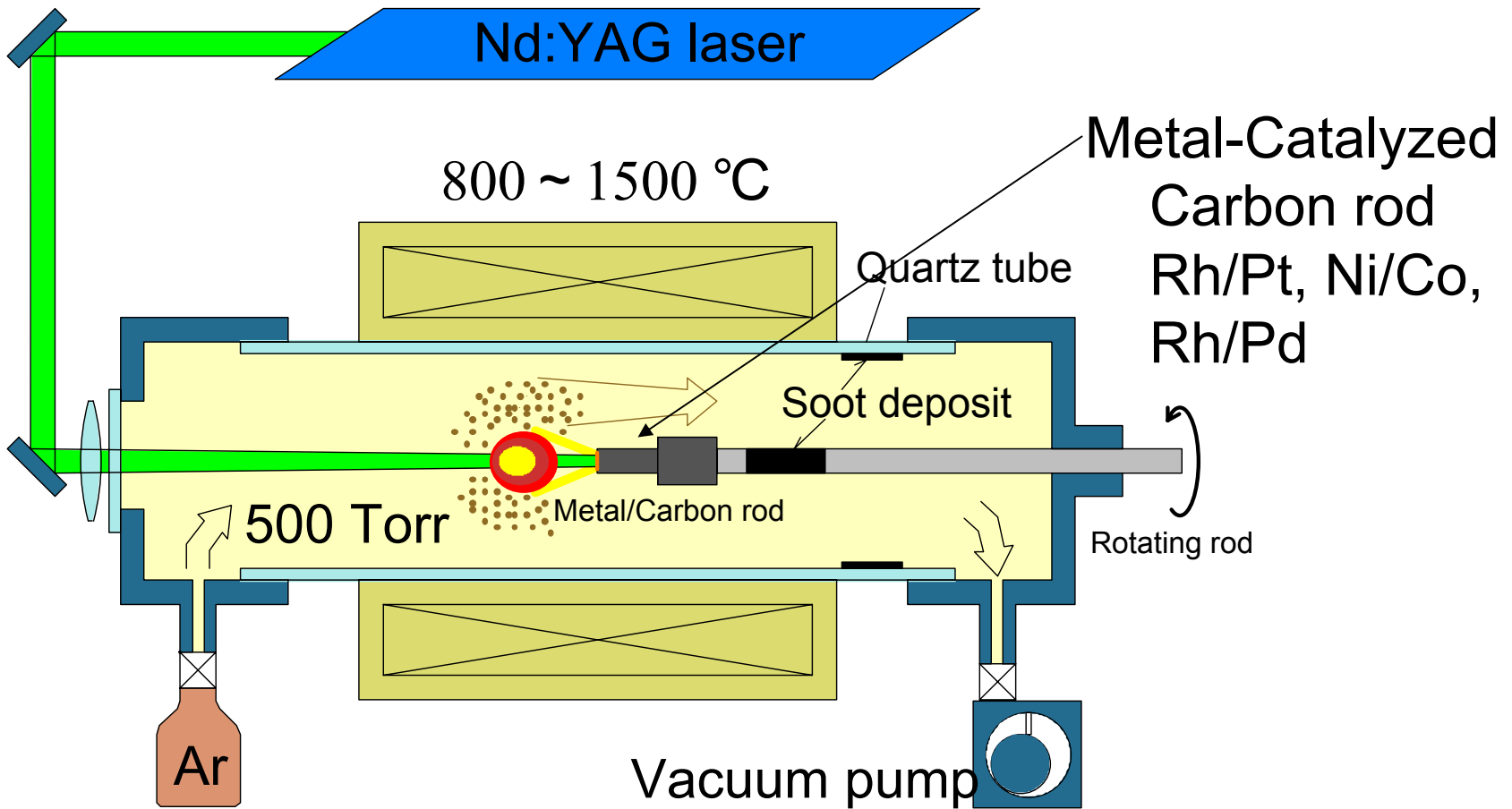


A. Thess *et al*. *Science*
273 483 (1996)



Pulsed Laser Ablation

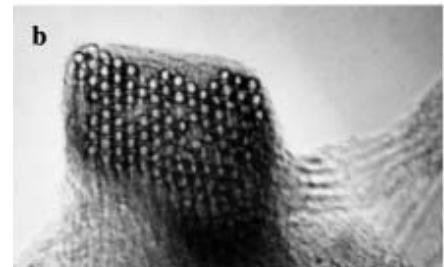
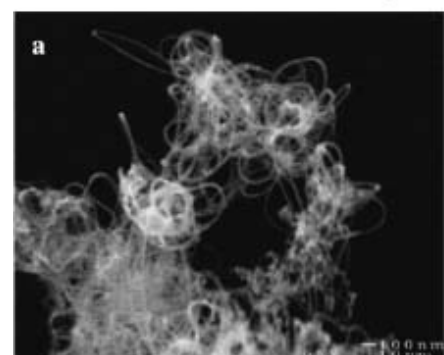
H. Kataura, unpublished (2001)



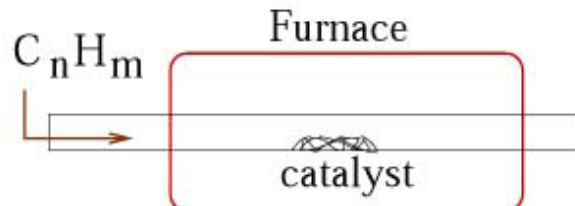
Isolated single wall carbon nanotubes by CVD method

(from J.H.Hafner and C.M.Lieber, Harvard Univ.)

conventional sample

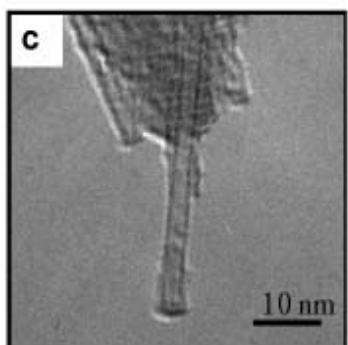


laser ablation method
(fig. from Prof. R. Smalley)

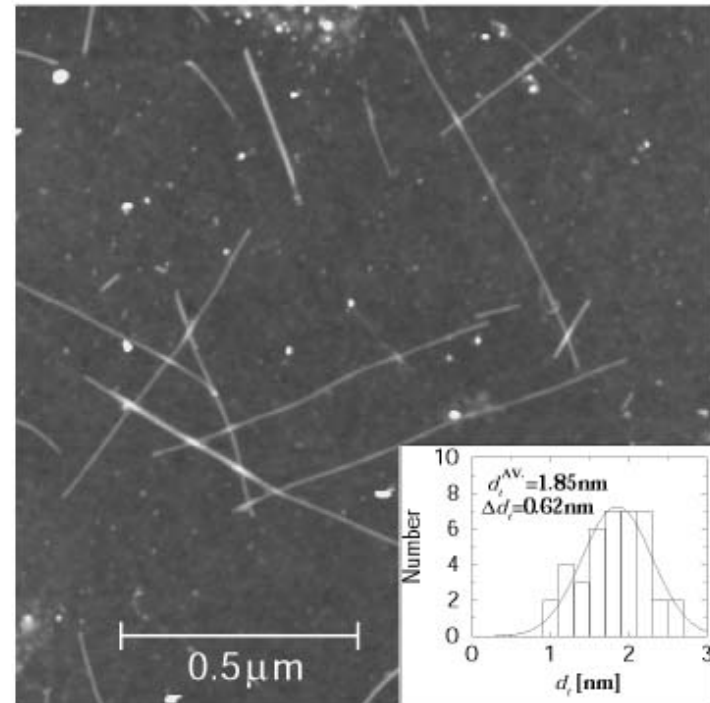


1 – Deposit Fe catalysts
on a Si/SiO₂ surface

2 – Evaporate ethylene
on the substrate at
800°C



TEM
image

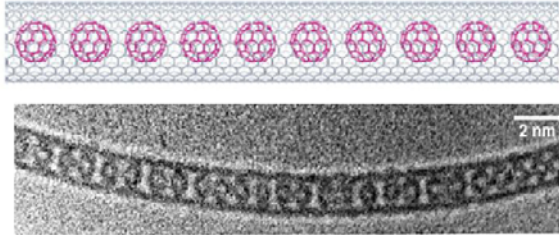


1 – 10 SWNTs / μm^2
laser spot $\sim 1 \mu\text{m}^2$

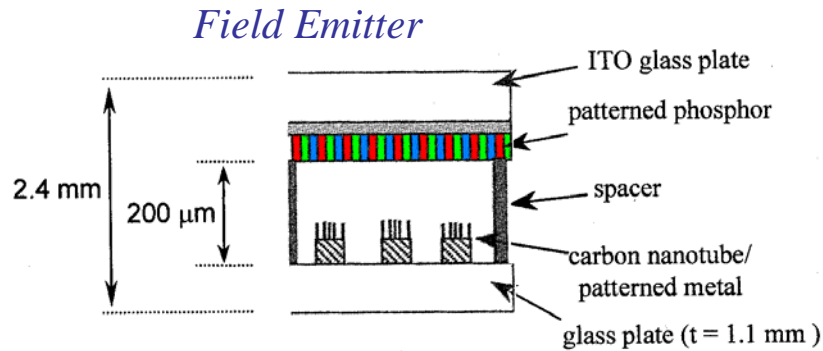
Applications for Nanotubes

- ✓ Field emitters
- ✓ Semiconductor devices
- ✓ STM/AFM tips
- ✓ Imaging of Biological molecules
- ✓ New Materials
- ✓ Battery additives
- ✓ Polymer composites

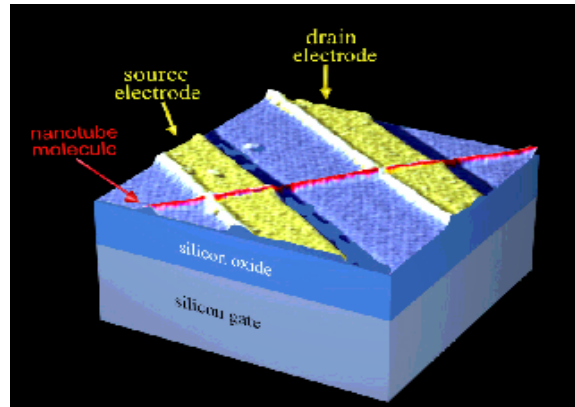
New Materials



Fullerenes C₆₀ inside nanotubes

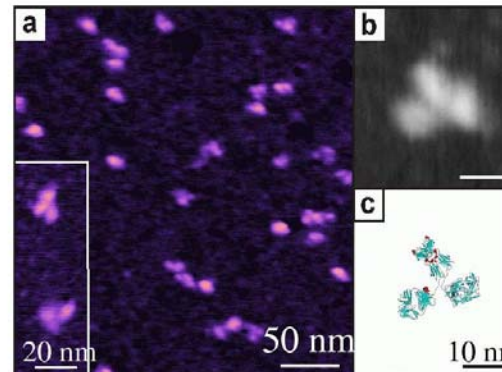


Transistor



S.J. Tans *et al. Nature*, 393, 49 (1998)

Imaging biological molecules



AFM image of Immunoglobulin G resolved by nanotube tips

Diameter and Chiral Angle

R. Saito et al. , Physical Properties of Carbon Nanotubes, Imperial College Press (1998)

- Diameter : d_t

$$d_t = \frac{L}{\pi} = \frac{a\sqrt{n^2 + nm + m^2}}{\pi}$$

$$L = |C_h|$$

- Chiral Angle : θ

- zigzag $\theta=0$
- armchair $\theta=\pi/6$
- chiral $0 < \theta < \pi/6$

$$\theta = \tan^{-1} \frac{\sqrt{3}m}{2n+m}, 0 \leq |\theta| \leq \frac{\pi}{6}$$

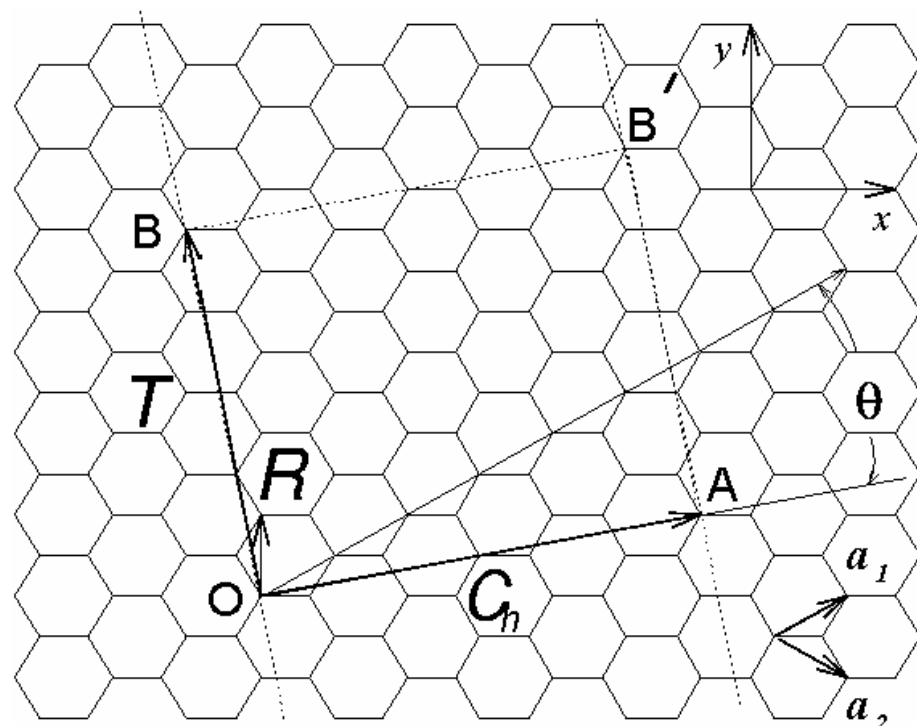
$$a_{\text{C-C}} = 1.42 \text{\AA}$$

$$a_1 = a_2 = 2.46 \text{\AA}$$

Ex. (10,10) armchair

$$d_t = 13.7 \text{\AA} = 1.37 \text{ nm}$$

$$(n,m)=(4,2)$$



Chiral Vectors : (n,m)

R. Saito *et al.*, Phys. Rev. **B46**, 1804
(1992)

$$a_{\text{C-C}} = 1.42 \text{\AA}$$
$$a_1 = a_2 = 2.46 \text{\AA}$$

- Chiral Vector (equator of nanotube): OA, C_h
- Translational Vector of 1D material: OB, T
- Unit Cell : OAB'B

$$C_h = n a_1 + m a_2 \equiv (n, m)$$

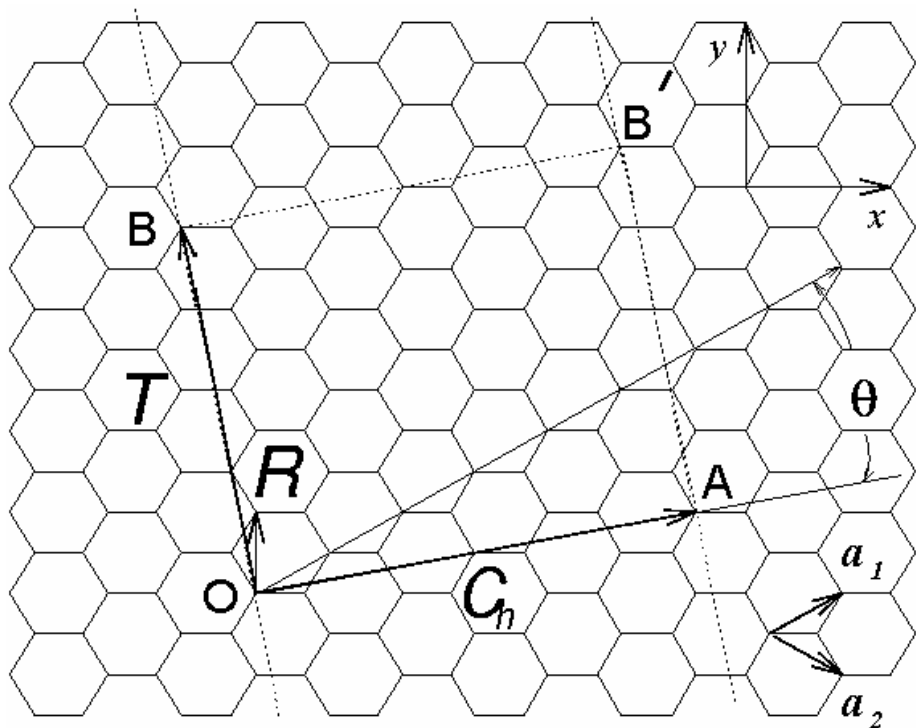
a_1, a_2 : primitive lattice vectors

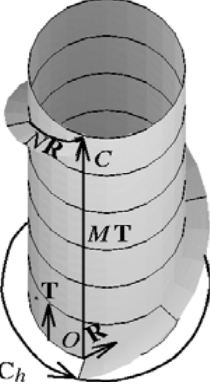
$$T = t_1 a_1 + t_2 a_2 \equiv (t_1, t_2)$$

$$t_1 = \frac{(2m+n)}{d_R}, t_2 = -\frac{(2n+m)}{d_R}$$

$$d_R = \gcd(2n+m, 2m+n)$$

gcd: greatest common divisor





Reciprocal Lattice and k Vectors

R. Saito et al., *Physical Properties of Carbon Nanotubes*, Imperial College Press (1998)

- Nanotube axis direction
 - 1 Dimensional Wave Vectors

$$-\frac{\pi}{T} \leq k \leq \frac{\pi}{T}, \quad T : \text{translational vector}$$

- Discrete in Circumferential Direction

$$C_h \cdot K_1 = 2\pi, \quad N = \frac{2(n^2 + m^2 + nm)}{d_R}$$

$$T \cdot K_2 = 2\pi, \quad d_R$$

$$K_1 = \frac{1}{N}(-t_2 b_1 + t_1 b_2), \quad K_2 = \frac{1}{N}(mb_1 - nb_2)$$

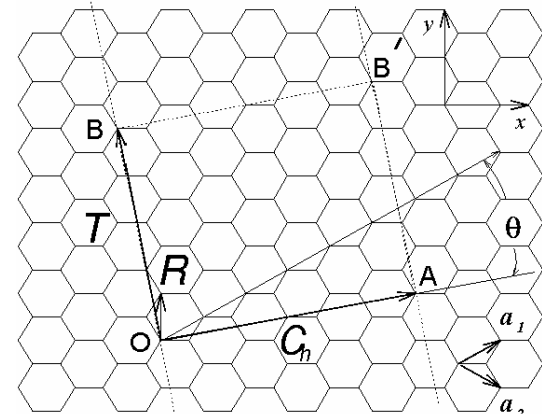
$$C_h = (4, 2), \quad T = (4, -5), \quad N = 28$$

$$K_1 = \left(\frac{5}{28}b_1 + \frac{1}{7}b_2\right), \quad K_2 = \left(\frac{1}{7}b_1 - \frac{1}{14}b_2\right)$$

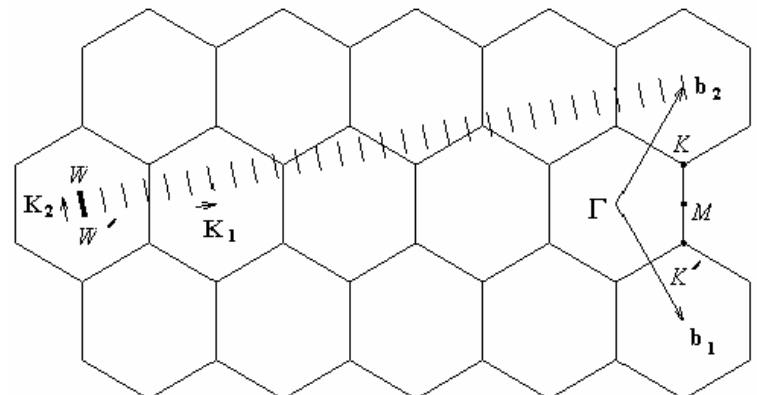
$$T = t_1 a_1 + t_2 a_2 \equiv (t_1, t_2)$$

$$t_1 = \frac{(2m+n)}{d_R}, \quad t_2 = -\frac{(2n+m)}{d_R}$$

$$d_R = \gcd(2n+m, 2m+n)$$

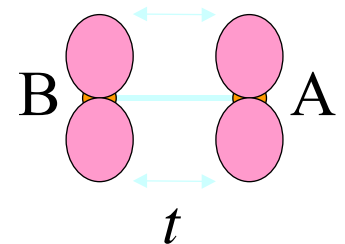


N Cutting lines



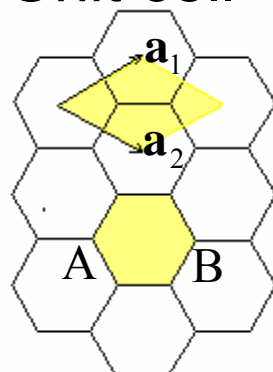
Energy bands of Graphite

P. R. Wallace, *Phys. Rev.*, **71** 622 (1947).

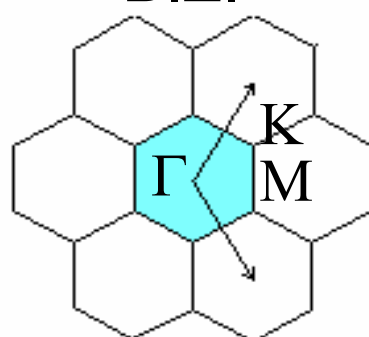


- π band of graphite
- Energy Band Model
 - Zero Gap Semiconductor

Unit cell

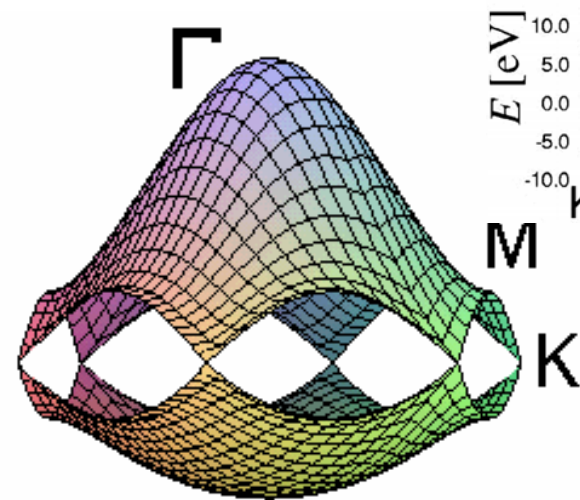


B.Z.



$$\mathbf{a}_1 = \left(\frac{\sqrt{3}}{2}, \frac{1}{2}\right)a, \mathbf{a}_2 = \left(\frac{\sqrt{3}}{2}, -\frac{1}{2}\right)a$$

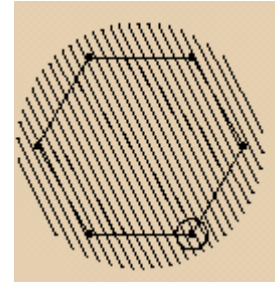
$$\mathbf{b}_1 = \left(\frac{1}{2}, \frac{\sqrt{3}}{2}\right) \frac{4\pi}{\sqrt{3}a}, \mathbf{b}_2 = \left(\frac{1}{2}, -\frac{\sqrt{3}}{2}\right) \frac{4\pi}{\sqrt{3}a}$$



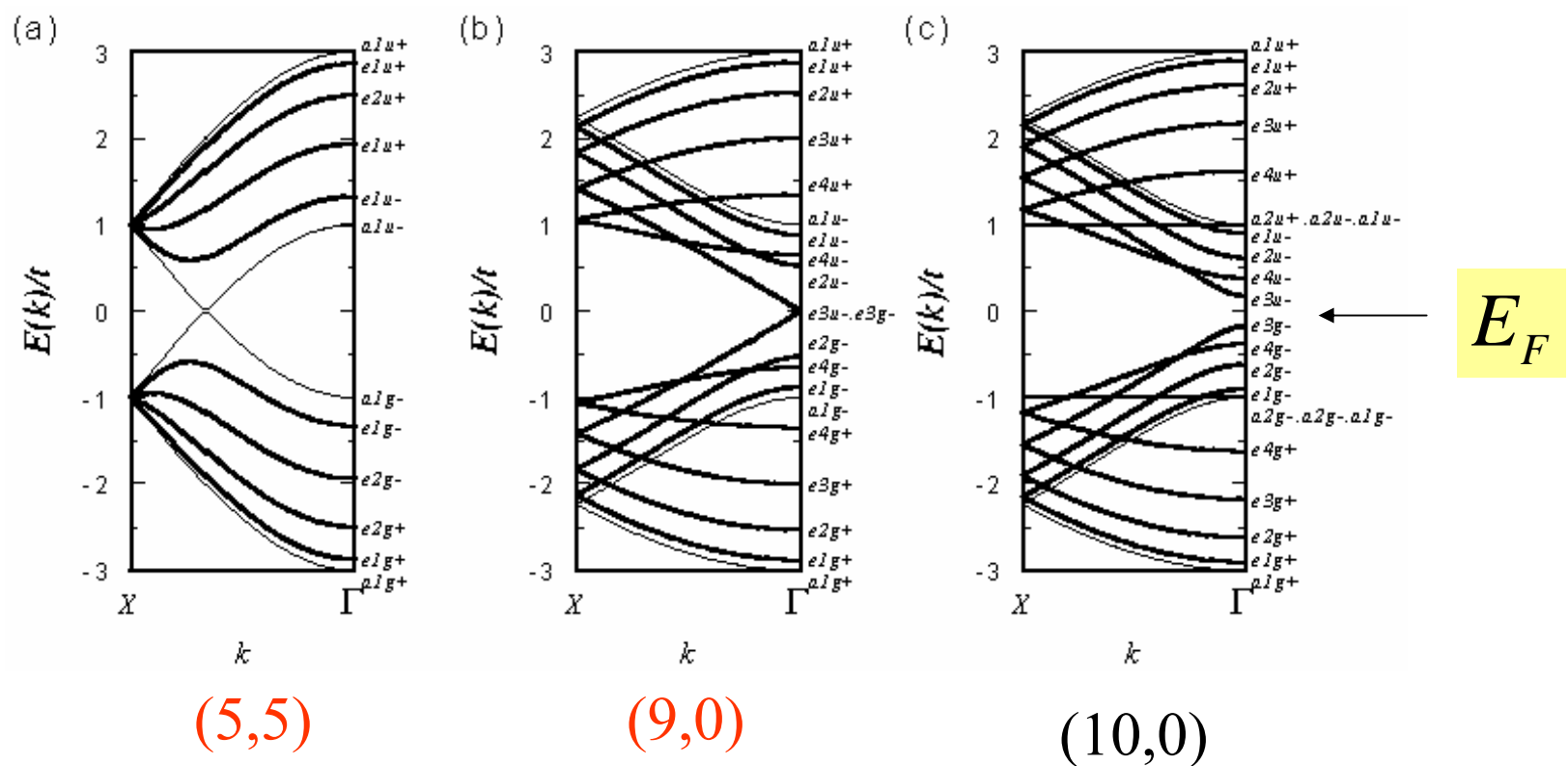
$$E_k = \pm t \sqrt{1 \pm 4 \cos \frac{k_y a}{2} \cos \frac{\sqrt{3} k_x a}{2} + 4 \cos^2 \frac{k_y a}{2}}$$

Energy Bands of Nanotubes

R. Saito *et al.*, *Phys. Rev. B* **46**, 1804 (1992)



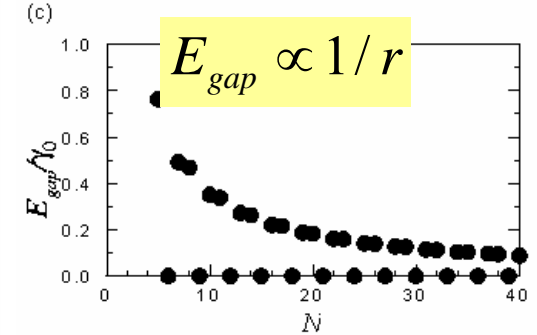
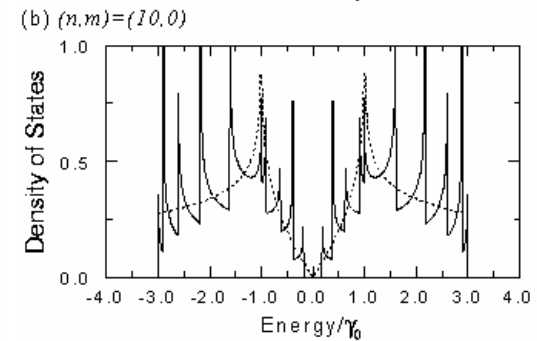
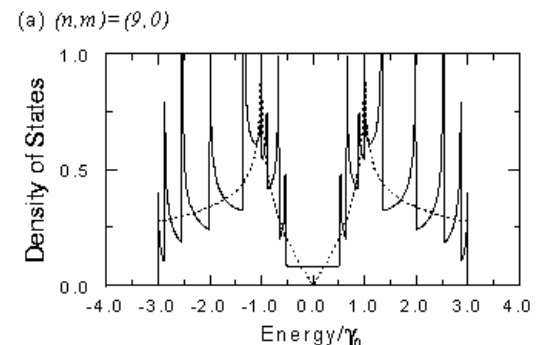
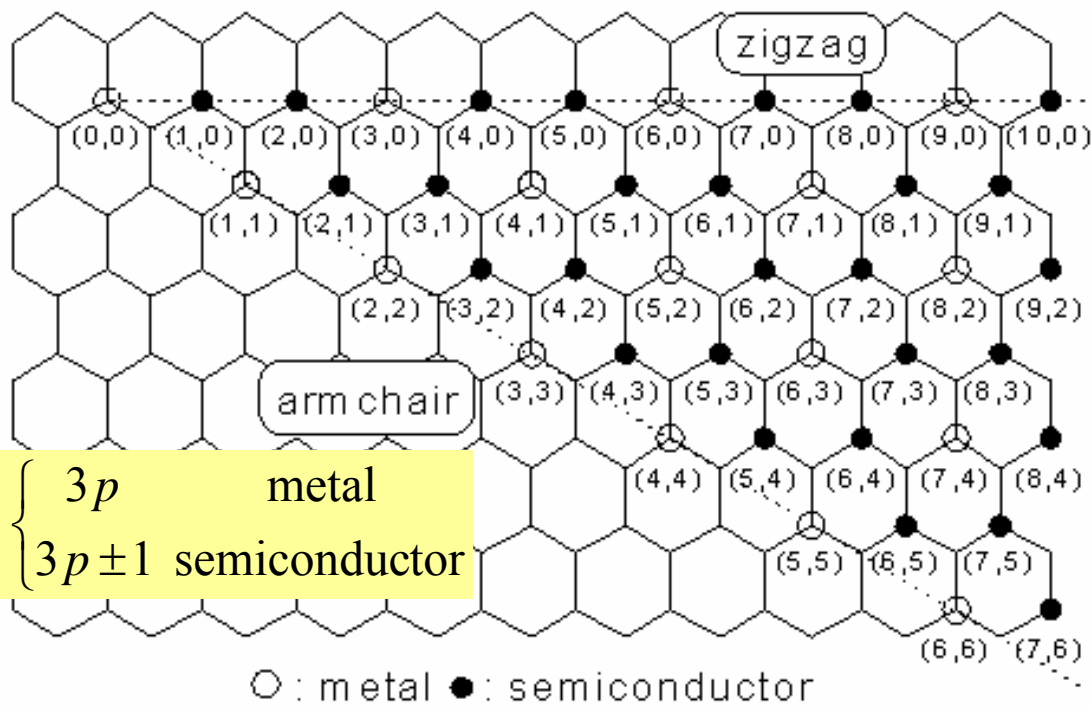
- N one-dimensional bands



Metal or Semiconductor

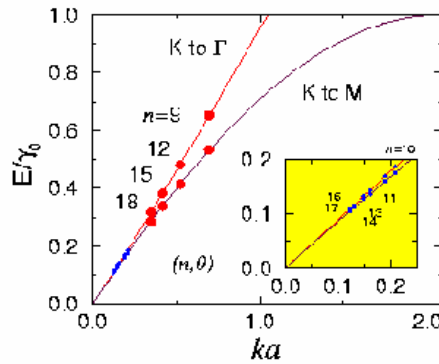
R. Saito *et al.*, *Appl. Phys. Lett.* **60**, 2204 (1992)

- Density of States
- depending on chirality

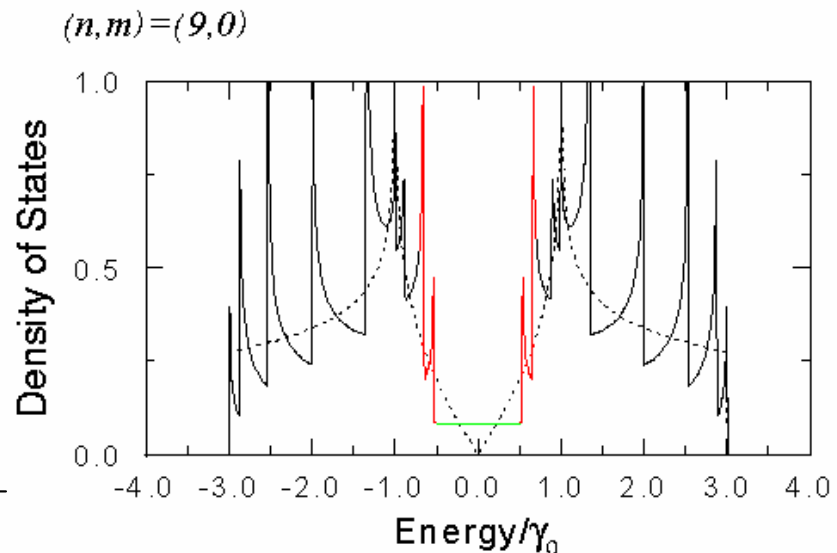
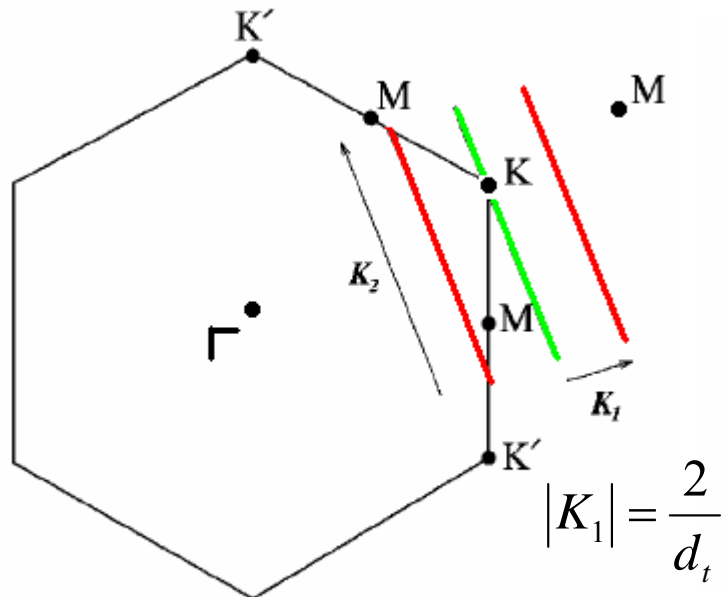


Metallic Carbon Nanotubes

R. Saito *et al*, Phys. Rev. B61, 2981(2000)



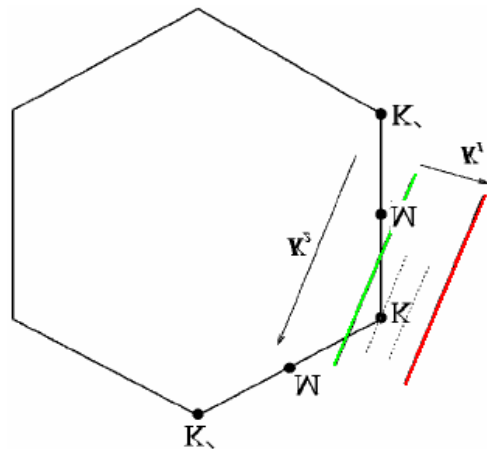
- 1D Energy Dispersion of SWNT
 - K point is always on a cutting line
 - Inequivalent two neighbor lines --- DOS Splitting



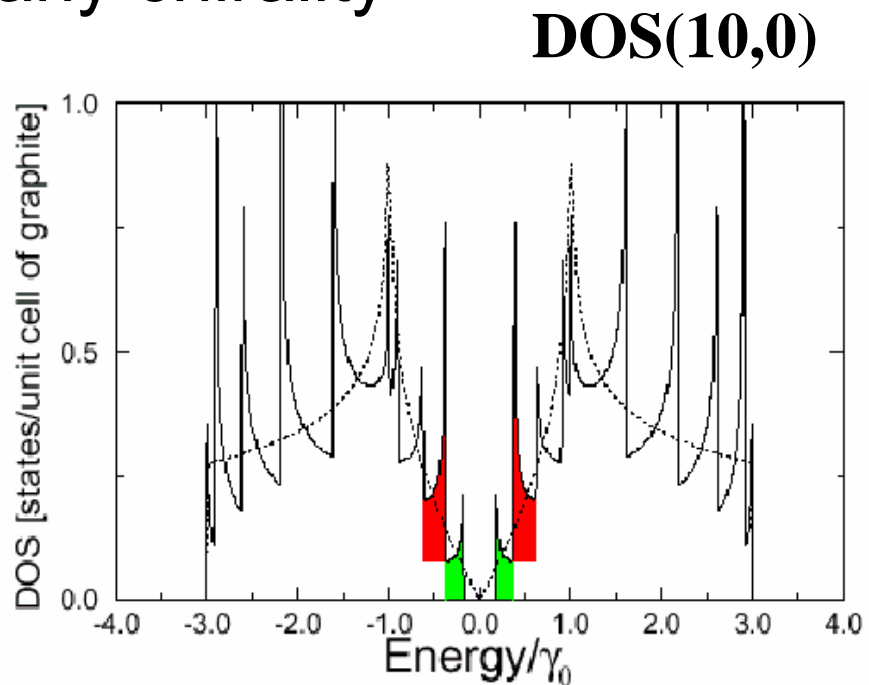
Semiconducting Carbon Nanotubes

R. Saito *et al*, *Phys. Rev. B* **61**, 2981(2000)

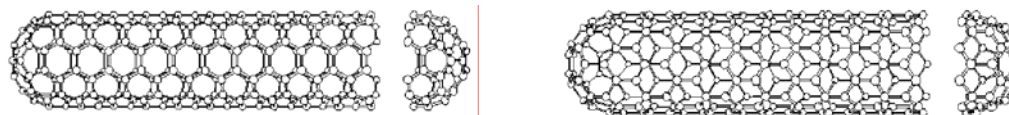
- K points are always at 1/3 (or 2/3) position
 - Two neighboring lines contribute to different energy singularities (e.g., E_1 and E_2)
 - **No DOS splitting** for any chirality



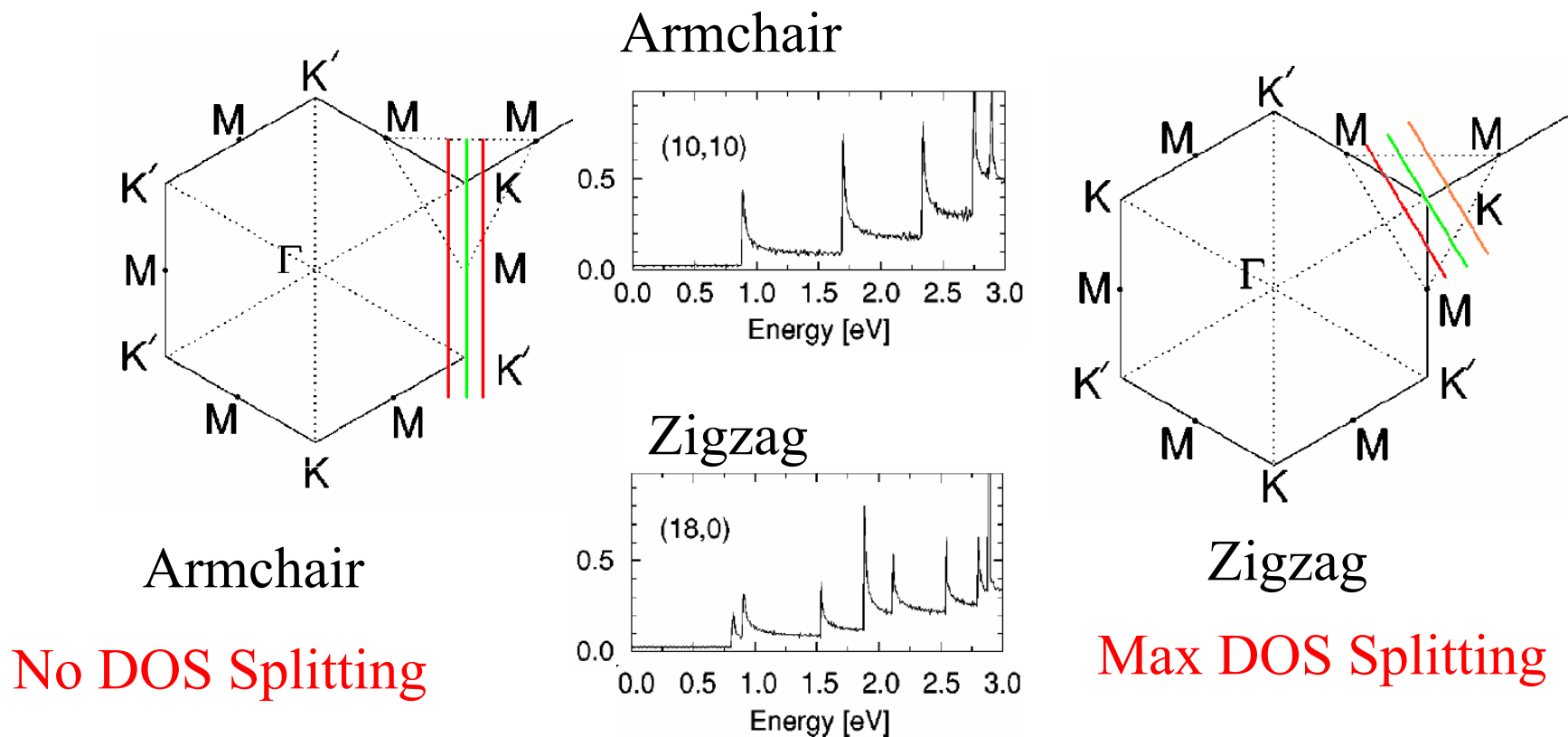
Magnetic Field induces
a Splitting



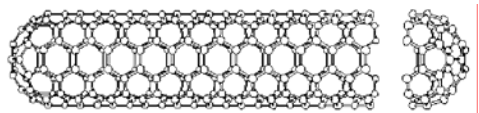
Armchair or Zigzag **metallic** SWNTs



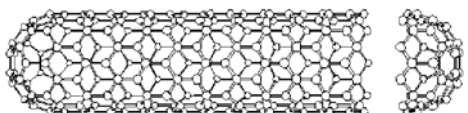
- Magnitude of the DOS splitting depends on *chirality*



Chirality Dependence of DOS splitting for metallic SWNTs

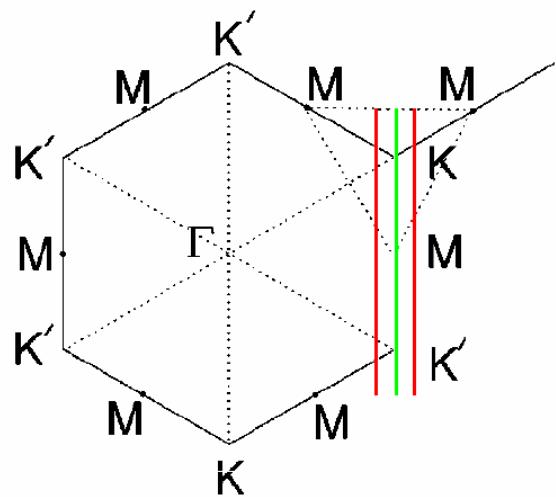


Armchair

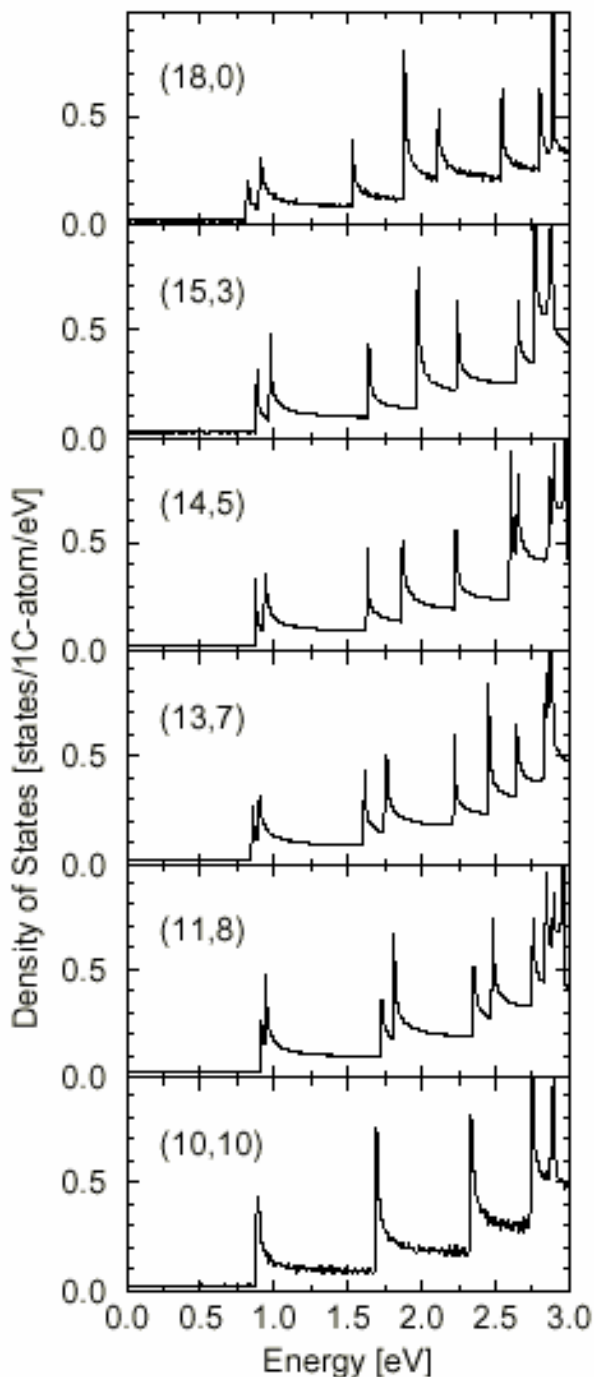
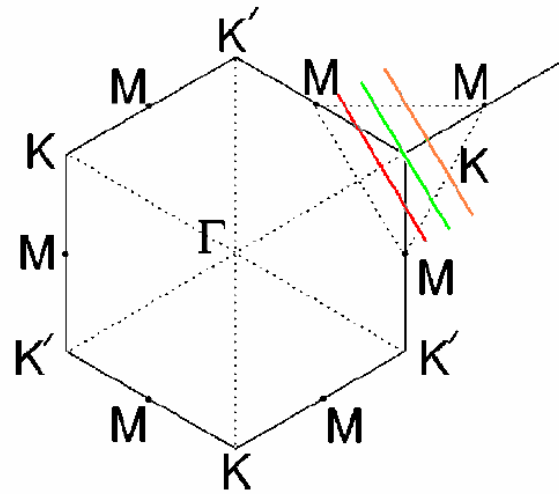


Zigzag

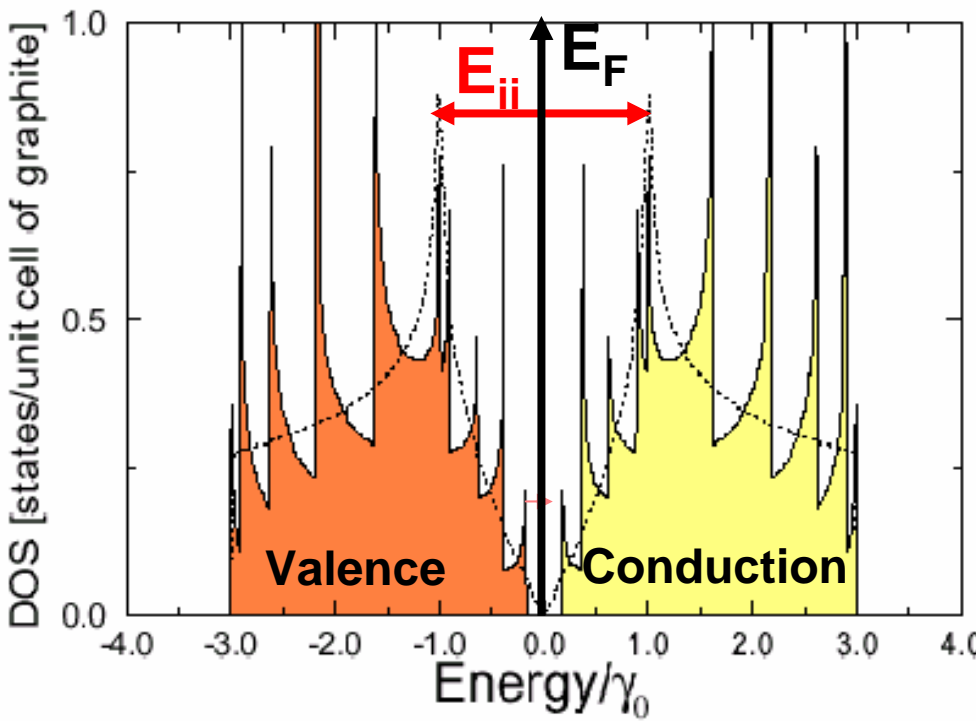
No DOS Splitting



Max DOS Splitting



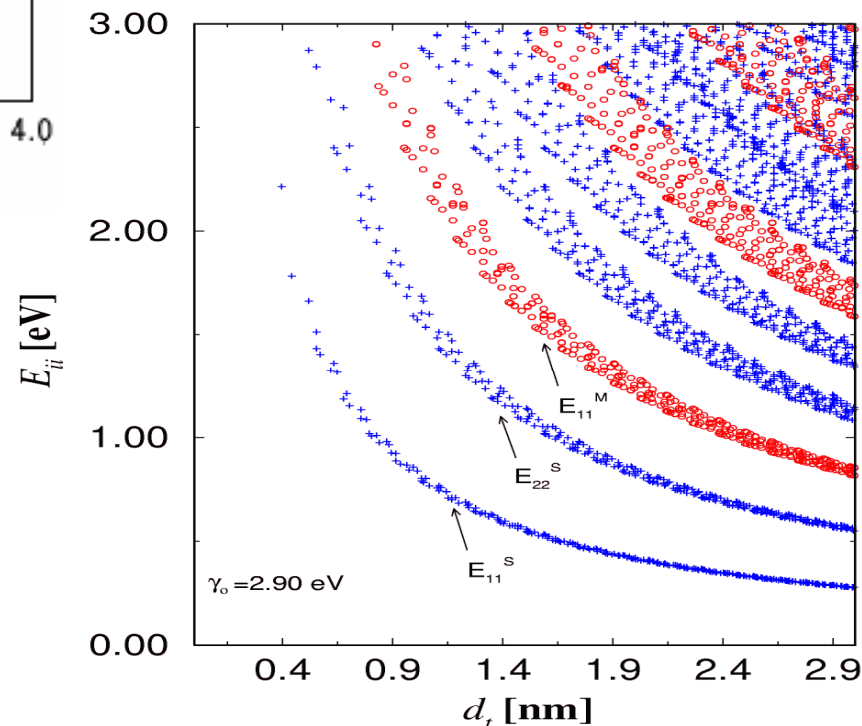
Transitions E_{ii} observed Optically



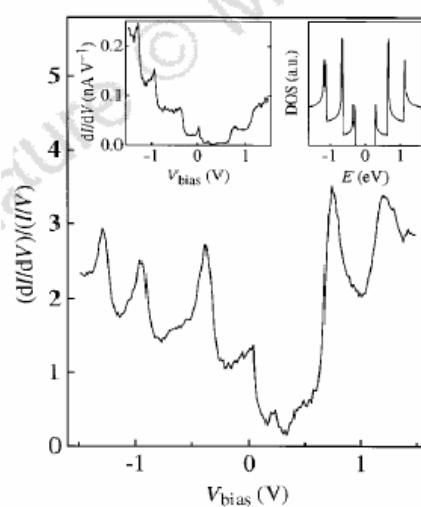
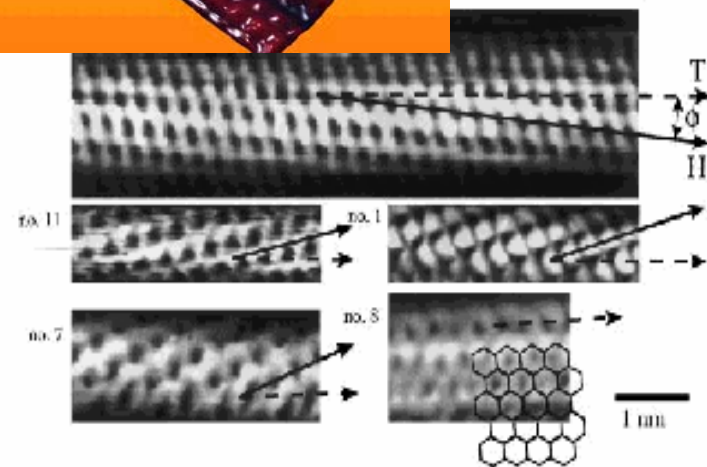
Optical transitions are strongly emphasized at 1D van Hove singularities in joint density of states E_{ii} .

Kataura Plot

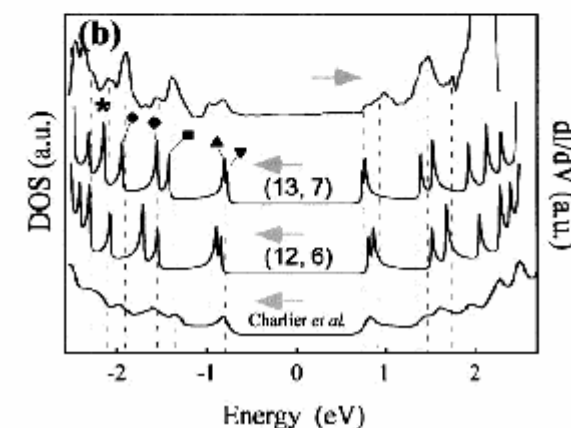
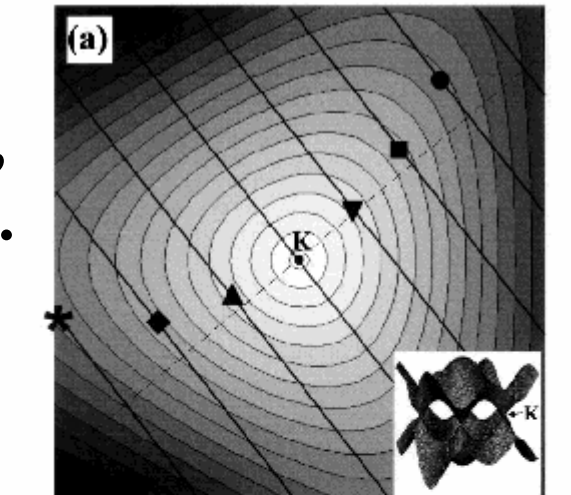
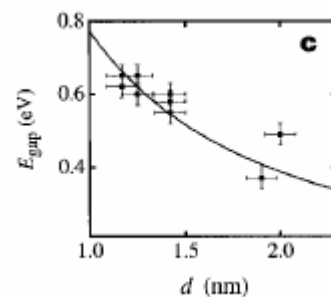
- E_{ii} vs. d_t
-Each (n,m) nanotube has distinct set of E_{ii}



STM/STS Experiments

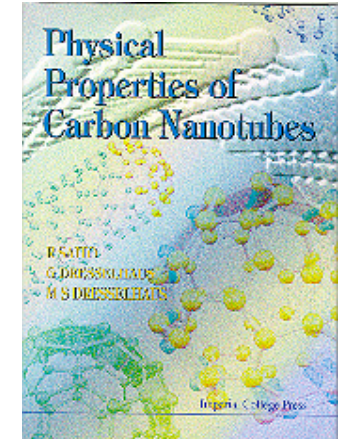


J. W. G. Wildoer et al,
Nature, 391 (1998) 59



Outline

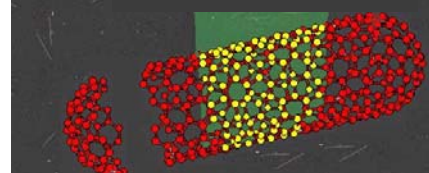
- Background
- **Phonon Properties**
- Overview of Raman Effect
- First-order Raman Processes
 - (the RBM and G-Band)
- Double Resonance Processes
- Photoluminescence
- Excitons



"Physical Properties of Carbon Nanotubes",
by R. Saito, G. Dresselhaus and M.S. Dresselhaus,
Imperial College Press (1998) ISBN 1-86094-093-5

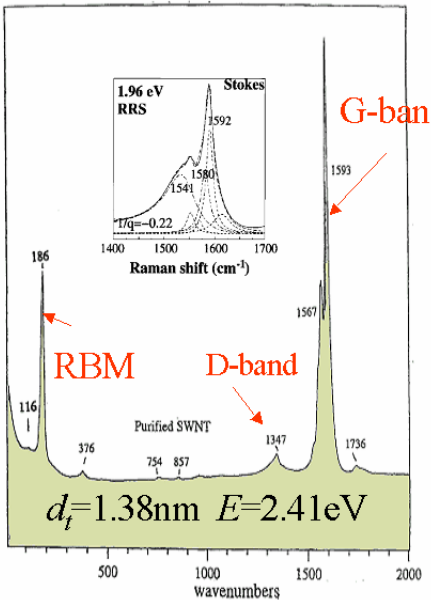


C. V. Raman

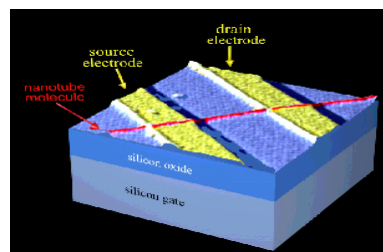
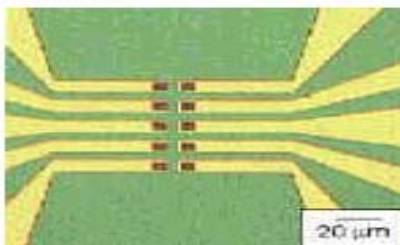


Raman Spectroscopy of Carbon Nanotubes

M. S. Dresselhaus and P. C. Eklund,
Advances in Physics 49 705 (2000)

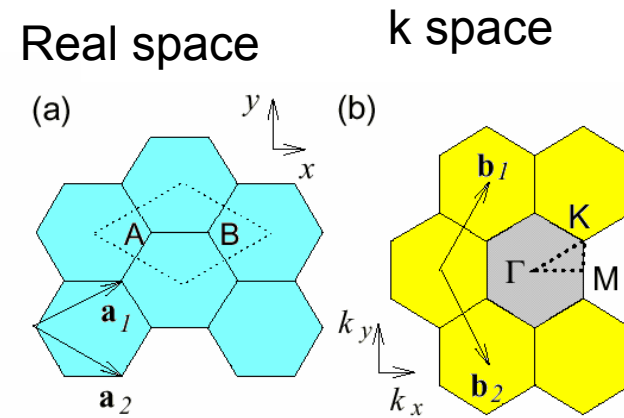
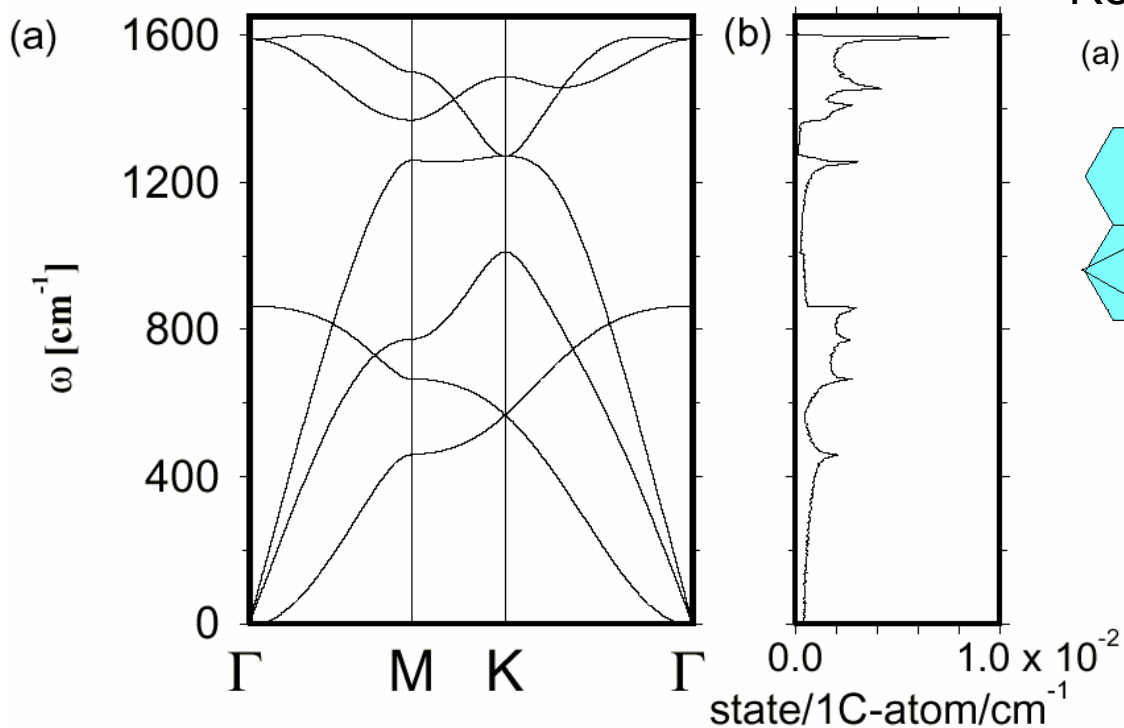


- Non-destructive, contactless measurement
 - Room Temperature
 - In Air at Ambient Pressure
 - Quick (1min), Accurate in Energy
- Diameter Selective (Resonant Raman Effect)
- Diameter and Chirality dependent phonons
 - Characterization of diameter distribution of tubes, their (n,m) values, phonon dispersion relations, presence of defects, and more



Phonon Dispersion of 2D graphite

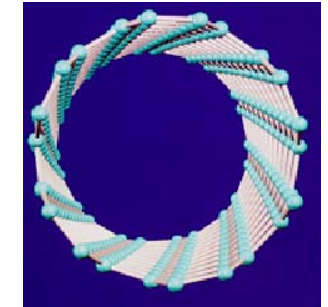
- E_{2g2} Raman mode at 1582cm^{-1} in graphite



R. Saito et al.,
“Physical Properties of
Carbon Nanotubes”
Imperial College Press
(1998)

Phonon Structure of SWNTs

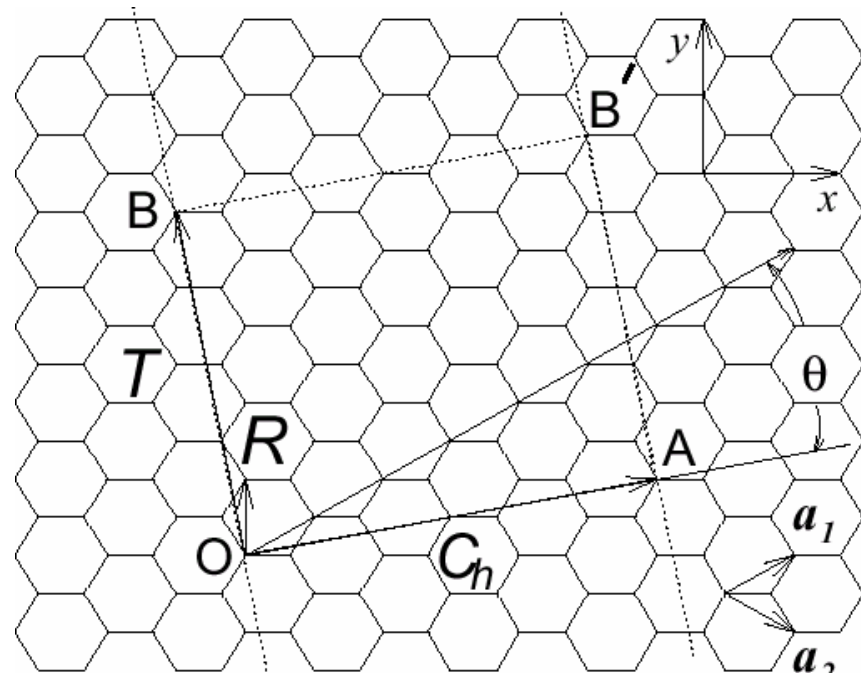
zone-folding is simplest model for $\omega(q)$



- OA: Chiral Vector
- OAB'B: Unit Cell
- $2N$ carbon atoms
- $6N$ phonon modes

$$N = \frac{2(m^2 + n^2 + nm)}{d_R}$$

$$d_R = \begin{cases} 3d & \text{if } n - m = 3d \cdot p \\ d & \text{otherwise} \end{cases}$$

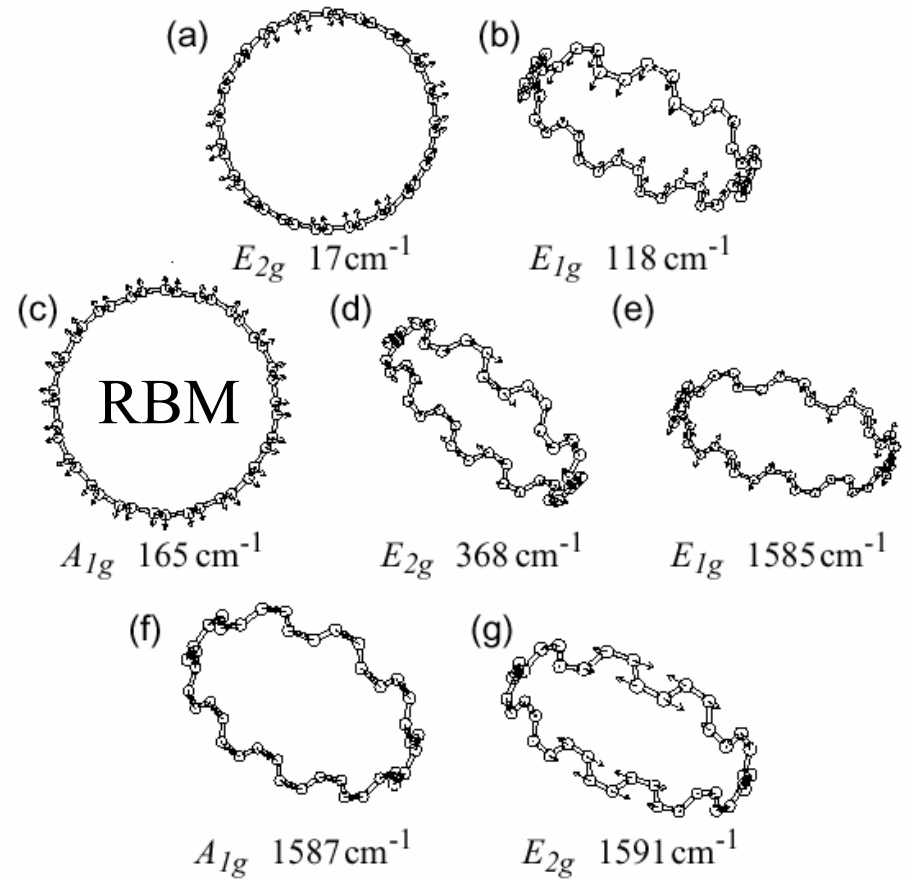
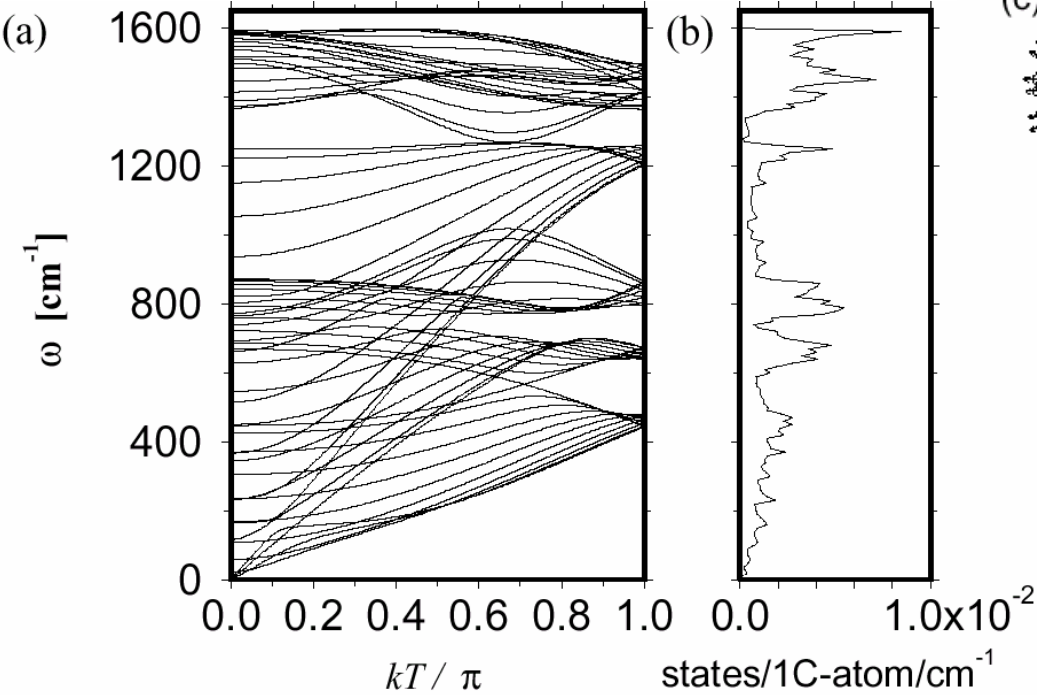


“Physical Properties of Carbon Nanotubes”
R. Saito, G. Dresselhaus, and M.S. Dresselhaus
Imperial College Press, (1998)

Phonon modes -- (10,10) Armchair

R.Saito *et al.* *Phys. Rev.* **B57** (1998) 4145

- $N=20$, $6N=120$ phonon modes
- 66 distinct, 4 acoustic
- 16 Raman (Group theory)

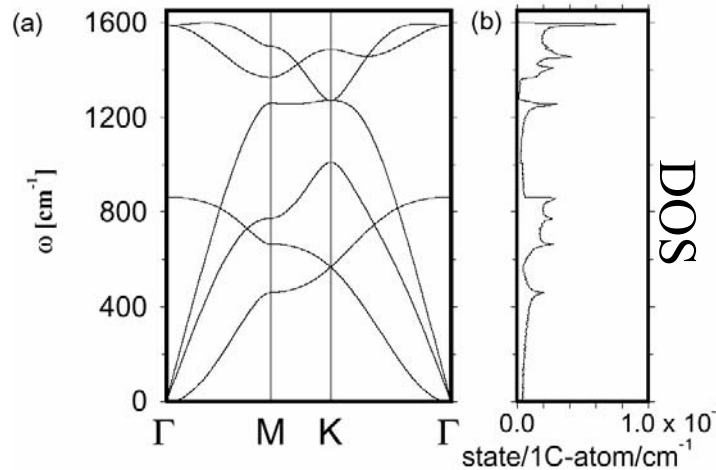


Predicts 7 strong Raman modes

Phonons in single wall carbon nanotubes

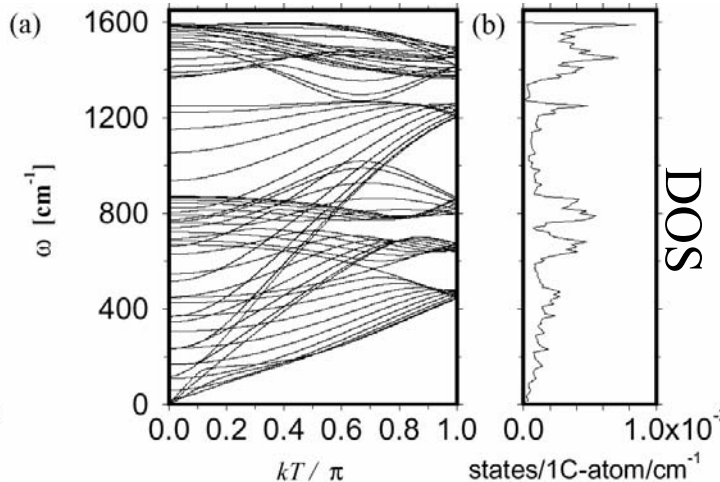
Main Features

Graphite Brillouin Zone



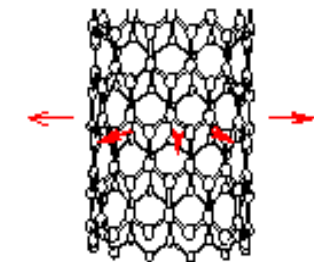
(Figs. From Prof. R. Saito)

(10,10) Brillouin Zone

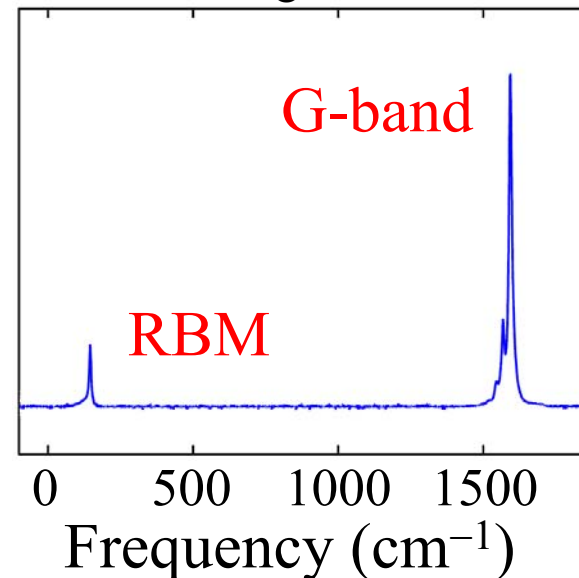


Zone folding of graphene sheet

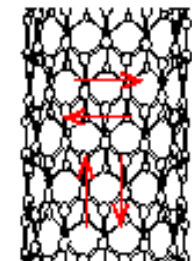
Radial
Breathing
Mode
(RBM)



SWNT signature



Tangential
Modes
(G-band)

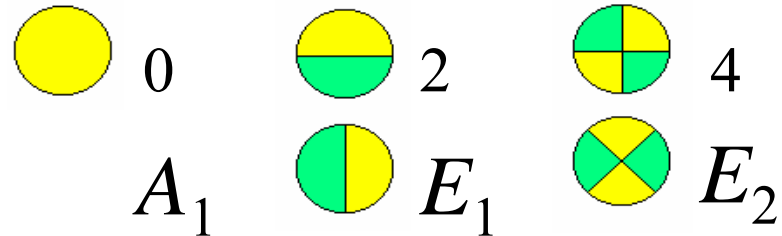


Raman Spectra of SWNTs:

Raman active modes:

- Chiral 15
- Zigzag 15
- Armchair
 - Even n 16
 - Odd n 15

Raman Active Modes



- Symmetry Requirements
 - Second-rank Tensor

$$x^2, xy, x^2 - y^2, 3z^2 - r^2, \text{etc}$$

$$\mathbf{P} = \sigma \mathbf{E}$$

σ : RamanTensor

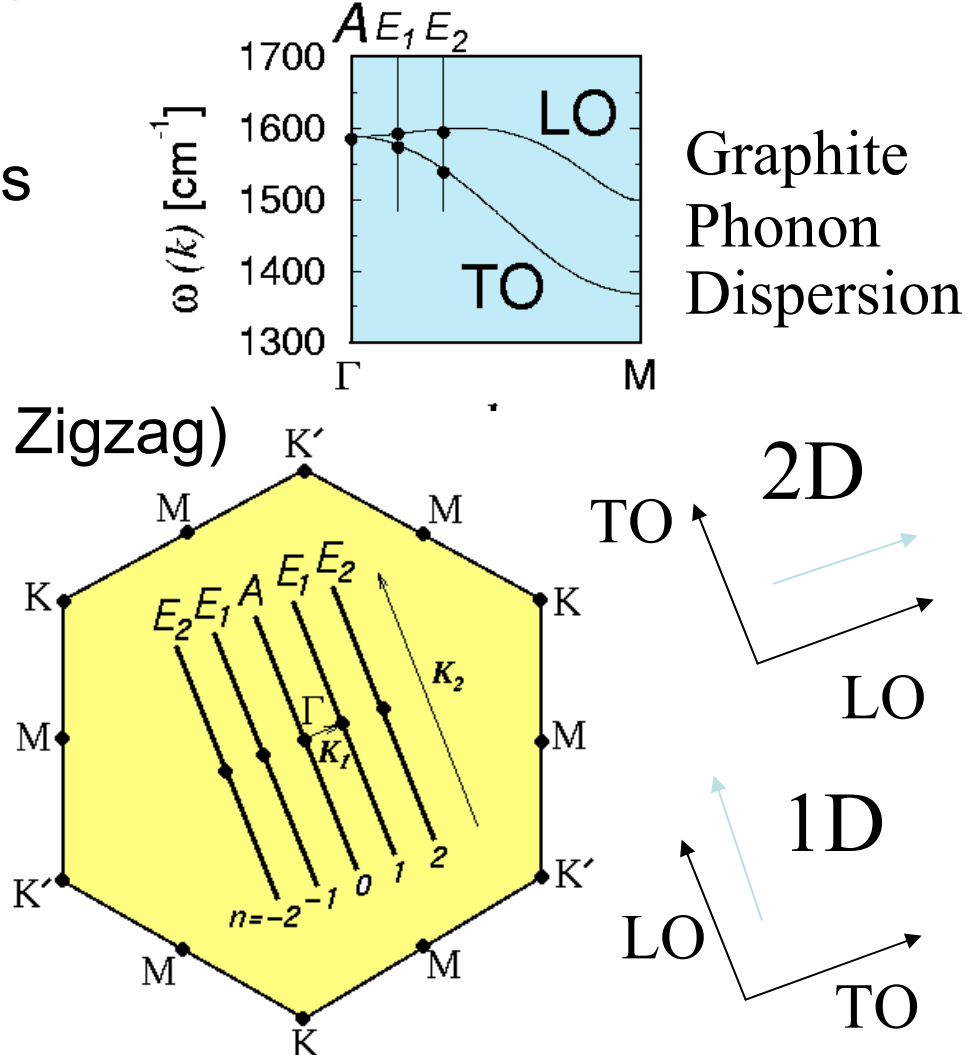
- 15 or 16 Raman Active Modes among $6N$ modes
 - No Node, 2 and 4 nodes (A_1 , E_1 , E_2) representations
 - In-phase and out-of-phase modes for A and B atoms

Nanotube structure	Point group	Raman-active modes	IR-active modes
armchair (n, n) n even	D_{nh}	$4A_{1g} + 4E_{1g} + 8E_{2g}$	$A_{2u} + 7E_{1u}$
armchair (n, n) n odd	D_{nd}	$3A_{1g} + 6E_{1g} + 6E_{2g}$	$2A_{2u} + 5E_{1u}$
zigzag $(n, 0)$ n even	D_{nh}	$3A_{1g} + 6E_{1g} + 6E_{2g}$	$2A_{2u} + 5E_{1u}$
zigzag $(n, 0)$ n odd	D_{nd}	$3A_{1g} + 6E_{1g} + 6E_{2g}$	$2A_{2u} + 5E_{1u}$
chiral (n, m) $n \neq m \neq 0$	C_N	$4A + 5E_1 + 6E_2$	$4A + 5E_1$

Zone-Folding & G-band Symmetry

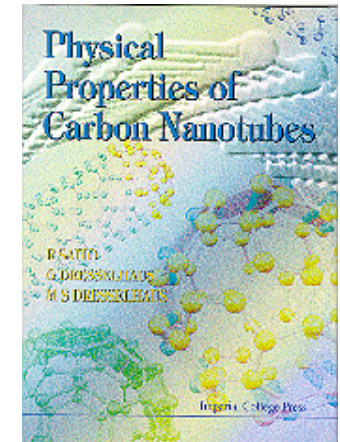
R.Saito *et al.* *Phys. Rev. B* **57** (1998) 4145

- Group Theory
 - $2A+2E_1+2E_2$ Raman Modes
 - 6 modes for chiral tubes
 - 3 modes for achiral tubes
 - A_{1g}, E_{1g}, E_{2g} (Armchair, Zigzag)
- 2D TO and LO modes
 - 1D LO and TO modes
- Curvature Effect
 - LO and TO vibrations



Outline

- Background
- Phonon Properties
- **Overview of Raman Effect**
- First-order Raman Processes
-(the RBM and G-Band)
- Double Resonance Processes
- Photoluminescence
- Excitons

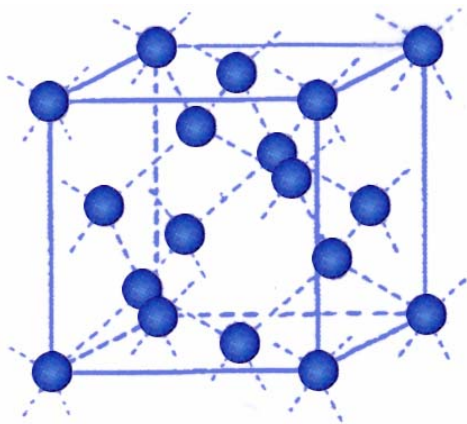


"Physical Properties of Carbon Nanotubes",
by R. Saito, G. Dresselhaus and M.S. Dresselhaus,
Imperial College Press (1998) ISBN 1-86094-093-5

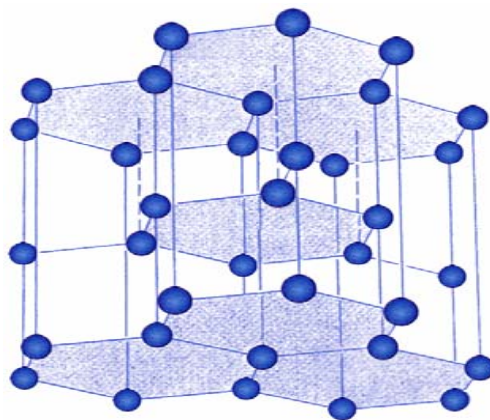
Raman Modes in Carbon Materials



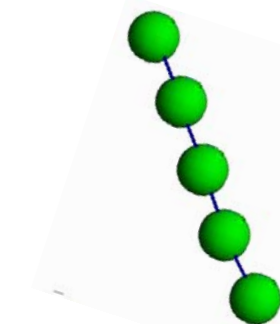
¿?



Diamond
 sp^3 (3D) 1332 cm⁻¹



Graphite
 sp^2 (2D) 1582 cm⁻¹

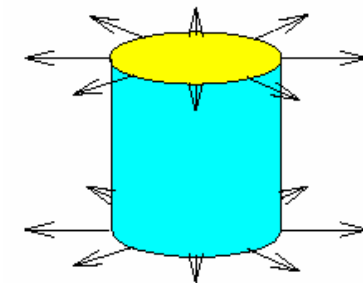


Chain
 sp^1 (1D) 1855 cm⁻¹

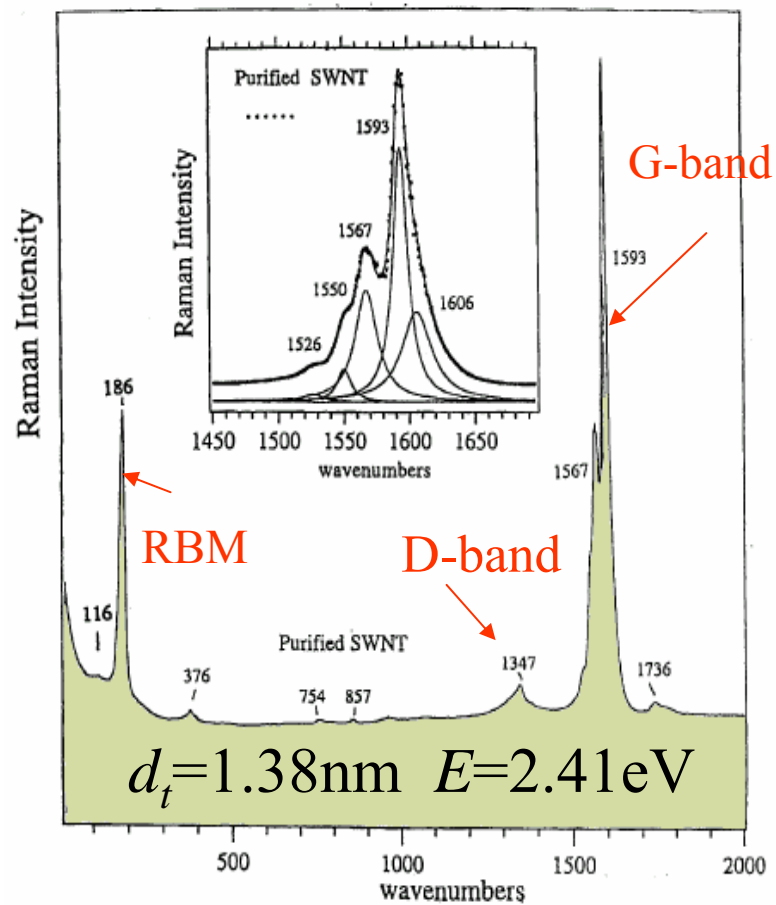
Carbon Mode Frequencies

Raman Signal of SWNTs

A.M. Rao et al, Science 275 (1997) 187



- Radial Breathing Mode
 - Observed up to 3nm in SWNTs and MWNTs
- D-band (1350 cm^{-1})
 - Resonant Nature
- G-band ($1530\text{-}1620\text{ cm}^{-1}$)
- G'-band (overtone of D)
- Other weak features



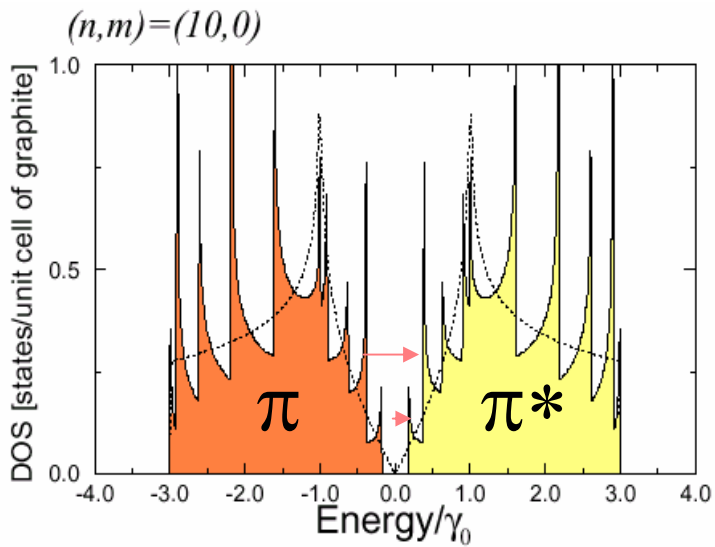
Resonance is diameter selective

Resonant Raman Spectroscopy (RRS)

A. M. Rao *et al.*, *Science* **275** (1997) 187

- Enhanced Signal

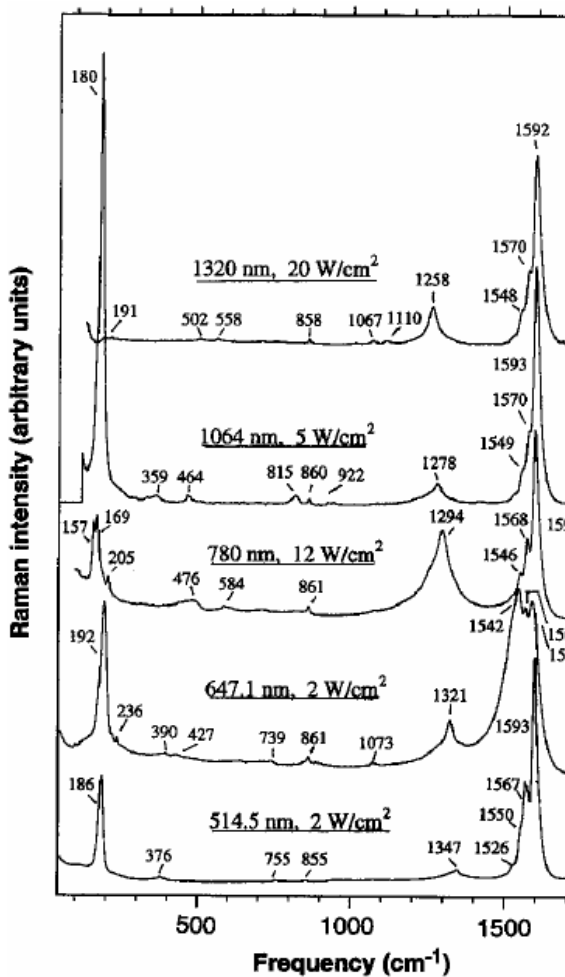
- ✓ Optical Absorption
- ✓ e-DOS peaks



diameter-selective resonance process

$$\omega_{\text{RBM}} = \alpha / d_t$$

Raman spectra from SWNT bundles



$$E = 0.94\text{eV}$$

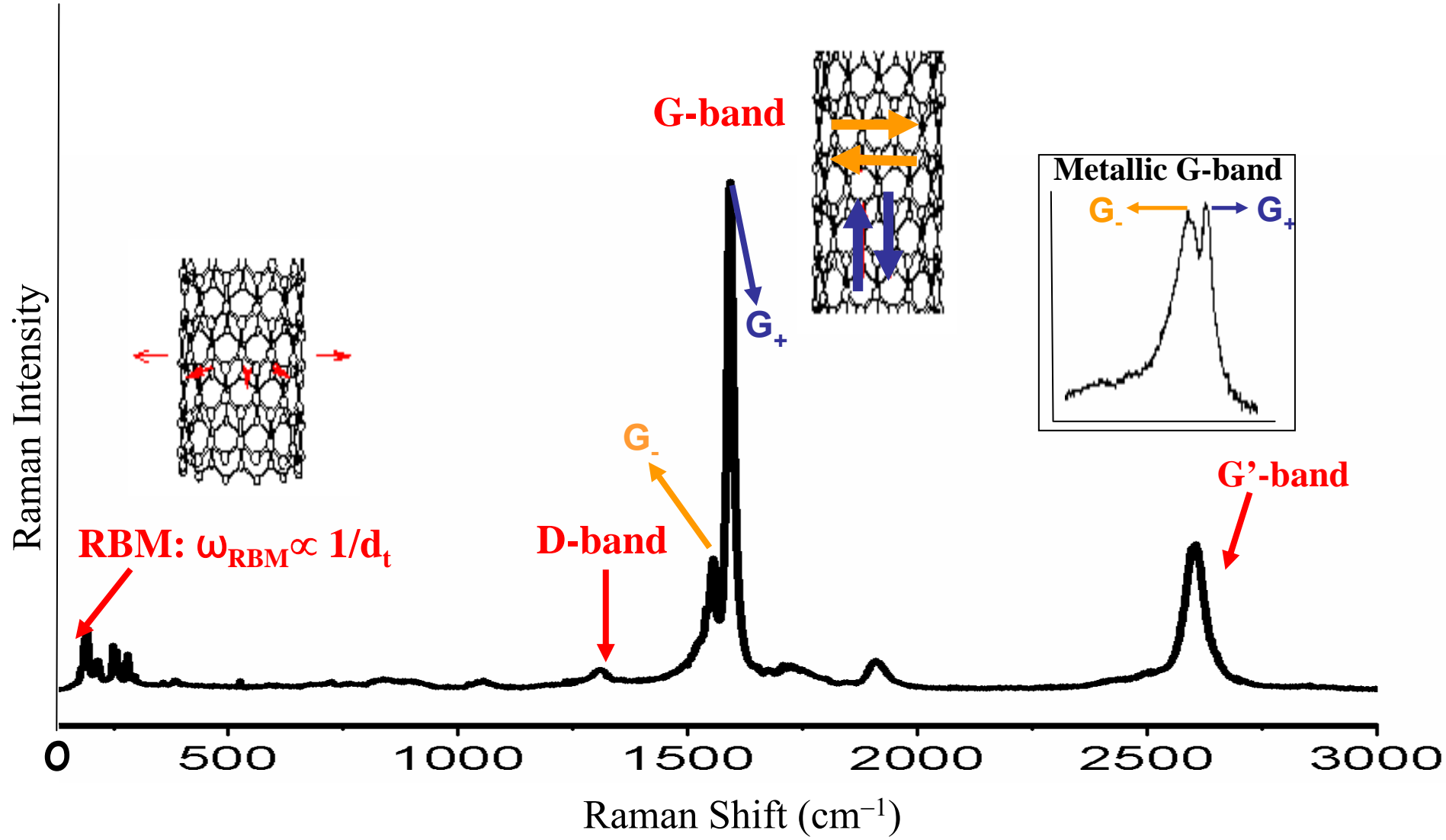
$$= 1.17\text{eV}$$

$$= 1.58\text{eV}$$

$$= 1.92\text{eV}$$

$$= 2.41\text{eV}$$

Raman Spectra of SWNT Bundles

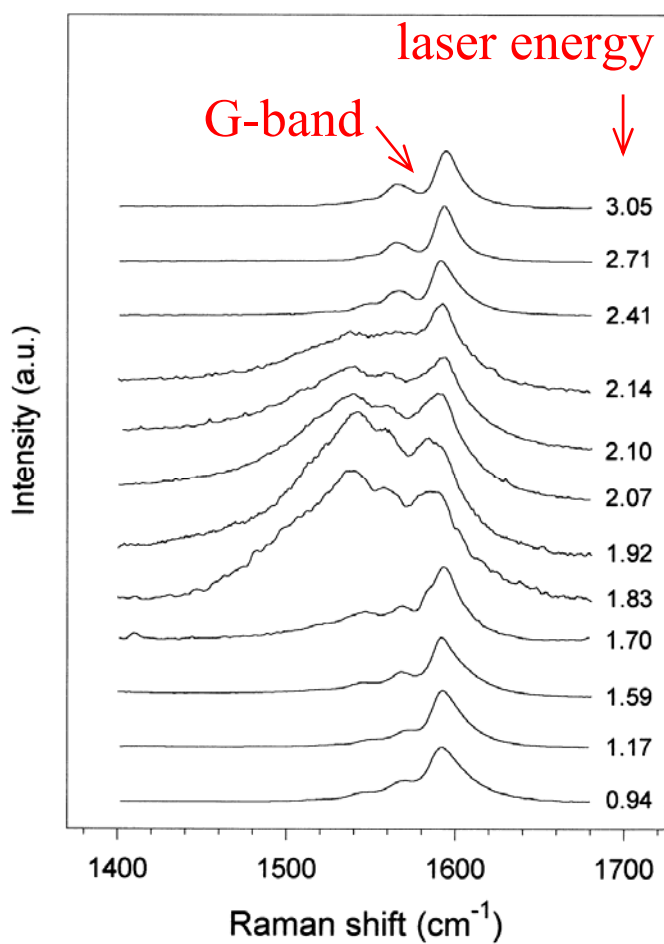


Radial breathing mode (RBM) and G-band are first-order processes

Distinguishing Metallic and Semiconducting Nanotubes

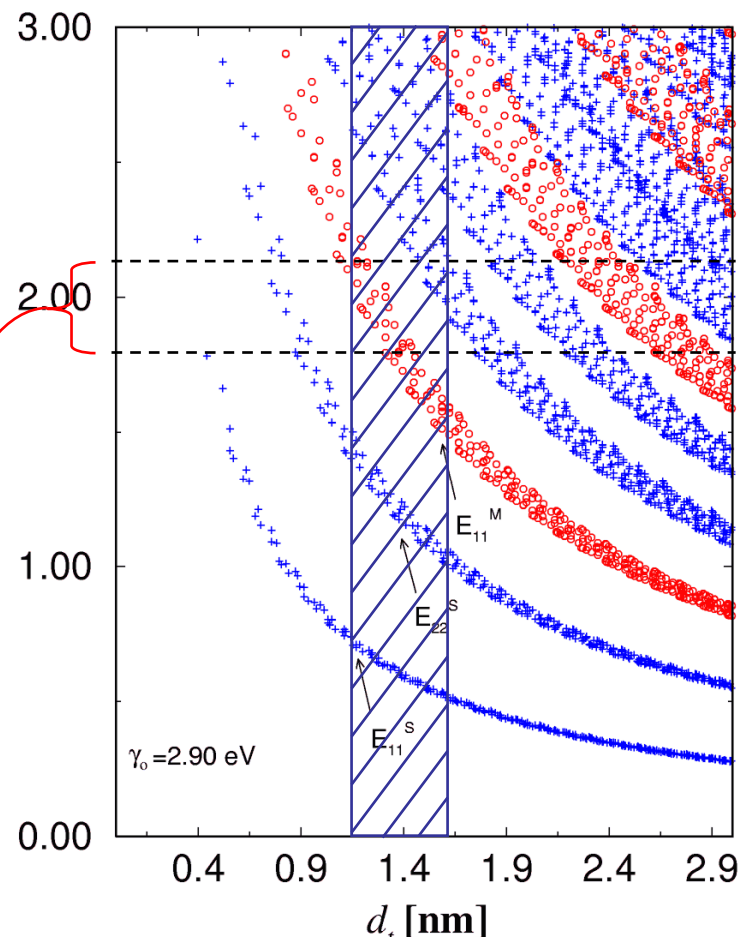
M. A. Pimenta *et al.*, *Phys. Rev. B* 58, R16016 (1998)

G-band resonant Raman spectra



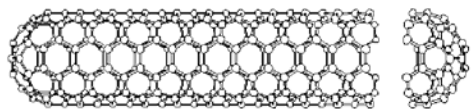
$$d_t = 1.37 \pm 0.18 \text{ nm}$$

Diameter dependence of the Van-Hove singularities

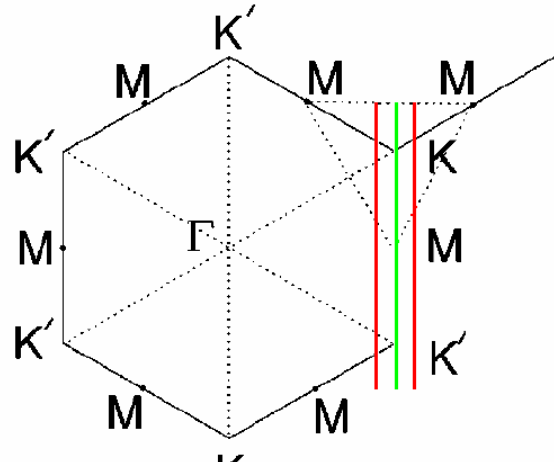
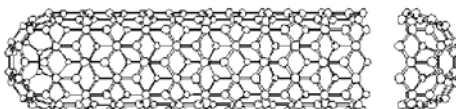


The DOS splitting depends on chirality through the trigonal warping effect

Armchair



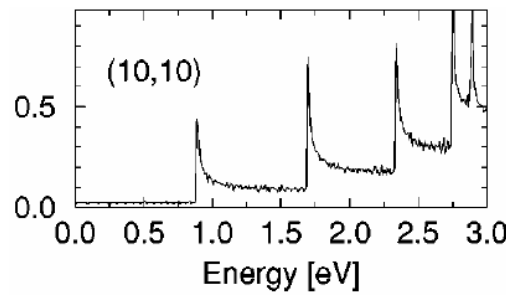
Zigzag



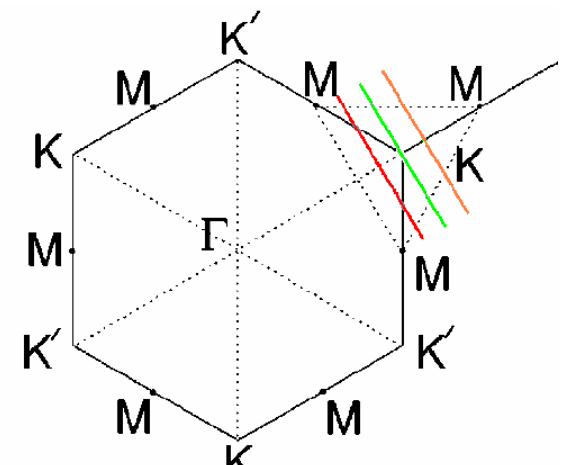
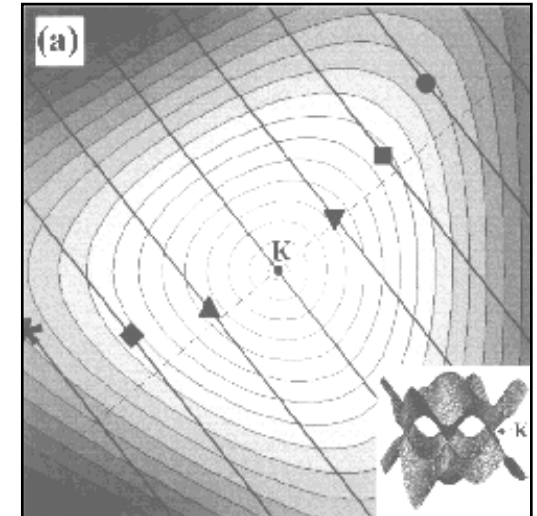
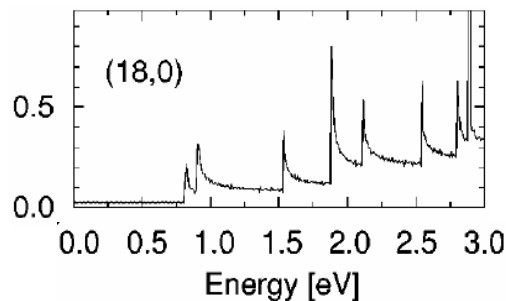
Armchair

No DOS Splitting

Armchair



Zigzag



Zigzag

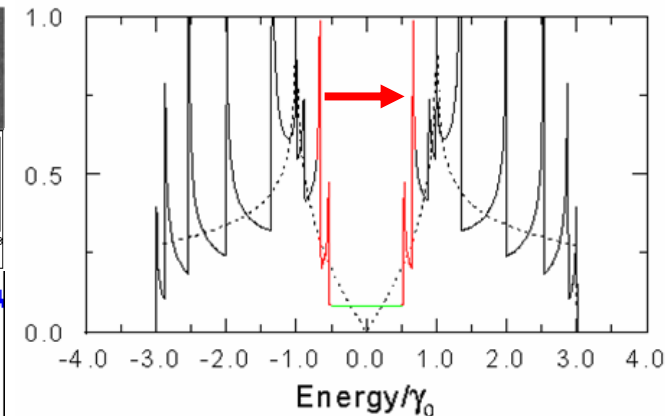
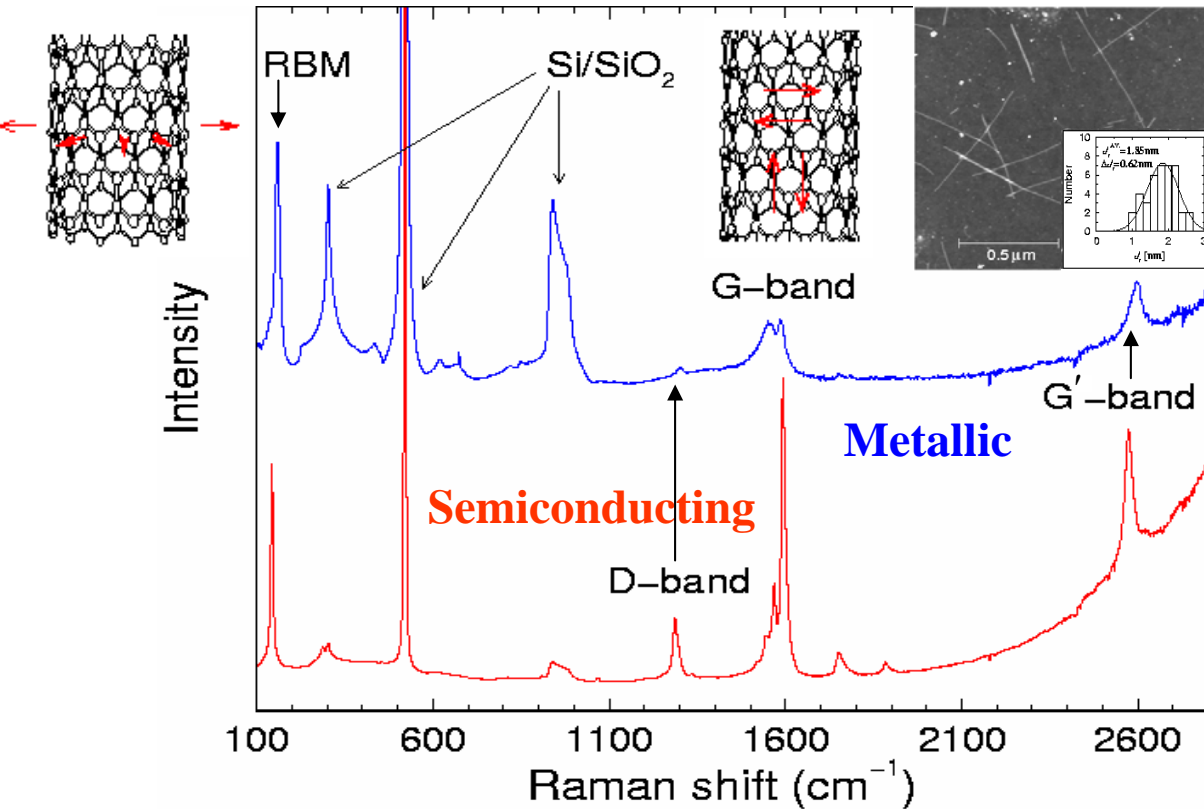
Max DOS Splitting

Single Nanotube Spectroscopy

Resonant Raman spectra for isolated single-wall carbon nanotubes grown on Si/SiO₂ substrate by the CVD method

A. Jorio et al., Phys. Rev. Lett. 86, 1118 (2001)

RBM



(n,m) identification

$$\omega_{\text{RBM}} = 248/d_t$$

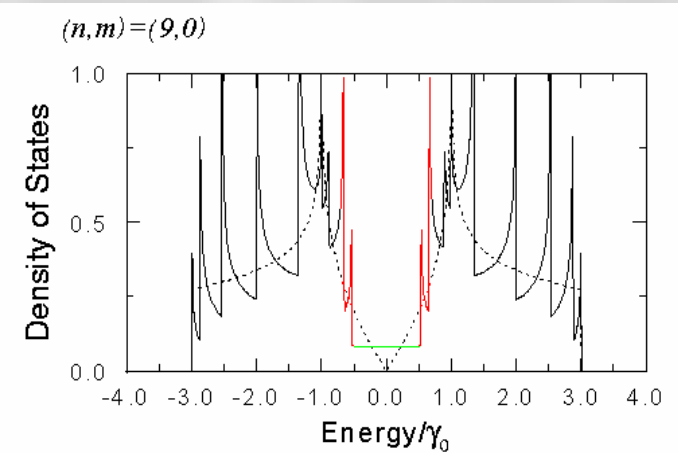
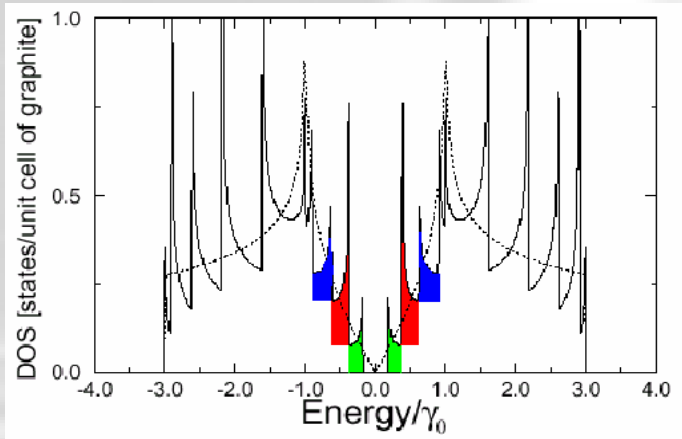
$$E_{ii} \approx E_{\text{laser}}$$

$$d_t \sim 1.5 \text{ nm}$$

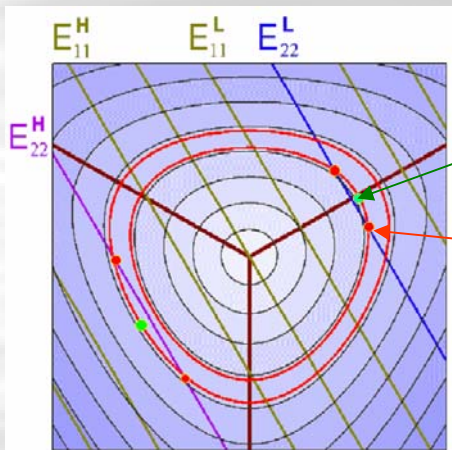
For isolated SWNTs on
Si/SiO₂

Raman signal from *one* SWNT indicates a strong resonance process in order to see Raman spectra at the single nanotube level

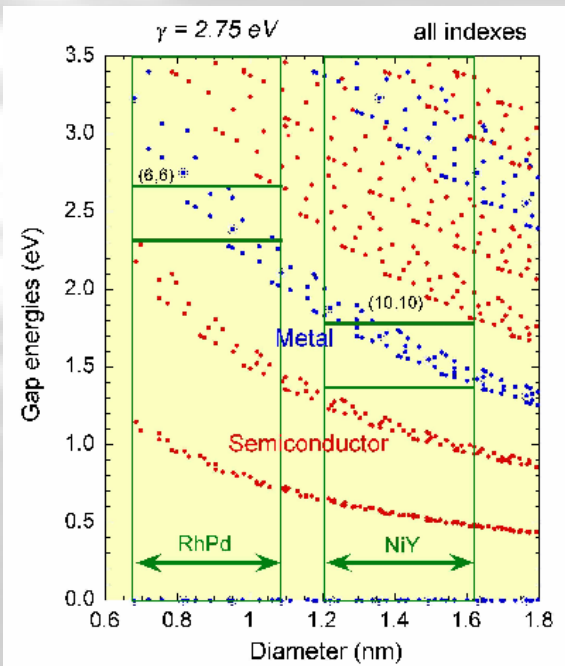
Electronic Density of States



Trigonal warping of constant energy contours



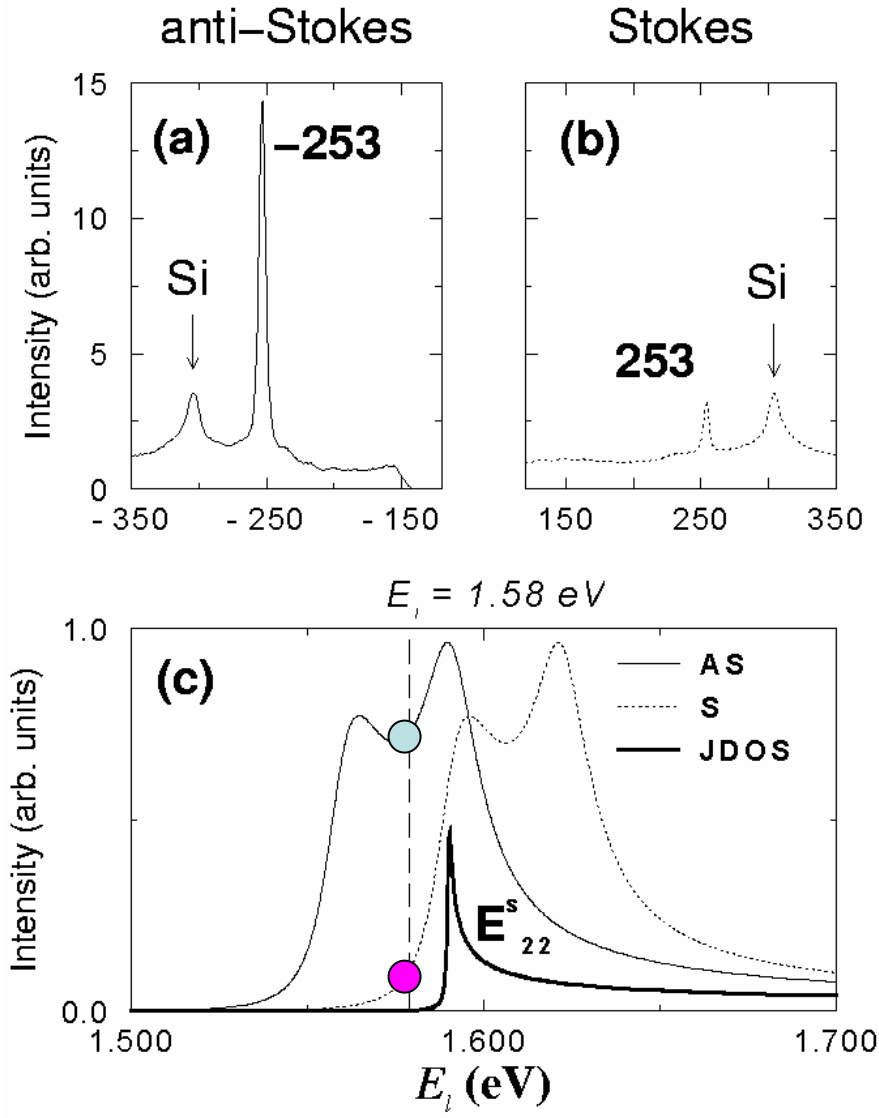
Kataura's Plot of $E_{ii}(d_t)$
H. Kataura et al., Synth. Metals,
103 2555 (1999)



Determination of (n,m) from Intensity Ratio of Anti-Stokes to Stokes

A. G. Souza-Filho *et al*, Phys. Rev. B63(2001)

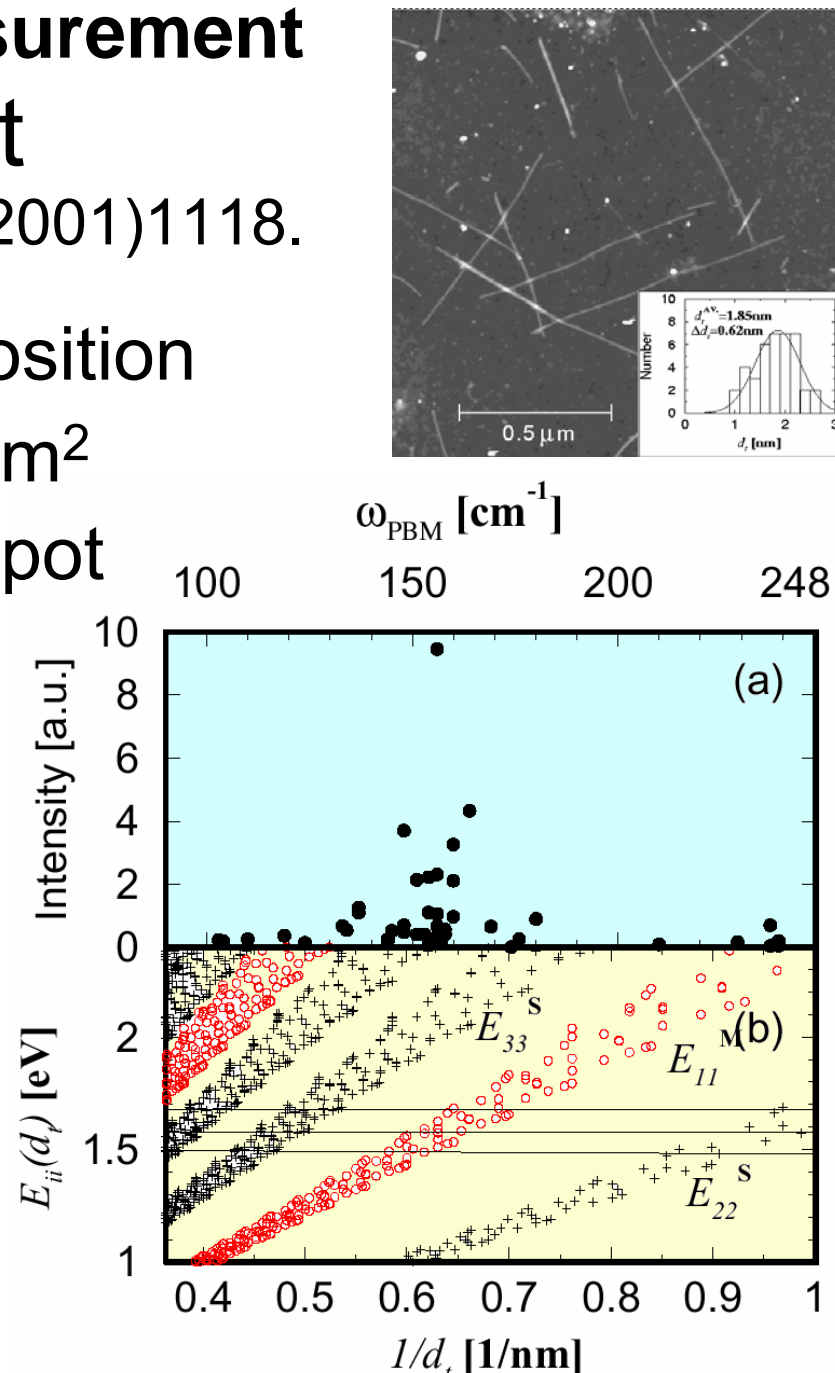
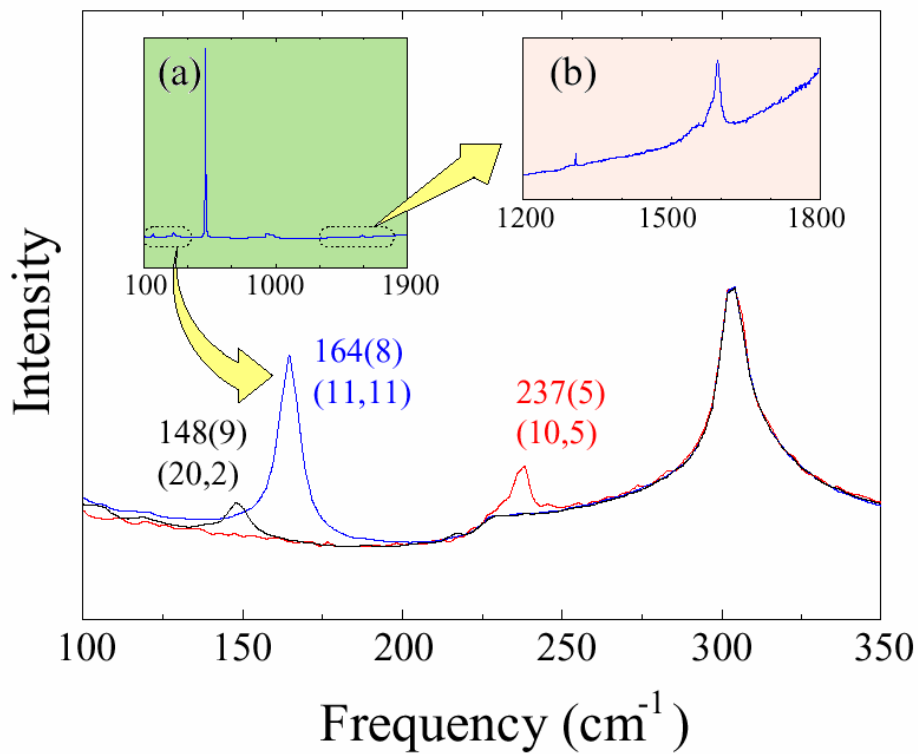
- Resonant Conditions
 - Incident light
 - Scattered light
 - Precise (n,m) Assignment
 - $(12,1), (11,3)$
 - $d_t = 0.98\text{nm}$, $\omega_{\text{RBM}}=253\text{cm}^{-1}$
 - $E_{22}^{\text{S(obs)}} = 1.587\text{eV}$
 - $E_{22}^{\text{S(cal)}} = 1.585, 1.564\text{eV}$
- $\gamma_0 = 2.89\text{eV}$ (12,1), (11,3)



Confocal Micro Raman Measurement (n, m) Assignment

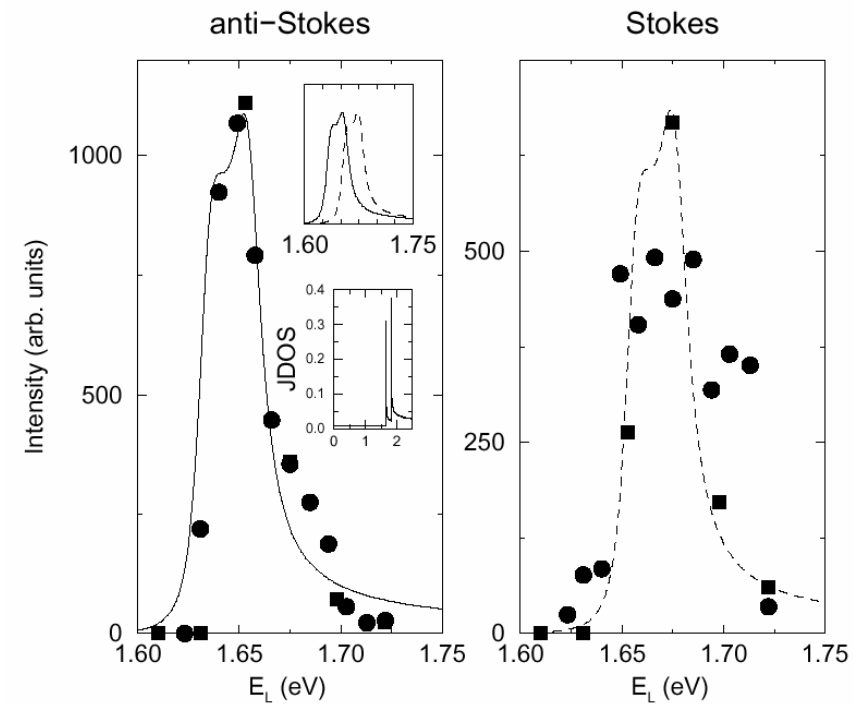
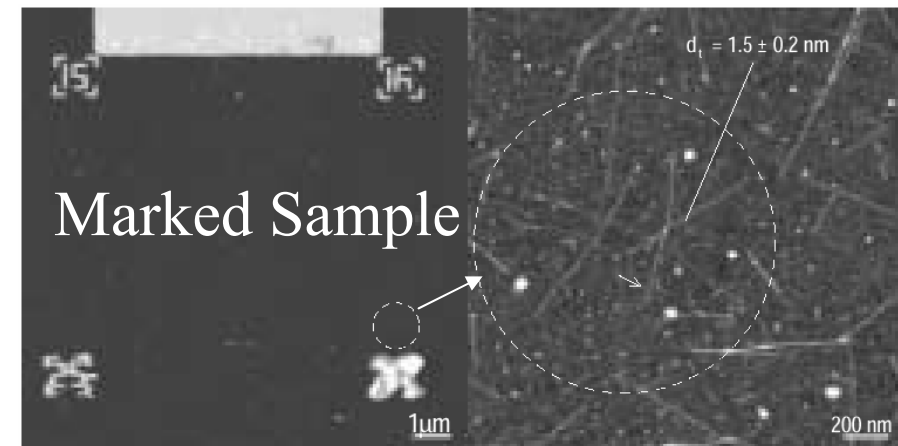
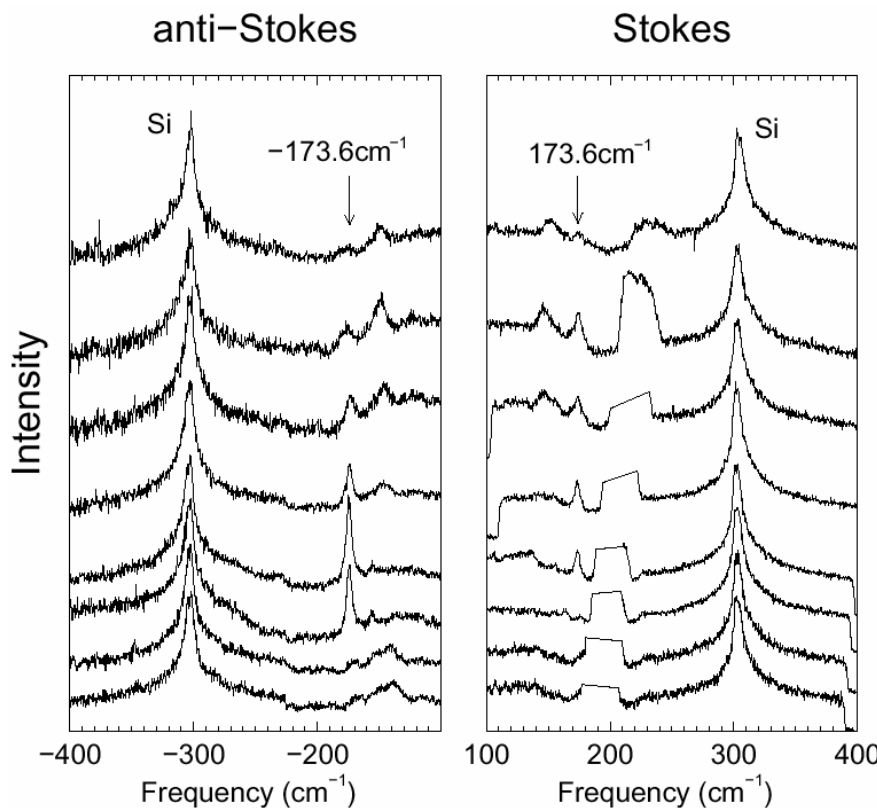
A. Jorio *et al.*, *Phys. Rev. Lett.* **86** (2001)1118.

- Carbon Vaporization Deposition
 - 6 SWNTs on Si/SiO₂ / μm^2
 - 1/10 resonant SWNT/ spot



Resonant Raman Spectra with Tunable Laser

A. Jorio et al, PRB **63**, 245416 (2001)

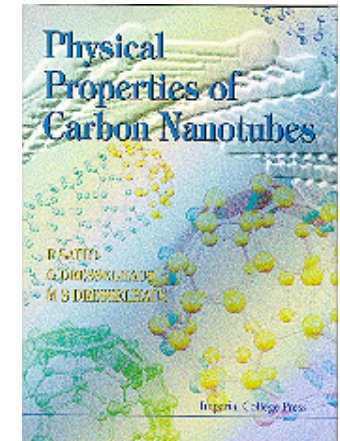


See Menendez et al PRB **65**, 201402 (2002)

(18,0) zigzag metallic nanotube
 $E_{ii}^M = 1.655 \text{ eV}, 173.6 \text{ cm}^{-1}$

Outline

- Background
- Phonon Properties
- Overview of Raman Effect
- **First-order Raman Processes**
 - (the RBM and G-Band)
- Double Resonance Processes
- Photoluminescence
- Excitons

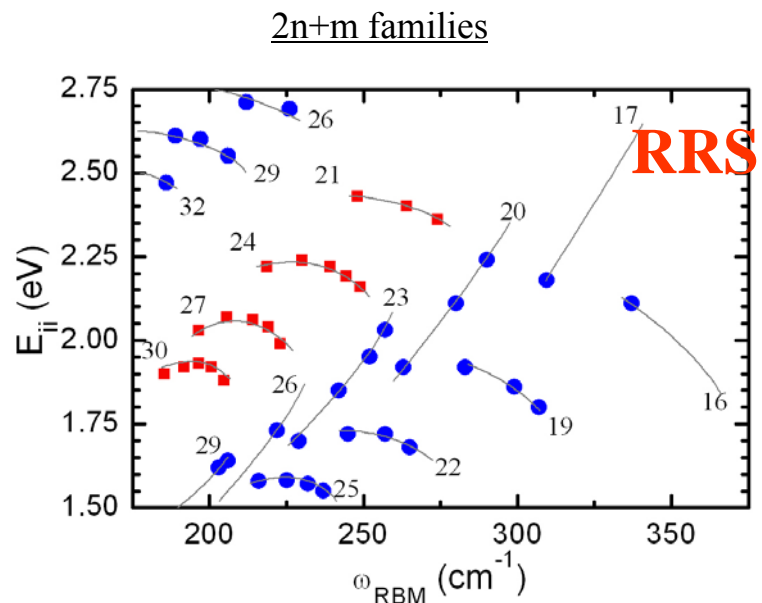


"Physical Properties of Carbon Nanotubes",
by R. Saito, G. Dresselhaus and M.S. Dresselhaus,
Imperial College Press (1998) ISBN 1-86094-093-5

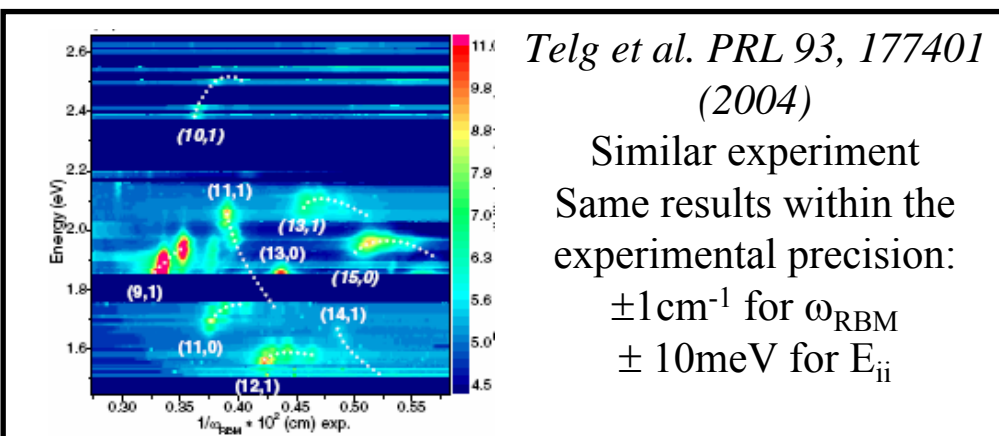
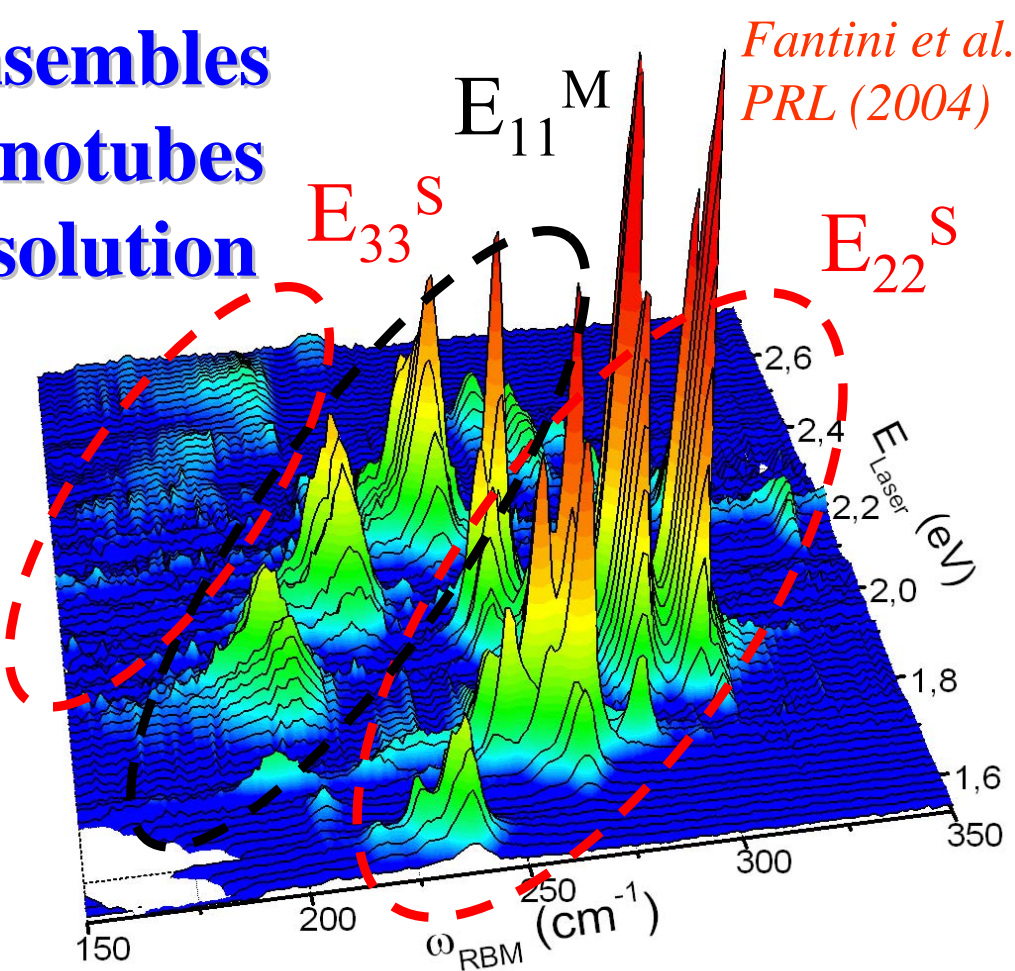
Radial Breathing Mode

- (n,m) identification
- Resonance window
- Making Kataura plots and diameter determination
- Analysis of (n,m) SWNTs in your sample
- Evaluation of parameters important for nanotube synthesis
- Evaluation of effectiveness of (n,m) separation process
- Evaluation of environmental effects

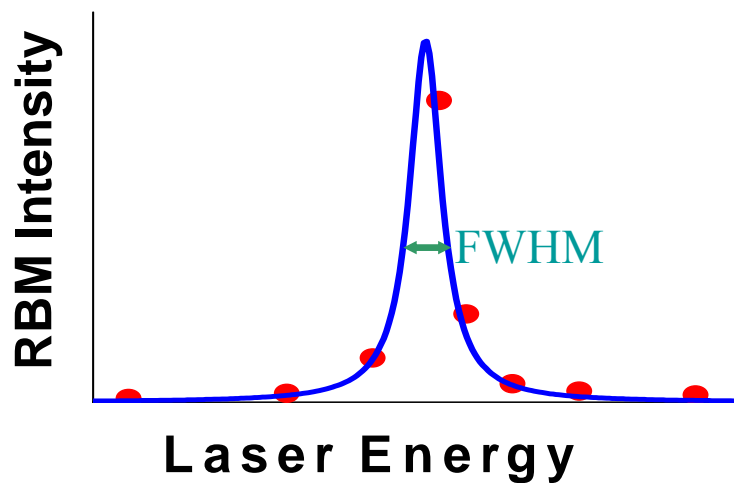
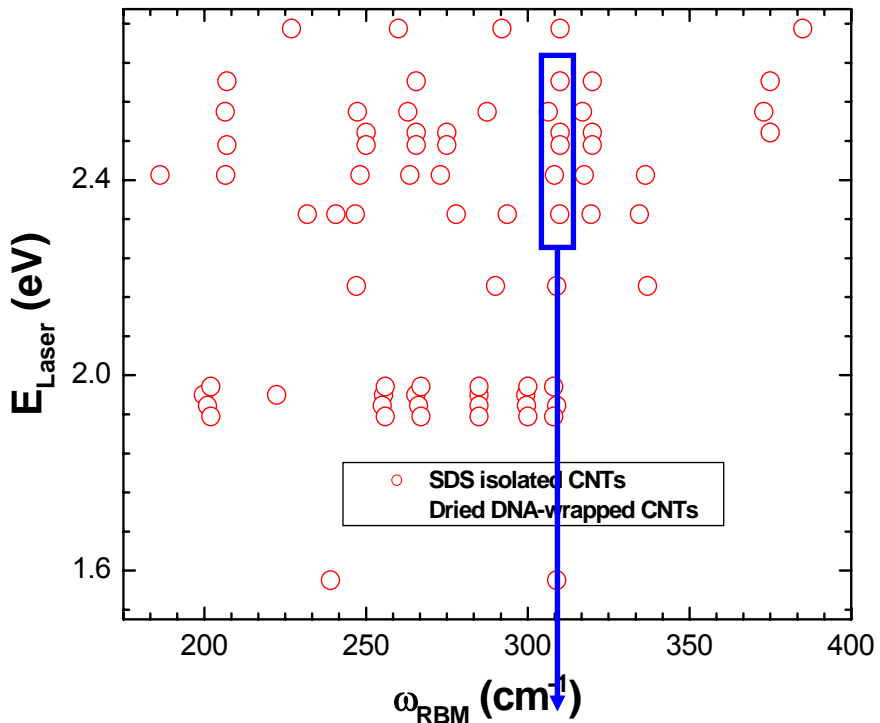
(n,m) identification for ensembles of SWNTs, e.g., HiPco Nanotubes wrapped in (SDS) and in solution



From E_{ii} vs ω_{RBM} and the relation $\omega_{RBM} \approx 218.3/d_t + 15.9 \text{ cm}^{-1}$
We obtain the Kataura plot of E_{ii} vs d_t for small diameter tubes



Resonance Window Measurements

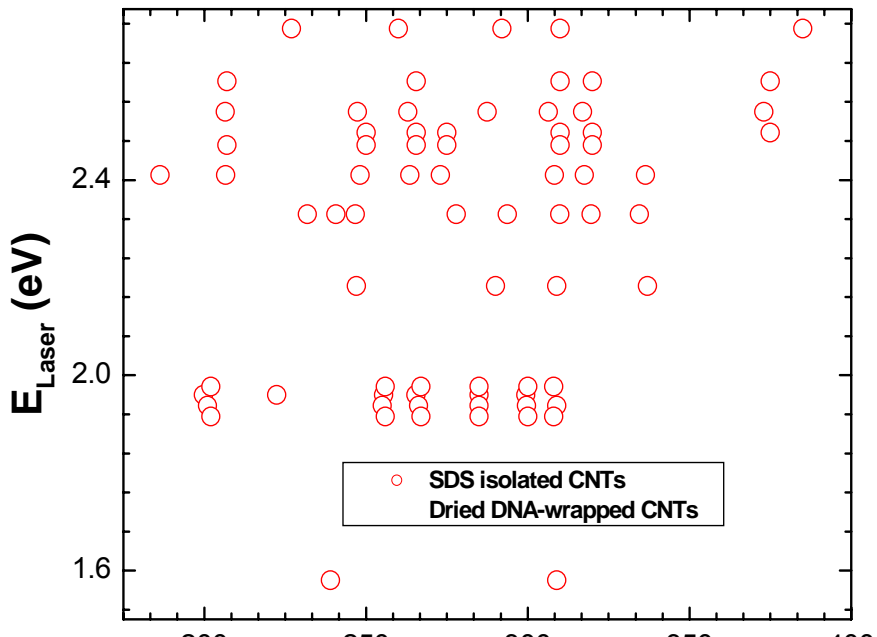


- Closely spaced E_{laser} provide information about the width of resonance window.
- Stokes and anti-Stokes profiles give E_{ii}

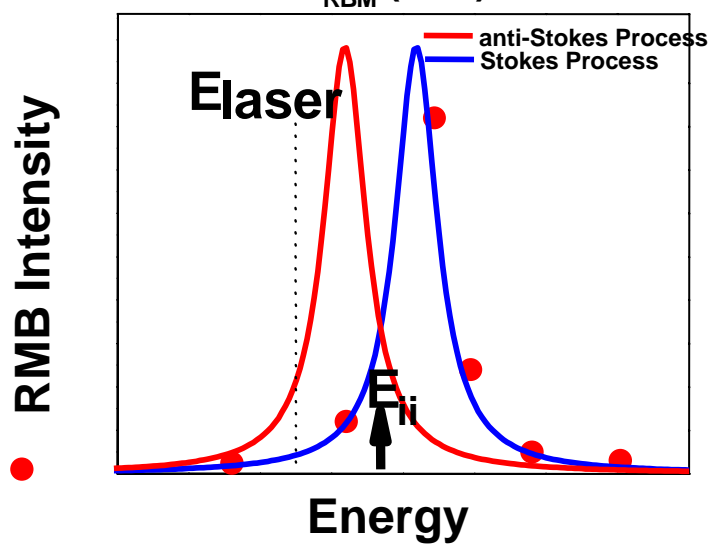
Widths of Resonance Windows:

- Isolated SWNTs on substrate: <10meV
- SDS-wrapped SWNTs in solution: 60meV
- Bundled SWNT: ~100meV
- Dried DNA-wrapped SWNTs: 15meV

Resonance Window Measurements



- Closely spaced E_{laser} provide information about the width of resonance window.
- Stokes and anti-Stokes profiles give E_{ii}



Widths of Resonance Windows:

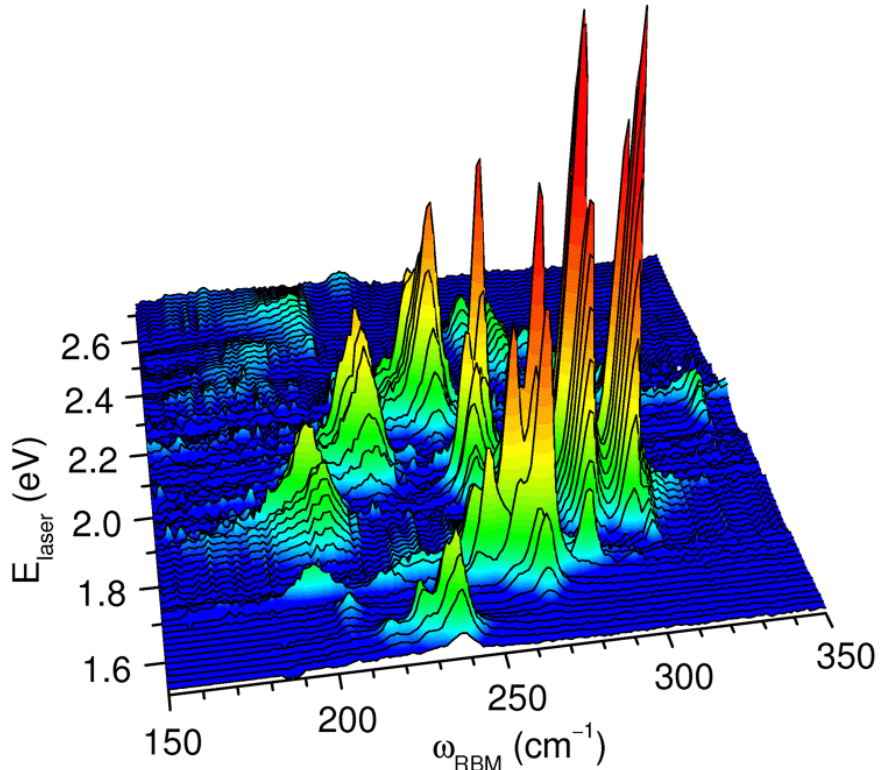
- Isolated SWNTs on substrate: <10meV
- SDS-wrapped SWNTs in solution: 60meV
- Bundled SWNT: ~100meV
- Dried DNA-wrapped SWNTs: 15meV

Challenges for Carbon Nanotube Synthesis

- Control synthesis process to produce tubes with same diameter and chirality (n,m)
- Until control of synthesis process is achieved, develop effective separation methods:
 - ✓ metallic from semiconducting
 - ✓ by diameter
 - ✓ by chirality
- Develop method for large-scale, cheap synthesis
- Improve nanotube characterization and manipulation
- Develop commercial scale applications

RAMAN (RRS) MAPS

Possible if many laser lines are available



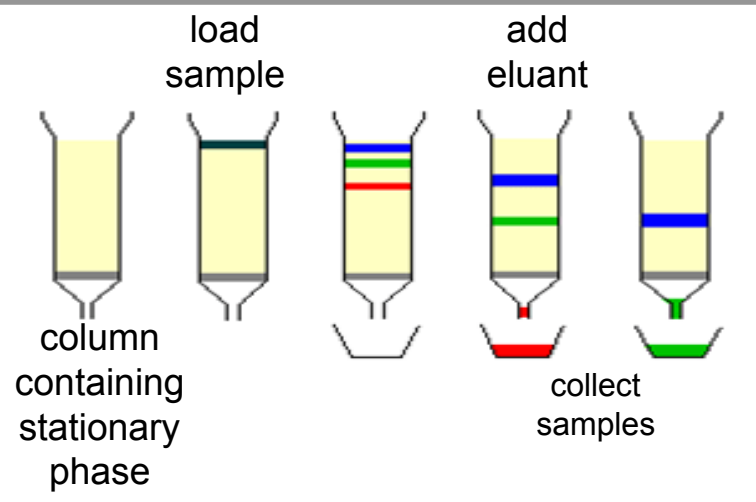
- Allows determination of (n,m) SWNTs in your sample using calculated cross section for each (n,m) SWNT,
- Determines Kataura plot E_{ii} vs d_t
- Determines the number of each (n,m) species in your sample
- Allows study of environmental effects

Data taken on SDS (sodium dodecyl sulfate) wrapped SWNTs

Evaluate Efficiency of DNA Wrapping Agent for M/S and (n,m) Separation

DNA-Assisted SEPARATION

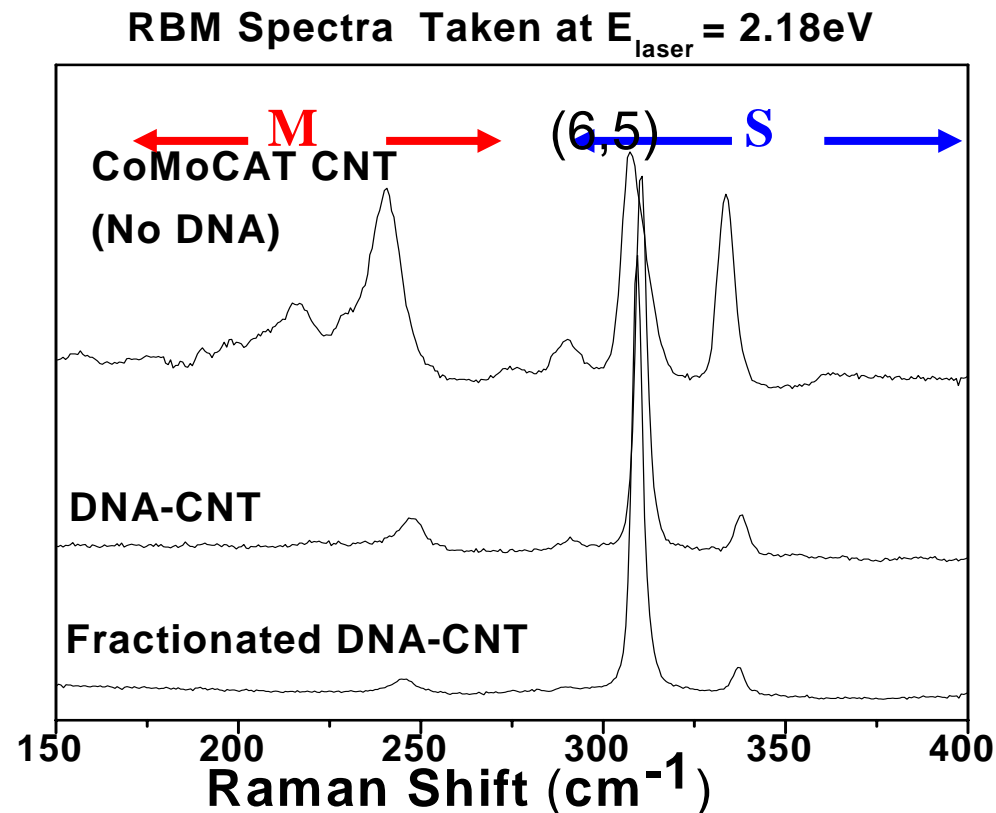
M. Zheng *et al.*, *Science*,
302, 1546 (2003).



Ion-exchange chromatography (IEC)

Hybrid DNA-SWNTs:

- M-SWNTs have different surface charge density, higher polarizability, and elute before S-SWNTs



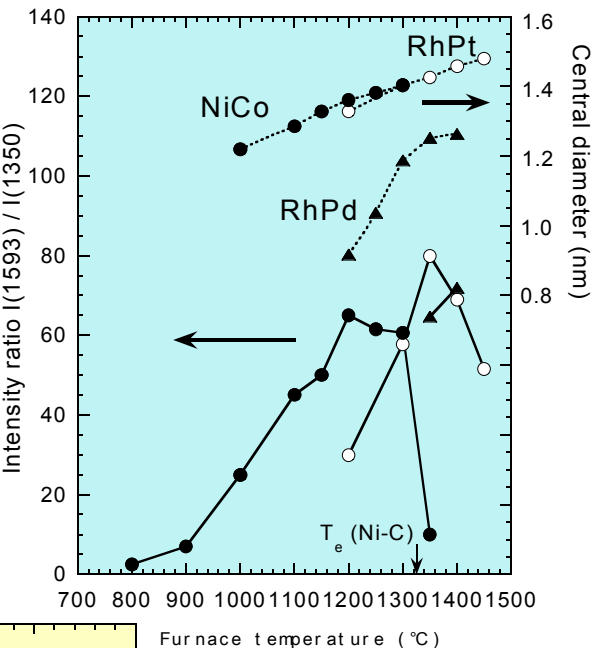
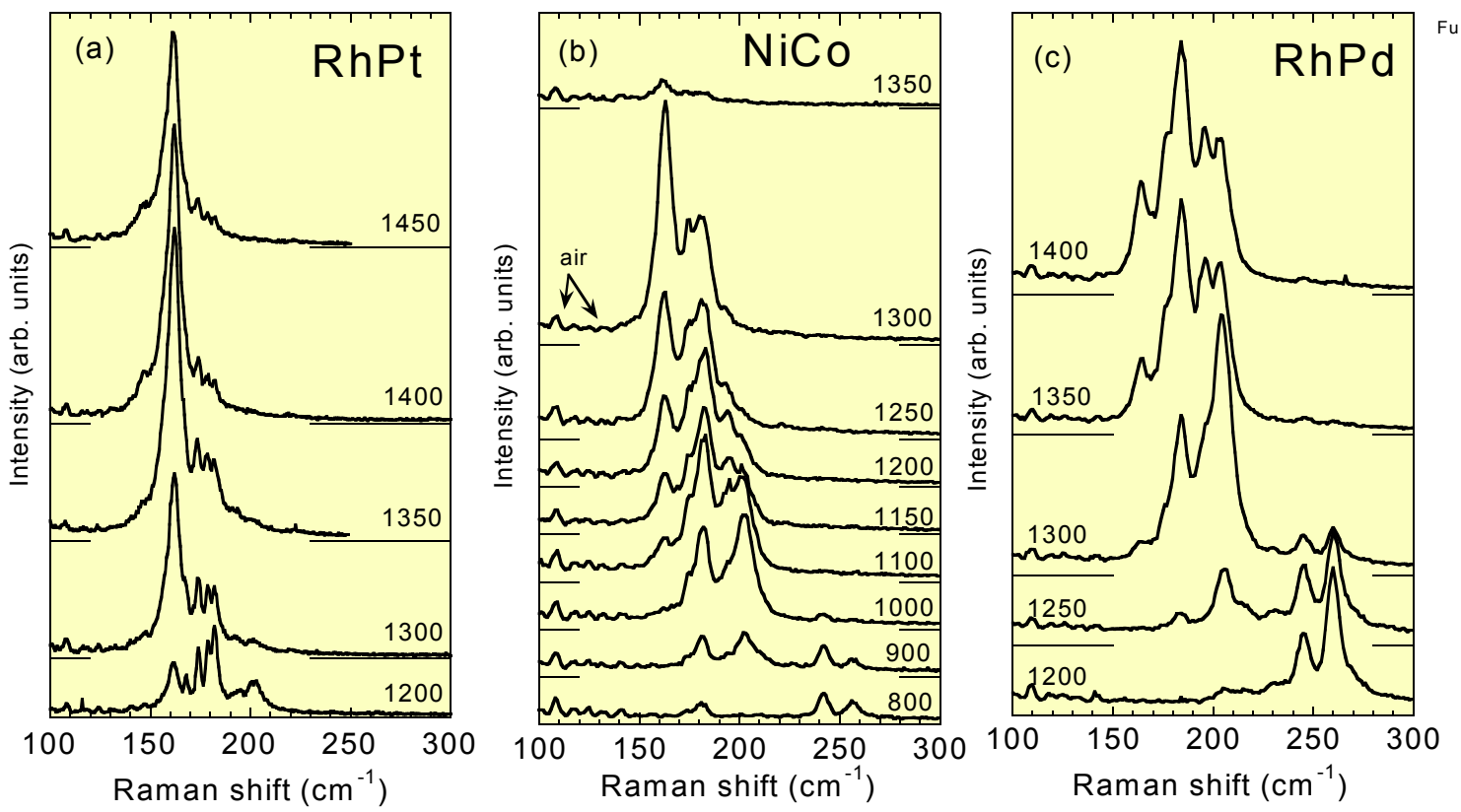
Separations

- by metallic vs semiconducting tubes
- by (n,m) values

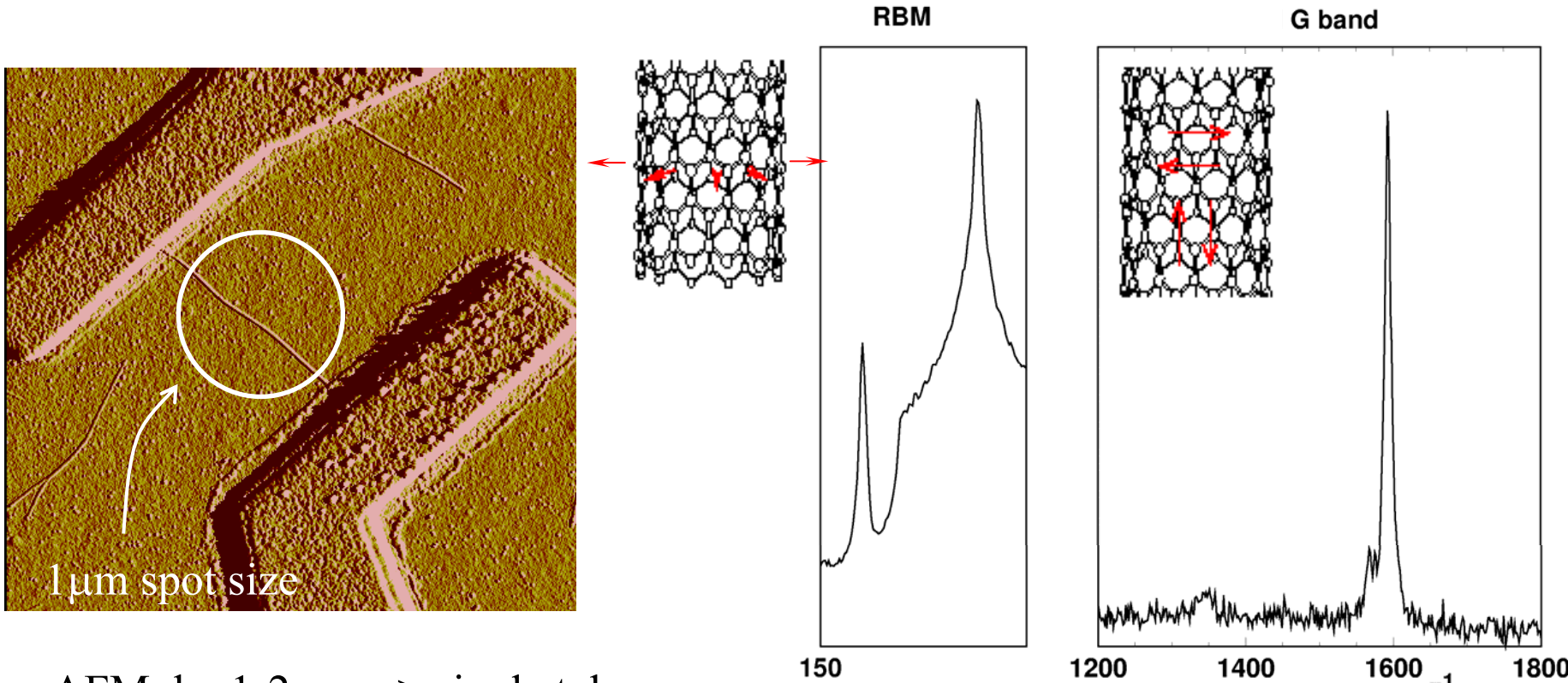
Raman used as early diagnostic for Diameter Control of SWNTs

H. Kataura *et al.*, Carbon 38, 1691 (2000)

- Variation of Catalysts and Furnace temperature



Raman Spectra and Transport for One SWNT New Research Directions for RRS



- AFM $d_t = 1\text{-}2\text{nm}$ \Rightarrow single tube.
- No voltage applied to sample during Raman Spectroscopy.

$$\omega_{\text{RBM}} = \frac{248}{d_t}$$

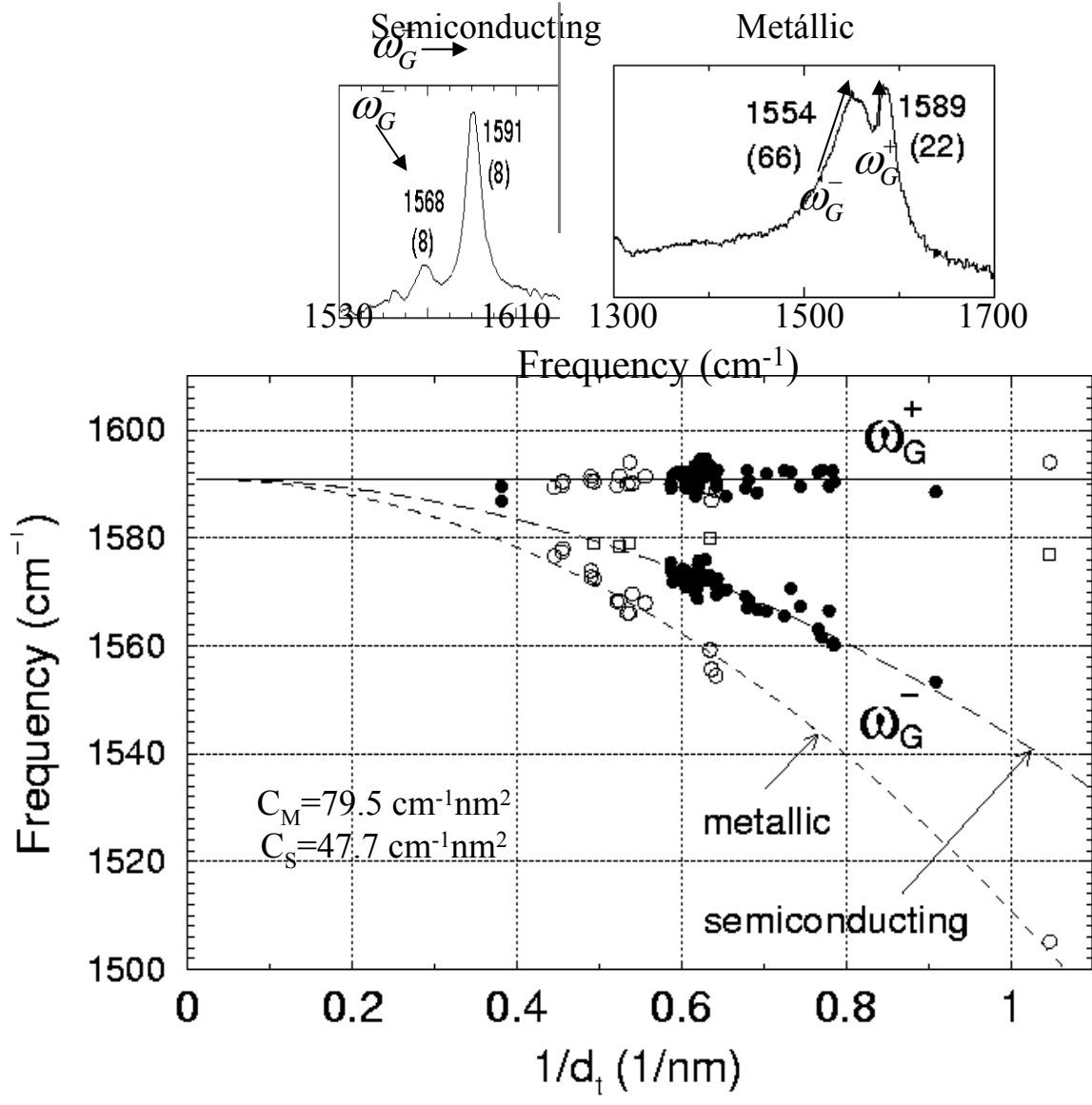
$$\omega_{\text{RBM}} = 185 \text{ cm}^{-1} \Rightarrow d_t = 1.34 \text{ nm}$$

S. B. Cronin *et al.*, *Appl. Phys. Lett.* **84**, 2052 (2004)

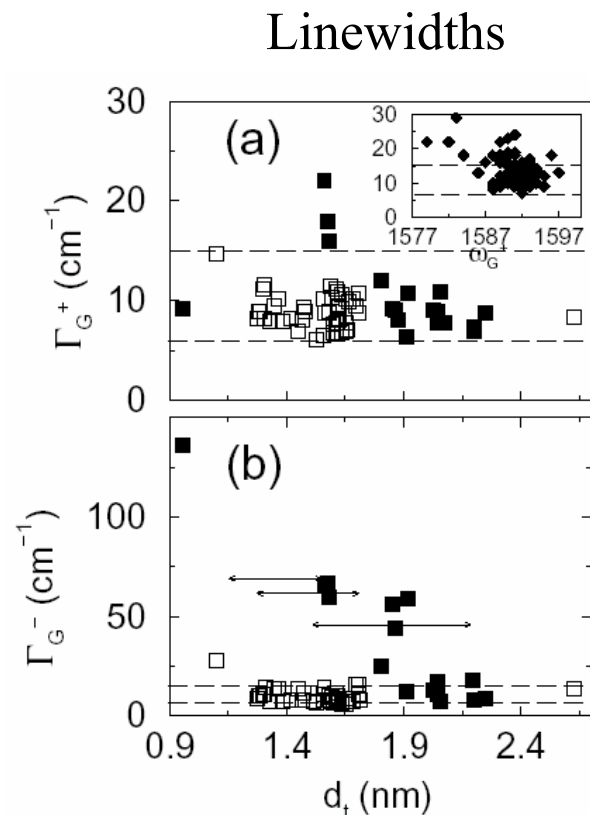
Properties of G-band Spectra

- Characteristic lineshape
- Linewidth for G^+ and G^-
- Diameter dependence
- Polarization effect for semiconducting SWNTs
- Breit-Wigner-Fano lineshapes for metallic tubes

Diameter dependence of the G mode frequencies from spectra at the single nanotube level



$E_{\text{laser}} = 1.58, 2.41, 2.54 \text{ eV}$

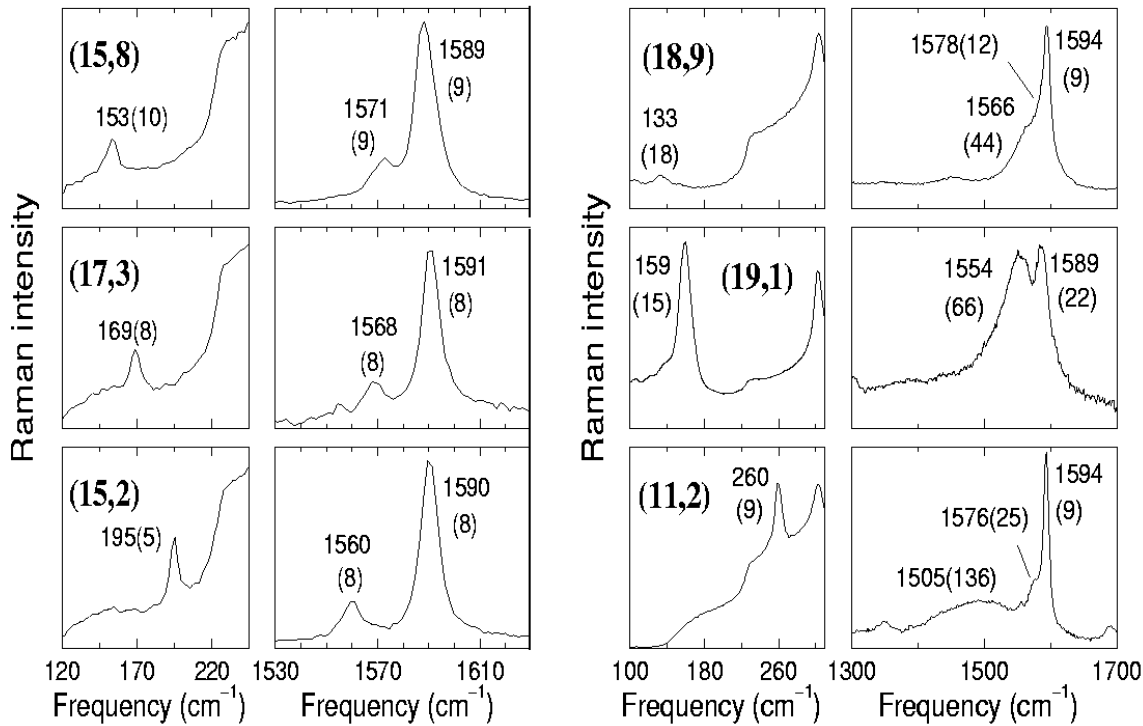
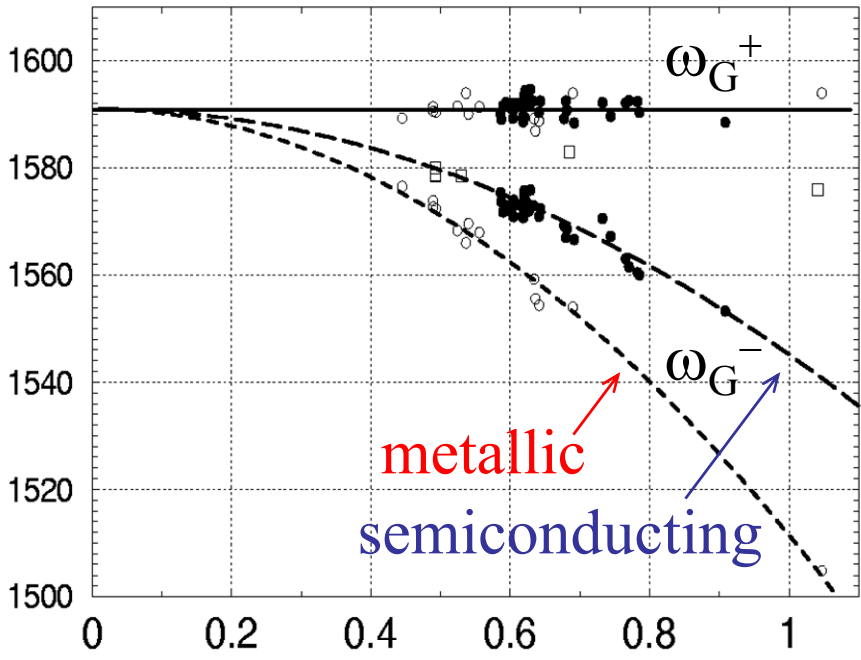


- Γ_G down to 5 cm^{-1}
- Γ_{BWF} depends on d_t

G-band frequency dependence on tube diameter

A. Jorio *et al.*,
Phys. Rev. B
 65, 155412 (2002)

Frequency (cm^{-1})



RBM G band
Semiconducting

RBM G band
Metallic

$$\omega_G^+ \sim 1591 \text{ cm}^{-1}$$

$$\omega_G^- = \omega_G^+ - C/d_t^2$$

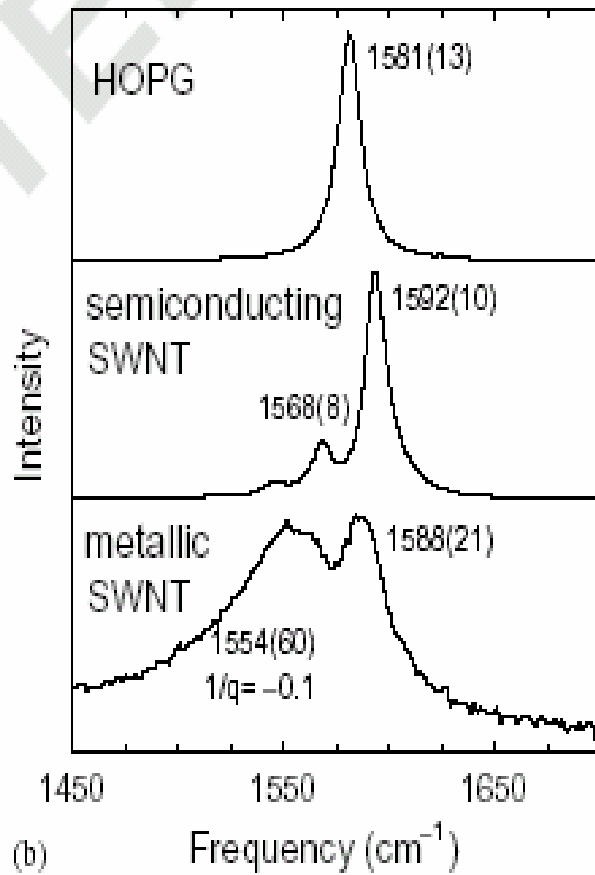
$$C_S = 47.7 \text{ cm}^{-1} \text{ nm}^2$$

$$C_M = 79.5 \text{ cm}^{-1} \text{ nm}^2$$

Selection rules in the Raman spectra of Nanotubes

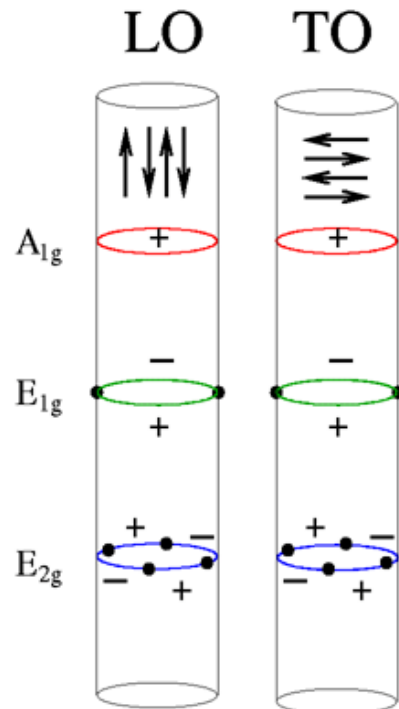
Tangential modes (G-band)

Polarization analysis is best done
for semiconducting SWNTs



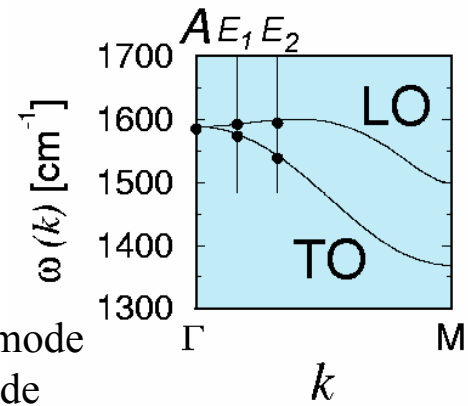
(b) Pimenta et al., PRB 58 R16016 (1998)

Selection rules:
6 Raman active modes



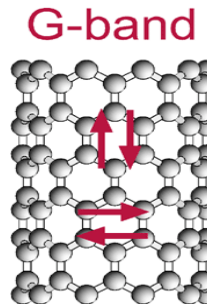
Group Theory

basis function	D _{nd}	D _{nh}	D _{NΩ}
(x ² +y ²), z ²	A _{1g}	A _{1g}	A
xz, yz	E _{1g}	E _{1g}	E ₁
(x ² +y ²), xy	E _{2g}	E _{2g}	E ₂



LO – longitudinal phonon mode
TO – transverse phonon mode

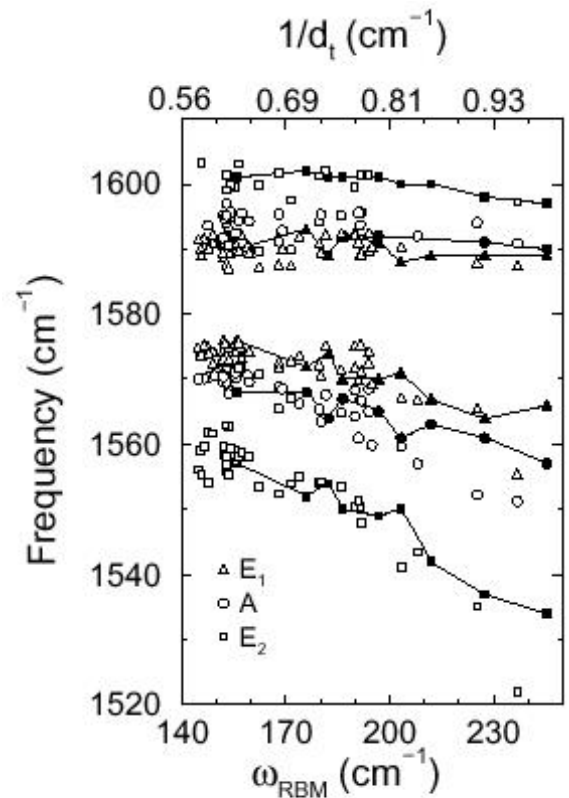
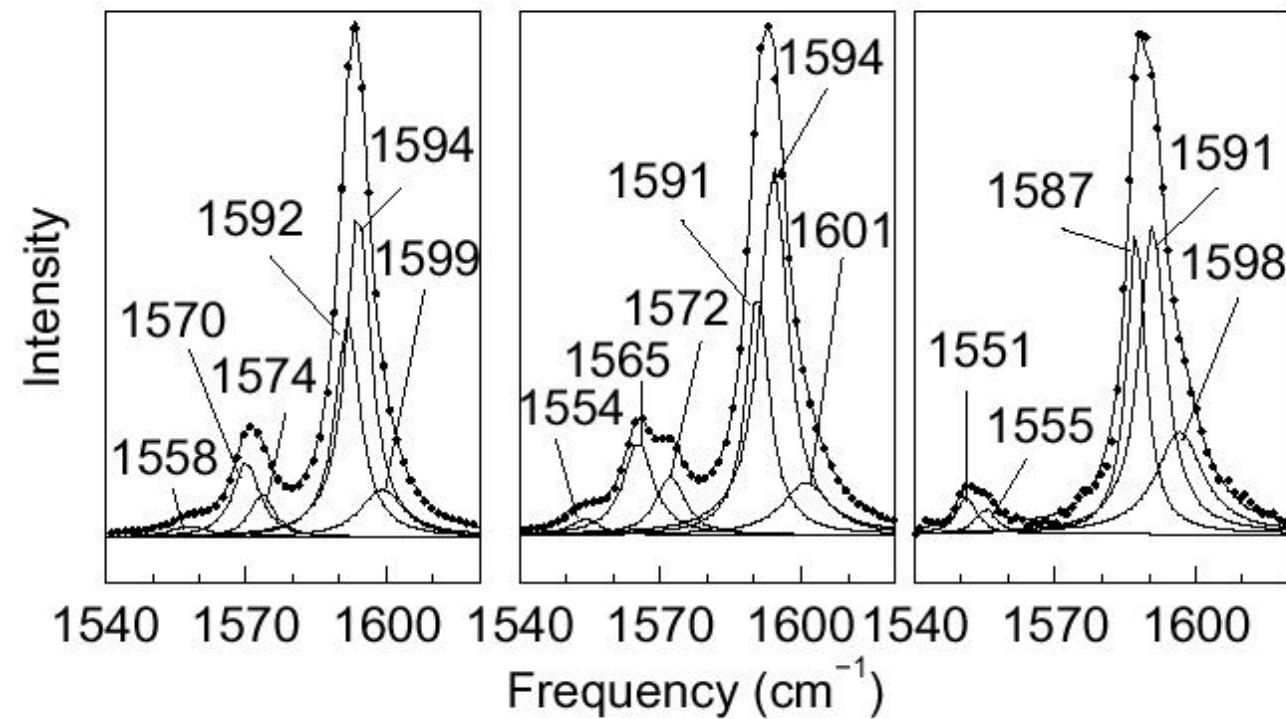
A. Jorio et al., Phys. Rev. Letters 85, 2617 (2000)



G band for isolated SWNTs

- 6 peaks are usually necessary for a good G-band fit
- ω_G vs d_t in agreement with *ab initio* calculations

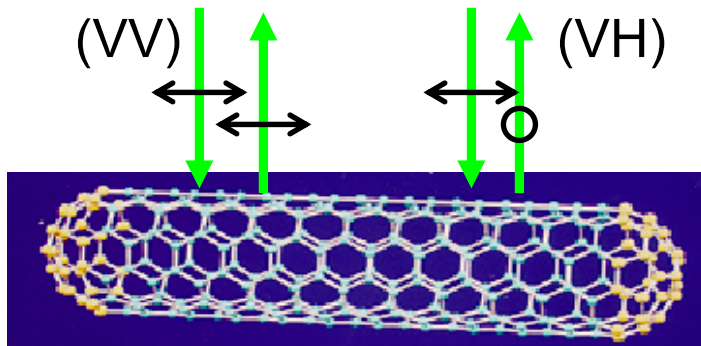
G-band for 3 different SWNTs



A. Jorio *et al.*, Phys. Rev. Letters **90**, 107403 (2003)

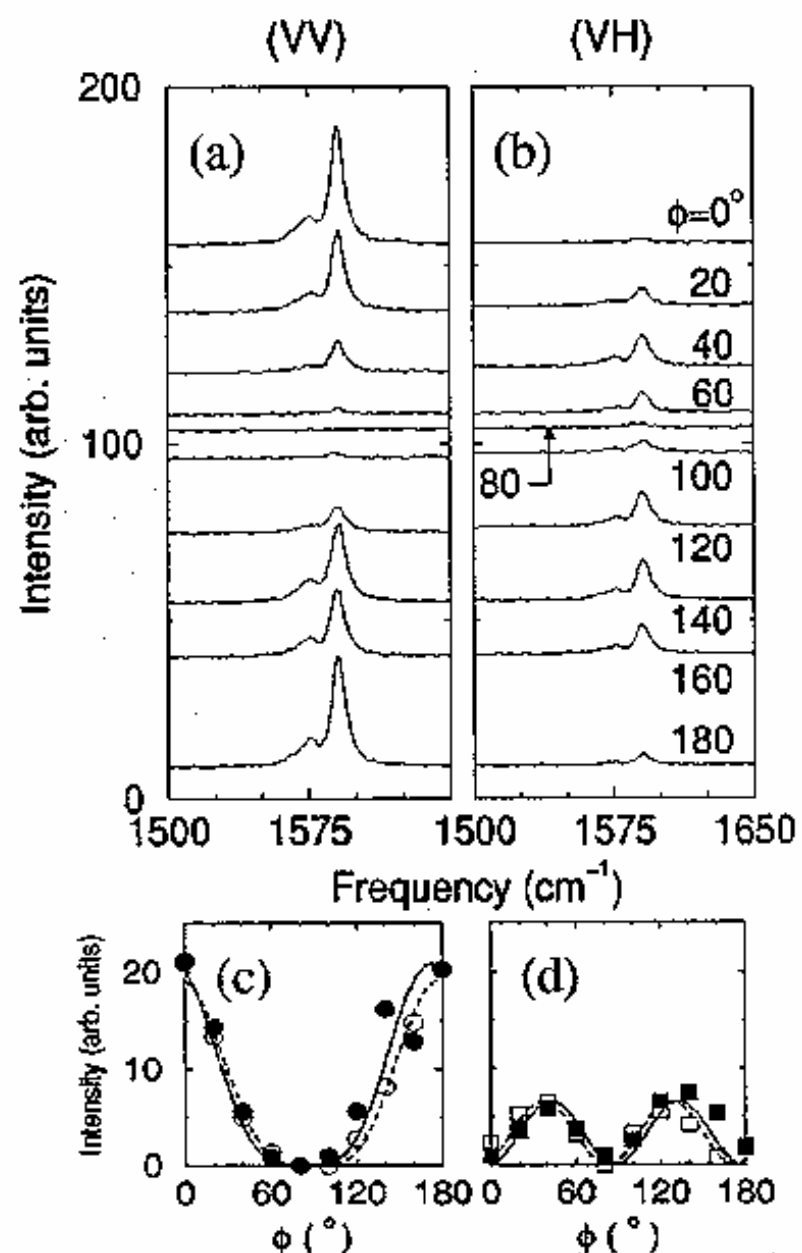
ab initio from Dubay et al.
Phys. Rev. Lett. **88**, 235506 (2002)

Antenna (depolarization) effect in isolated SWNT



SWNT emits and
absorbs light polarized
along the nanotube
axis

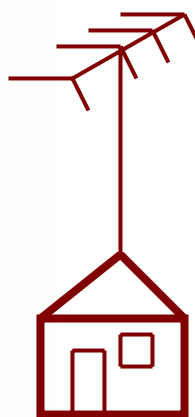
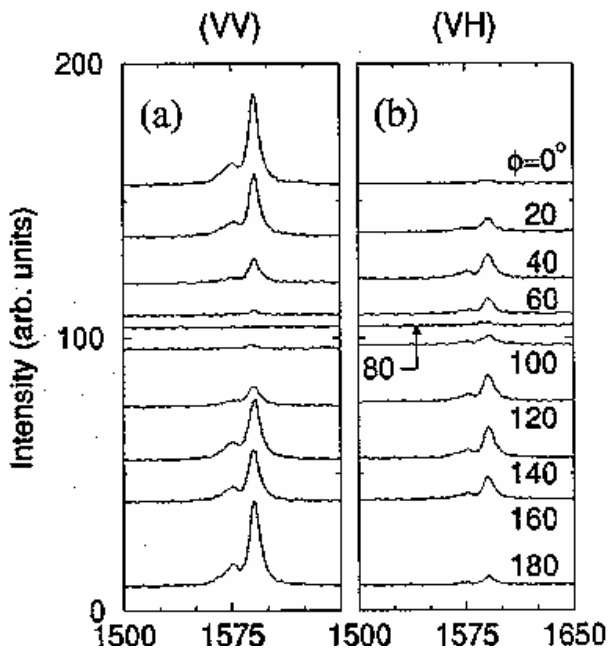
Duesberg et al., *PRL* (2000)
Rinzler et al., *PRB* (2001)
A. Jorio et al., *PRB* (2002)



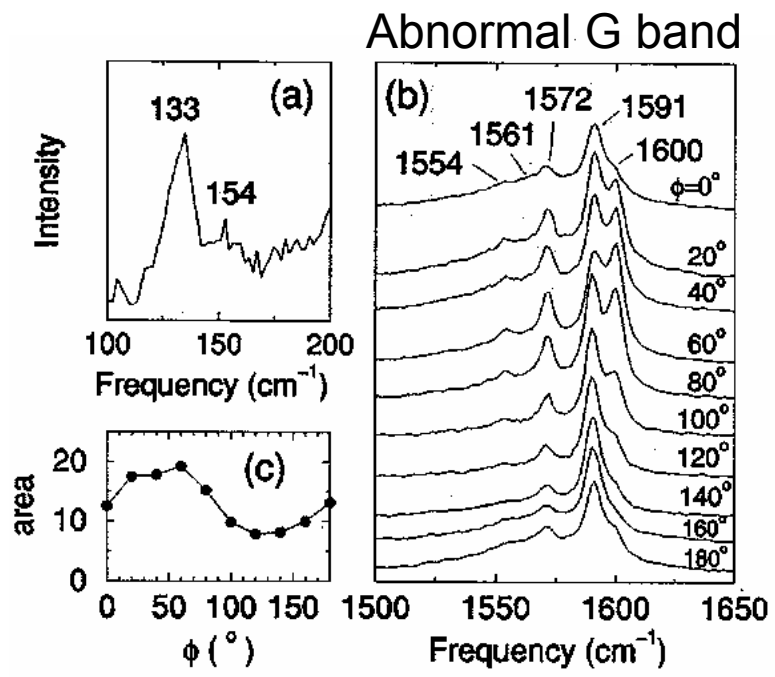
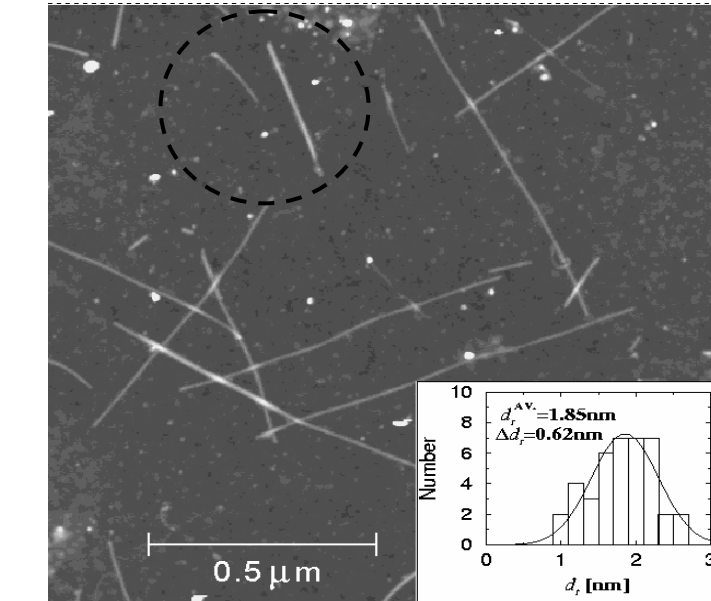
ϕ = angle between optical E field and nanotube axis

Polarization analysis of G band modes in carbon nanotubes

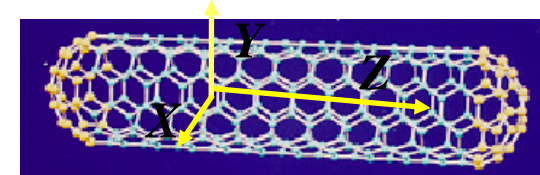
Selection rules, dipolar and multipolar antenna behaviours



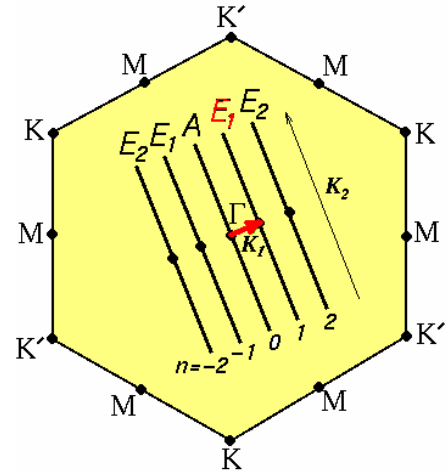
Normal nanotube antenna behavior.
 Φ is the angle between the optical E field and the nanotube axis.



Selection rules for resonance Raman



Unfolded BZ picture

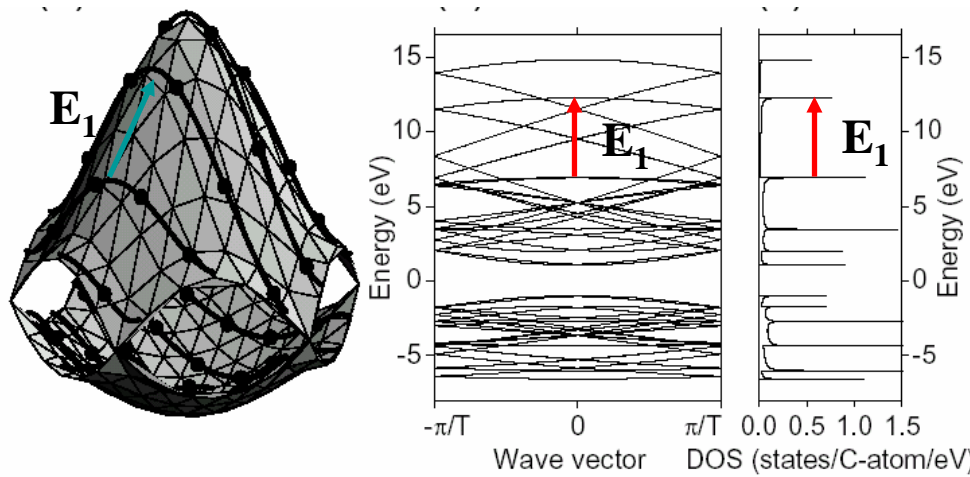


$$E_\mu \xrightarrow{\mathbf{E}_n} E_{\mu \pm \mathbf{n}}$$

- **A modes do not change cutting line**
- **E_1 change by $\pm \mathbf{K}_1$**
- **E_2 change by $\pm 2\mathbf{K}_1$**

$$\begin{array}{ll}
 \text{(I)} & E_\mu^{(v)} \xrightarrow{Z} E_\mu^{(c)} \xrightarrow{A} E_\mu^{(c)} \xrightarrow{Z} E_\mu^{(v)} \\
 \text{(II)} & E_\mu^{(v)} \xrightarrow{X} E_{\mu \pm 1}^{(c)} \xrightarrow{A} E_{\mu \pm 1}^{(c)} \xrightarrow{X} E_\mu^{(v)} \\
 \text{(III)} & E_\mu^{(v)} \xrightarrow{Z} E_\mu^{(c)} \xrightarrow{E_1} E_{\mu \pm 1}^{(c)} \xrightarrow{X} E_\mu^{(v)} \\
 \text{(IV)} & E_\mu^{(v)} \xrightarrow{X} E_{\mu \pm 1}^{(c)} \xrightarrow{E_1} E_\mu^{(c)} \xrightarrow{Z} E_\mu^{(v)} \\
 \text{(V)} & E_\mu^{(v)} \xrightarrow{X} E_{\mu \pm 1}^{(c)} \xrightarrow{E_2} E_{\mu \mp 1}^{(c)} \xrightarrow{X} E_\mu^{(v)}
 \end{array}$$

A. Jorio et al., Phys. Rev. Letters 90, 107403 (2003)
Group Theory

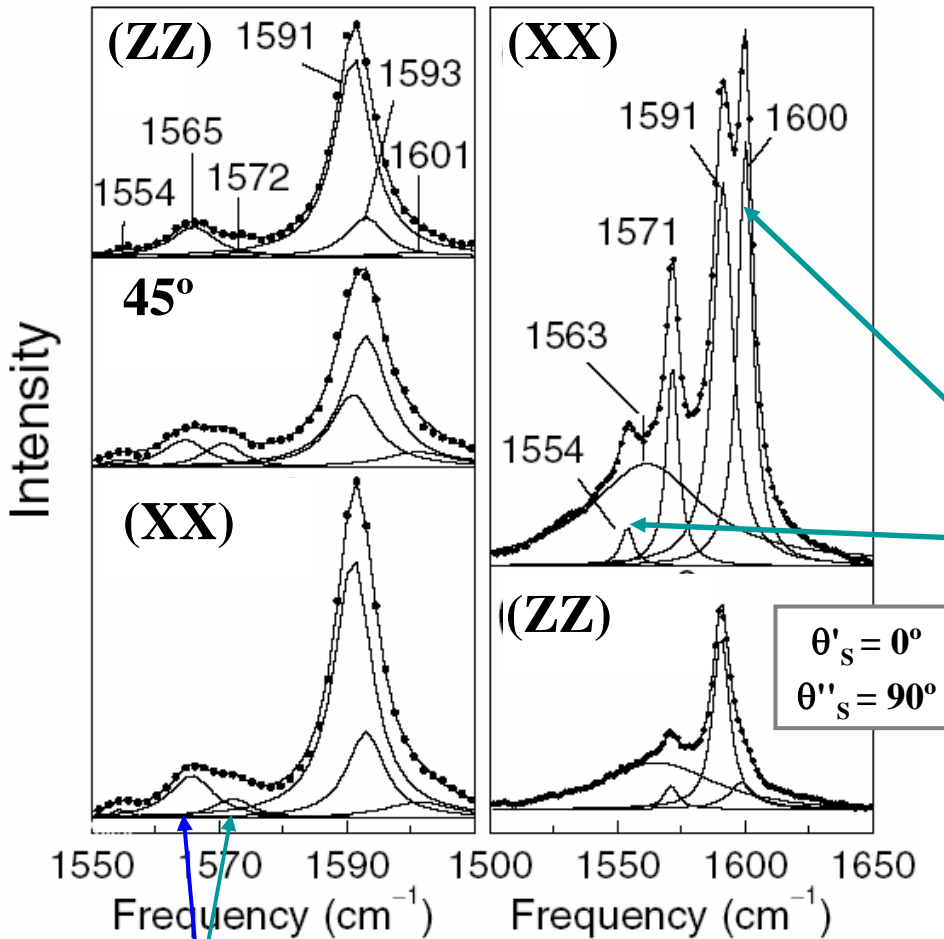


basis functions for the Raman active
 Irreducible Representations (C_N, D_{nh}, D_{nd})

Raman-active modes		Basis functions	
Chiral	Achiral		
A	A_{1g}	$X^2 + Y^2$	Z^2
E_1	E_{1g}	XZ	YZ
E_2	E_{2g}	$X^2 - Y^2$	XY

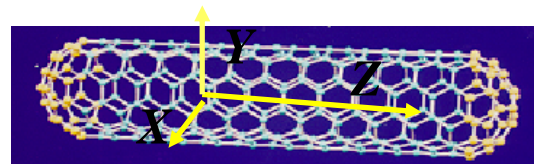
Polarization study of isolated SWNTs

Observation of symmetry selection rules



Observation of resolved A and E₁ modes with intensity dependence on polarization

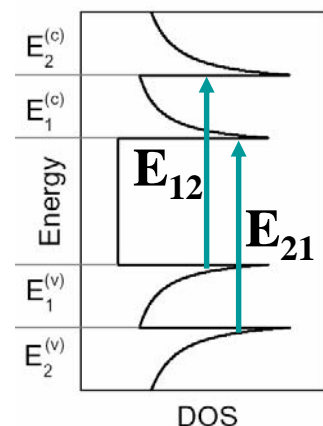
A. Jorio *et al.*, Phys. Rev. Letters 90, 107403 (2003)



Raman-active modes		Basis functions	
Chiral	Achiral		
A	A _{1g}	X ² + Y ²	Z ²
E ₁	E _{1g}	XZ	YZ
E ₂	E _{2g}	X ² - Y ²	XY

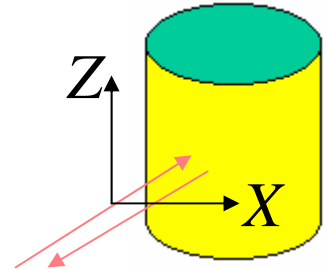
Observation of strong E₂ modes with intensity dependence on polarization implies $E_\mu^{(v)} \rightarrow E_{\mu \pm 1}^{(c)}$ transition

Asymmetry with respect to the Fermi level (s parameter) can be obtained from $E_{12} \neq E_{21}$



Polarized G-band Spectra for aligned bundles

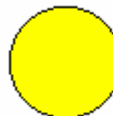
A. Jorio *et al.* *PRL* **85**, 2617 (2000)



- Symmetry Assignment

- $1550\text{-}60\text{cm}^{-1}$ E_2^{LO}
- $1560\text{-}70\text{cm}^{-1}$ $A_1^{\text{TO}} + E_1^{\text{LO}}$
- $1580\text{-}90\text{cm}^{-1}$ $A_1^{\text{LO}} + E_1^{\text{TO}}$
- 1600cm^{-1} E_2^{TO}

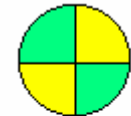
- Nodes of Modes



0

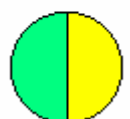


2

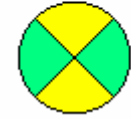


4

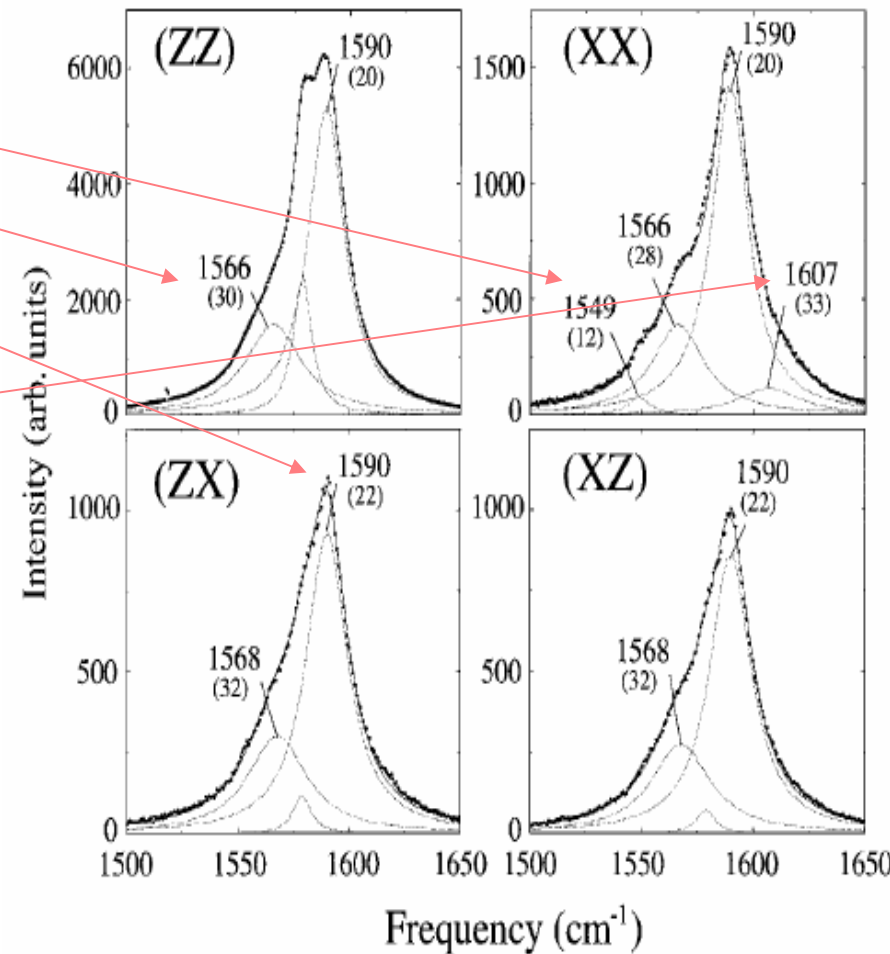
A_1

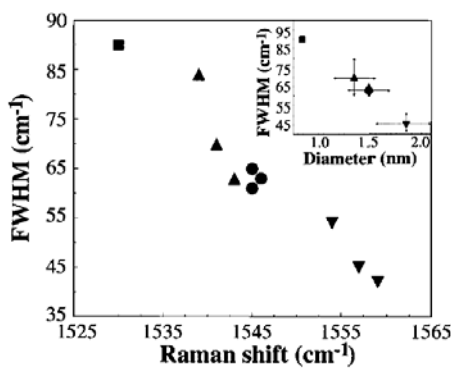


E_1



E_2

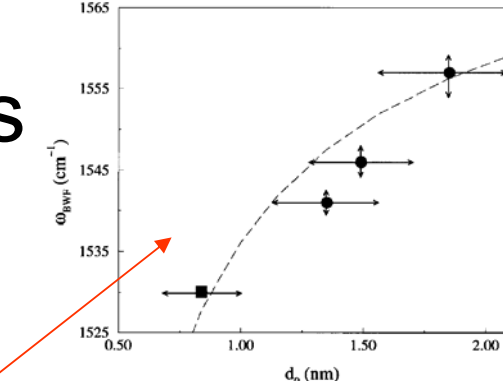




Breit-Wigner-Fano Peaks

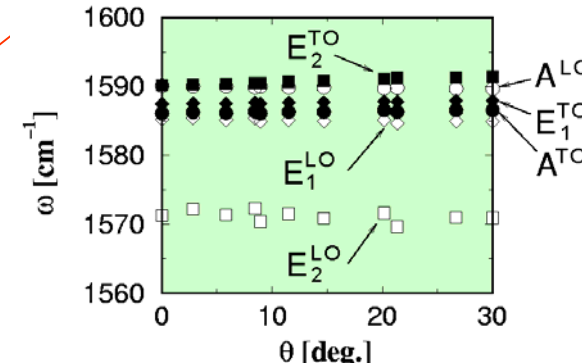
S.D.M. Brown et al, *Phys. Rev. B* **63**, 5414 (2001)

BWF effect is largest in SWNT bundles

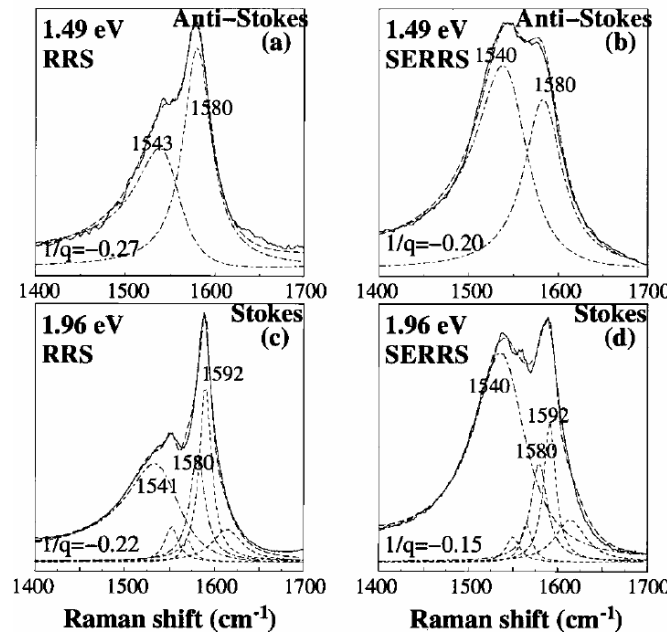


- Metallic SWNTs, GICs
 - A_{LO} mode is Lorentzian ($q=0$)
 - A_{TO} mode is of BWF origin

$$I(\omega) = I_0 \frac{[1 + (\omega - \omega_{BWF})/q\Gamma]^2}{1 + [(\omega - \omega_{BWF})/\Gamma]^2}$$



- Diameter Dependent ω_{BWF}
 - Coupling constant q and width
- Chirality Dependent Intensity

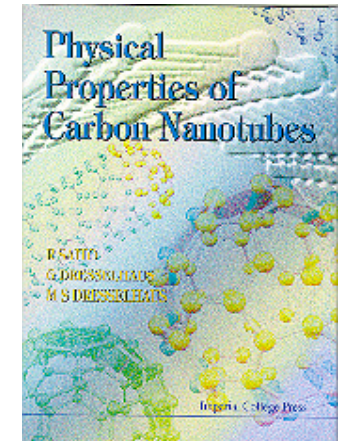


Coffee Break time

- Back in 10 minutes

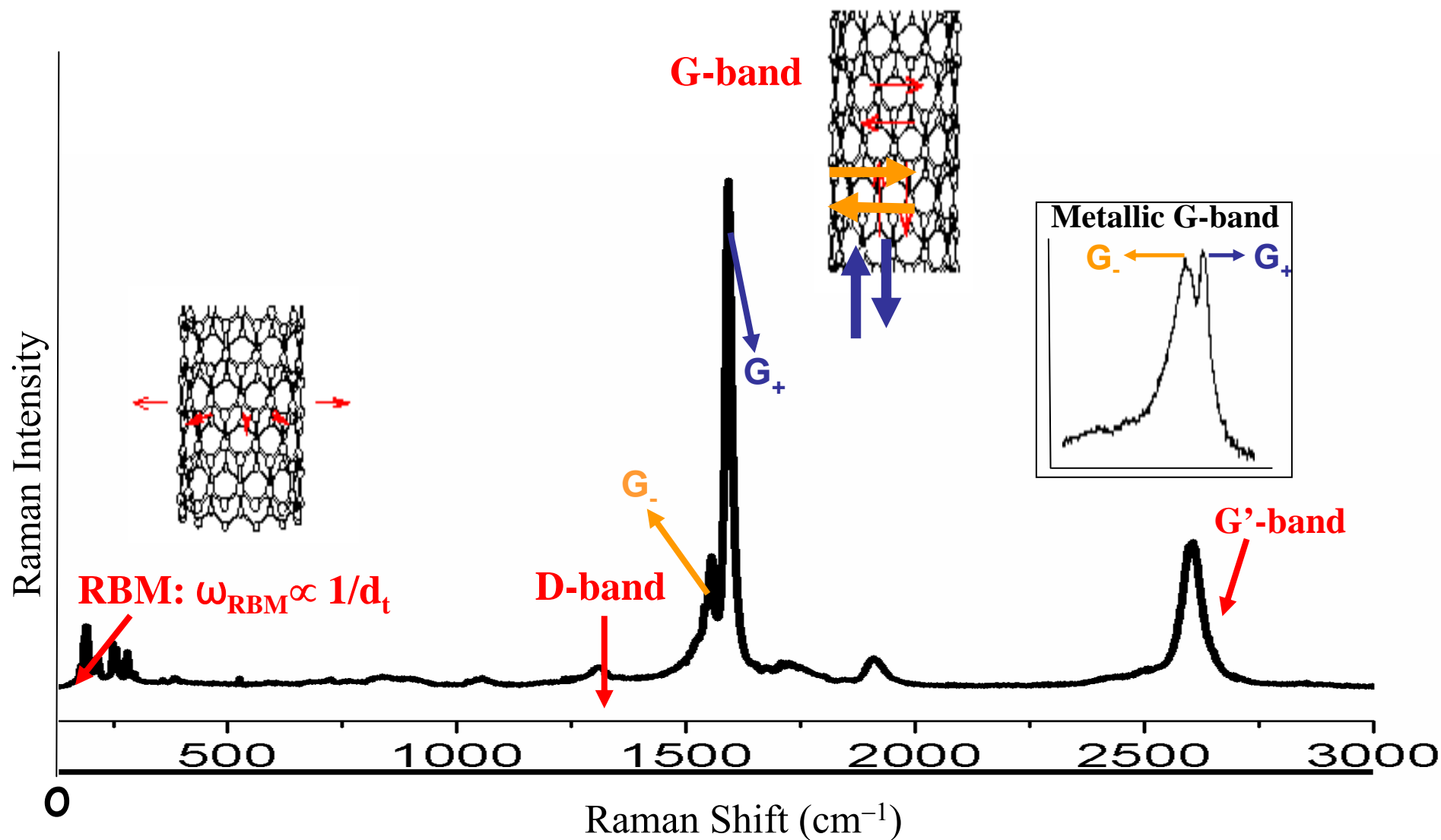
Outline

- Background
- Phonon Properties
- Overview of Raman Effect
- First-order Raman Processes
 - (the RBM and G-Band)
- **Double Resonance Processes**
- Photoluminescence
- Excitons



"Physical Properties of Carbon Nanotubes",
by R. Saito, G. Dresselhaus and M.S. Dresselhaus,
Imperial College Press (1998) ISBN 1-86094-093-5

Raman Spectra of SWNT Bundles



- Radial breathing mode (RBM) and G-band are first-order processes
- D-band, G'-band and other weak features are second-order processes

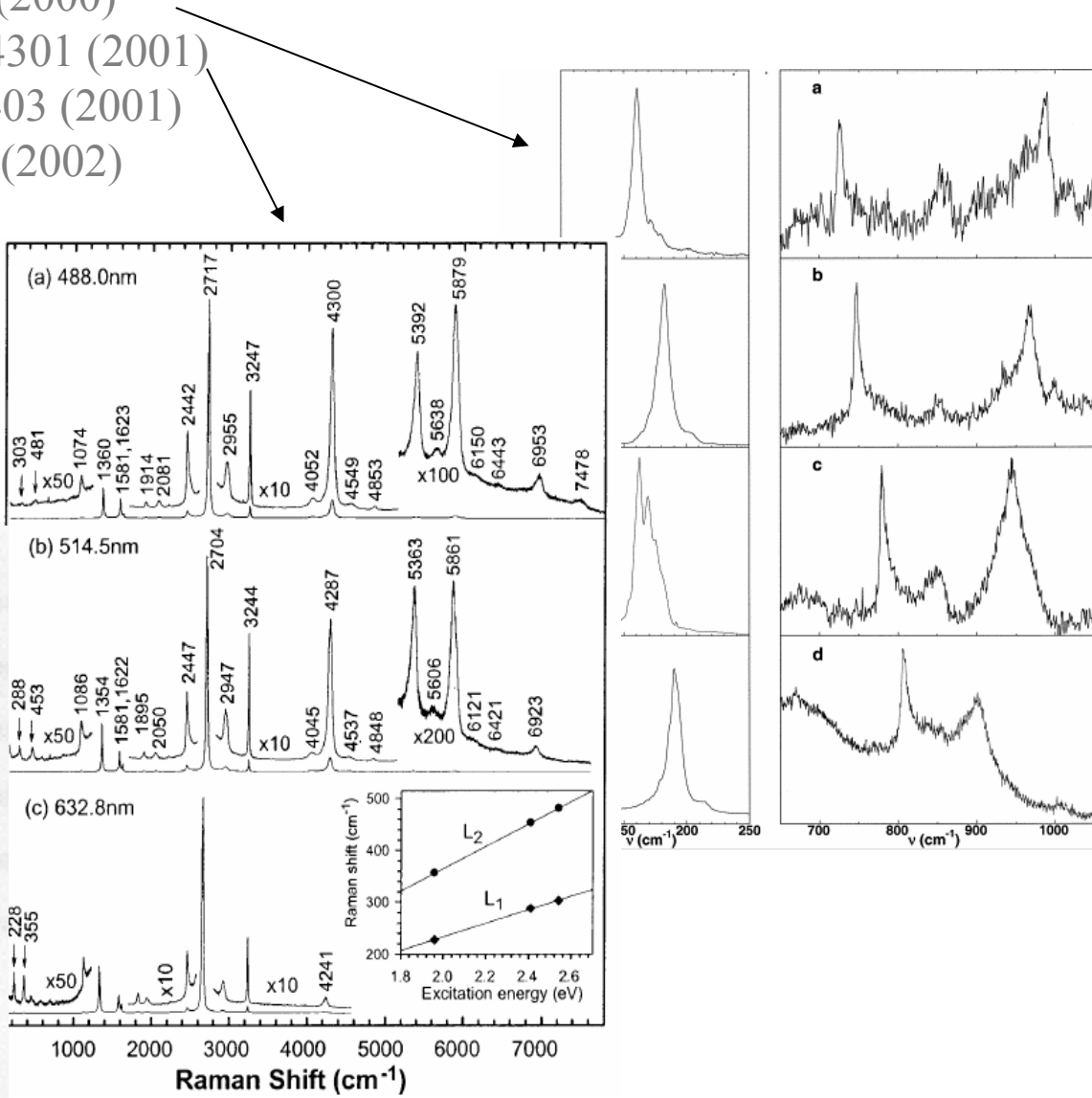
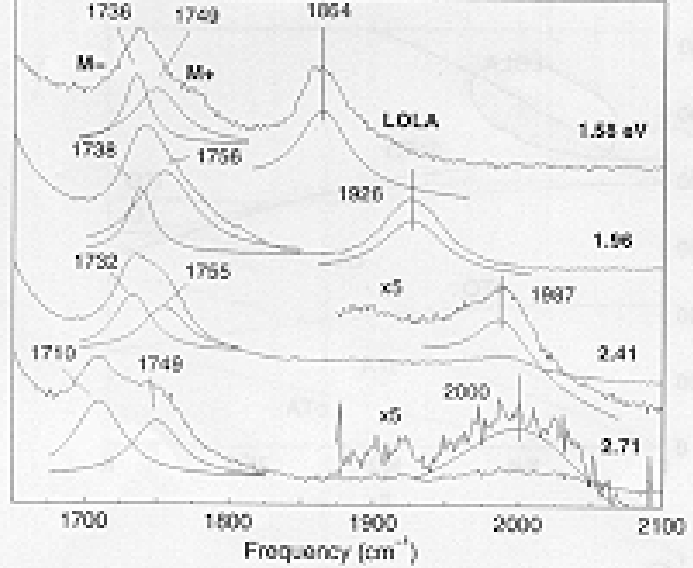
Dispersive modes in sp^2 carbons

L. Alvarez et al, *CPL* **320** 441(2000)

P. H. Tan et al. *Phys. Rev B* **64**, 214301 (2001)

S.D.M.Brown et al, *PRB* **64**, 073403 (2001)

V. Brar et al. *PRB* **66**, 155418 (2002)



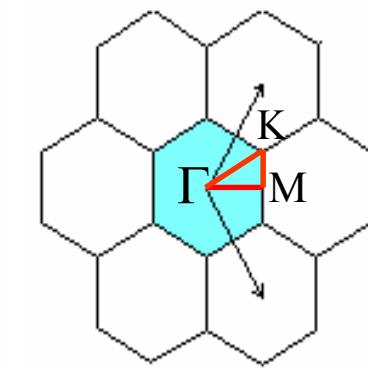
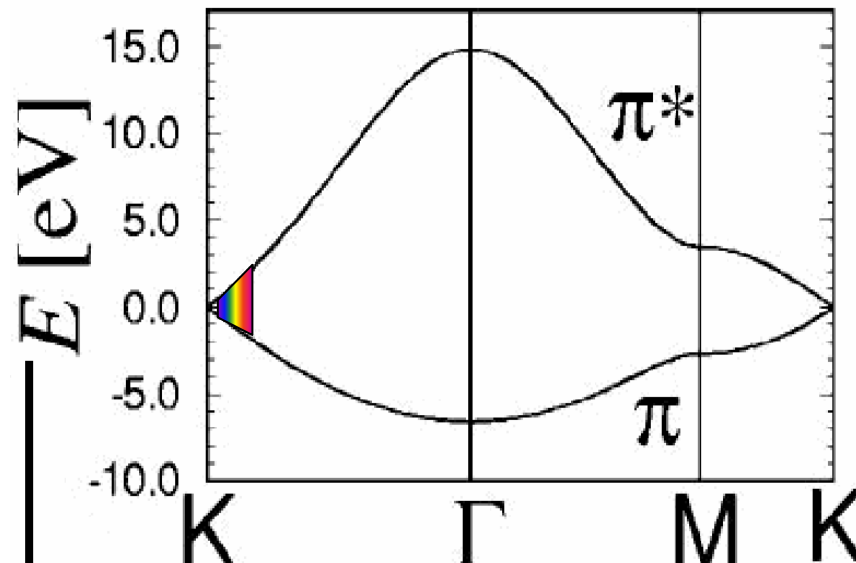
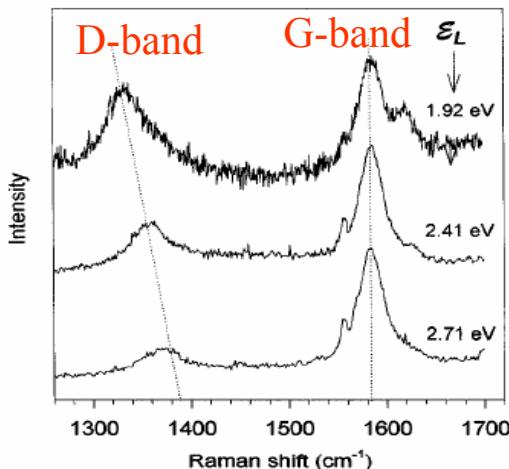
Properties of D-band and G'-band Spectra

- Highly dispersive with variation of E_{laser}
- Due to a Double Resonance Process
- Possibility of Triple Resonance
- Oscillatory behavior of D-band and G'-band dispersion
- Double Resonance selects resonant q vector
- Trigonal warping for electrons
- Monitoring edge defects
- Monitoring nanotube coalescence

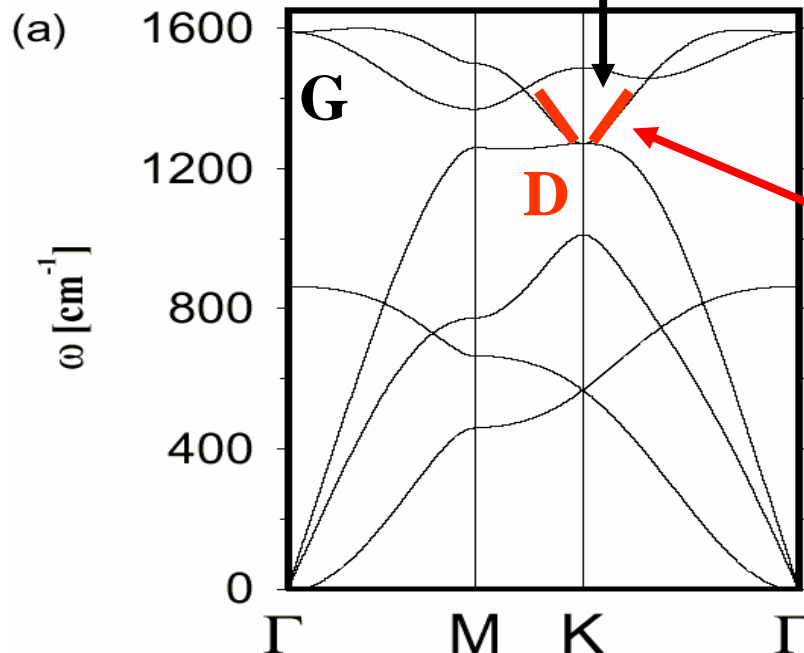
Graphite

Matthews et al., PRB 59, R6585 (1999)

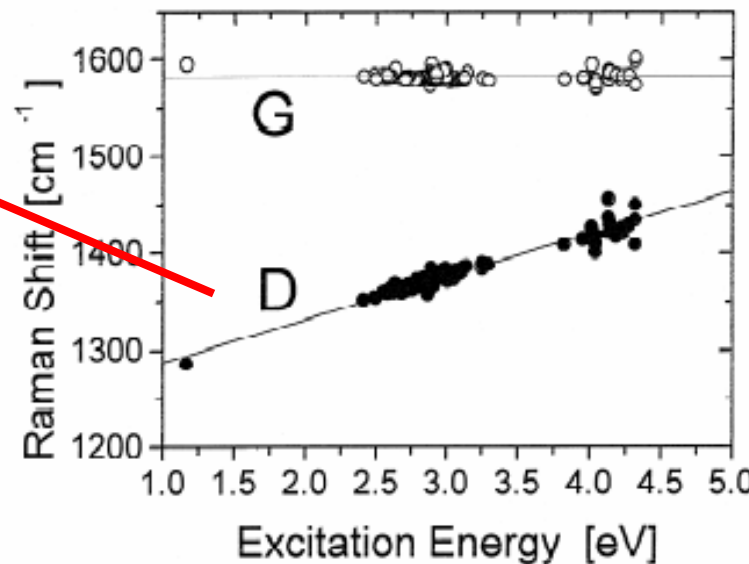
Electrons



Phonons

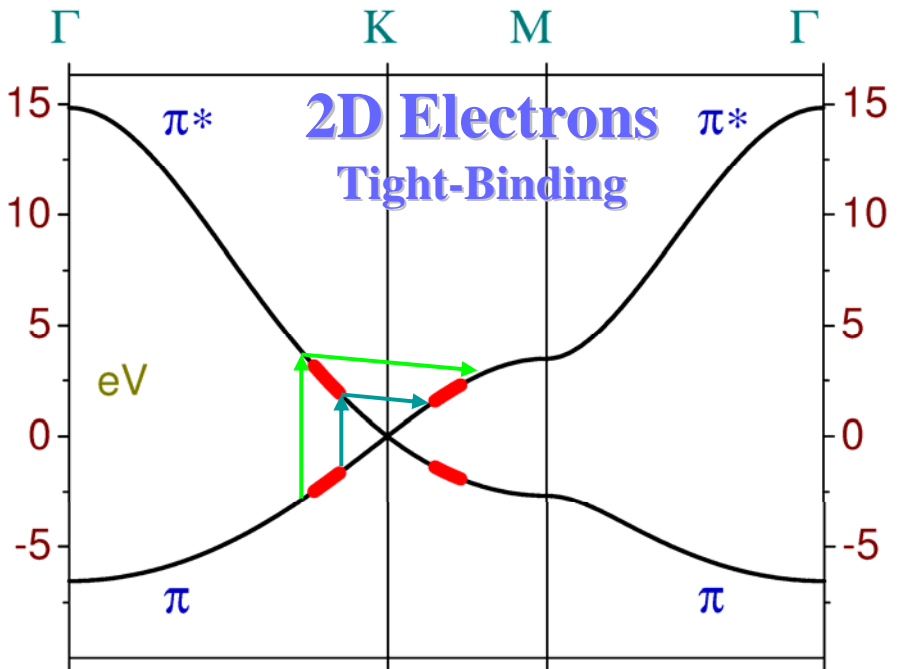


I. Pócsik et al. / Journal of Non-Crystalline Solids 227–230 (1998) 1083–1086

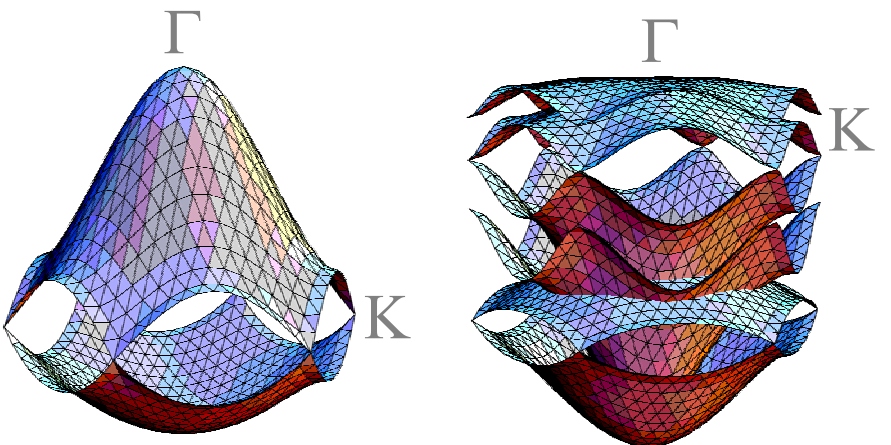


Dispersion of D-band = $53 \text{ cm}^{-1}/\text{eV}$

Determination of phonon dispersion for 2D graphite with double resonance Raman effect

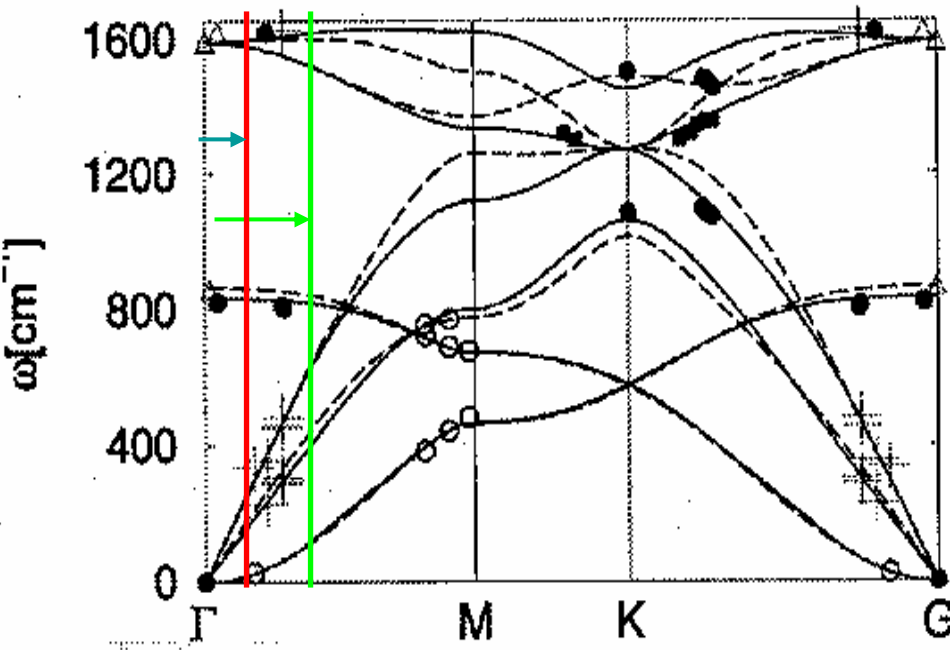
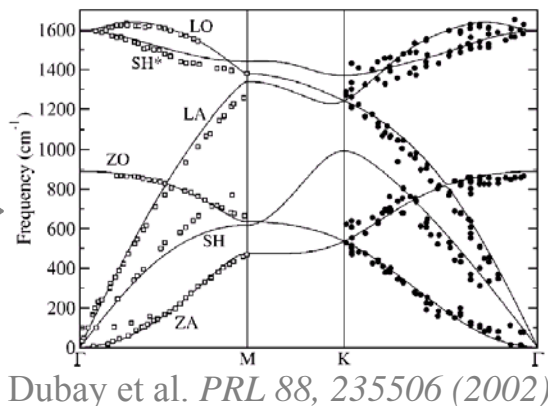


R. Saito et al., *Phys. Rev. Lett.* 88, 027401 (2002)
A. Grüneis et al., *Phys. Rev. B* 65 155405 (2002)



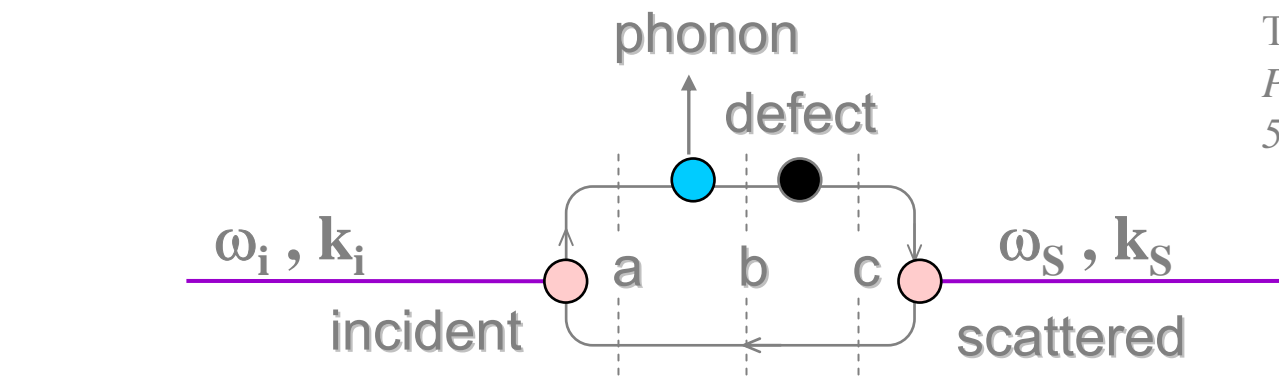
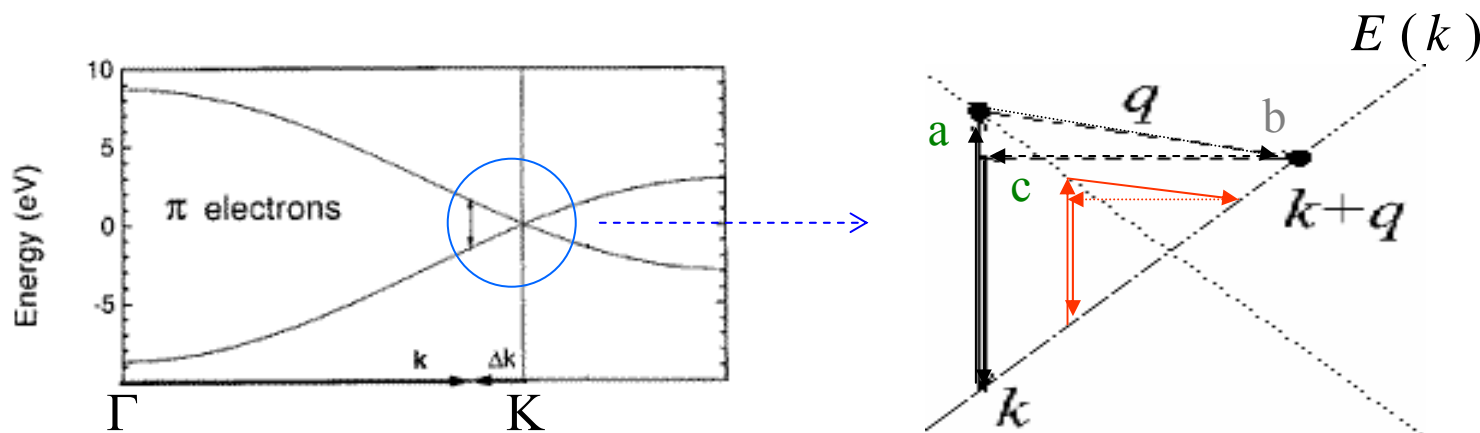
EELS →

**2D Phonons
Force Constant**



Special phonons (ω, q) give rise to double resonance (high intensity) providing a new technique for phonon dispersion determination

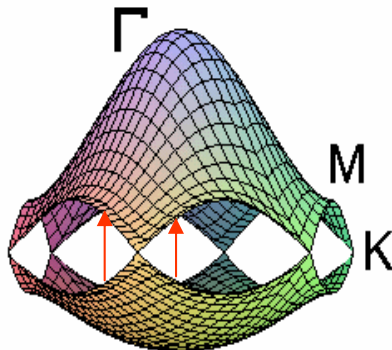
Double Resonance Model



Thomsen and Reich,
Phys. Rev. Letters 85,
5214 (2000)

$$I = C \sum_{A,B,C} \frac{M}{(\hbar\omega_i - E_a - i\gamma)(\hbar\omega_i - \hbar\omega_q - E_b - i\gamma)(\hbar\omega_i - \hbar\omega_q - E_c - i\gamma)}$$

Double resonance: Two terms in the denominator go to zero simultaneously

Γ 

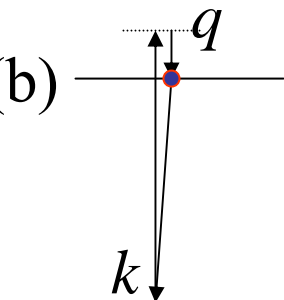
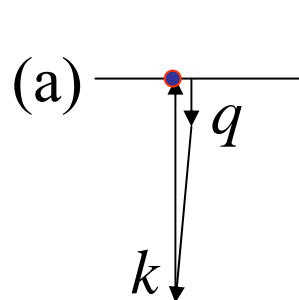
Double Resonance Raman processes

C. Thomsen and S. Reich, *Phys. Rev. Lett.* **85** 5214 (2000)

R. Saito et al., *Phys. Rev. Lett.* **88**, 027401 (2002)

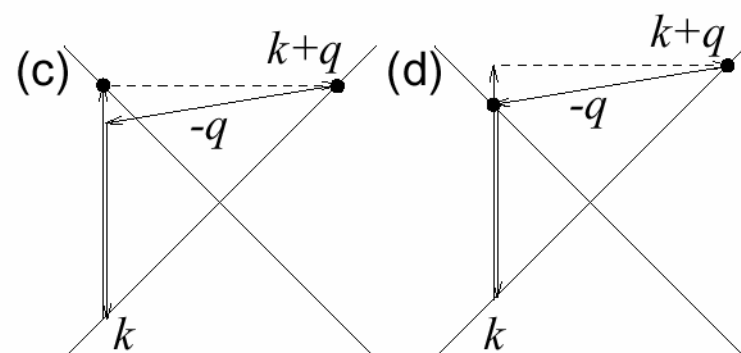
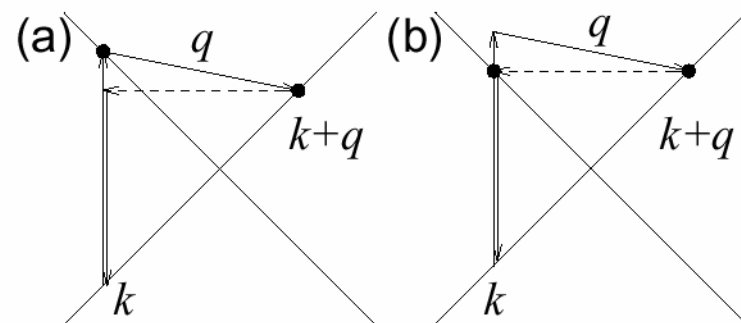
Resonant Raman Processes

- 1st order $q < k$, $k \approx 0$
 - $q \sim 0$ (only near Γ point)
- 2nd order (1 phonon, 2 phonons)
 - $q \gg 1$ (depend on E(laser))



1st order Raman

One phonon emission

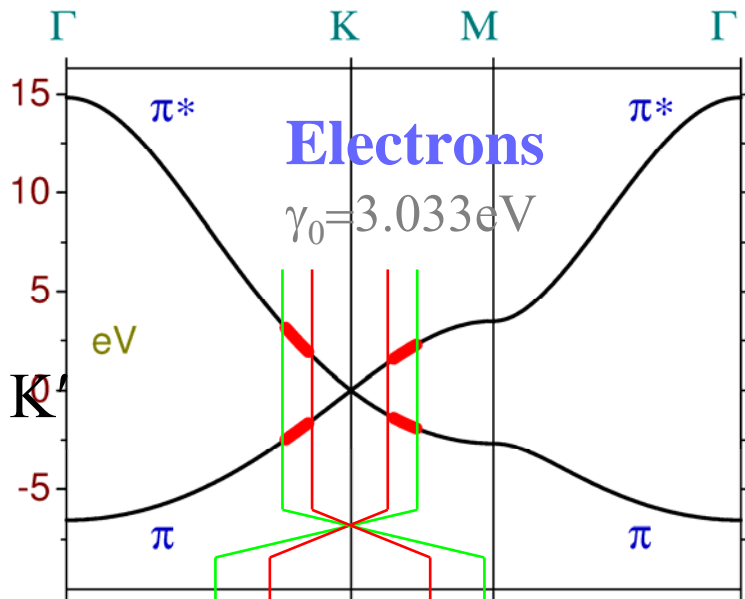
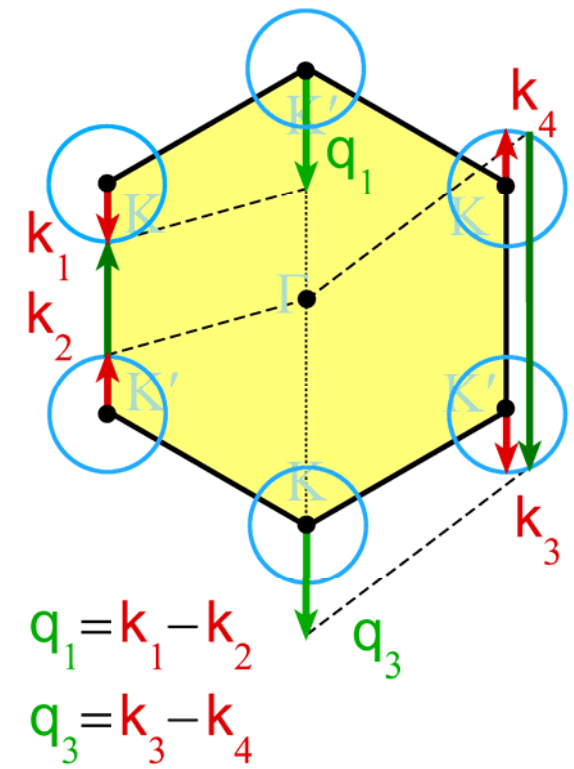
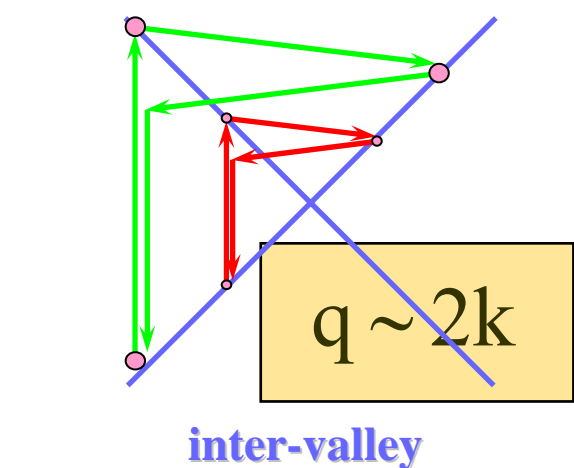


Double resonance condition

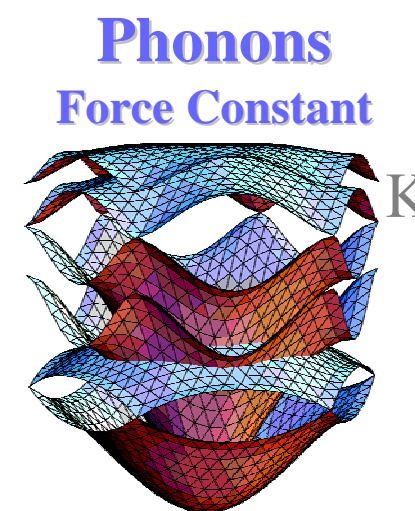
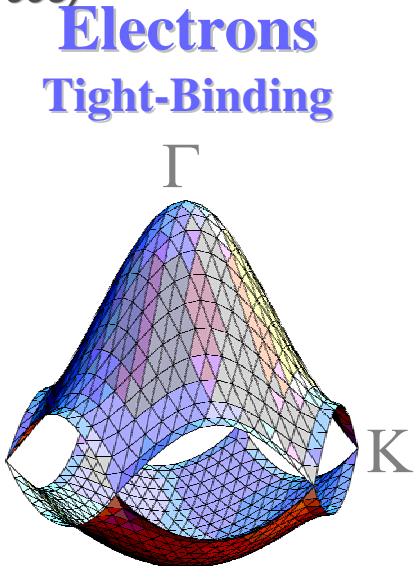
2nd order Raman

Electrons and Phonons

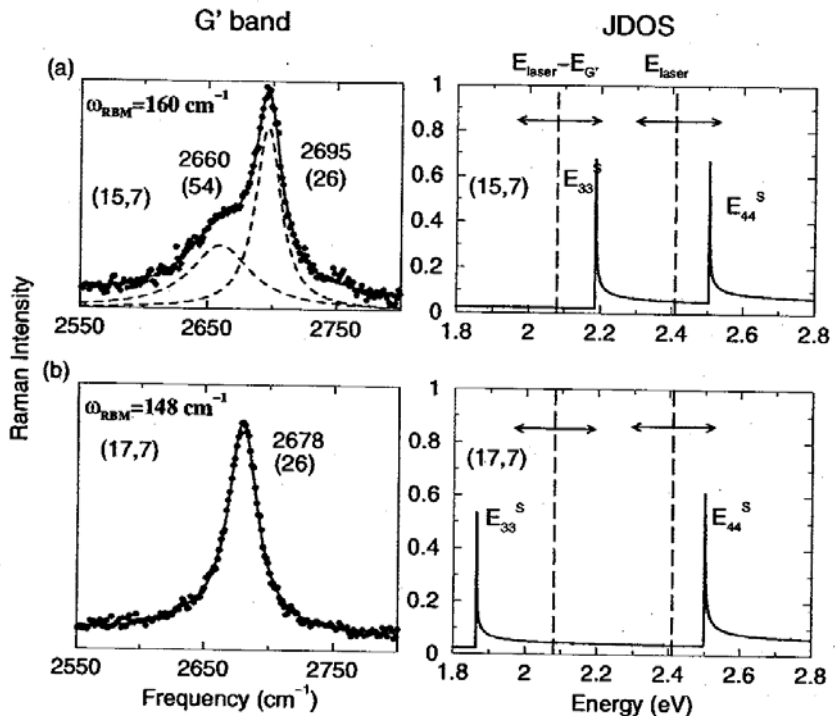
R. Saito et al, Physical Properties of Carbon Nanotubes, Imperial College Press (1998)



Phonons

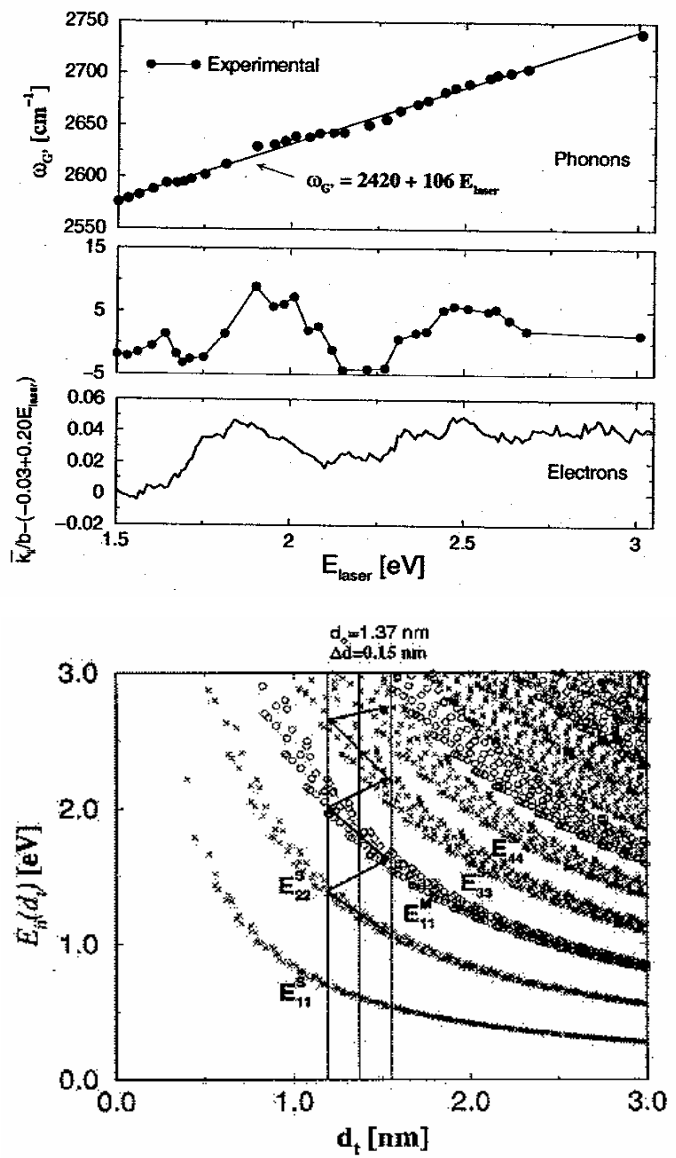


Anomalous results for Double Resonance in carbon nanotubes - vHs



G' band in isolated SWNTs:
1 or 2 peaks (for triple resonance)

A. G. Souza Filho *et al*, PRB 65, 085417 (2001)



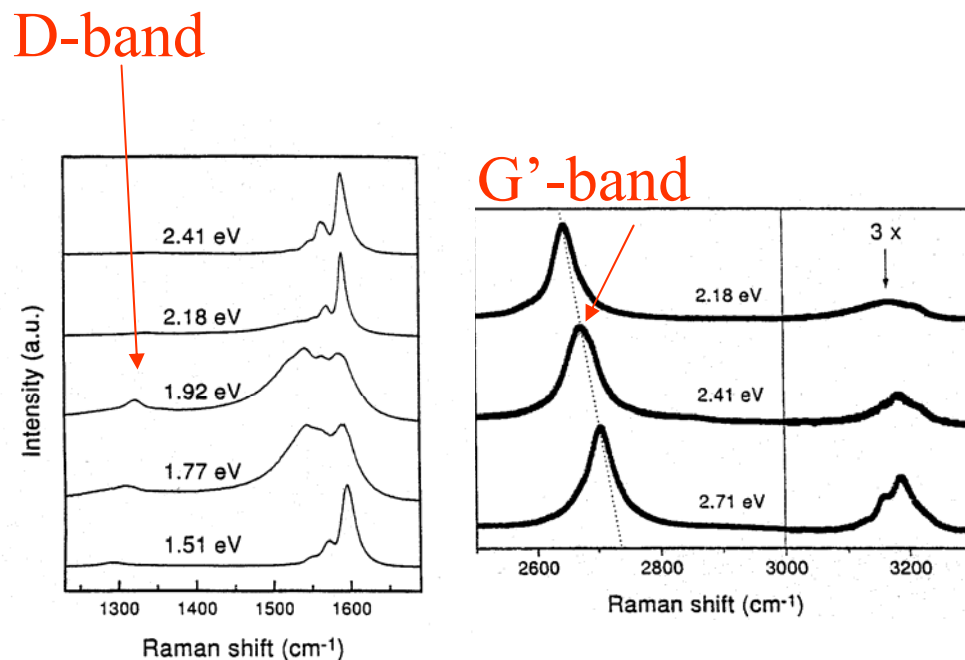
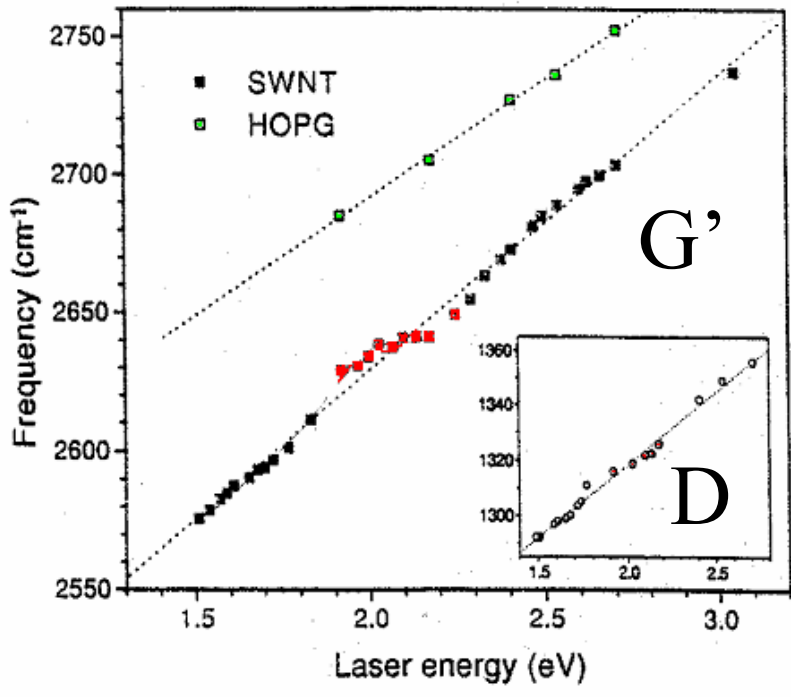
Oscillatory behavior for D band dispersion in bundles

A. G. Souza Filho *et al*, PRB 65, 035404 (2001)

D(G')-band Spectra of SWNT

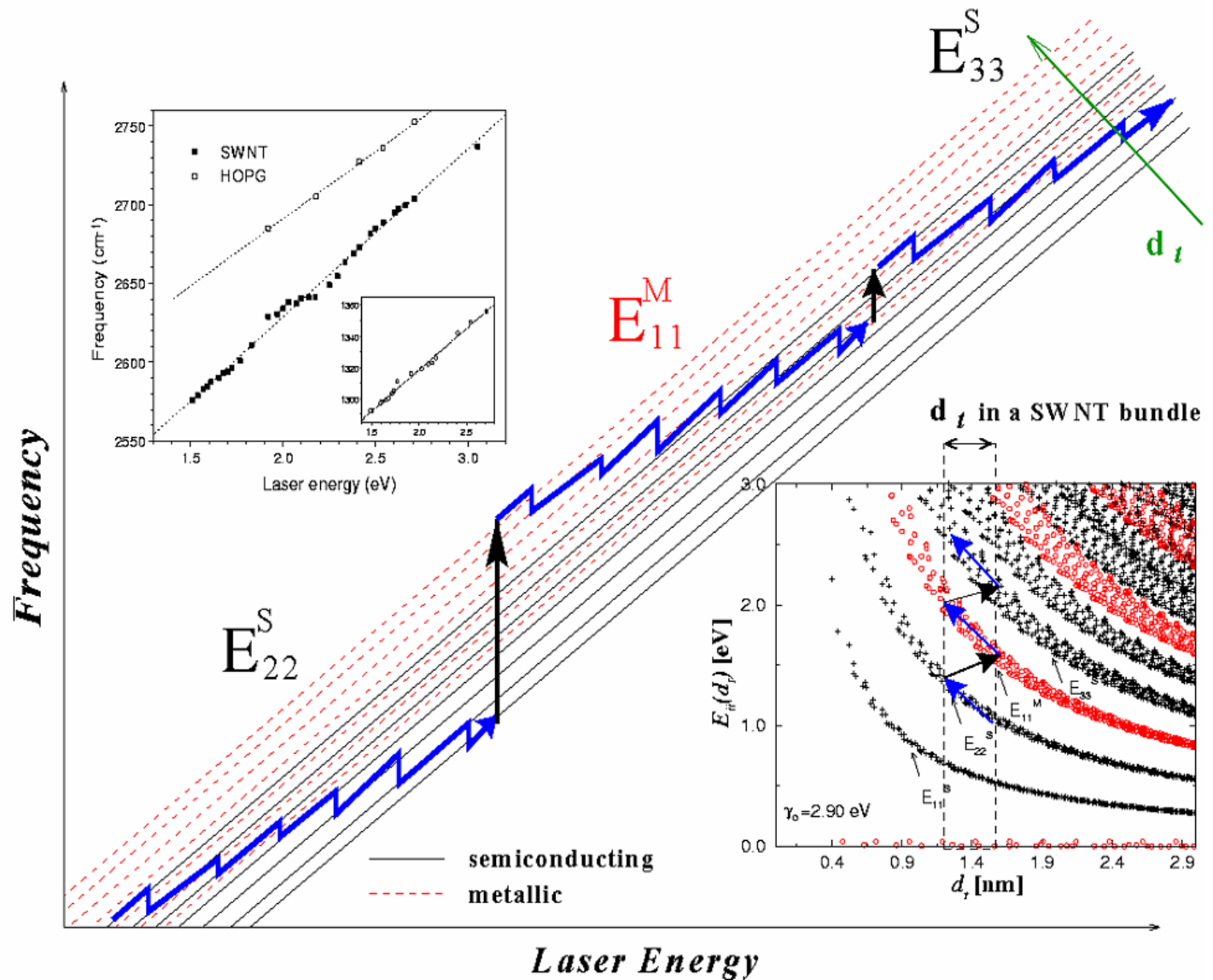
M. A. Pimenta *et al.*, *Brazilian J. Phys.* **30**, 423 (2000).

- Laser Energy Dependence
 - $\omega(E_{\text{laser}}) = 2420 + 106 E_{\text{laser}}$ (cm^{-1})
 - Resonant Nature (incident and scattered)
- Diameter Dependence



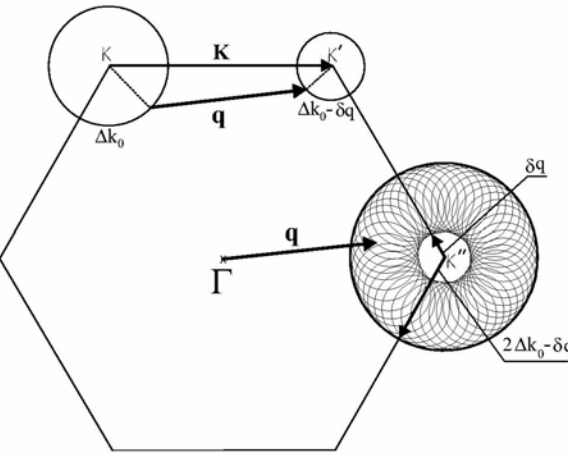
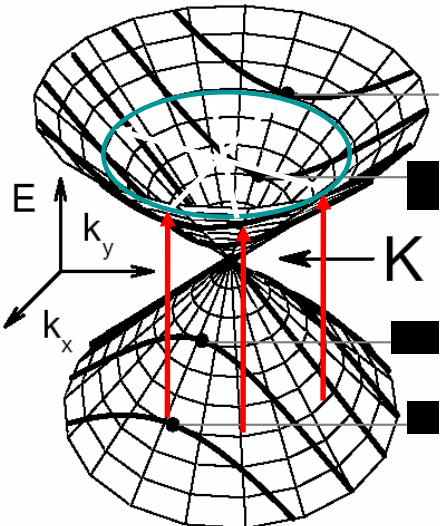
Anomalous Dispersion of D(G') band

M. Pimenta et al., Brazilian J. Phys. 30, 423 (2000)

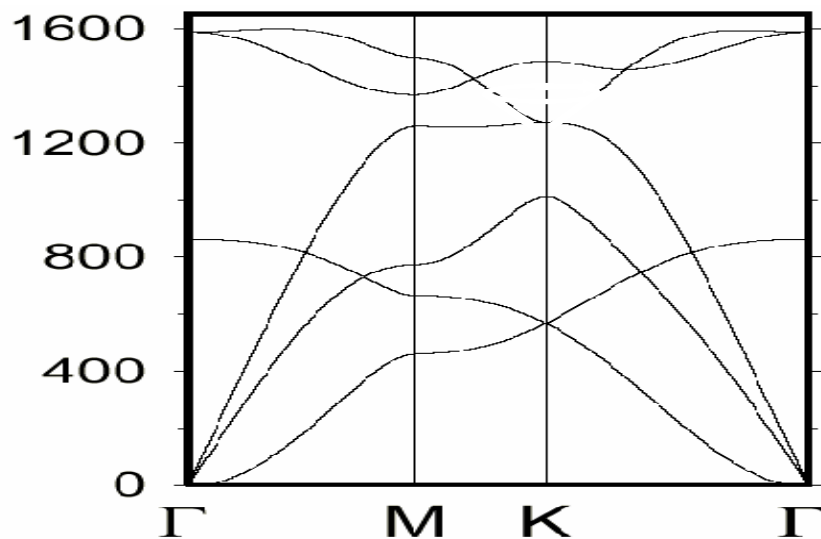


Double resonance selects q vectors

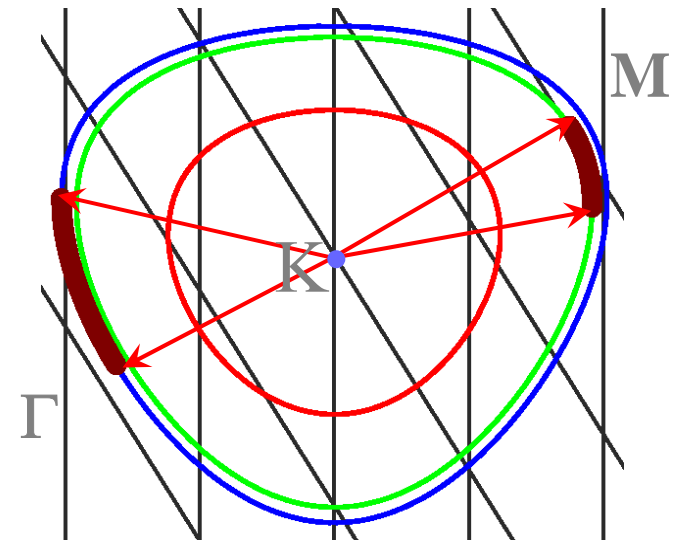
Momentum and energy double resonance requirements in graphite
only selects q magnitude around high symmetry Γ and K points



Cançado et al., PRB 66, 35415 (2002)



1D cutting lines define
allowed q and k vectors



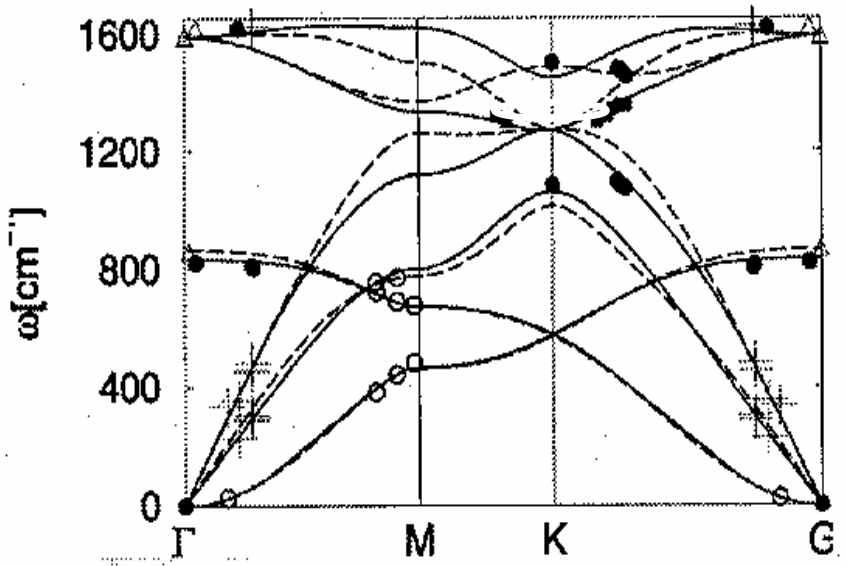
1D quantum confinement allow
determination of not only
magnitude of q but also direction

Samsonidze et al., PRL 90, 027403 (2003)

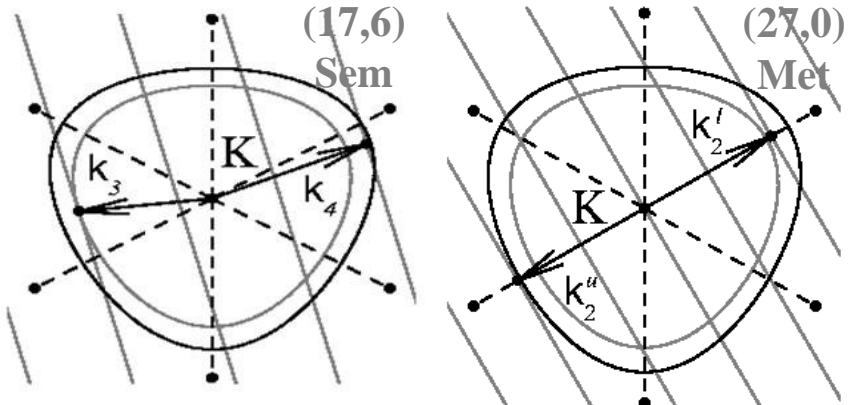
Trigonal warping effect for phonons

Measured by Raman spectroscopy

SWNT chiral angle θ defines q direction on 2D Brillouin zone

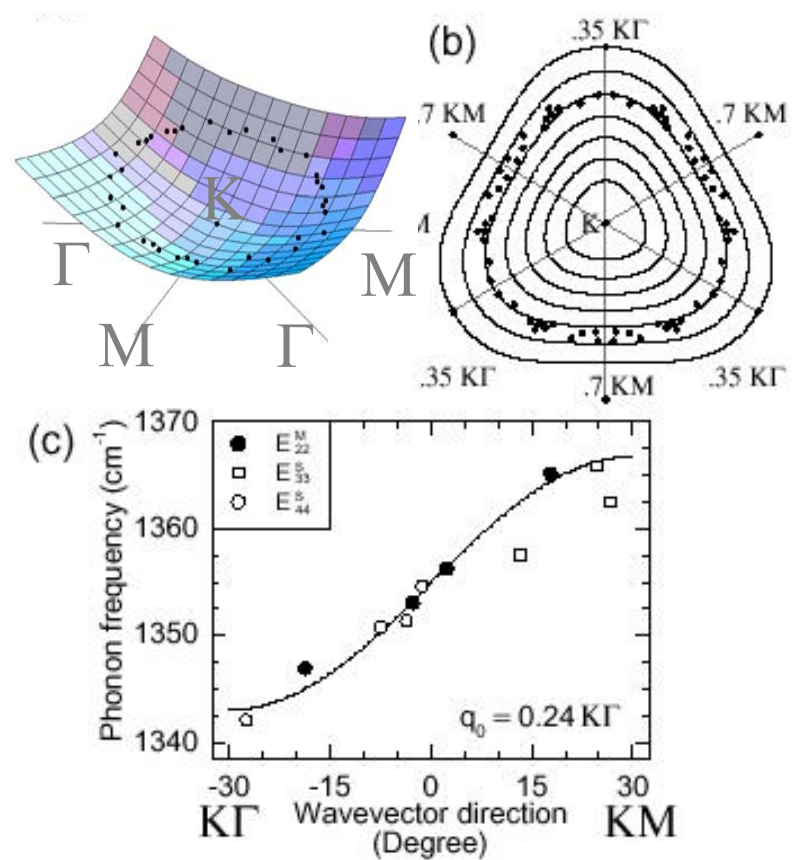


A. Grüneis et al., *Phys. Rev. B* 65 155405 (2002)



Samsonidze et al., *PRL* 90, 027403 (2003)

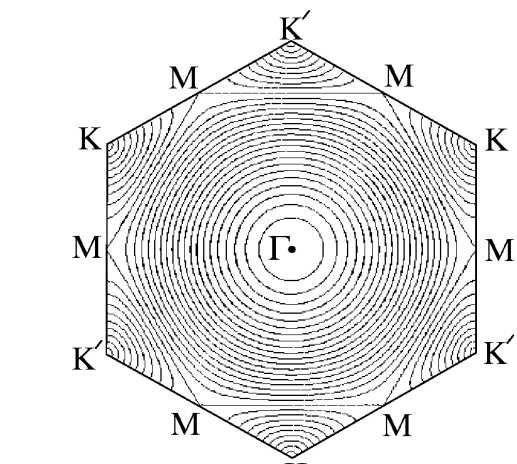
Experimental results



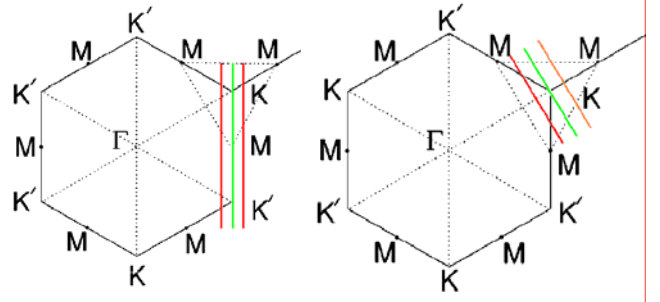
Phonon trigonal warping around K point $\sim 24 \text{ cm}^{-1}$

Trigonal Warping Effect in Carbon Nanotubes

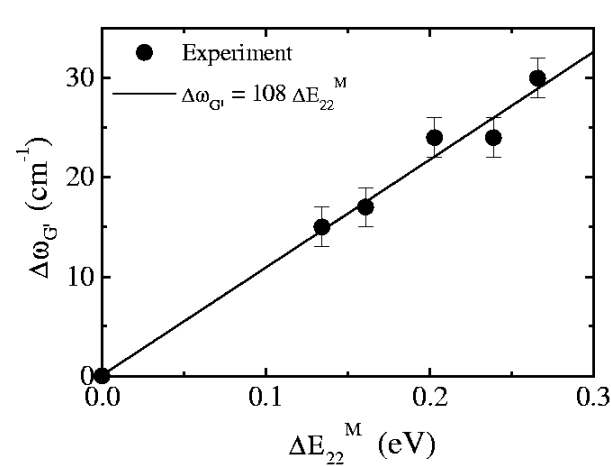
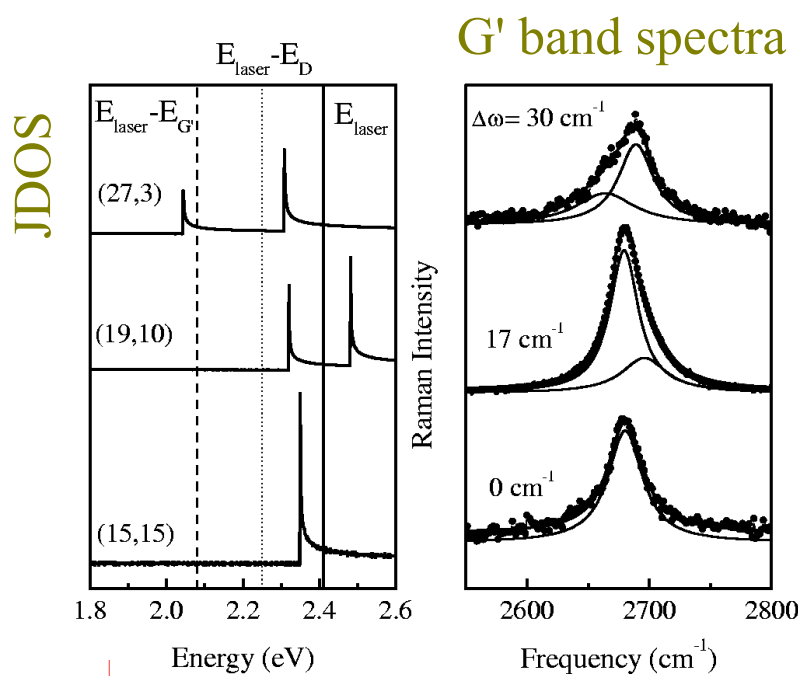
R. Saito *et al.*, PRB
61, 2981 (2000)



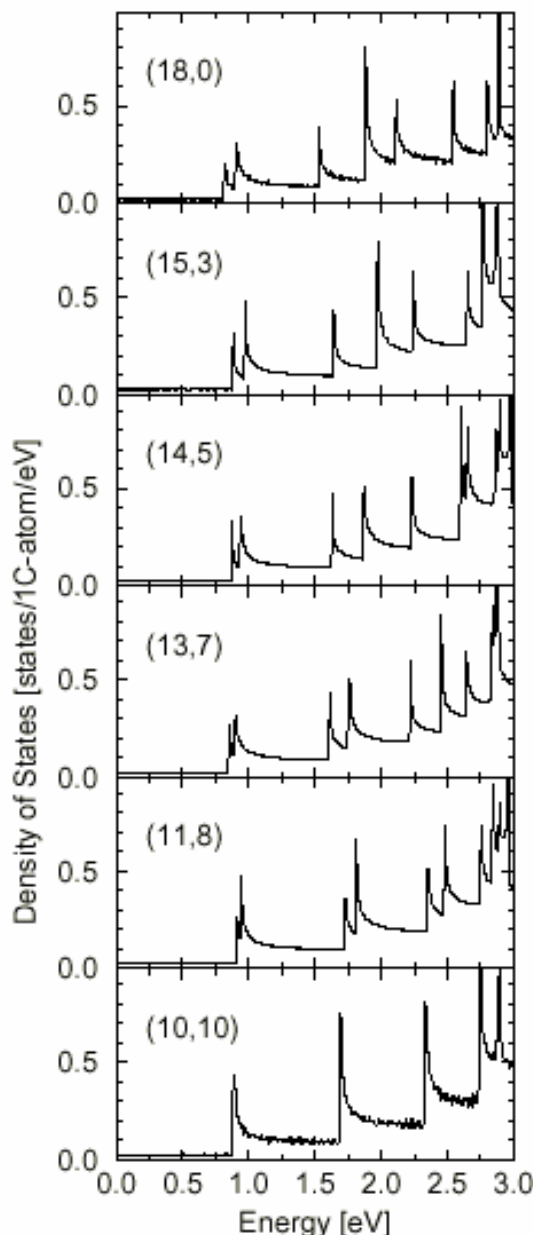
armchair zigzag



A. G. Souza Filho *et al.*,
CPL 354, 62 (2002)



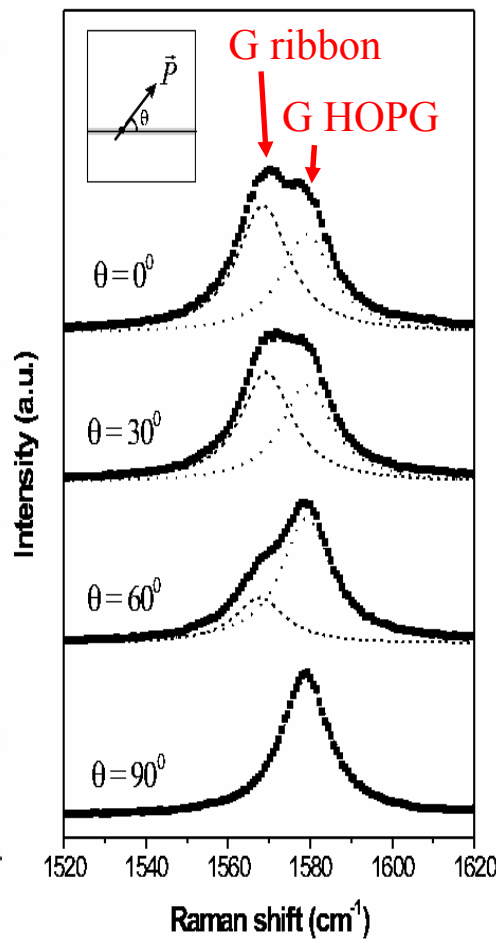
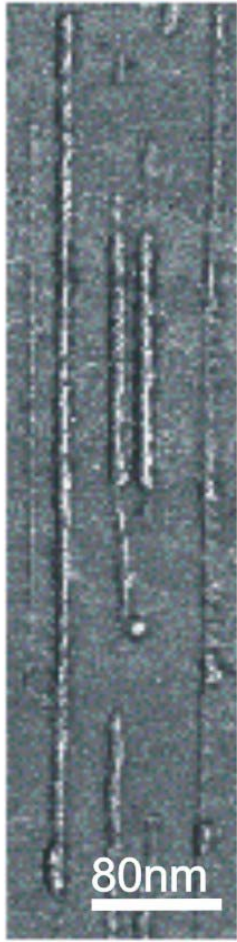
Splitting of the vHs
in **metallic** SWNTs



Slope $\delta\Delta\omega_G/\delta\Delta E$ ($108 \text{ cm}^{-1}/\text{eV}$) gives G' band dispersion
($106 \text{ cm}^{-1}/\text{eV}$) from measurements with one laser line

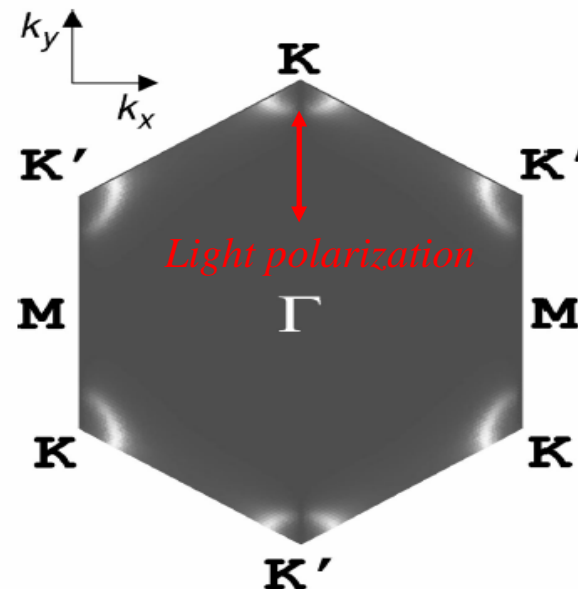
Raman on Nanographite ribbons

Nanographite ribbons on top of HOPG substrate



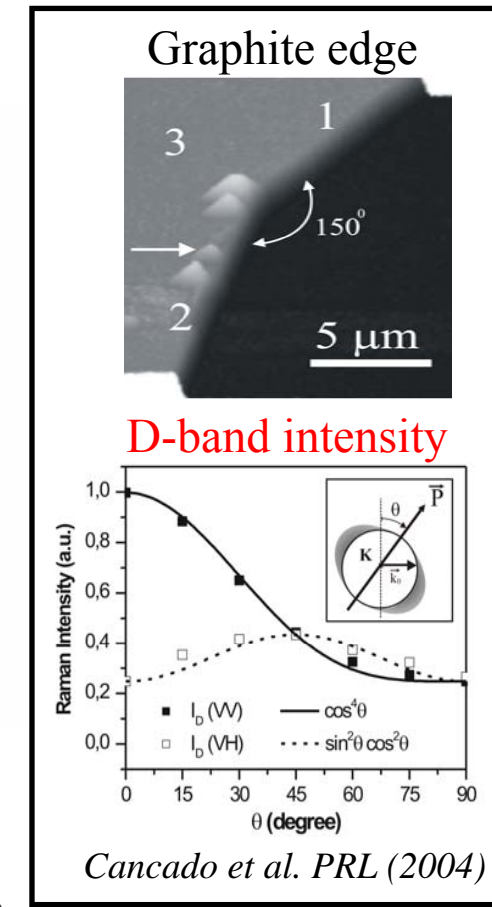
Cancado et al. PRL (2004)

The Raman signal drops for light polarized perpendicular to the nanoribbon axis



Nodes in the optical absorption
Gruneis and Saito PRB 67 (2003)

Same polarization behavior for HOPG edges

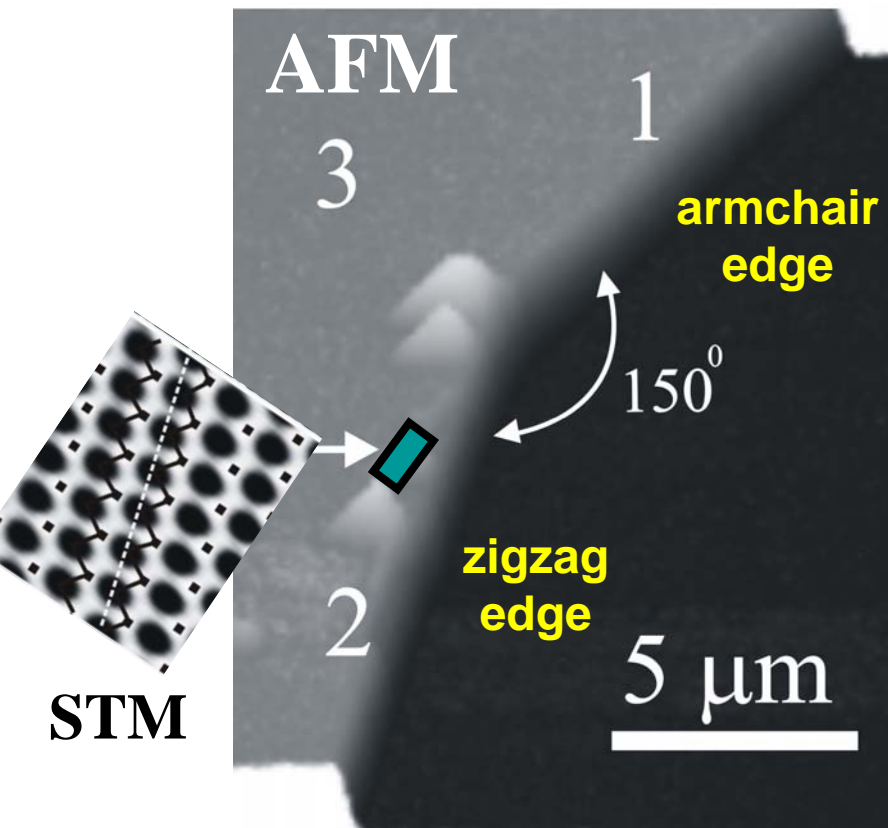


Cancado et al. PRL (2004)

Reflects the anisotropic optical absorption at the graphite edge

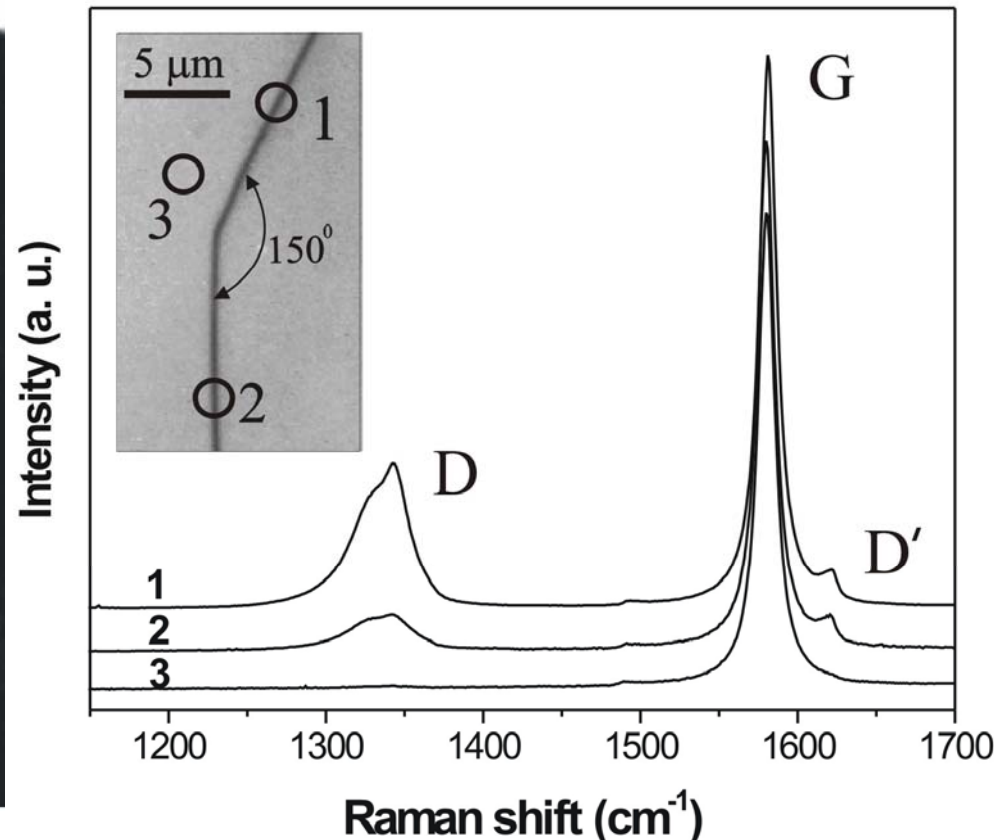
Micro-Raman spectra from graphite edges

HOPG substrate



Cancado et al. PRL (2004)

Raman Spectra

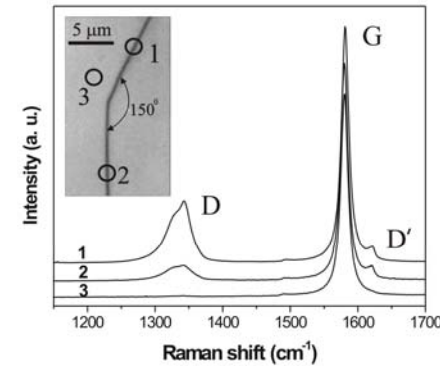
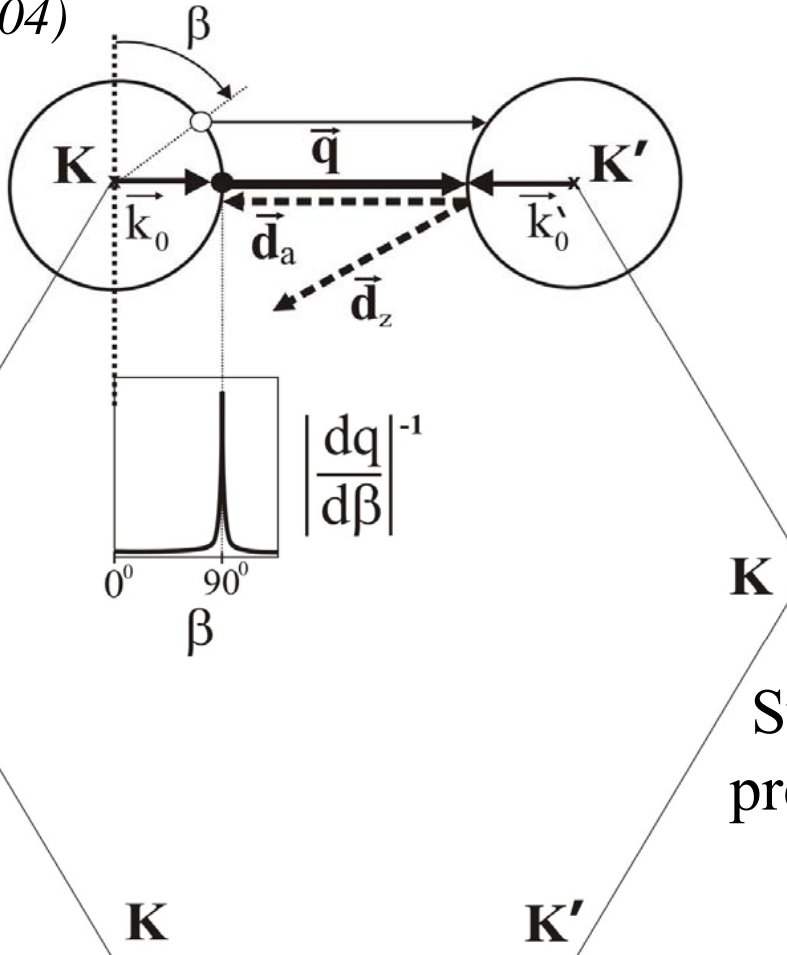
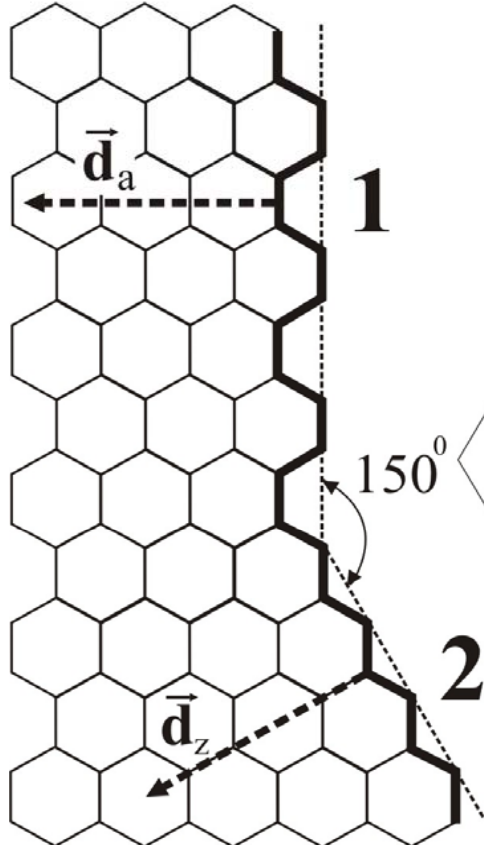


**D band is strong for armchair edge
and weak for zigzag edge**

Micro-Raman spectra from graphite edges

Double resonance one “1D defect” explains the result

Cancado et al. PRL (2004)

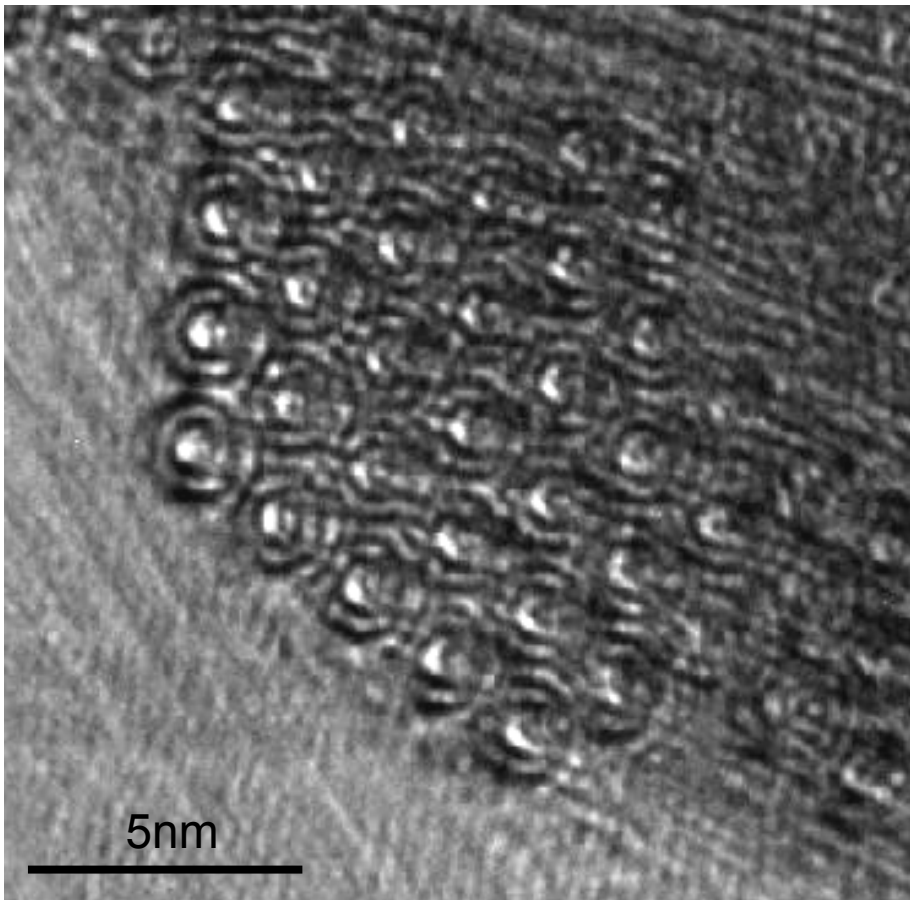


Such an effect was previously predicted for SWNTs
[Maultzsch et al., PRB(2001)]

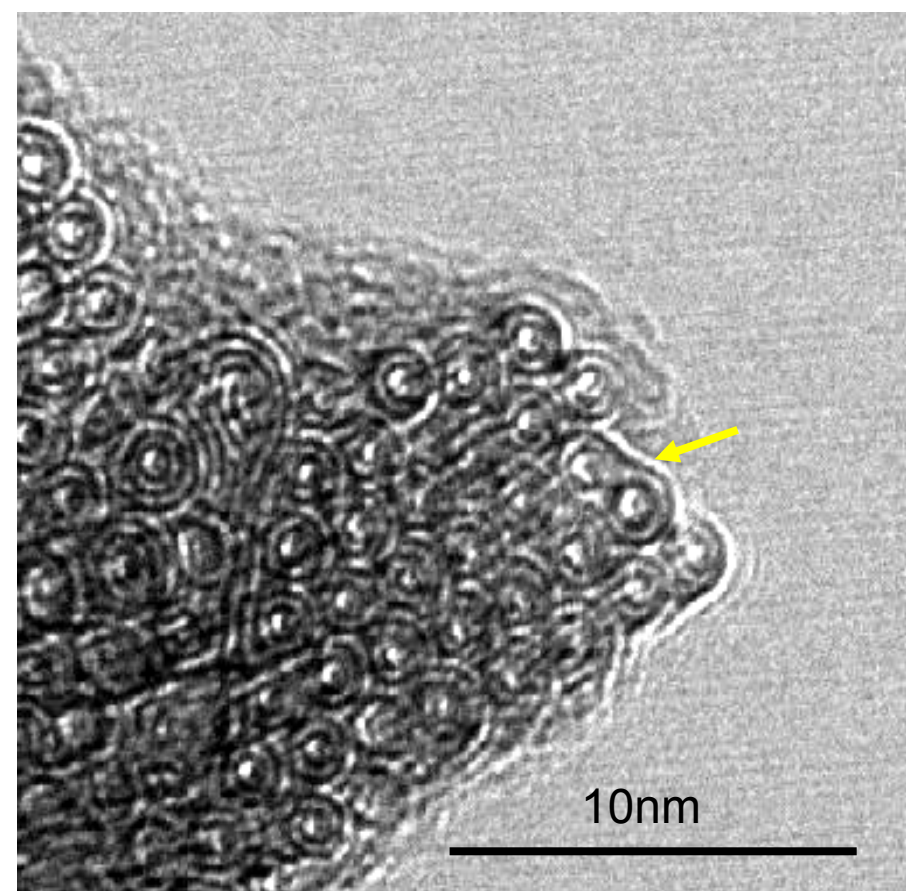
Raman can tell us if the edge has an armchair or zigzag structure

DWNT coalescence by heat treatment

High resolution TEM images of DWNTs doped with B



Heat treated at 1200°C



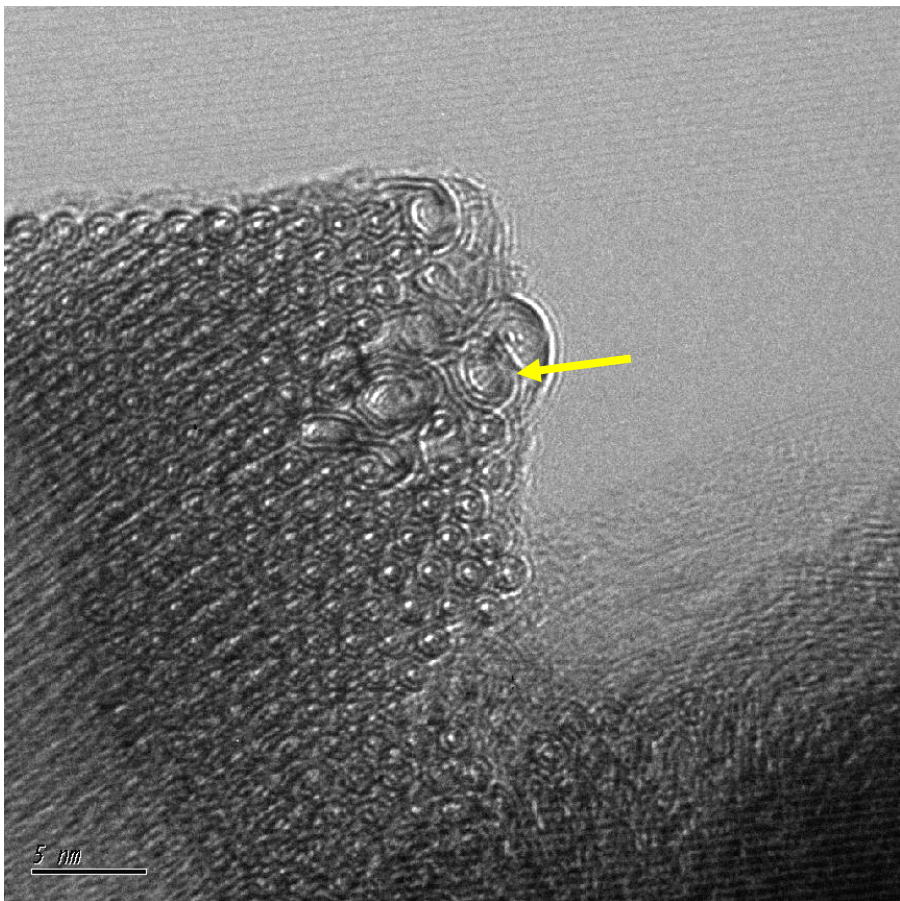
Heat treated at 1500°C

Coalescence of DWNTs outer shells are observed for 1500°C heat treatment

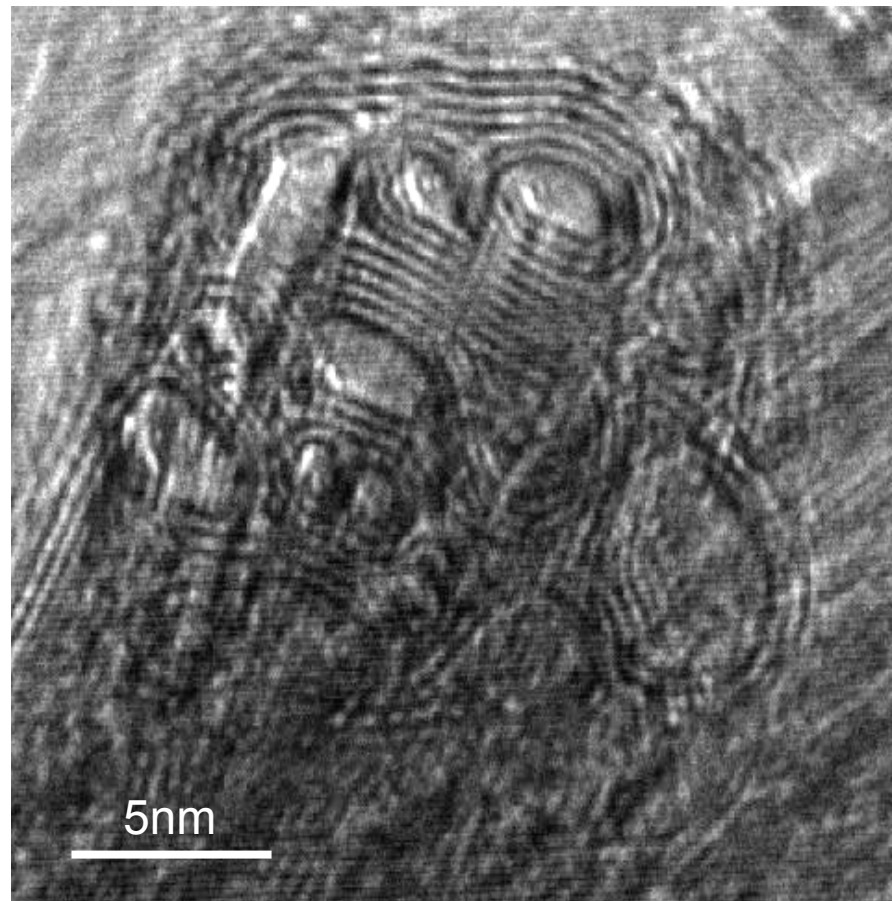
TEM images from Endo et al, Nano. Lett. (2005)

DWNT coalescence by heat treatment

High resolution TEM images of DWNTs doped with B



Heat treated at 1600°C



Heat treated at 2000°C

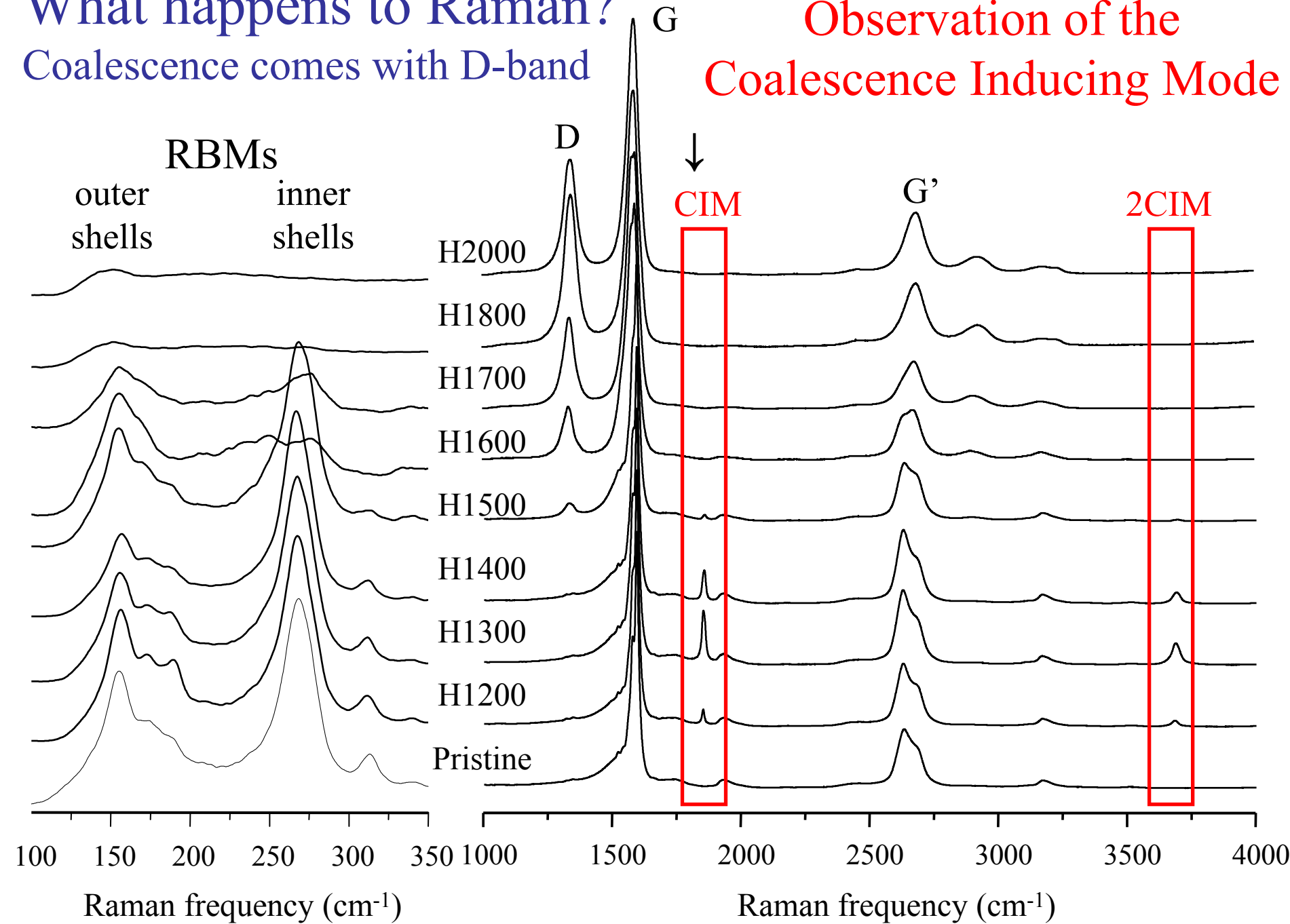
Coalescence of DWNTs is very strong for higher temperatures heat treatment

TEM images from Endo et al, Nano. Lett. (2005)

What happens to Raman?

Coalescence comes with D-band

Observation of the
Coalescence Inducing Mode

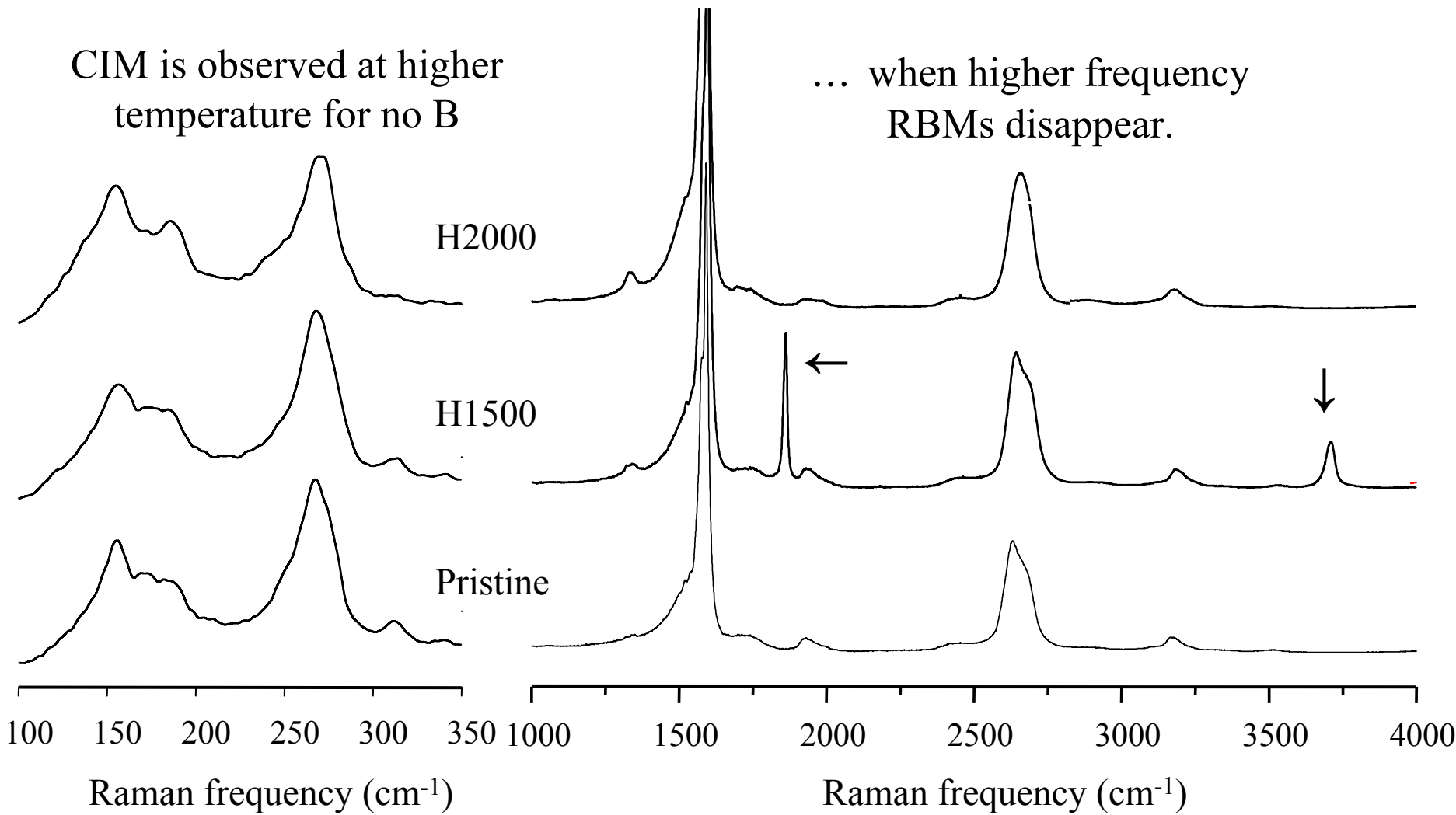


DWNT coalescence by heat treatment

Raman spectra of DWNTs with no B

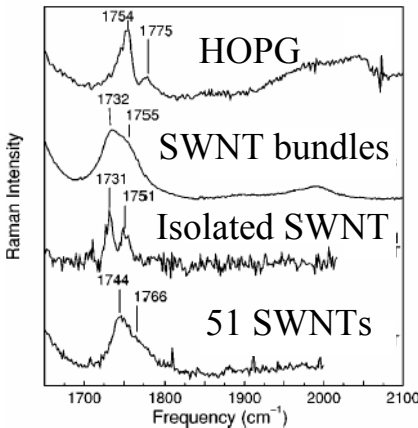
CIM is observed at higher temperature for no B

... when higher frequency RBMs disappear.



What is the physics of the CIM?

Does it tell us how coalescence occurs? How to control?



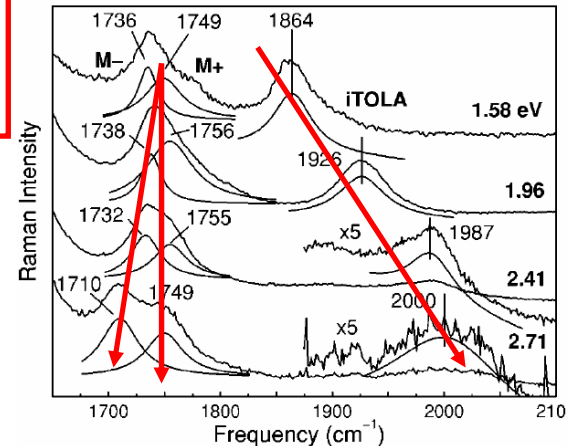
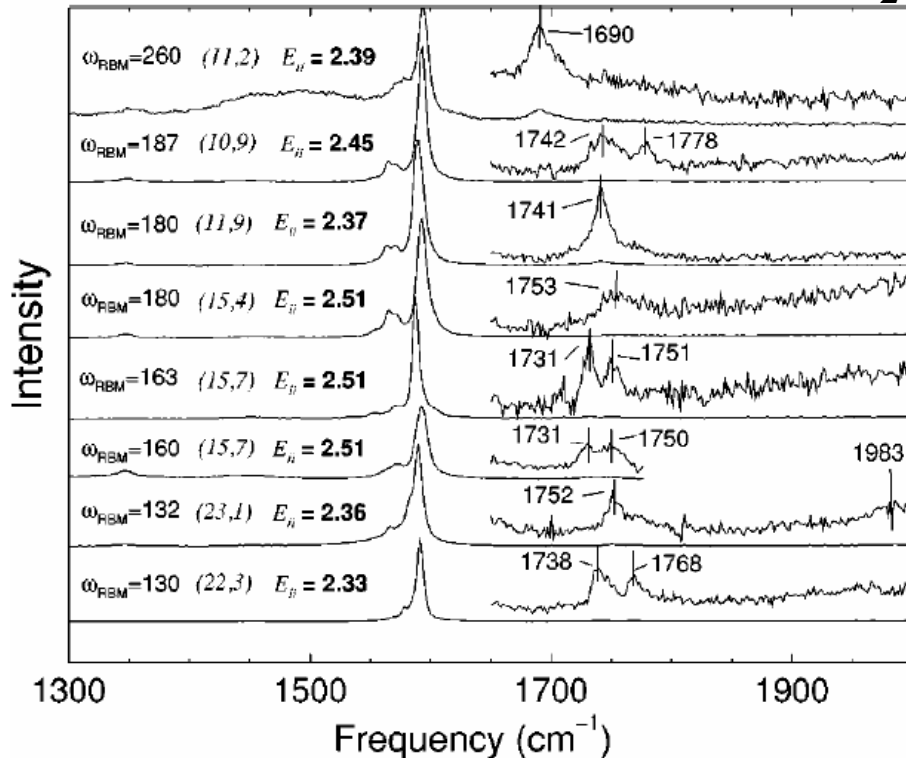
Features just above the G band

The 2oTO and iTO+LA double resonance peaks

Arc discharge SWNT bundles

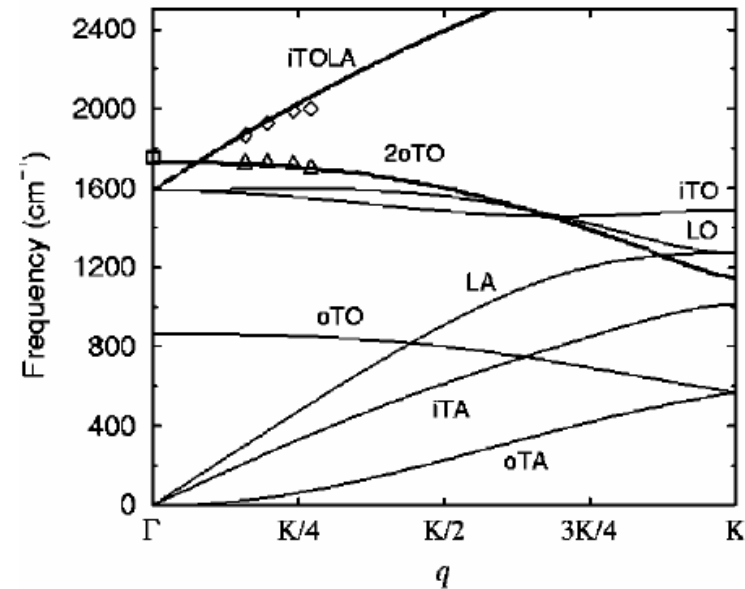
Please remember there is
nothing around 1850cm^{-1}

Different Isolated SWNTs on SiO_2



E_{laser}

Double resonance – Thomsen and Reich PRL (2001)



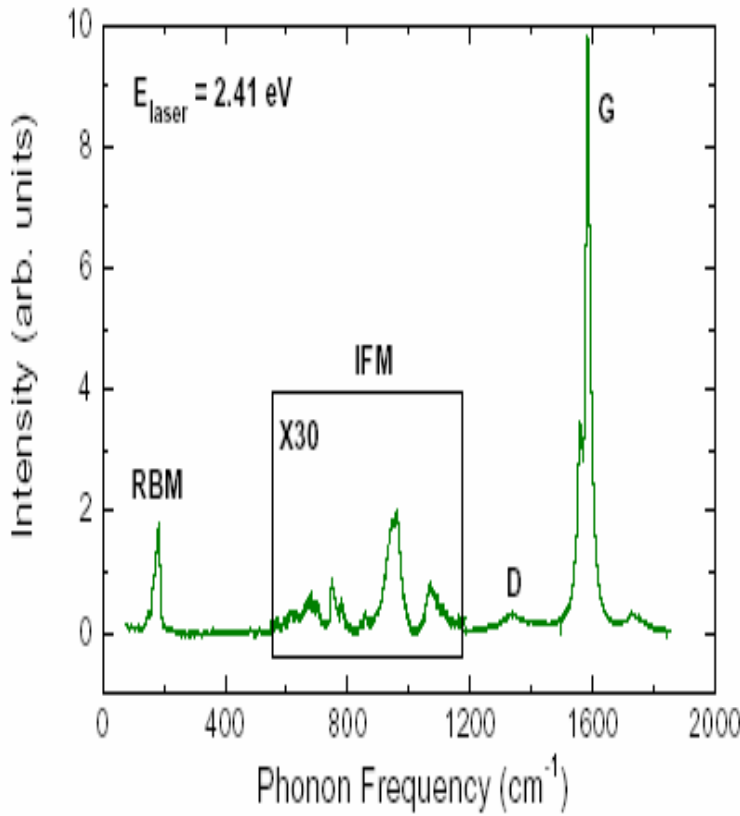
Raman Spectra of Carbon Nanotubes

Intermediate frequency modes (IFM): large number of peaks appearing between the RBM and D/G band frequencies

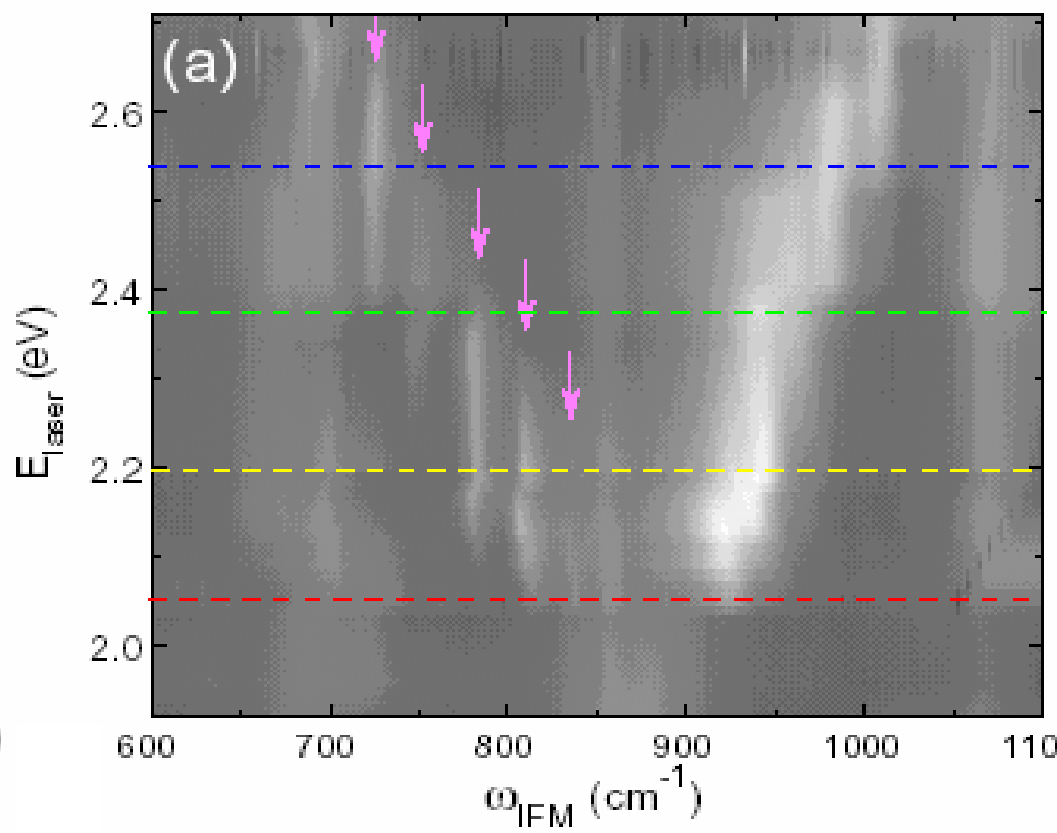
Arc discharge sample $1.2 < d_t < 1.8$ nm

C. Fantini *et al.*, *Phys. Rev. Lett.* **93**, 147406 (2004)

E_{laser} dispersion for the IFMs

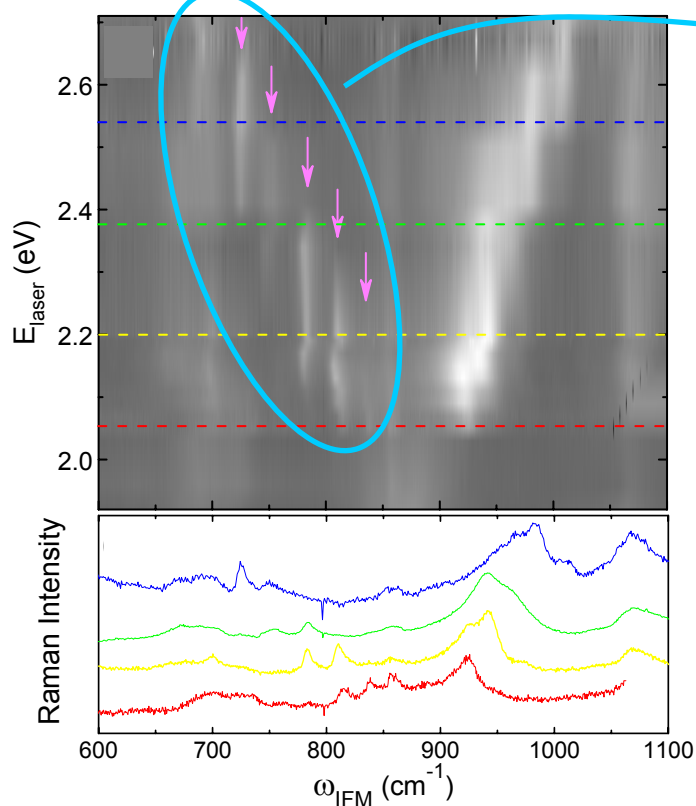


Many E_{laser} experiment:

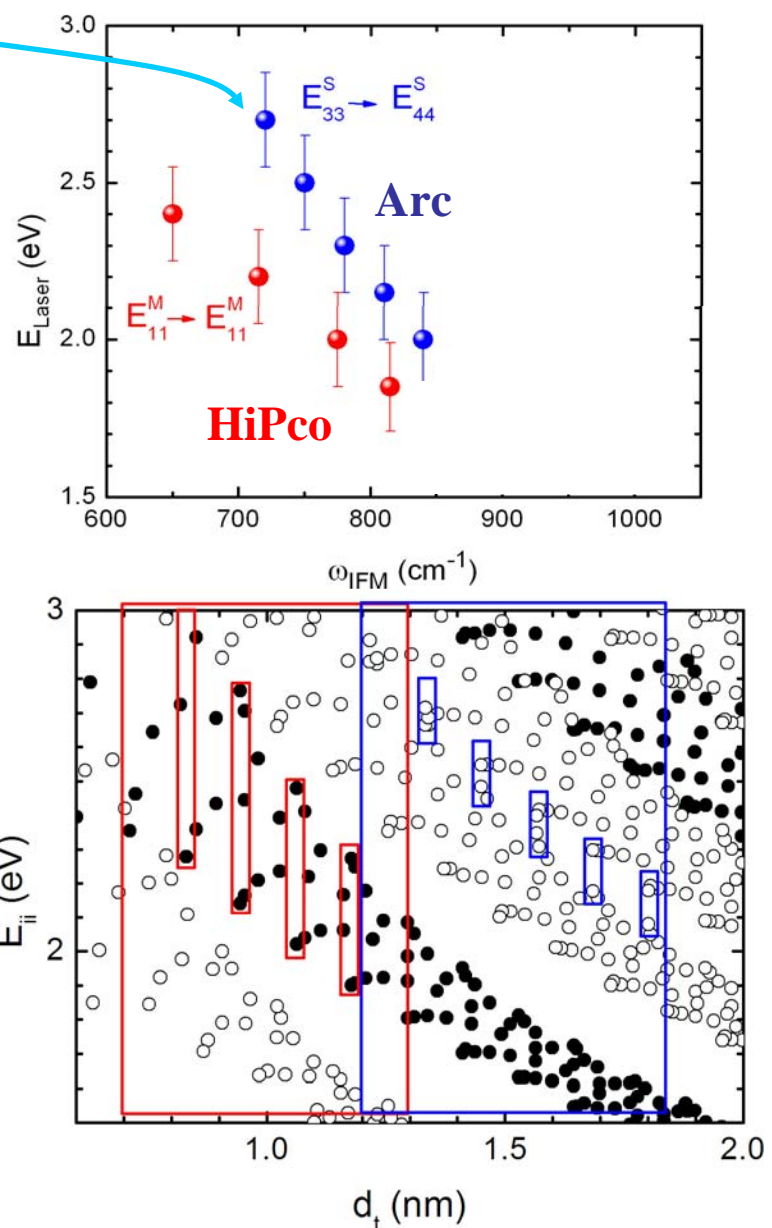


The intermediate frequency modes (IFMs)

Arc discharge sample $1.2 < d_t < 1.8$ nm



Fantini et al. PRL 92, 087401 (2004)

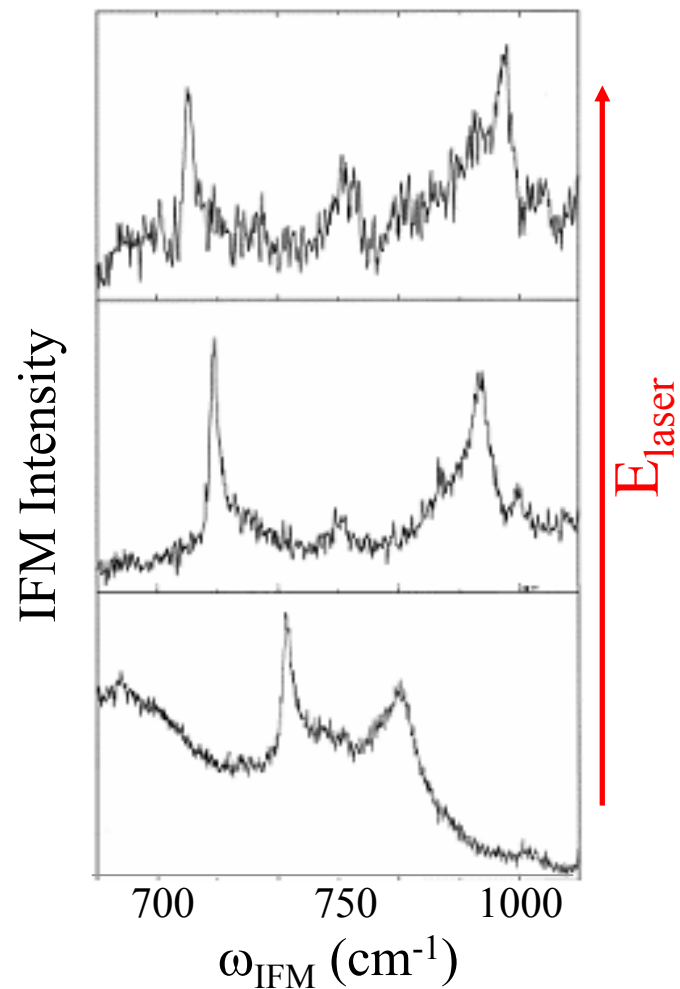
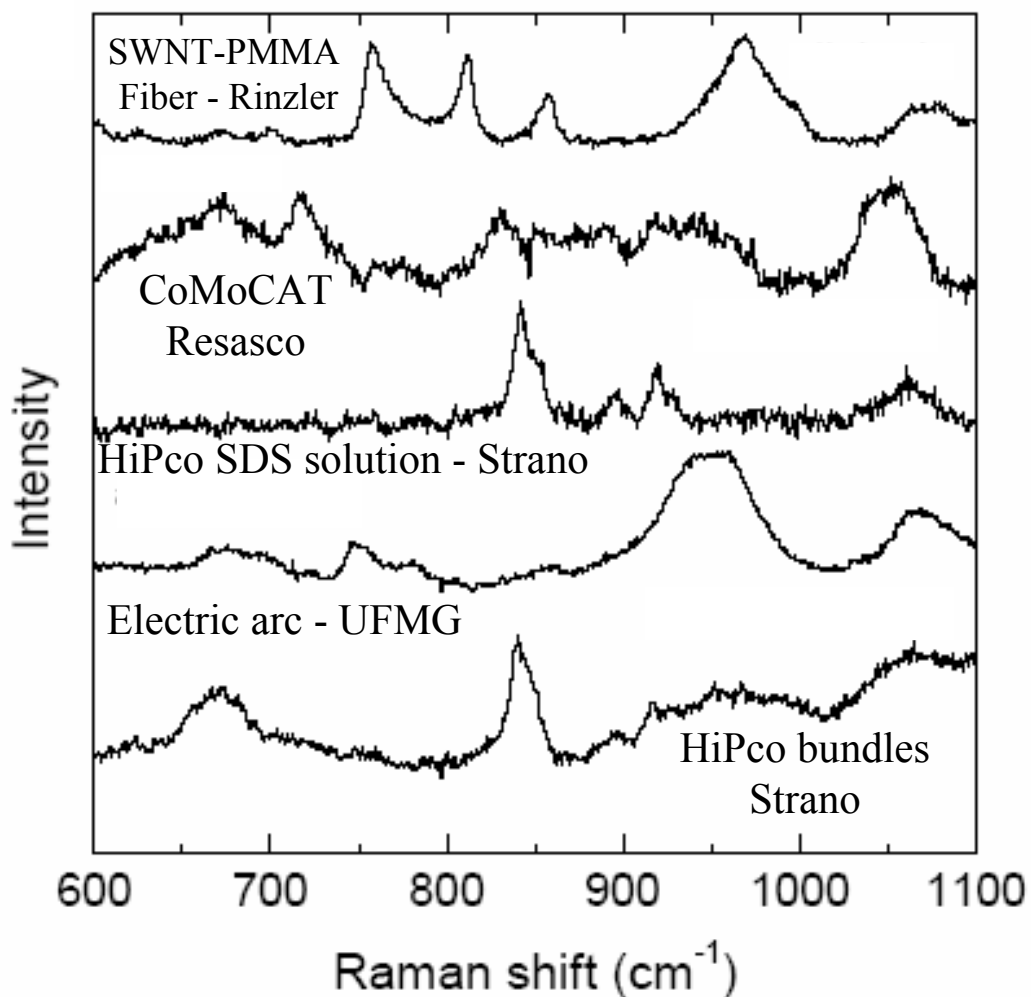


There is a close connection of IFMs with the Kataura plot – we assign (n,m)

The phonon assignments are not yet fully understood

The intermediate frequency modes (IFMs)

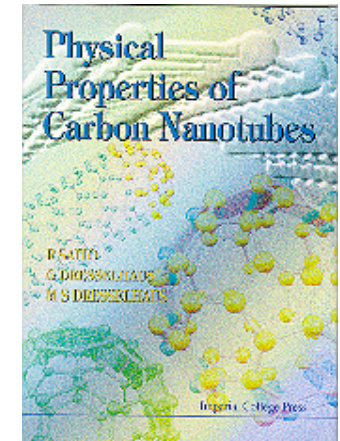
L. Alvarez et al, Chem. Phys. Lett. 320 441(2000)



Many features change from sample to sample,
and with laser line within the same sample

Outline

- Background
- Phonon Properties
- Overview of Raman Effect
- First-order Raman Processes
-(the RBM and G-Band)
- Double Resonance Processes
- **Photoluminescence**
- Excitons



"Physical Properties of Carbon Nanotubes",
by R. Saito, G. Dresselhaus and M.S. Dresselhaus,
Imperial College Press (1998) ISBN 1-86094-093-5

Advances in RRS through Photoluminescence (PL) Studies

(n,m) identification through PL

Kataura Plots and (2n+m) family effects from PL

First principles Extended Tight Binding calculations

Characterization of environmental effects by RRS and PL

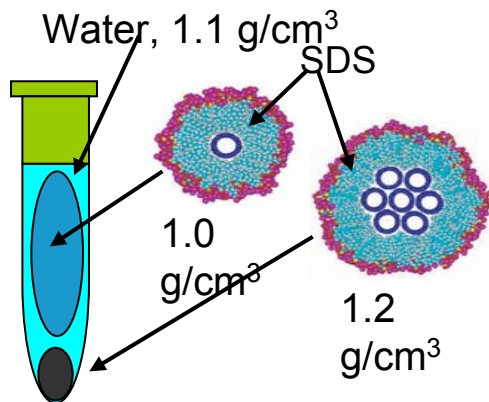
- Different synthesis methods: HiPco and CoMoCAT
- Different wrapping agents: SDS, DNA, etc.
- Different substrates: Si/SiO₂, sapphire, freely suspended

Phonon-Assisted processes

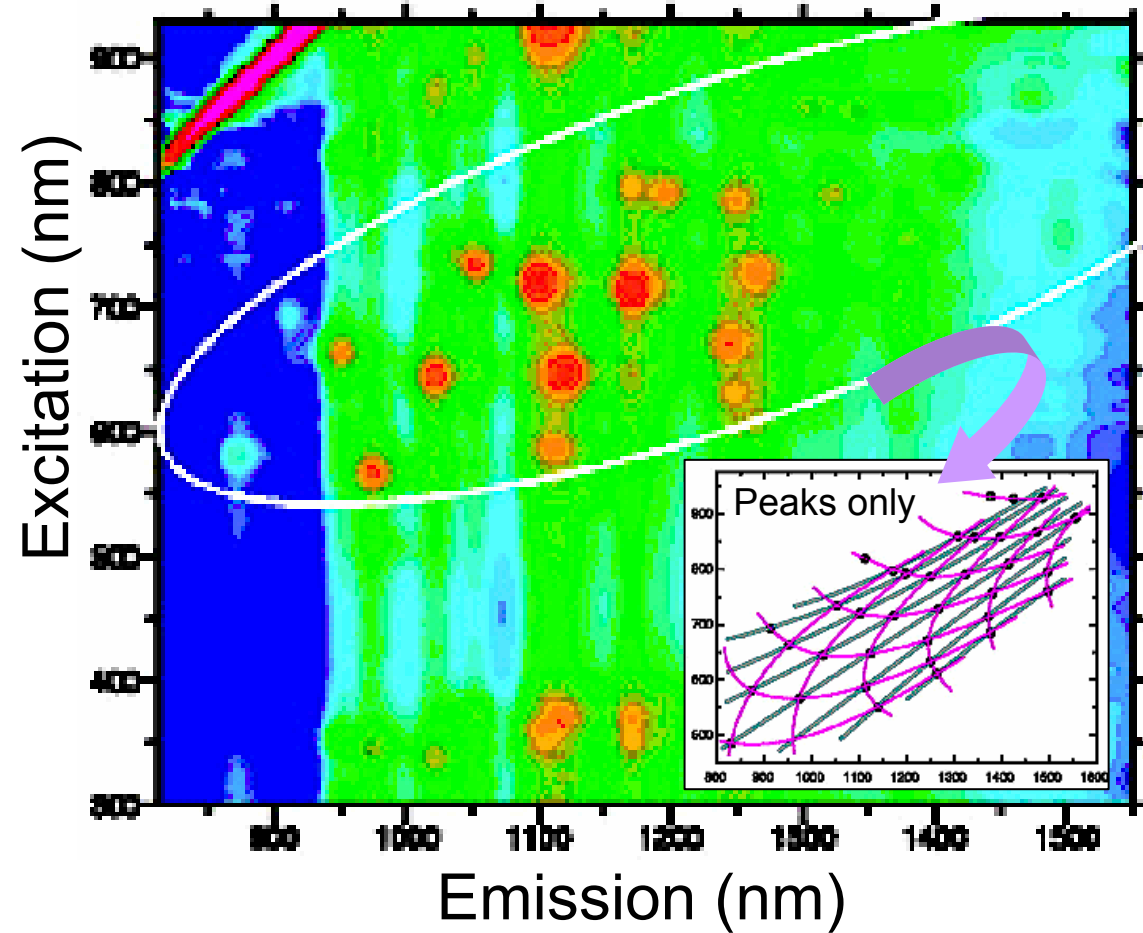
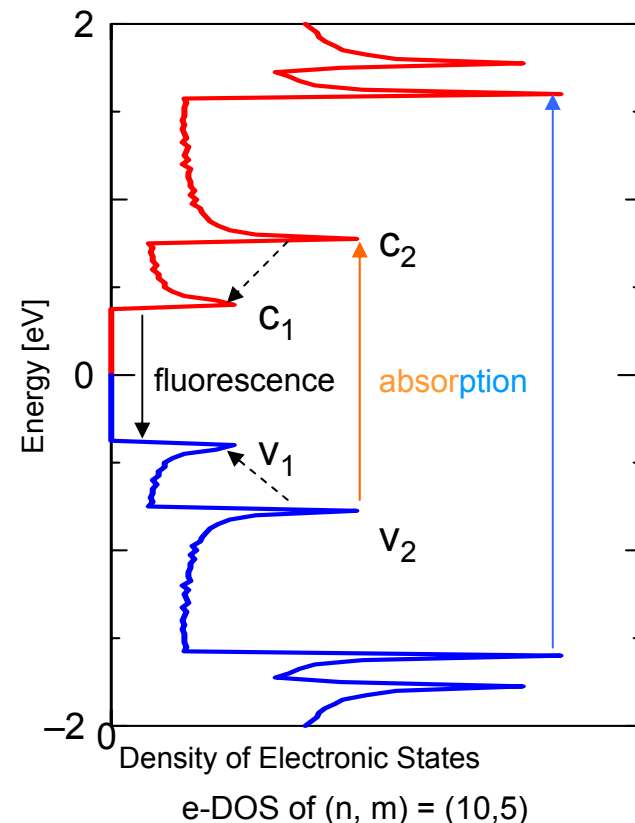
- Frequency domain
- Time domain (fast optics)

Band Gap Fluorescence

M. J. O'Connell *et al.*, Science 297 (2002) 593
S. M. Bachilo *et al.*, Science 298 (2002) 2361.



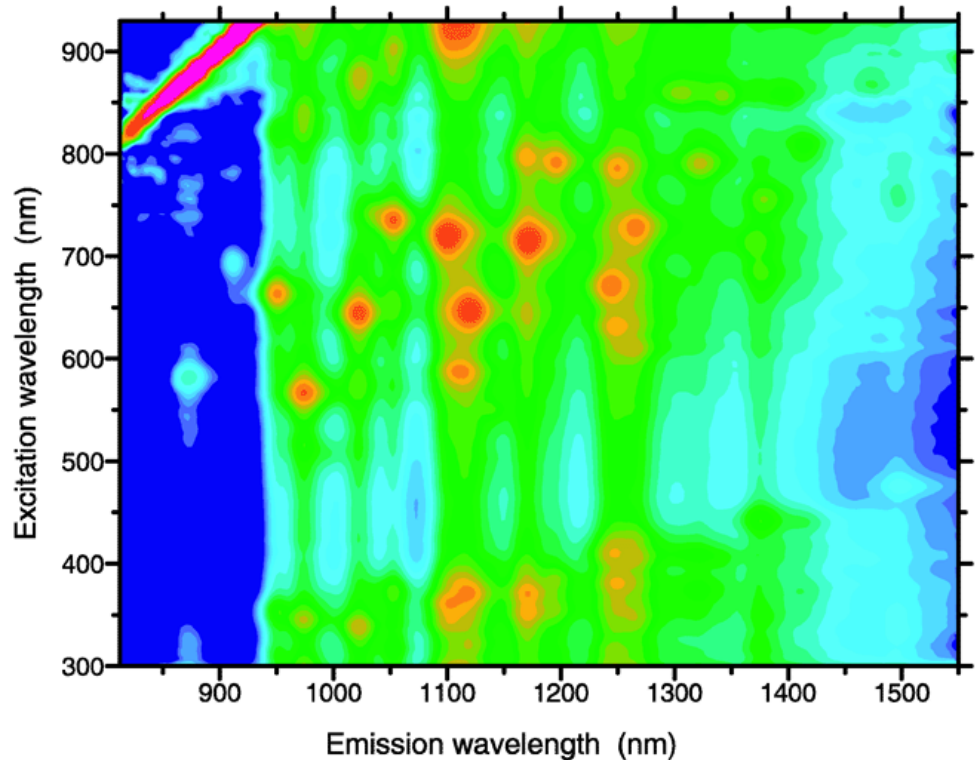
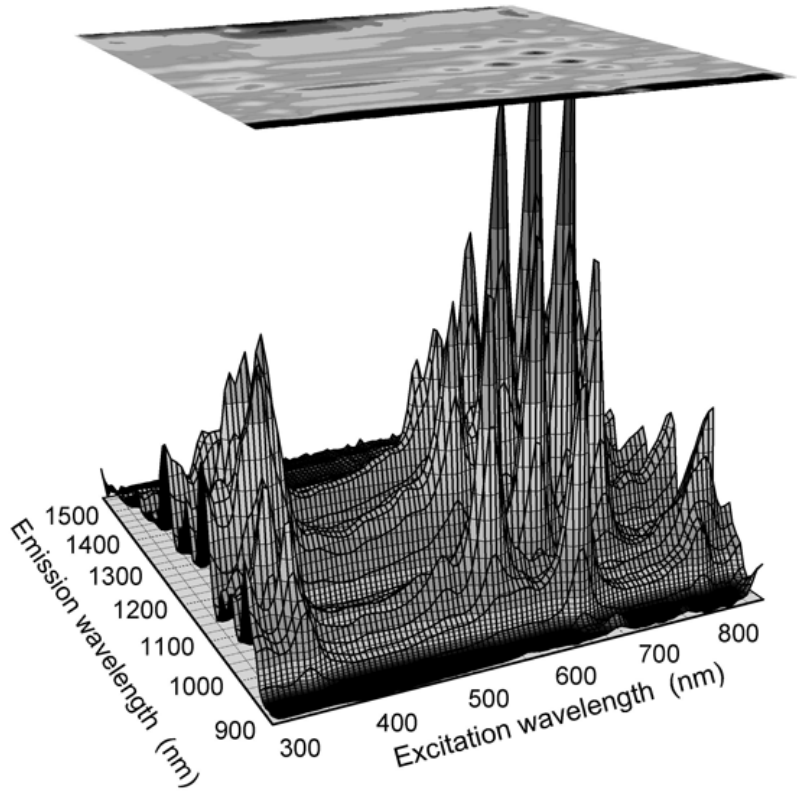
Wrapping agents
SDS=Sodium Dodecyl Sulfate



(n,m) Assignments Made by Empirical
Excitation-Emission Pattern

PHOTOLUMINESCENCE

SDS-wrapped HiPco nanotubes in solution

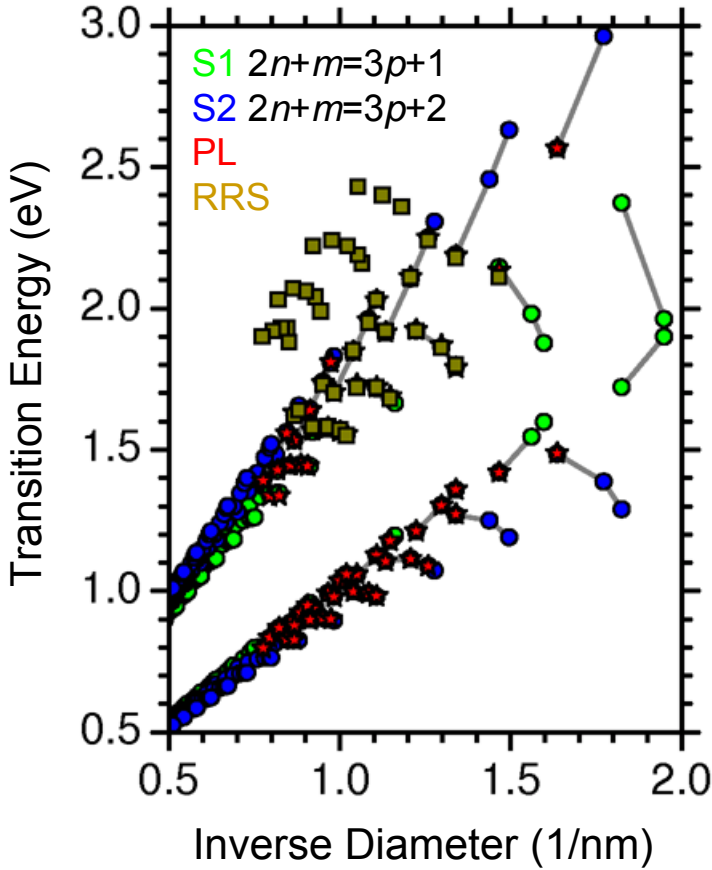


$2n+m=\text{constant}$ family patterns are observed in the PL excitation-emission spectra
3D maps, first shown for PL spectra, but influenced future RRS experiments

S. M. Bachilo et al., Science 298, 2361 (2002)

EMPIRICAL KATAURA PLOT

based on fitting PL experiments



Family behavior (small diameter limit)

- ❖ Strong difference between E_{ii}^{S1} and E_{ii}^{S2}
- ❖ Strong chirality dependence of E_{ii}^S
(chirality changes from armchair to zigzag along family lines)

$$\bar{\nu}_{11}(\text{mod 1}) = \frac{1 \times 10^7 \text{ cm}^{-1}}{157.5 + 1066.9d_t} - 771 \text{ cm}^{-1} \frac{[\cos(3\alpha)]^{1.374}}{d_t^{2.272}}$$

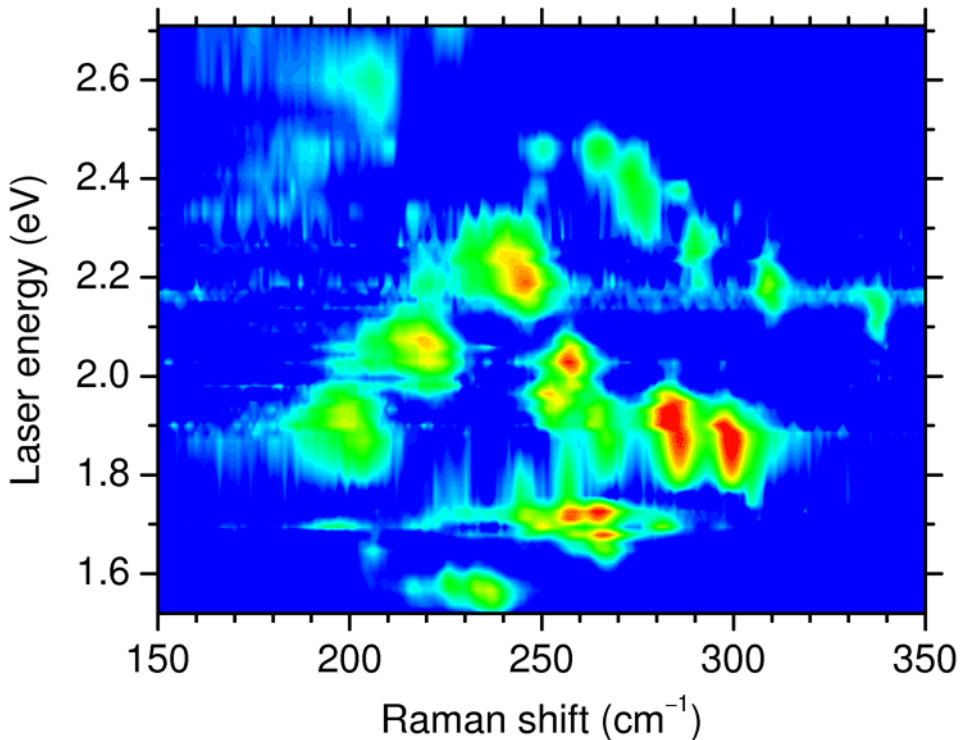
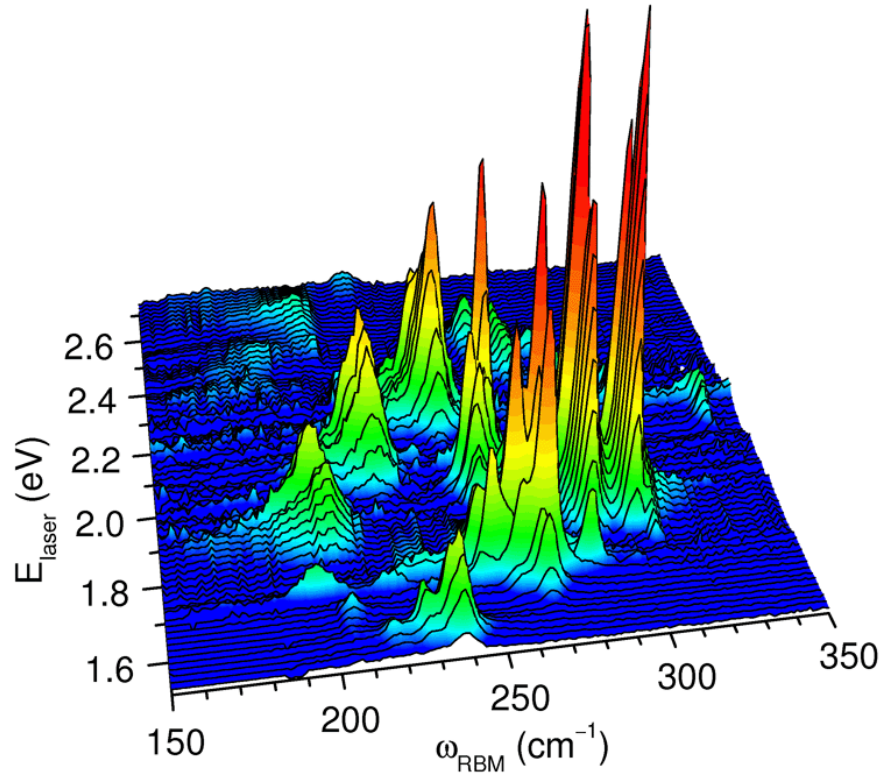
$$\bar{\nu}_{11}(\text{mod 2}) = \frac{1 \times 10^7 \text{ cm}^{-1}}{157.5 + 1066.9d_t} + 347 \text{ cm}^{-1} \frac{[\cos(3\alpha)]^{0.886}}{d_t^{2.129}}$$

$$\bar{\nu}_{22}(\text{mod 1}) = \frac{1 \times 10^7 \text{ cm}^{-1}}{145.6 + 575.7d_t} + 1326 \text{ cm}^{-1} \frac{[\cos(3\alpha)]^{0.828}}{d_t^{1.809}}$$

$$\bar{\nu}_{22}(\text{mod 2}) = \frac{1 \times 10^7 \text{ cm}^{-1}}{145.6 + 575.7d_t} - 1421 \text{ cm}^{-1} \frac{[\cos(3\alpha)]^{1.110}}{d_t^{2.497}}$$

RAMAN (RRS)

SDS-wrapped HiPco nanotubes in solution used for RRS and PL

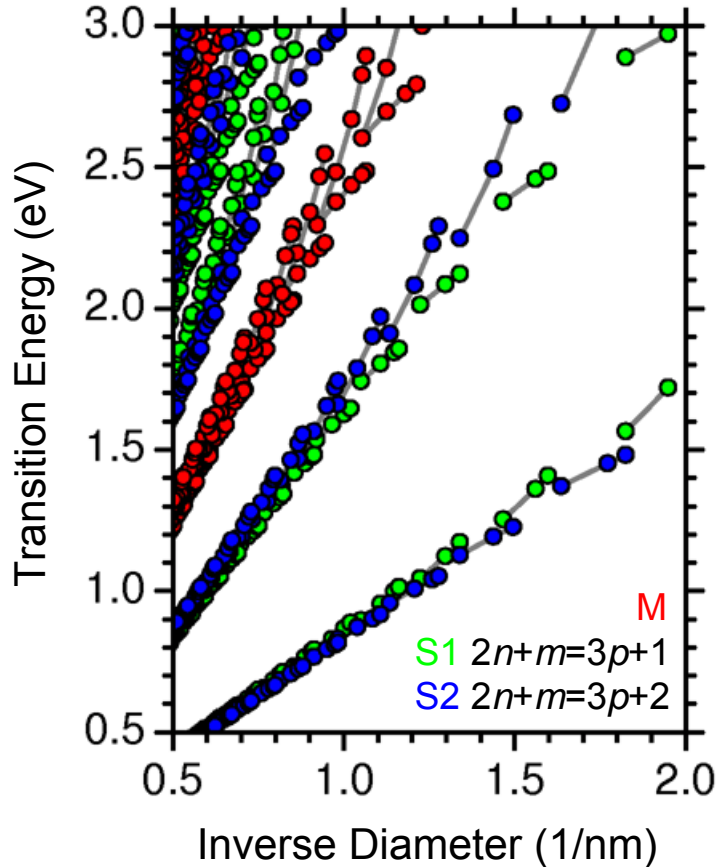


The same optical transition energies E_{ii} are observed in RRS and PL

C. Fantini et al., PRL 93, 147406 (2004)

SIMPLE TIGHT BINDING MODEL

π -band nearest-neighbor model



Simple tight binding model has been successfully used for small diameter SWNTs

Problems of simple tight binding model

Family behavior problem (small diameter limit)

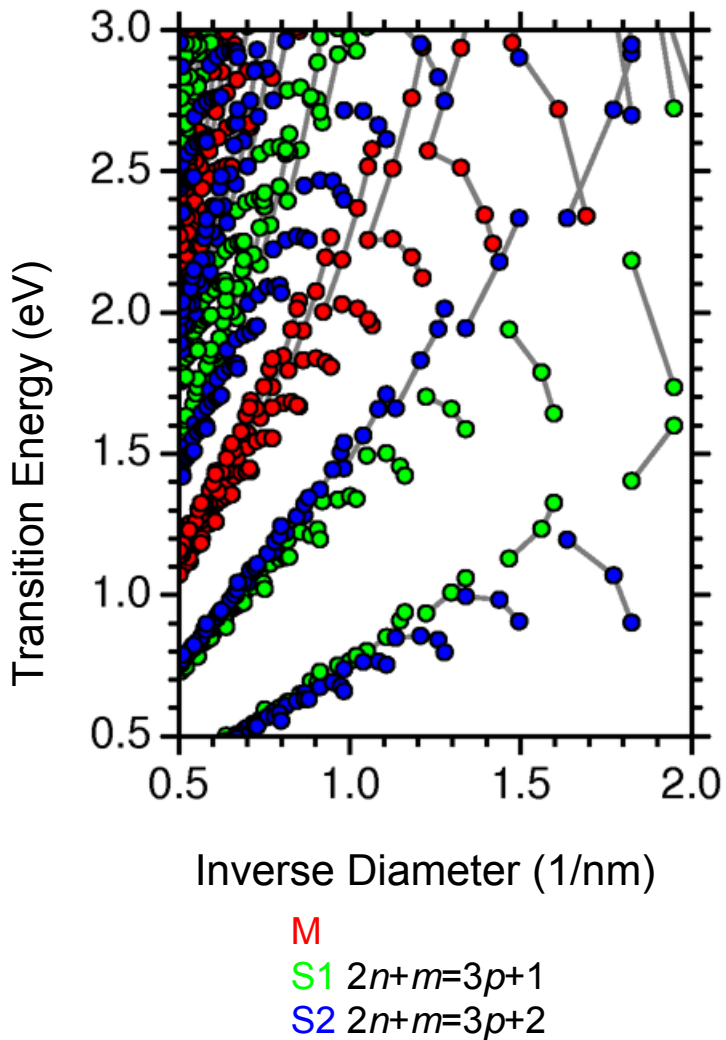
- ❖ Small difference between E_{ii}^{S1} and E_{ii}^{S2}
- ❖ Weak chirality dependence of E_{ii}^S
(chirality changes from armchair to zigzag along family lines)

Ratio problem (large diameter limit)

- ❖ E_{22}^S to E_{11}^S ratio
~2 from simple tight-binding
~1.75 from PL empirical fit

transfer integral $t = 2.89$ eV
overlap integral $s = 0$

EXTENDED TIGHT BINDING MODEL



Kataura plot is calculated within the extended tight-binding approximation using Popov/Porezag approach:

- ❖ curvature effects ($ss\sigma$, $sp\sigma$, $pp\sigma$, $pp\pi$)
- ❖ long-range interactions (up to $\sim 4\text{\AA}$)
- ❖ geometrical structure optimization



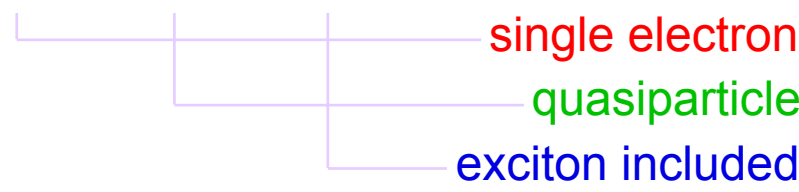
The extended tight-binding calculations show family behavior (differentiation between S1 & S2 and strong chirality dependence) similar to that of PL empirical fit

COMPARISON of ETB TO FIRST PRINCIPLES

C. D. Spataru et al., PRL 92, 077402 (2004)

Lowest two optical transition energies for the (8,0) SWNT.

TB	Present work			Deduced from experiment
	LDA	GW	BS	
ν_{11} (eV)	...	1.39	2.54	1.55
ν_{22} (eV)	...	1.51	2.66	1.80
ν_{22}/ν_{11}	1.6	1.09	1.05	1.16



$$\begin{aligned} E_{ii} &= E_{ii}^e \\ E_{ii} &= E_{ii}^e + E_{ii}^{ee} \\ E_{ii} &= E_{ii}^e + E_{ii}^{ee} + E_{ii}^{eh} \end{aligned}$$

The ETB model with many-body corrections was applied to the (8,0) S1 nanotube

Reference	E_{11}^e	E_{22}^e	E_{11}^{ee}	E_{22}^{ee}	E_{11}^{eh}	E_{22}^{eh}	E_{11}	E_{22}	E_{22} / E_{11}
Weisman	—	—	—	—	—	—	1.60	1.88	1.18
Spataru	1.39	1.51	1.15	1.15	-0.99	-0.86	1.55	1.80	1.16
This work	1.33	1.64	1.22	1.03	-0.95	-0.82	1.60	1.85	1.16

Good agreement is achieved. ETB model is used to interpret experiments

Characterization for Environmental Effects

Both RRS and PL are being used to measure environmental effects on E_{ij} and ω_{RBS} according to :

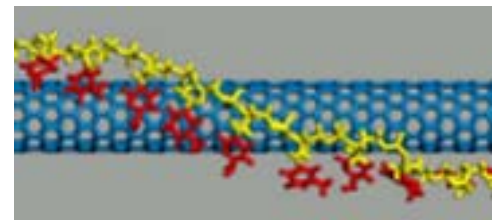
- Synthesis methods: HiPco, CoMoCAT, etc
- Wrapping agents: SDS, DNA, etc
- Substrate: Freely suspended, in solution, on Si/SiO₂, Sapphire substrates, etc.

Different Wrapping Agents

DNA – an Alternative SWNT Isolation Method to SDS Dispersion

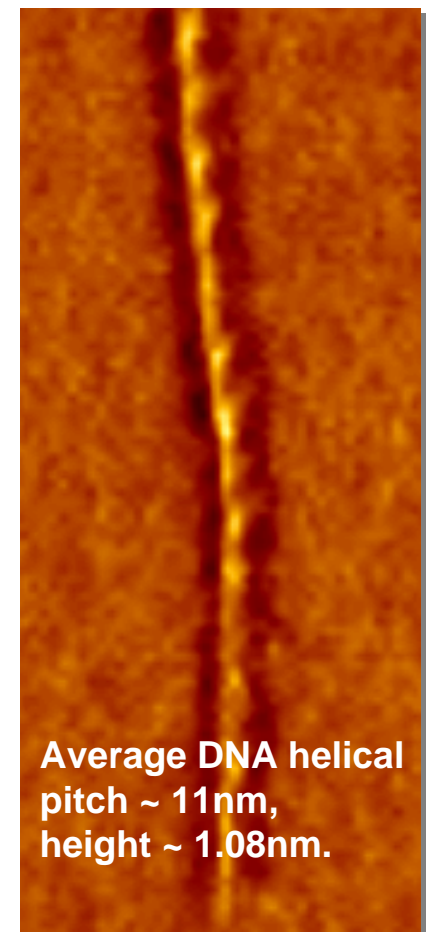
DNA Wrapping:

- Aromatic interaction
- Partial coverage, different perturbation



Chromatography and Fractionation:

- DNA strands selects smaller d_t SWNTs
- Ion exchange chromatography separation by charge
- Fractionated sample enriched in a single (n,m) species

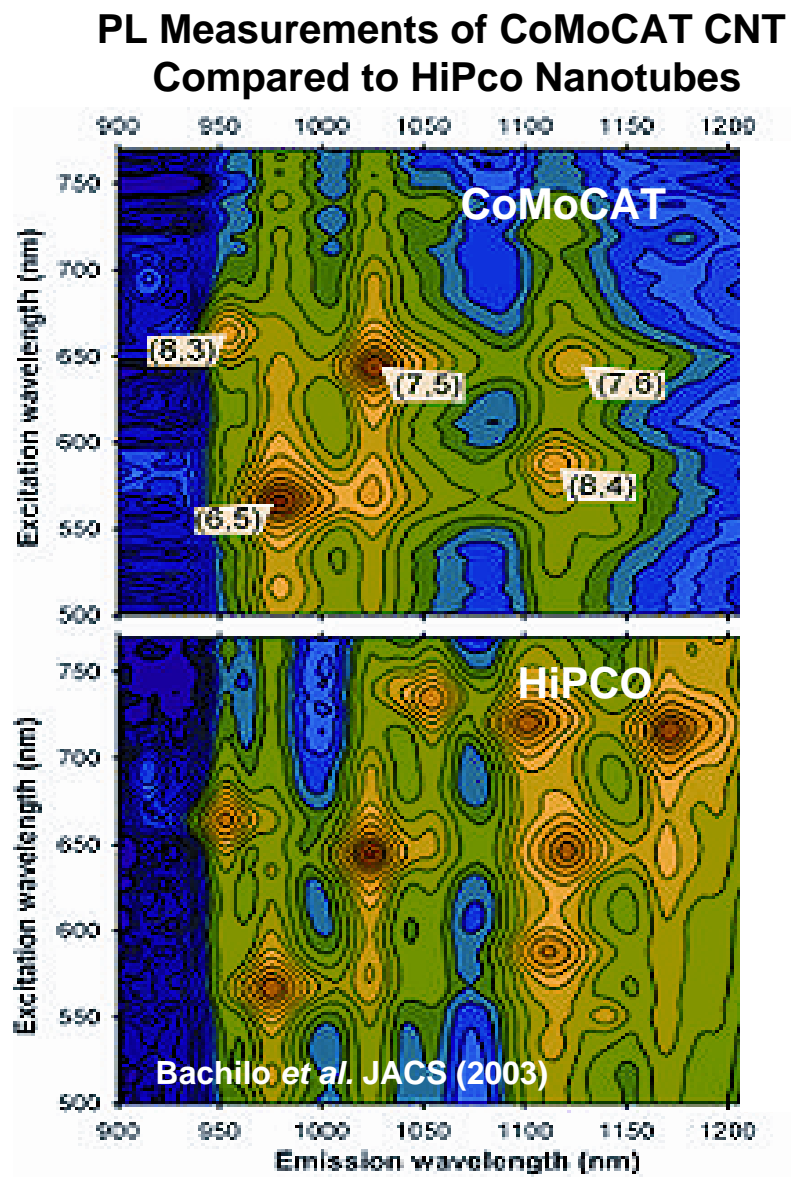


Interesting Science:

- Environment effects on optical processes.
- Phonon-assisted processes

Different Synthesis Methods for Small Diameter SWNTs: CoMoCAT and HiPco Growth Processes

- SWNT bundles synthesized using silica supported Co-Mo catalysts, with Co:Mo ratio optimized to produce a narrow d_t distribution.
- PL Intensity analysis shows that (6,5) and (7,5) nanotubes account for 57% of the CoMoCAT sample, (not including the metallic and non-fluorescing species.)
- HiPco SWNTs have a wider diameter distribution, with a wider distribution of (n,m) values and an average diameter larger than that of CoMoCAT CNTs.
- Average d_t
 - HiPco = $1.05 \text{ nm} \pm 0.15$
 - CoMoCAT = 0.81 nm



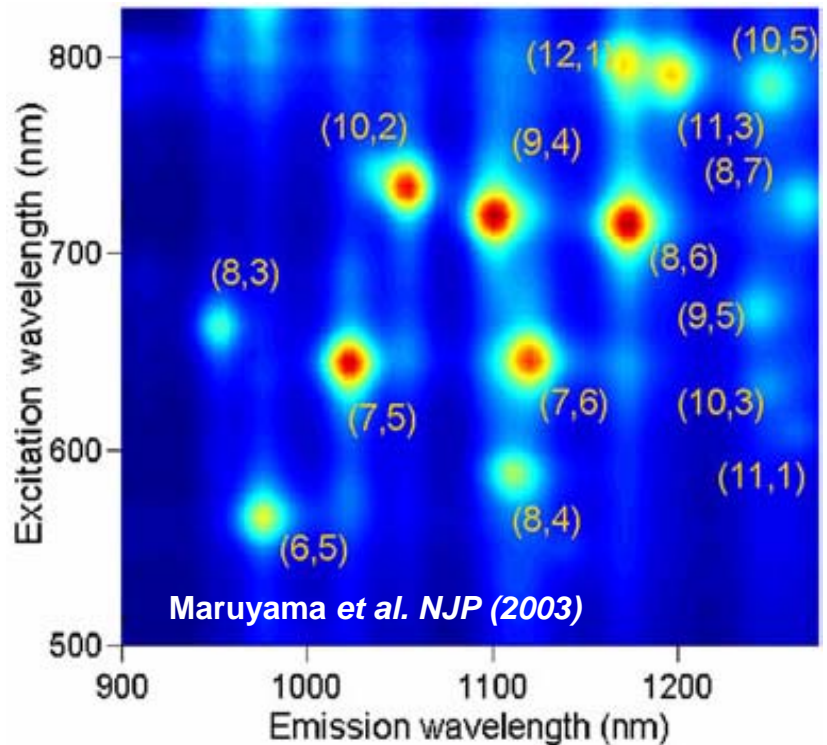
Nanotube PL Spectroscopy

Measurements in 2002-3

Excitation at E_{22} , and emission at E_{11}

- measured with Xe lamp
- $(2n+m)$ family patterns give (n, m) identifications.
- Reports of mysterious “orphan” transitions

PL map of SDS- dispersed HiPco CNTs

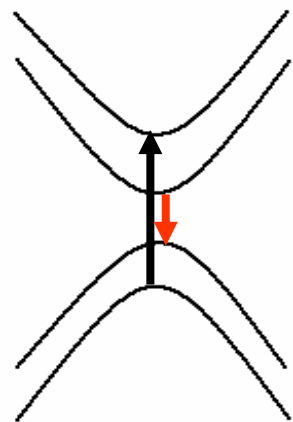


Maruyama work suggests study of detailed phonon-assisted excitonic relaxation processes for different phonon branches.

Study of Phonon-Assisted PL Spectra

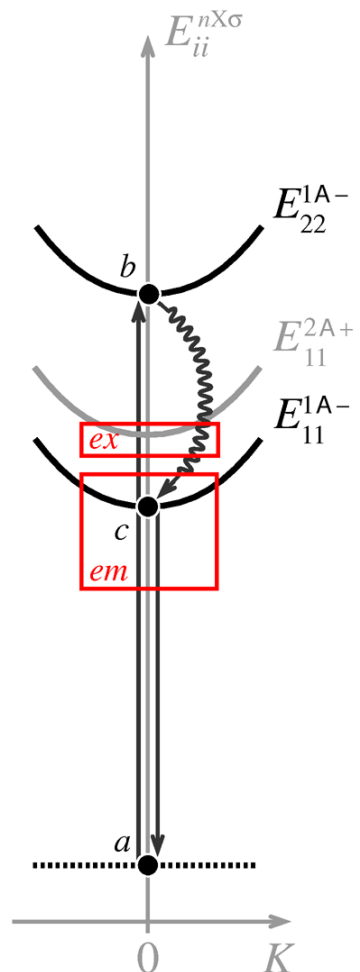
- Carried out on DNA wrapped CoMoCAT samples with dominant (6,5) species
- Used laser light excitation source

Free e-h model



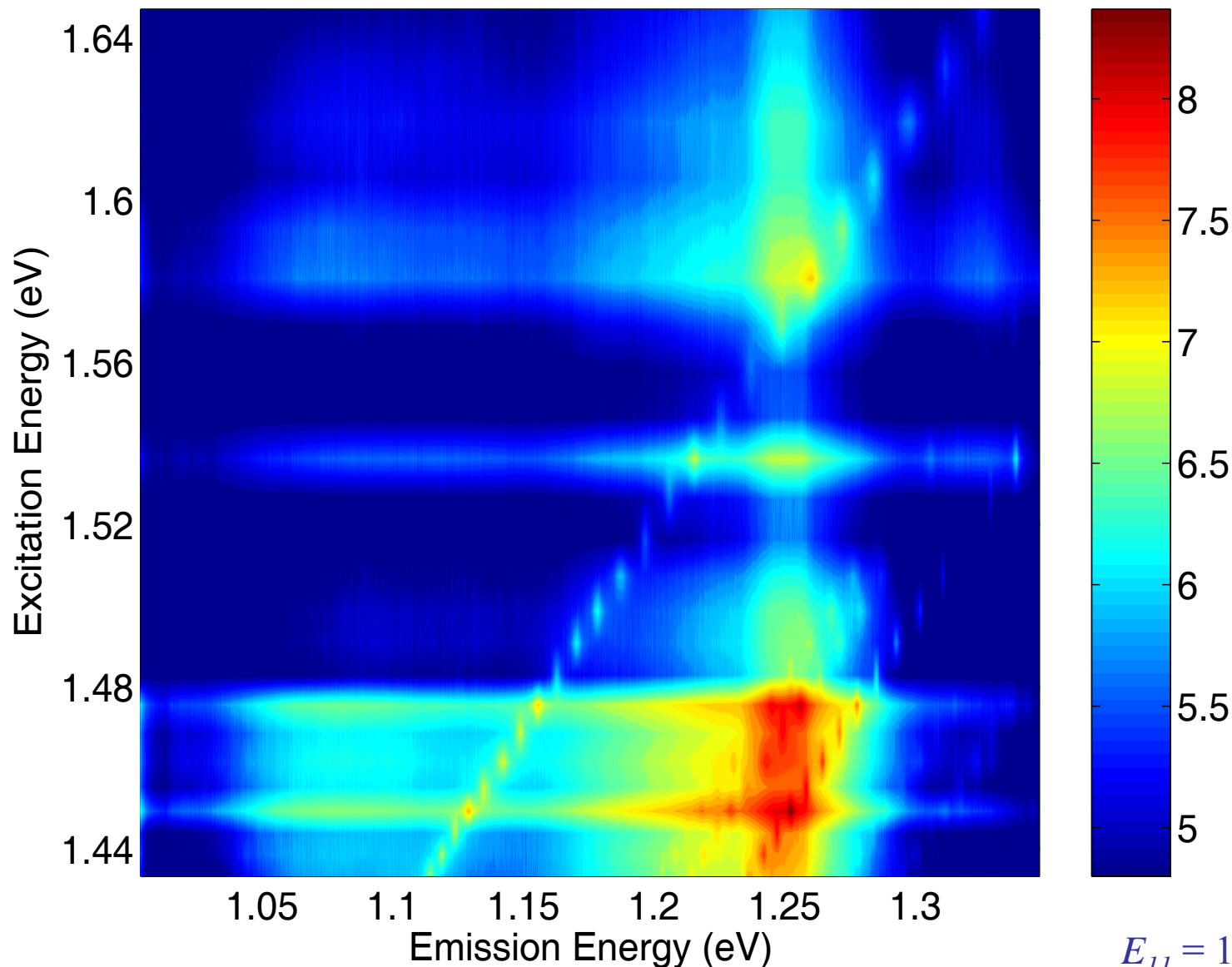
$$E_{\text{ex}} = E_{22}$$
$$E_{\text{PL}} = E_{11}$$

Excitonic model



J. Jiang, et al., Phys. Rev. B, **71**, 045417 (2005)
S.G. Chou, et al, PRL **94**, 177402 (2005)

PL Spectra of (6,5) Nanotubes



$$E_{11} = 1.26\text{eV}$$

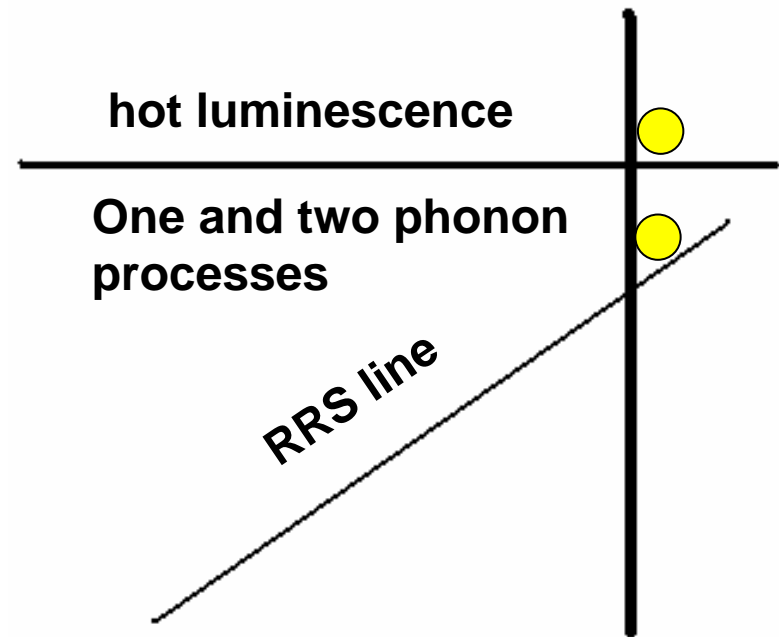
$$E_{22} = 2.18\text{eV}$$

Orphan transitions on an expanded scale
Chou, et al PRL 94, 127402 (2005)

Different Channels of Phonon-Assisted Relaxation Processes are Observed

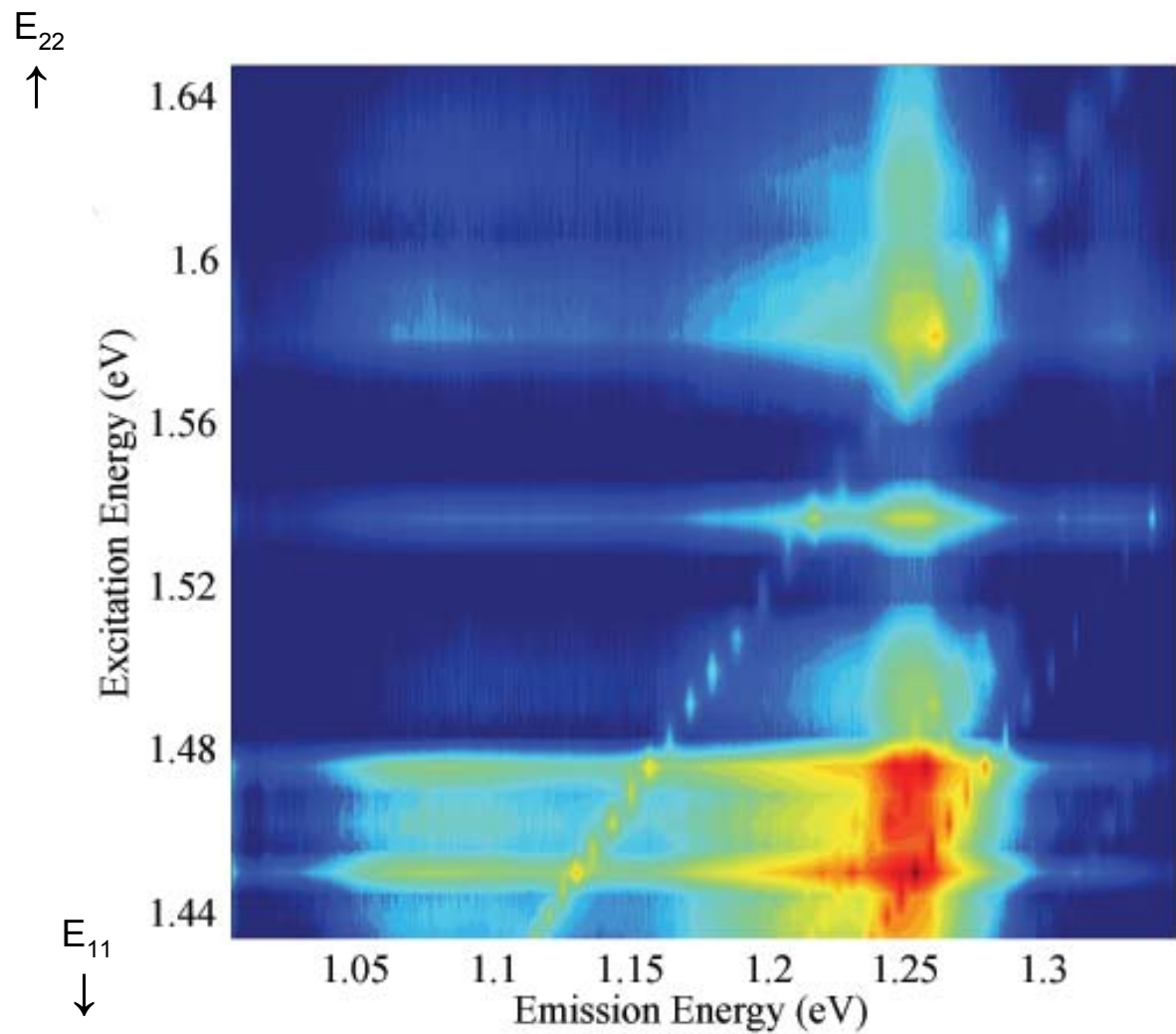
- Two phonon processes
- One phonon process
- Hot Luminescence
- RRS process (1 phonon)
- RRS process (2 phonons)

Phonons observed by Photoluminescence (PL) are same phonons seen by Resonance Raman Spectroscopy (RRS)

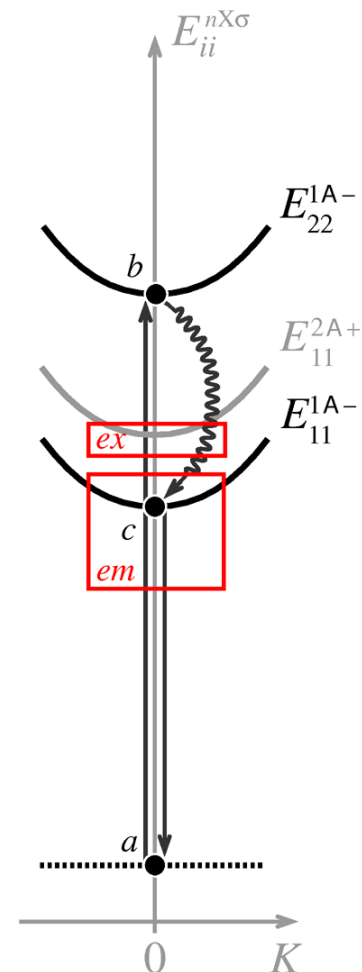


$$E_{\text{PL}} = E_{11}$$

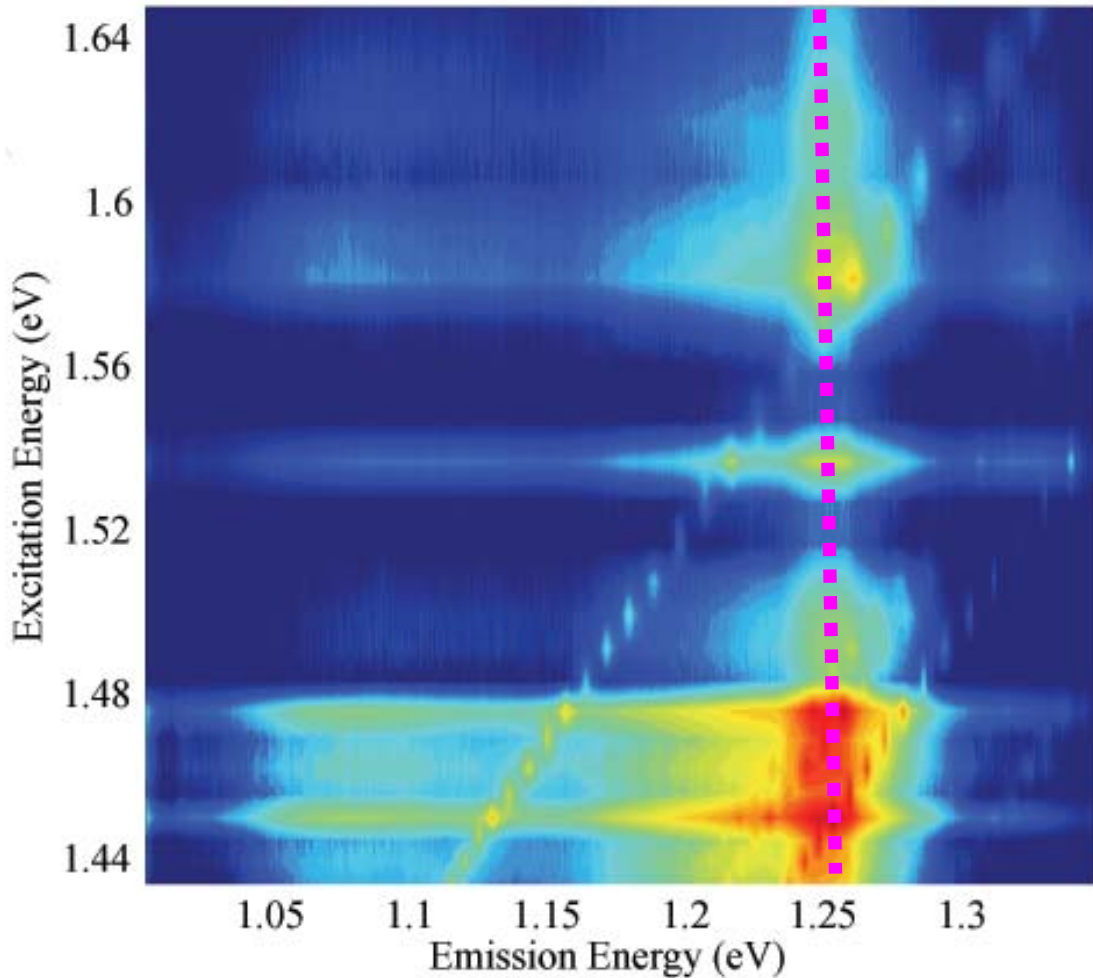
Emission at the Band Edge for Special Excitation Energies



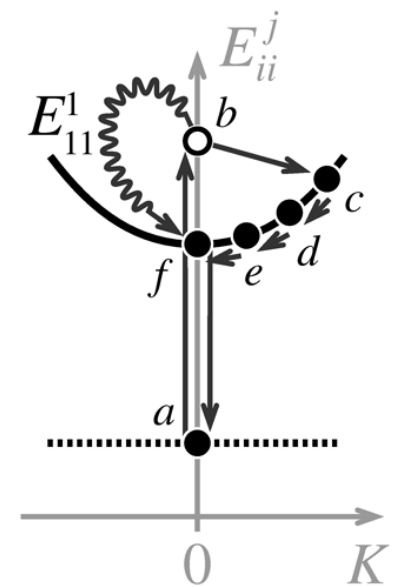
Absorption at E_{22}
Emission at E_{11}



Emission at the Band Edge

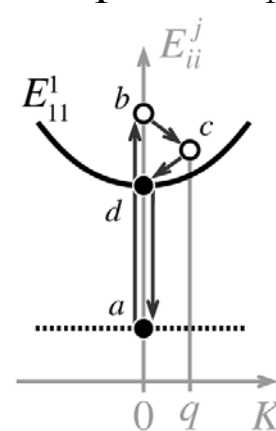
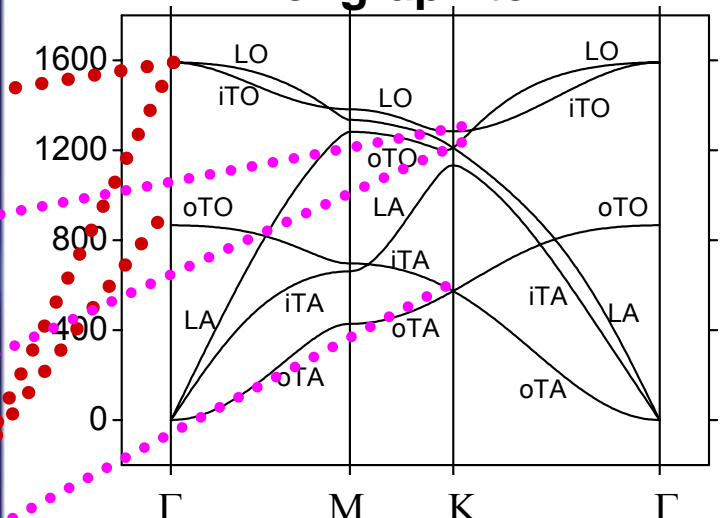
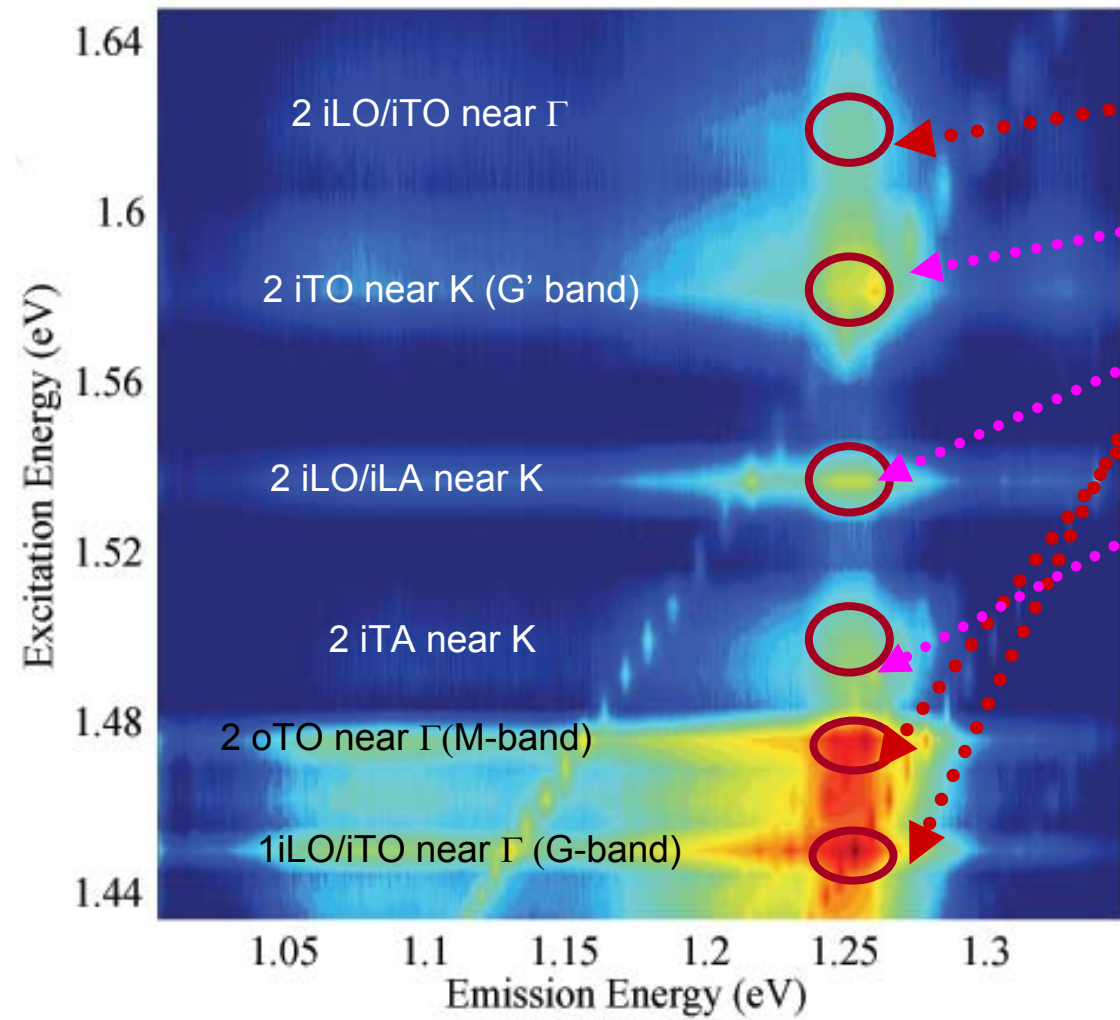


Multiphonon processes
 E_{PL} at E_{11}

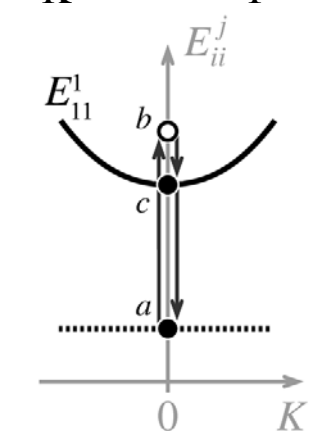


Emission Identified with One and Two Phonon Processes:

Phonon dispersion relations of graphite



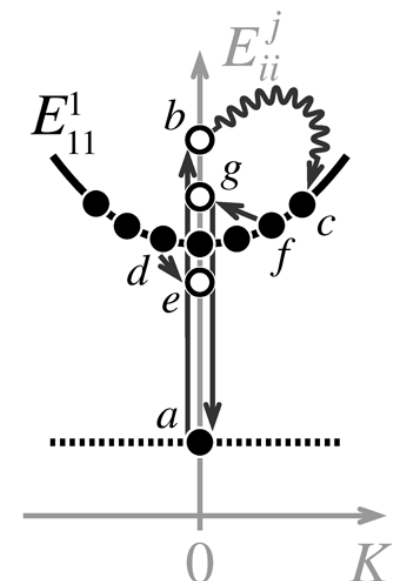
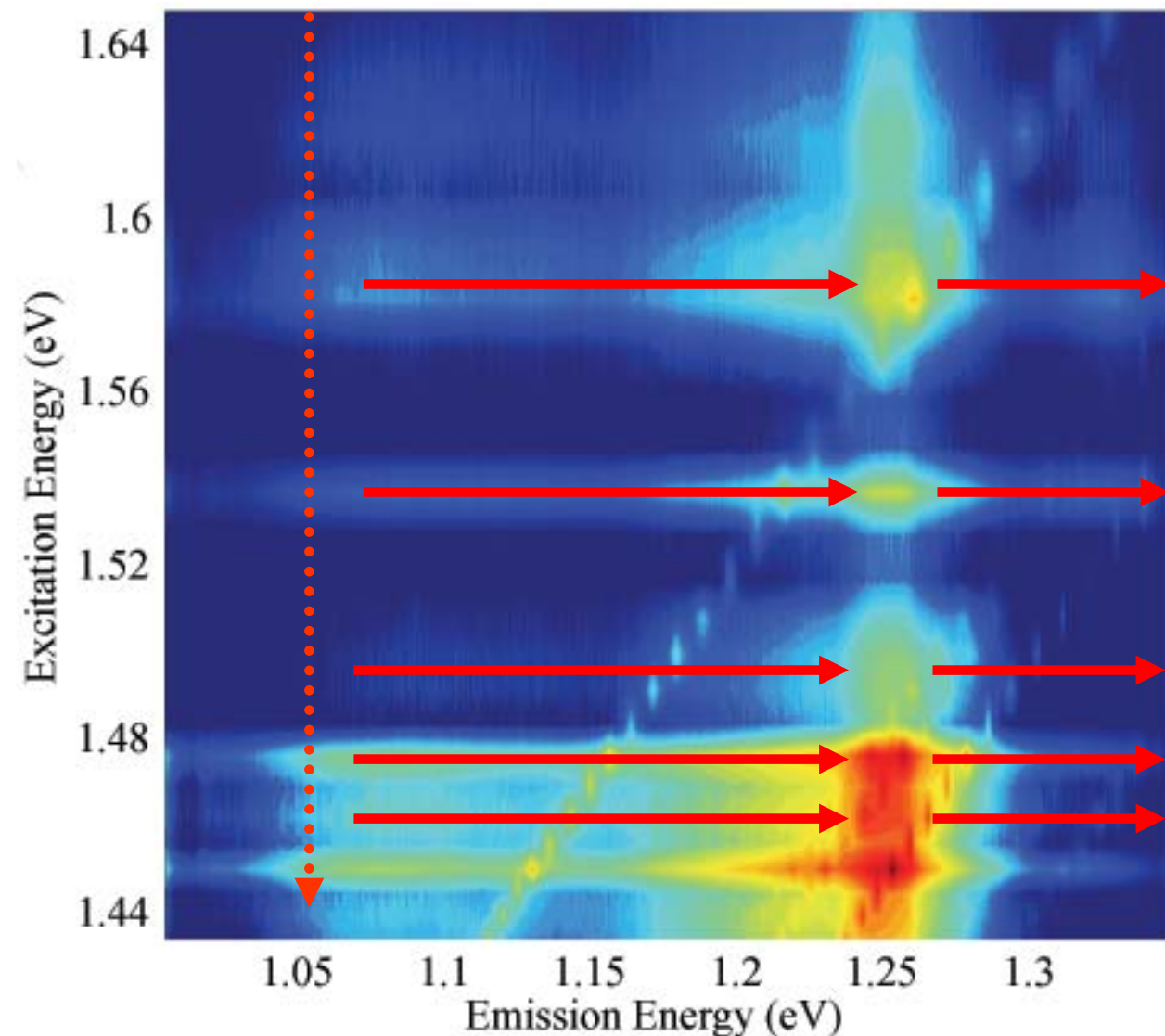
Two phonon process



One phonon process

Hot Luminescence

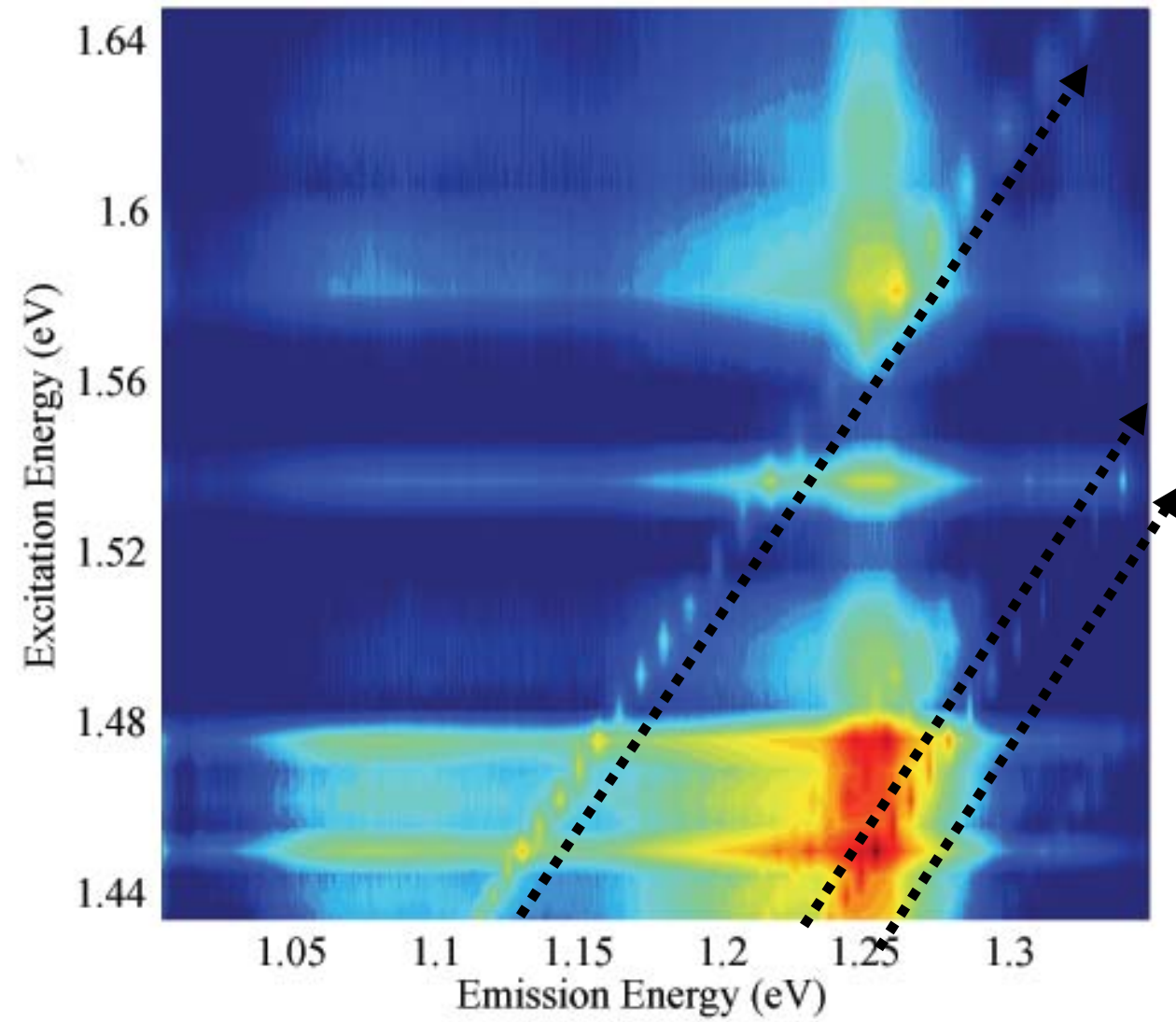
$E_{\text{cut-off}} \sim 1.06\text{eV}$



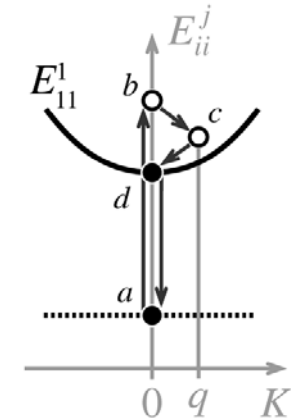
$E_{11} - E_{\text{cut-off}} \sim 0.20\text{eV}$

- Corresponding to largest possible E_{phonon}
- Observed in first order Raman spectra

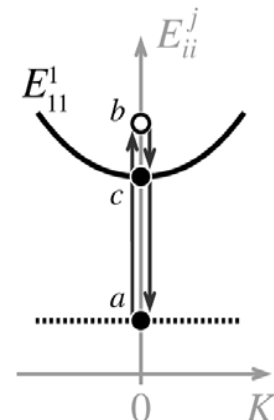
Resonance Raman Peaks



Two Phonon Process
(G'-band, iToLA)

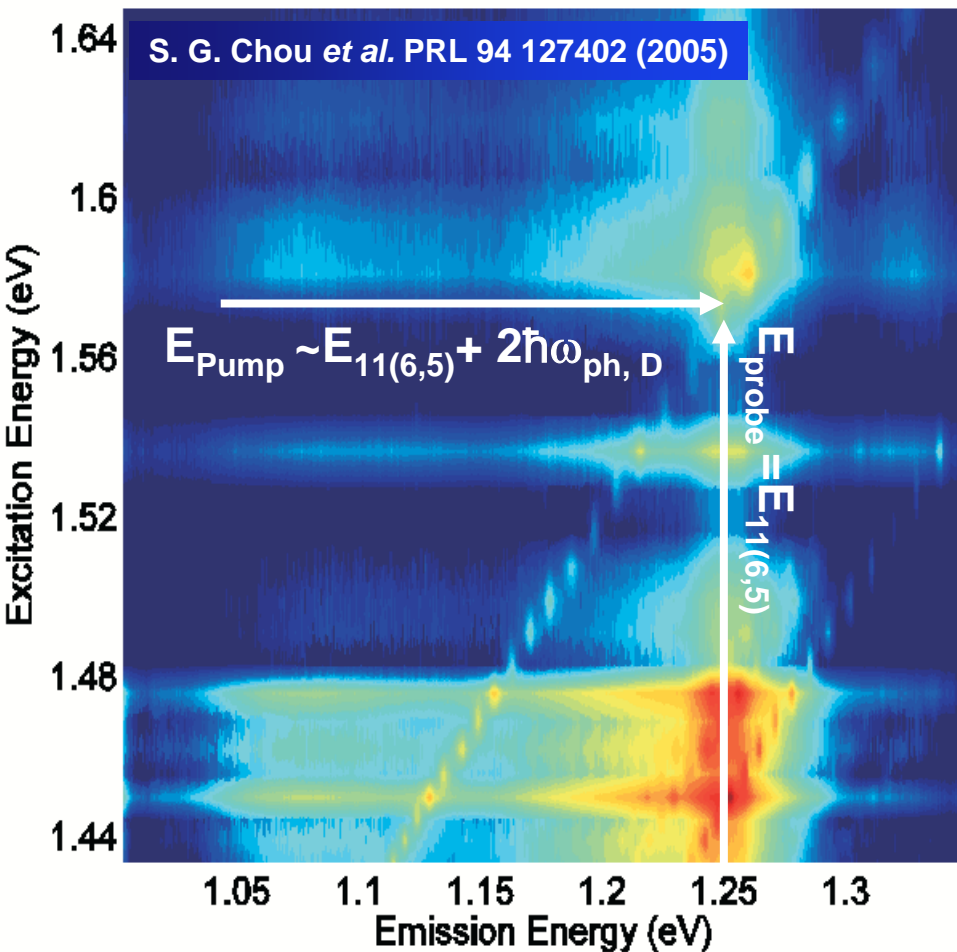


One Phonon Process
(G-band, RBM)



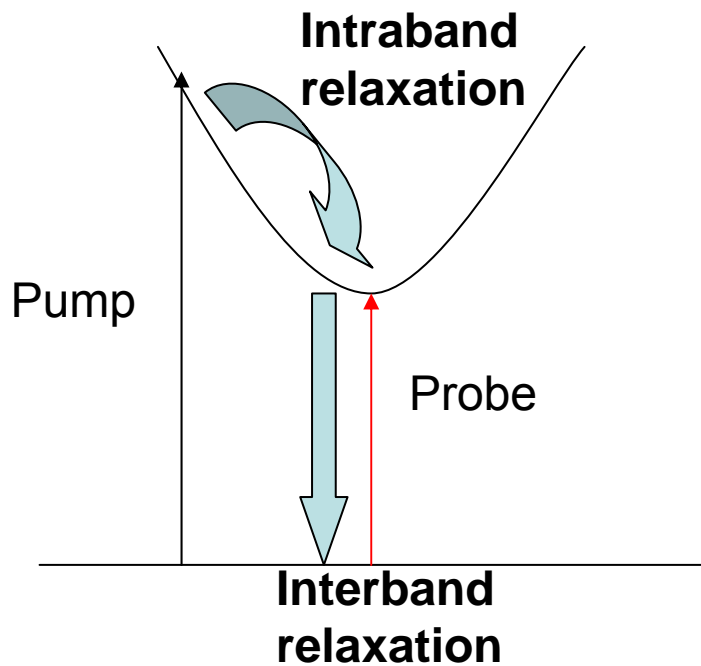
Non-degenerate Pump-Probe

Frequency domain



Fast optics, Time domain

$E_{\text{pump}} = 1.57 \pm 0.01 \text{ eV}$, $\sim E_{11}(6,5) + 2\hbar\omega_D$
 $E_{\text{probe}} = \text{around } E_{11}\text{ of } (6,5)$ nanotube
(Instrument resolution $\sim 250 \text{ fs}$)

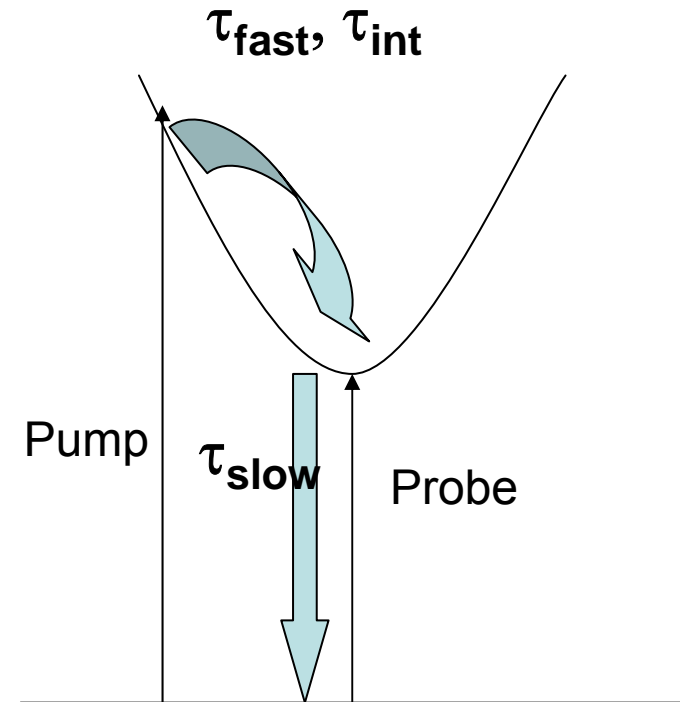
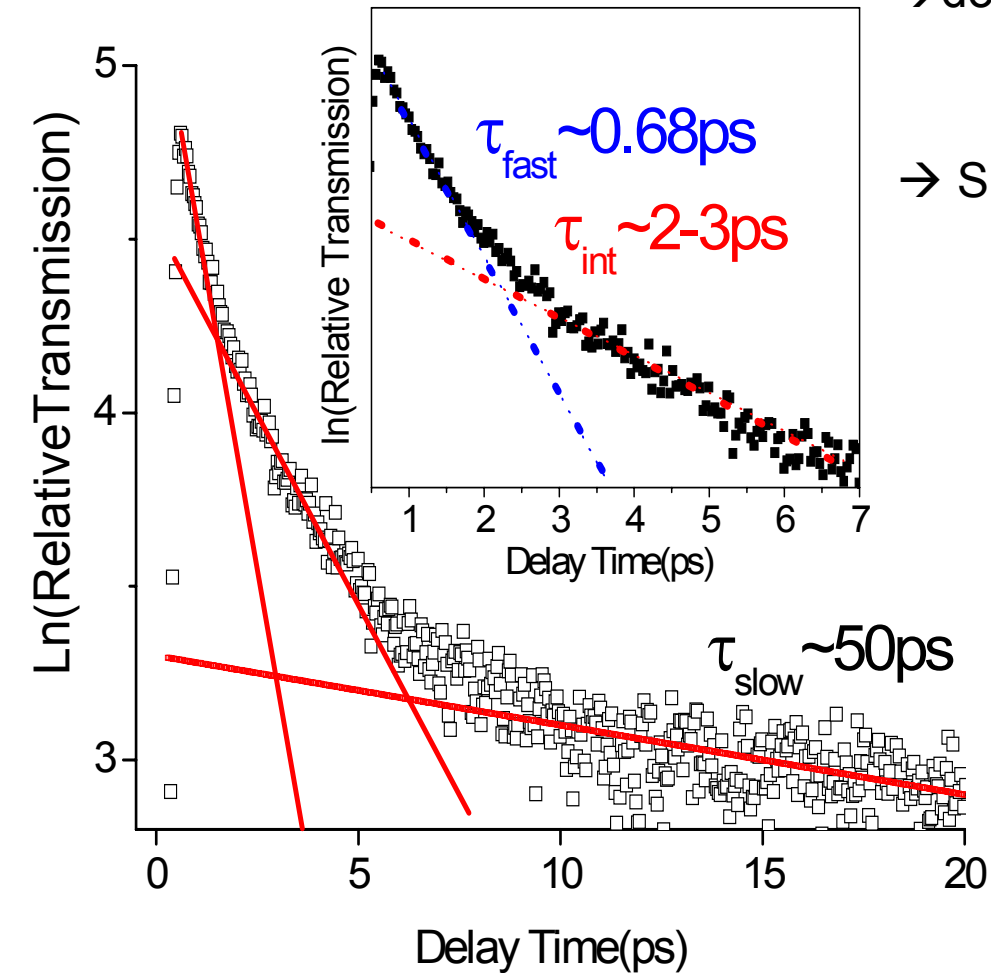


S. G. Chou et al. (unpublished)

Transient Spectrum of DNA-CNT

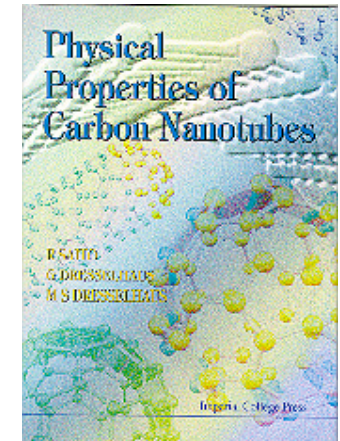
Phonon-assisted excitation (probing at band edge):

- dominated by two fast processes:
 - ~680fs and 3ps
 - non-radiative, e-e and e-ph scattering
- Small tail of slow $\tau \sim 50\text{ps}$ process
 - Interband, radiative process (Small)



Outline

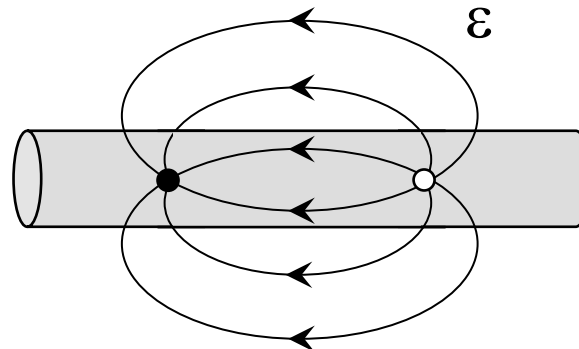
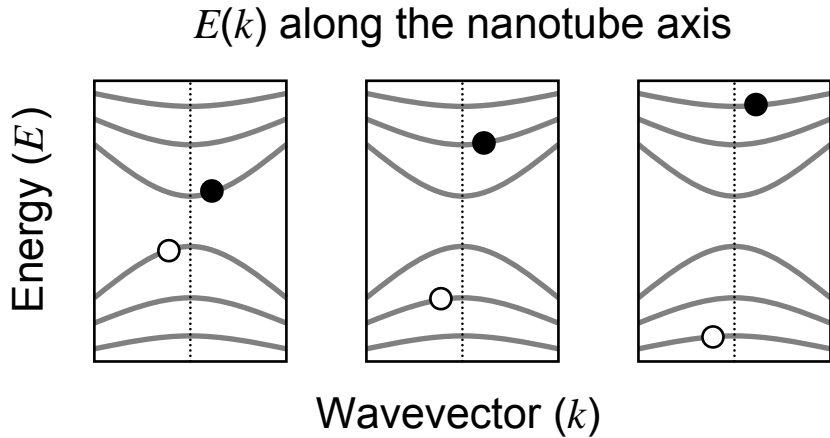
- Background
- Phonon Properties
- Overview of Raman Effect
- First-order Raman Processes
 - (the RBM and G-Band)
- Double Resonance Processes
- Photoluminescence
- **Excitons**



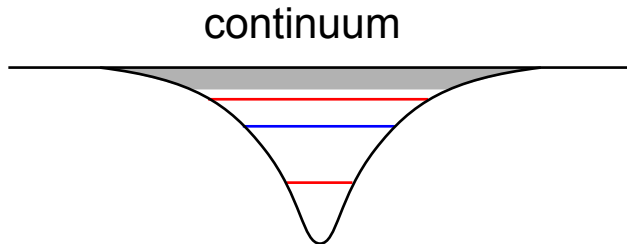
"Physical Properties of Carbon Nanotubes",
by R. Saito, G. Dresselhaus and M.S. Dresselhaus,
Imperial College Press (1998) ISBN 1-86094-093-5

EXCITONS IN CARBON NANOTUBES

Simple Hydrogenic Model – Indicates Subband Index



Electron-Hole Coulomb Interaction



Exciton Hydrogenic Levels
 $n=1,2,3\dots$

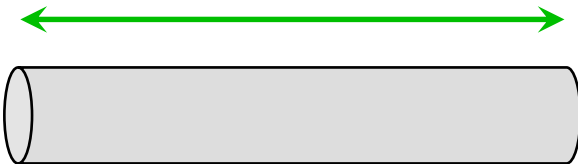
$$H_{eh} = -\frac{e^2}{\epsilon |\mathbf{r}_e - \mathbf{r}_h|}$$

results in the electron-hole binding that forms the exciton states below the conduction subband edge

EXCITON SYMMETRY

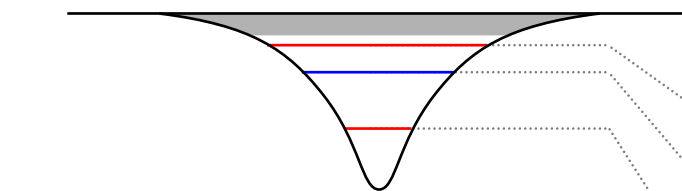
Envelope Function along the Nanotube Axis

Nanotube axial direction



HYDROGENIC MODEL

some authors refer to
the exciton states as
s ($n=1,3\dots$) & **p** ($n=2,4\dots$)



Electron and hole wavefunctions

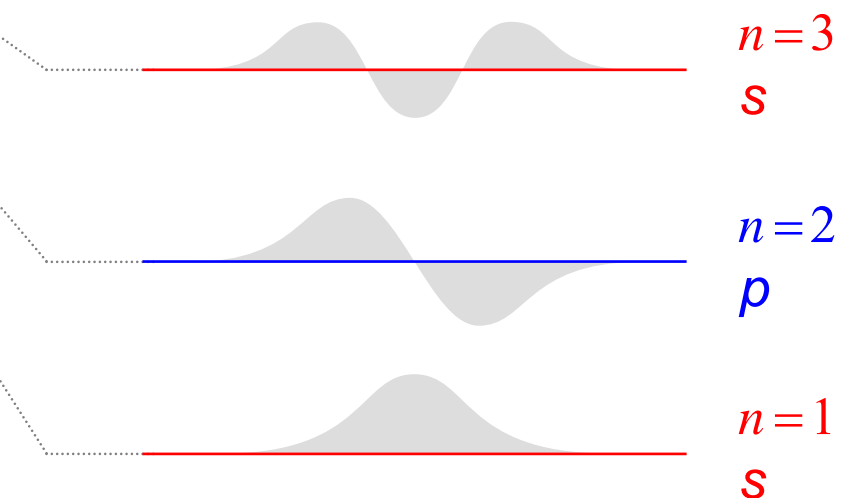
$$\psi_c = \phi_A - \phi_B$$

$$\Psi_v = \Phi_A + \Phi_B$$



Wavefunction for exciton ($\psi_c \Psi_v$) is
antisymmetric at $k=0$

Envelope Function symmetry



$n=3$

s

$n=2$

p

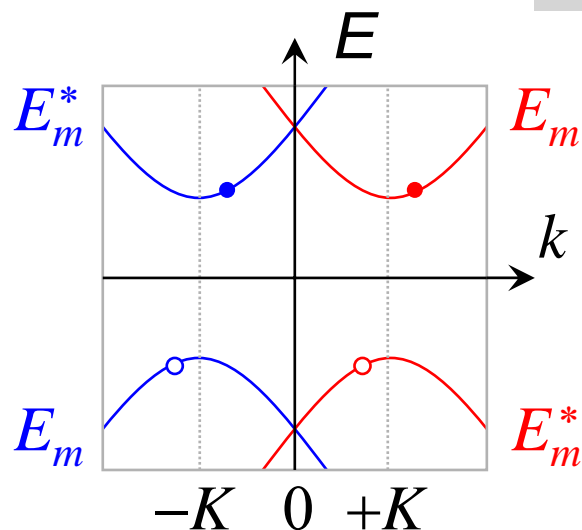
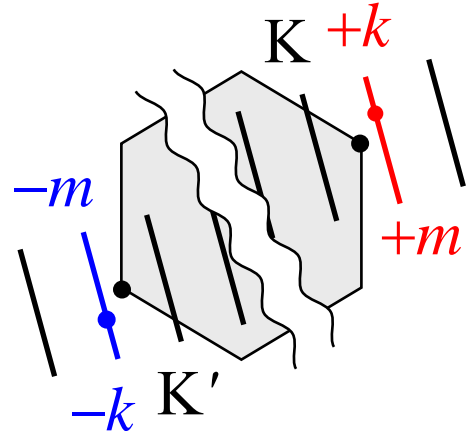
$n=1$

s

TOTAL EXCITON SYMMETRY

K and K' points

Nanotube Cross-section



Electron and hole dispersion

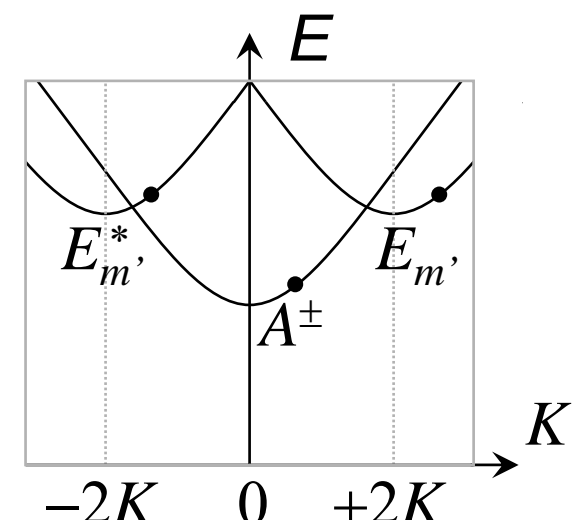
GROUP THEORY

Electron and Hole Symmetries

$$\text{Same } \mathbf{K} \text{ (Intra)} \quad E_m \otimes E_m^* = \begin{cases} A^+ \\ A^- \end{cases}$$

$$\text{K and K' (Inter)} \quad E_m \otimes E_m = E_m,$$

$$m' = \begin{cases} 2m, & \text{for } 2m \leq N/2 \\ N-2m, & \text{for } 2m > N/2 \end{cases}$$



Exciton dispersion

EXCITONS IN CARBON NANOTUBES

Notation based on Free Electron Picture

$E_{ij}^{nX\sigma}(k)$ – exciton binding energy with respect to the ground state

$k = (-2\pi/T; +2\pi/T]$ – linear momentum (continuous)

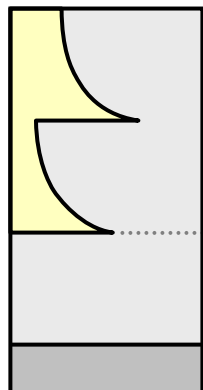
$i,j = 1,2,3,4\dots$ – van Hove singularities (i,j for valence & conduction bands)

$n = 1,2,3,4\dots$ – envelope function (hydrogenic model)

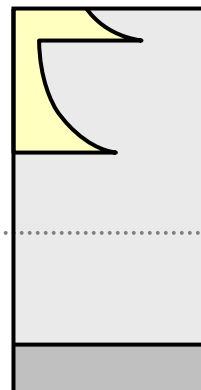
$X = A,E$ – total exciton symmetry (also B and G for achiral tubes)

$\sigma = +,-$ – total exciton parity

ground



quasiparticle



exciton



Free Electron Picture

Coulomb Repulsion

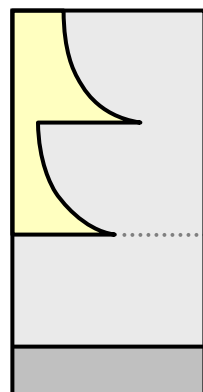
Exciton Bound States

EXCITONS IN CARBON NANOTUBES

Notation based on Line Group Theory

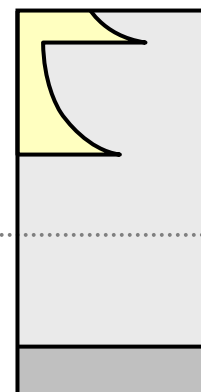
$k n X_m^\sigma$	- exciton binding energy with respect to the ground state
k	- linear momentum
m	- angular momentum
n	- envelope function
X	- total exciton symmetry
σ	- total exciton parity
	$k = (-2\pi/T; +2\pi/T]$
	$m = 2-N \dots N$
	$n = 1, 2, 3, 4 \dots$
	$X = A, B, E, G$
	$\sigma = +, -$

ground



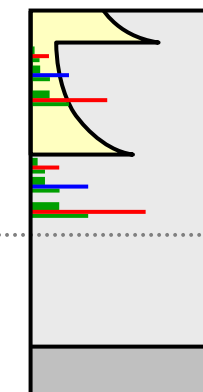
Free Electron Picture

quasiparticle



Coulomb Repulsion

exciton



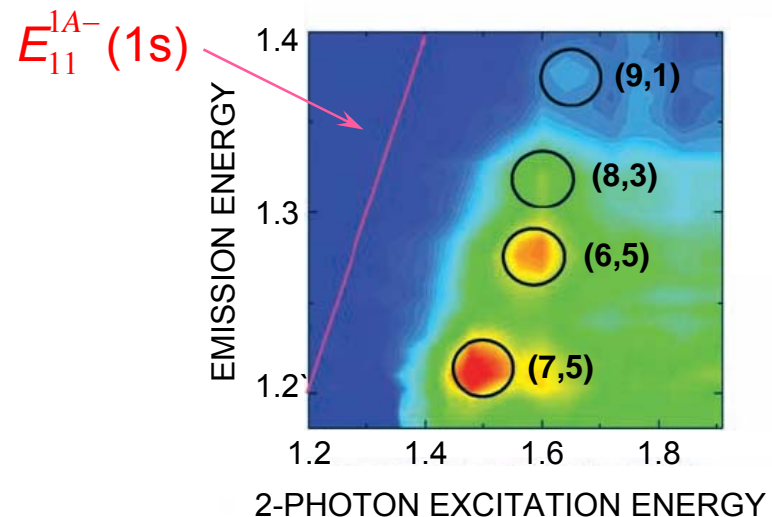
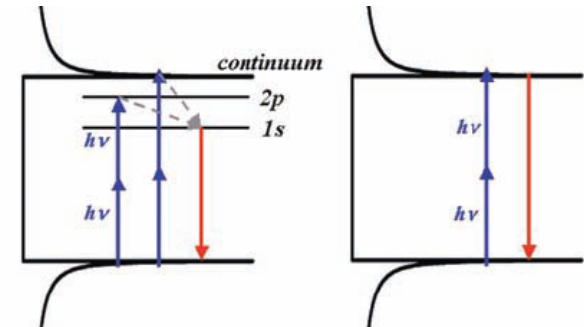
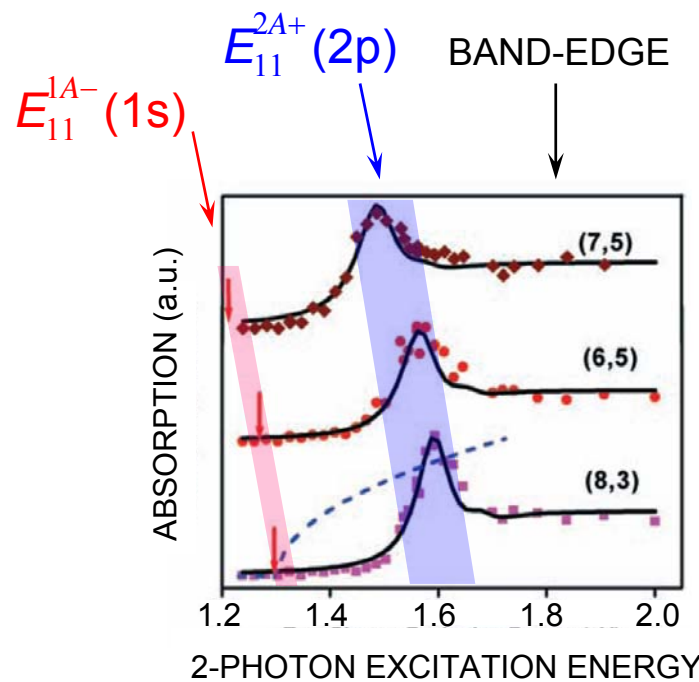
2 photon
1 photon
dark

Exciton Bound States

EXCITONS IN CARBON NANOTUBES

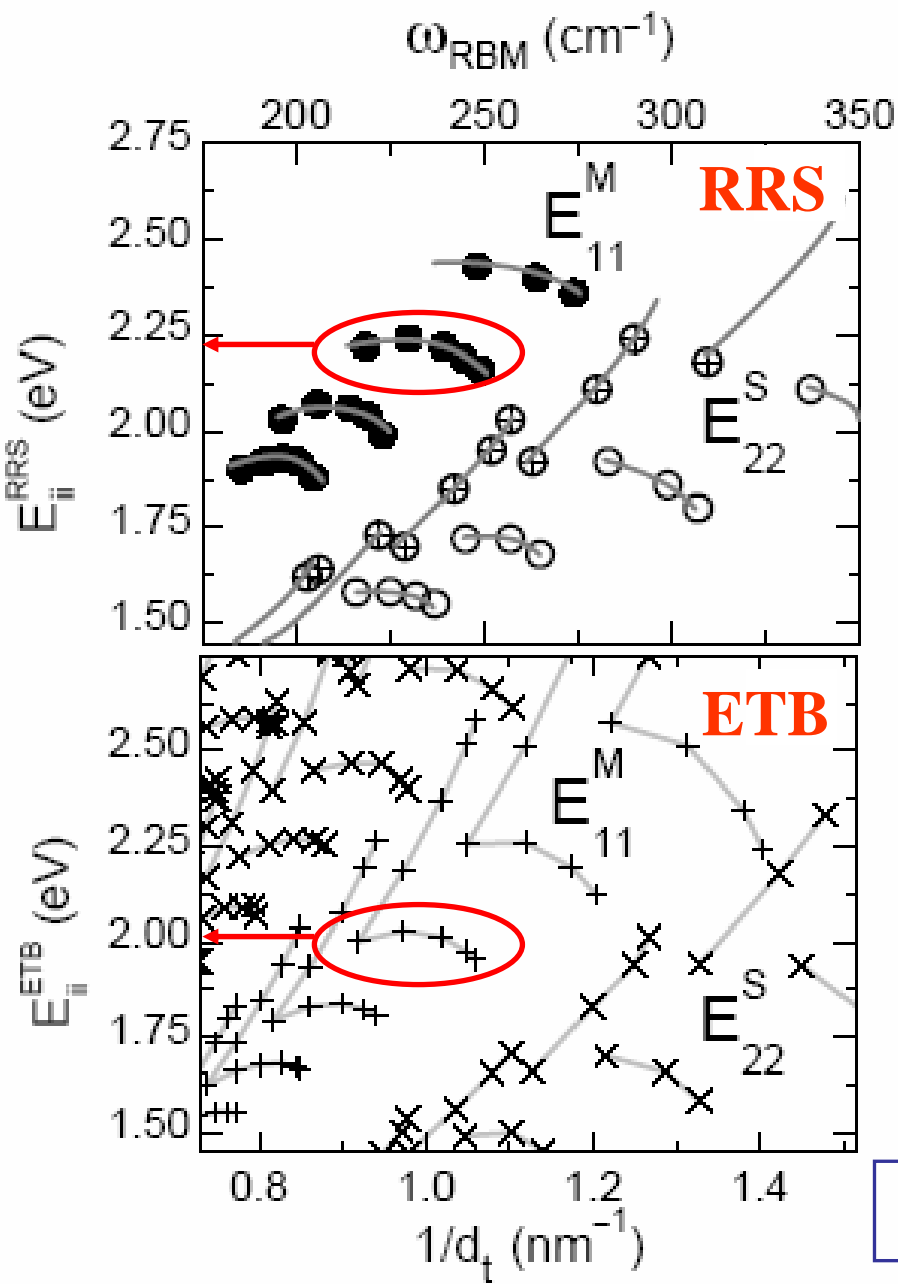
Experimental Justification

2-photon excitation to a $2A^+$ symmetry exciton (2p) and 1-photon emission from a $1A^-$ exciton (1s) cannot be explained by the free electron model



Wang et al. Science **308**, 838 (2005)
J. Maultzsch et al. submitted (2005).

The development of the E_{ii} vs d_t plot for SWNTs



Extended Tight Binding (ETB) model:

*Popov, NJP **6**, 17 (2004)*

*Samsonidze et al. APL **85**, 5703 (2004)*

Non-orthogonal tight-binding total energy calculations → beyond the simple π -only, orthogonal nearest neighbor approximation

ETB transfer and overlap integrals as functions of the C–C interatomic distance are calculated within DFT framework.

SWNT curvature is considered.

[Porezag et al., PRB **51**, 12947 (1995)]

- Geometrical family behavior is obtained
- ETB values are red-shifted from the experimental results

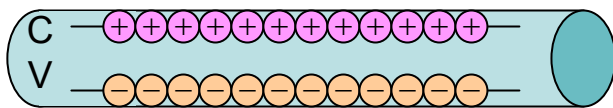
Many-body effect are not included

Many-body Effects

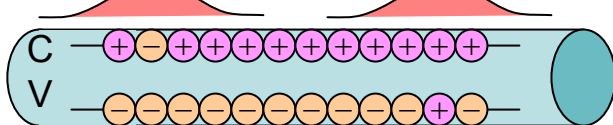
C. D. Spataru et al., PRL 92, 077402 (2004)

$$E_{ii} = E_{ii}^{\text{gr}} + E_{ii}^{\text{ee}} + E_{ii}^{\text{eh}}$$

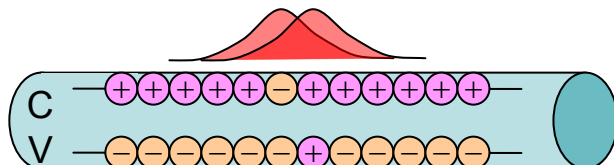
ground state
quasiparticle correction }
exciton binding } many-body
corrections
gs - ground state DFT-LDA or ETB



ee - quasiparticle correction (blueshift) GW

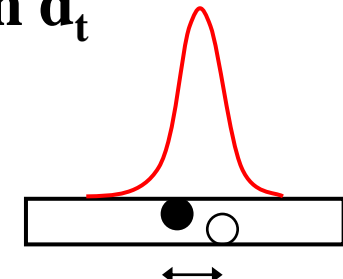
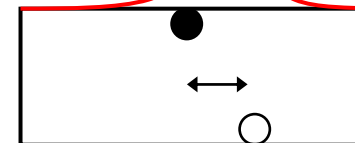


eh - exciton binding (redshift)



BS

- Dependence on d_t

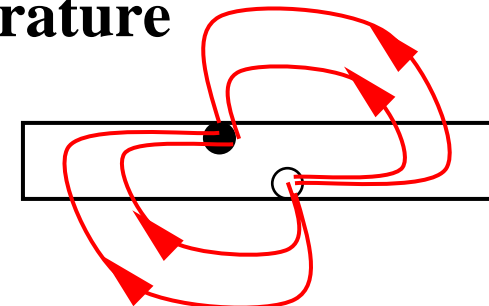


- Dependence on θ and
 $(2n+m)\text{mod}3$

effective mass \rightarrow mobility

- Dependence on environment
and temperature

dielectric
constant

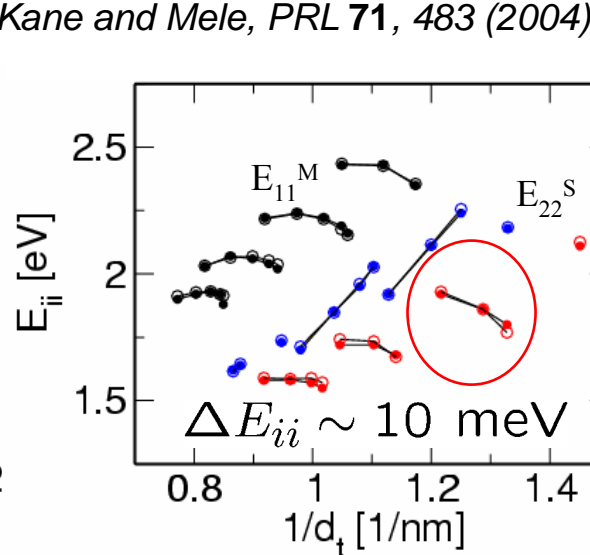
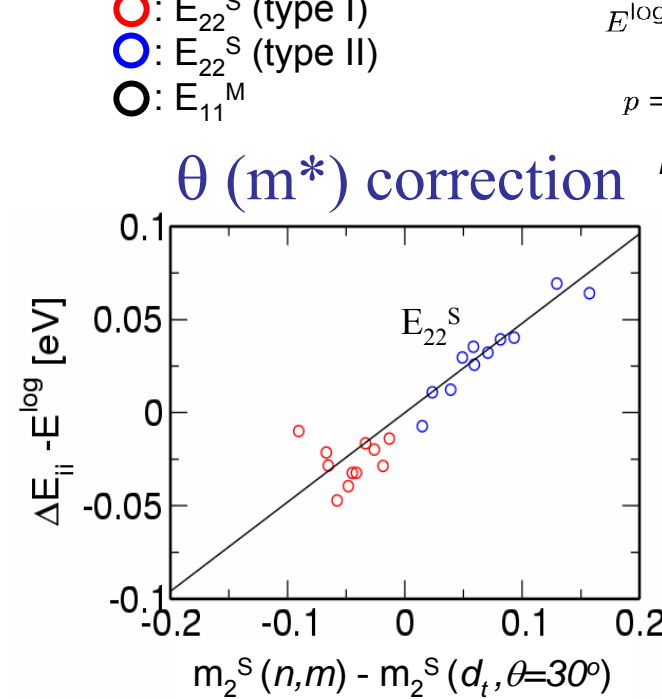
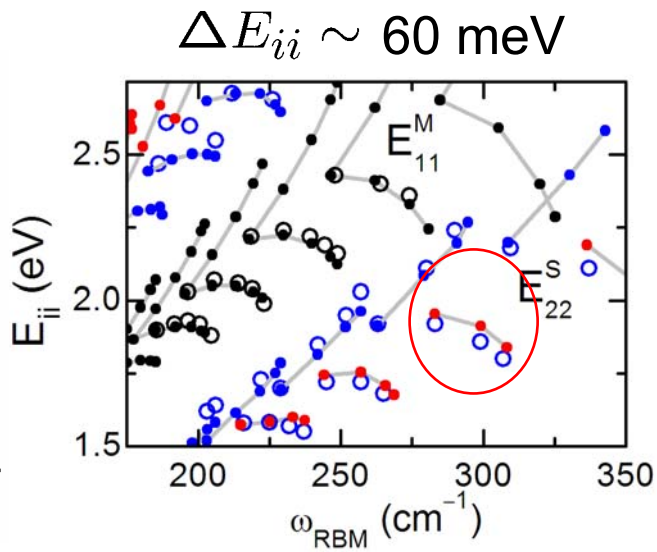
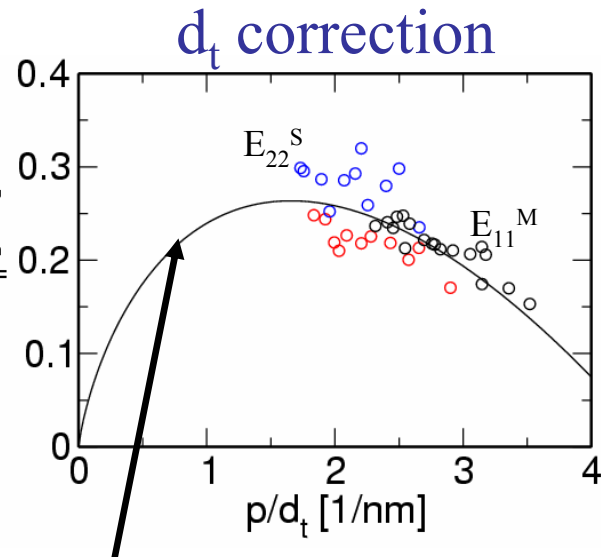
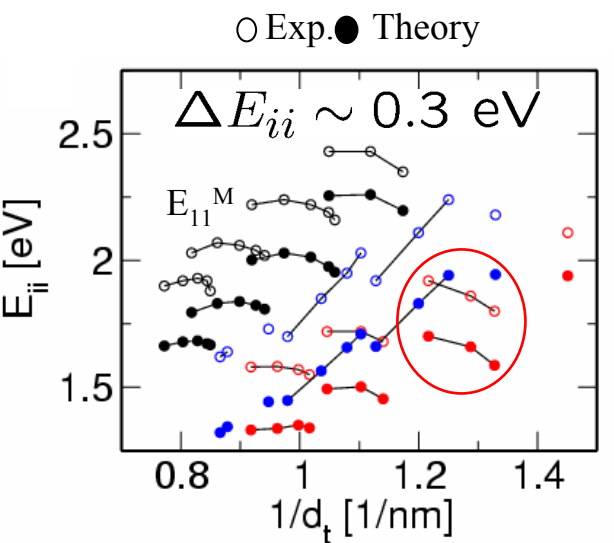


Ando, Kane & Mele, Avouris,
Steve Louie, ...

How to make those corrections to ETB?

Accounting for many-body effects

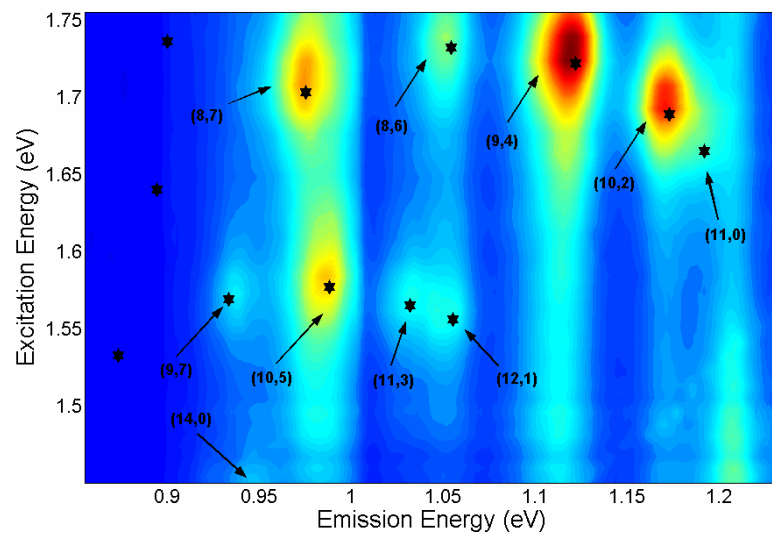
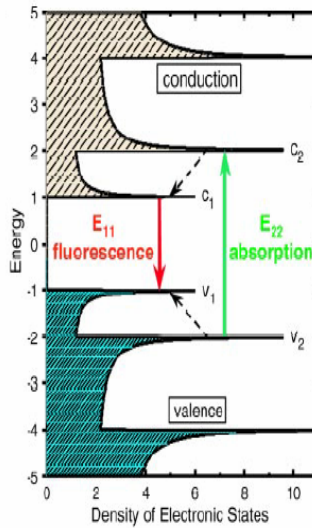
Jorio et al., PRB 71, 075401 (2005)



Theory explains experiment within experimental precision

What about the RBM frequency dependence on (n,m) ?

2 – Photoluminescence – excitons...

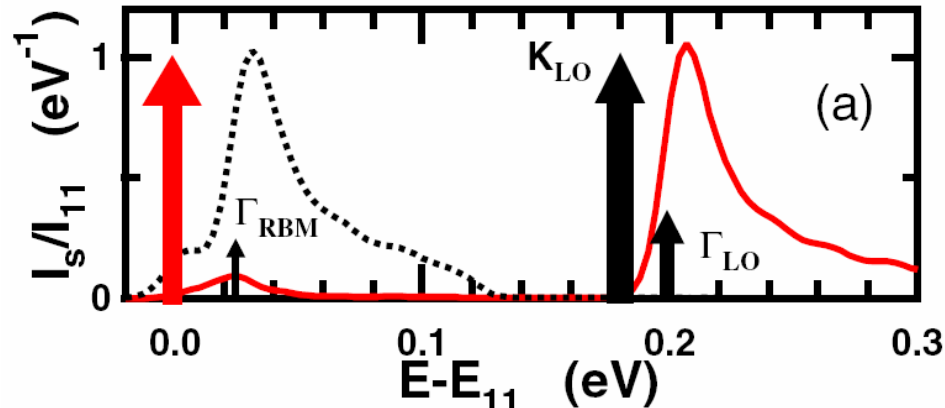


Main Process:
Absorption - E_{22}^S
Emission - E_{11}^S

Bachilo et al., Science 298, 2361 (2002)

...and phonons

Exciton-phonon coupling

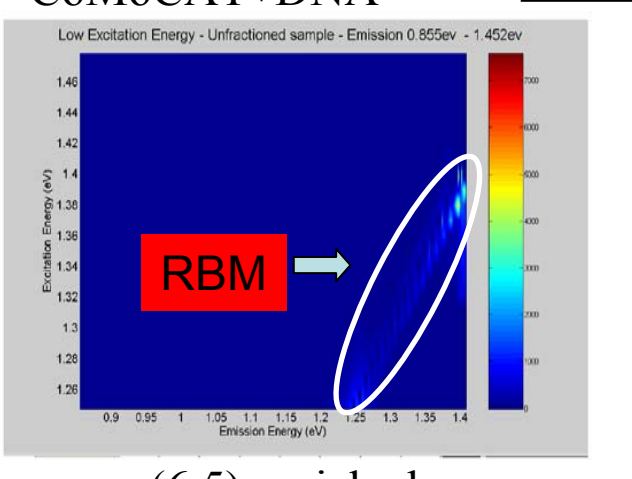
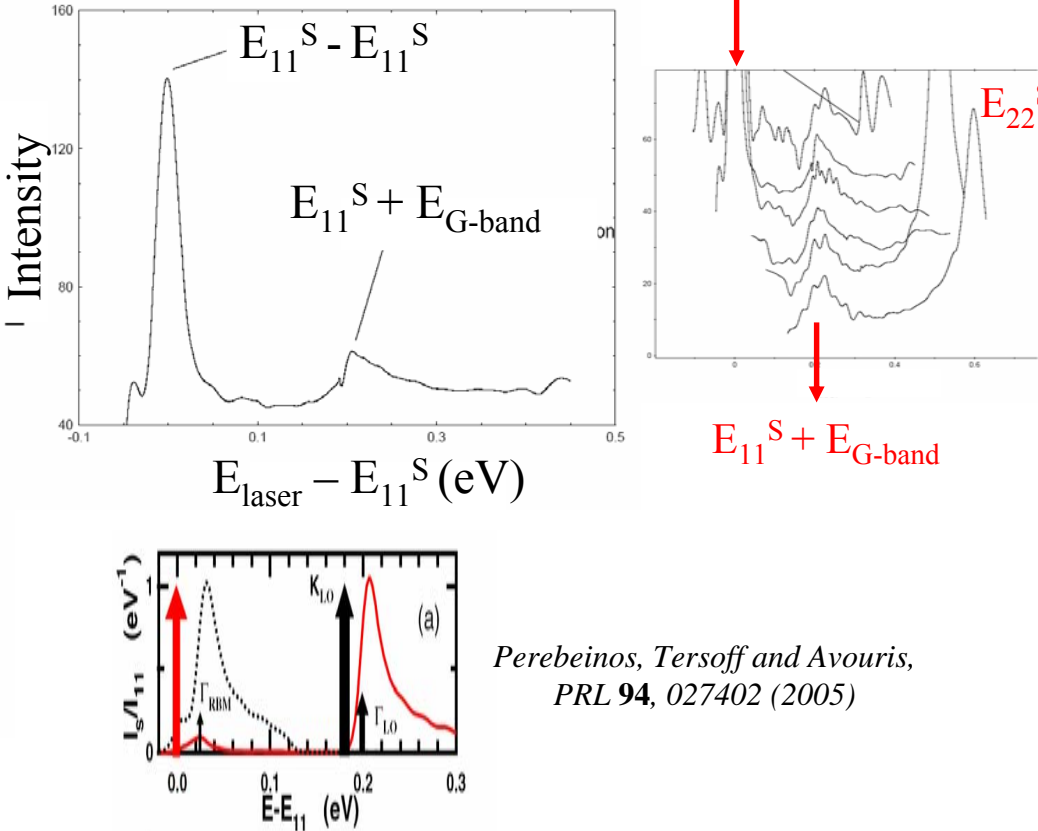
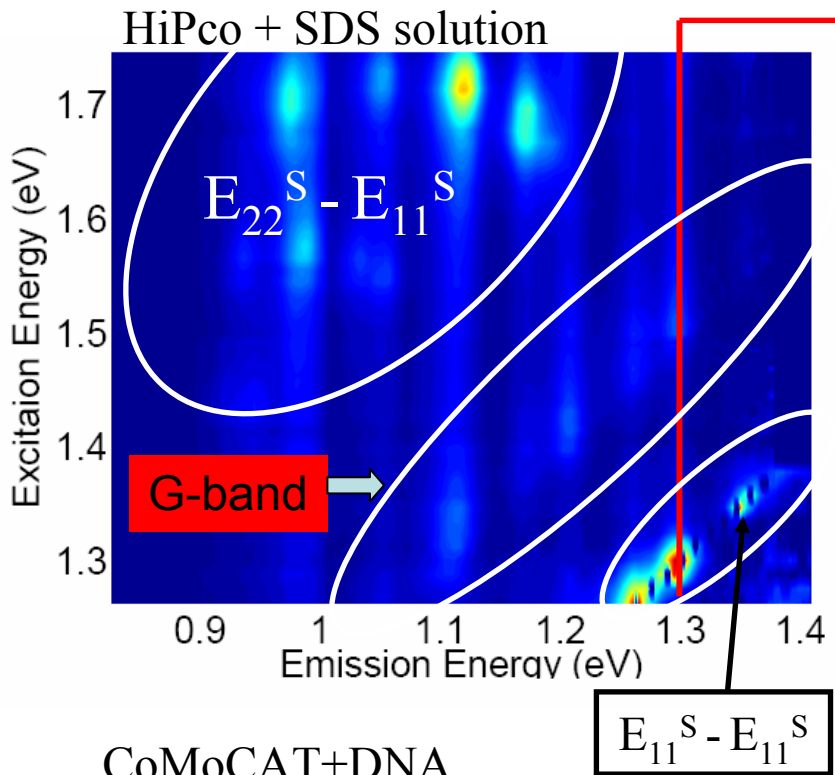


Perébeinos, Tersoff and Avouris, PRL 94, 027402 (2005)

Two exciton-phonons sideband
- $E_{ii} + E_{RBM}$
- $E_{ii} + E_{G\text{-band}}$

$E_{RBM} \sim 0.02\text{eV}$
 $E_{G\text{-band}} \sim 0.2\text{eV}$

The exciton-phonon sidebands



The exciton-RBM and exciton-G-band sidebands are there for all the (n,m) SWNTs.
But, there is more...

H. B. Ribeiro et al. unpublished

Summary

Raman spectroscopy and photoluminescence provide:

- Powerful tools for characterizing nano objects only about 1 nm in diameter
- These photophysical techniques also allow exploration of much beautiful new physics made available for the first time in these unique nano systems
- Although much new physics has already been revealed, many vital unanswered questions remain unresolved.

Collaborators

S. G. Chou	Chemistry, MIT, USA
Ge. G. Samsonidze	EECS, MIT, USA
H. Son	EECS, MIT, USA
E.B. Barros	EECS, MIT, USA
J. Kong	EECS, MIT, USA
D. Tokmakoff	Chemistry, MIT, USA
G. Dresselhaus	Bitter Magnet Lab, MIT, USA
M. Zheng	DuPont, USA
A. K. Swan	Comp. & Elec. Eng., BU, USA
B. B. Goldberg	Physics, BU, USA
S. M. Unlu	Comp. & Elec. Eng., BU, USA
R. Saito	Tohoku Univ., Japan
J. Jiang	Tohoku Univ., Japan
M. Endo	Shinshu Univ., Japan
M. Pimenta	Physics, UFMG, Brazil
A. Jorio	Physics, UFMG, Brazil
H. B. Ribeiro	Physics, UFMG, Brazil
C. Fantini	Physics, UFMG, Brazil
F. Plentz Filho	Physics, UFMG, Brazil
A.G. Souza Filho	Physics, UFC, Brazil
A. P. Santos	CDTN, Brazil
M. Terrones	San Luis Potosi, Mexico

The End